



Roger Taylor

# Gossans and Leached Cappings

Field Assessment

 Springer

## Gossans and Leached Cappings



Roger Taylor

# Gossans and Leached Cappings

Field Assessment

 Springer

Roger Taylor  
Townsville  
Queensland 4810  
Australia  
[rinkbowl@dodo.com.au](mailto:rinkbowl@dodo.com.au)

ISBN 978-3-642-22050-0 e-ISBN 978-3-642-22051-7  
DOI 10.1007/978-3-642-22051-7  
Springer Heidelberg Dordrecht London New York

Library of Congress Control Number: 2011934477

© Springer-Verlag Berlin Heidelberg 2011

This work is subject to copyright. All rights are reserved, whether the whole or part of the material is concerned, specifically the rights of translation, reprinting, reuse of illustrations, recitation, broadcasting, reproduction on microfilm or in any other way, and storage in data banks. Duplication of this publication or parts thereof is permitted only under the provisions of the German Copyright Law of September 9, 1965, in its current version, and permission for use must always be obtained from Springer. Violations are liable to prosecution under the German Copyright Law.

The use of general descriptive names, registered names, trademarks, etc. in this publication does not imply, even in the absence of a specific statement, that such names are exempt from the relevant protective laws and regulations and therefore free for general use.

*Typesetting & Prepress:* Elisabeth Sillmann, Landau, [www.blaetterwaldDesign.de](http://www.blaetterwaldDesign.de)

*Cover design:* deblik, Berlin

Printed on acid-free paper

Springer is part of Springer Science+Business Media ([www.springer.com](http://www.springer.com))

# Acknowledgements

Given a 30–40 years germination period, it is not surprising that the list of contributors is considerable, and it is not feasible to list the input of every student, colleague, and professional geologist. Thank you everybody.

Special thanks are extended to W.C. Lacy former Professor of Economic Geology at James Cook University, who passed on both his enthusiasm and extensive field knowledge of the subject.

Similarly Dr Peter Pollard and Dr Gavin Clarke contributed continuously over the years via rock collection, specimen preparation, and editorial help with this tome.

Many of the high quality plates are the work of Roger Yeldham and Brian Pump from the former photographic division of James Cook University.

Amongst the numerous students and active exploration geologists involved, the photographic and hand specimen contributions of David Andrews will be evident to the reader.

On the more recent front, the financial support via Ivanhoe Mines (Doug Kirwan and Richard Gosse) the local branch of the Australasian Institute of Mining and Metallurgy, and the Economic Geology Research Unit at James Cook University have made all the difference in stimulating progress from an occasionally reluctant author.

Marianne Drogemuller wrestled with the spider like writing at the typesetting stage, and many warm thanks are due to Elleni Caragianides for gallons of coffee and her ever tolerant company.

A desperate late stage plea for both field and rare mineral photographic help was willingly answered by the following contributors: – A.P. Rovera, M. Boni, C.S. Rugless, S. Close, S. Moore, S. Prihatmoko, H. Huehne, and P. Schumacher. Their top quality pictures have enhanced the book considerably.



This offering was probably initiated some forty years ago when a young geologist with an interest in mineral specimens and vision of El Dorado launched into the field with a borrowed copy of Blanchard's leached outcrops (Blanchard, 1968).

Despite youthful confidence and perhaps a mild arrogance "emanating" from attending "suitable" institutions the net result was one of confusion, disappointment, and in retrospect a complete lack of comprehension. Where were the marvellous boxworks, stunning mineral specimens and blindingly obvious places to dig?

This humbling experience has led to a still unfinished quest to gain a better concept of the visual skills required to produce a better result. Hopefully some of the knowledge gained along the way will be of value to younger professionals experiencing a similar problem.

To some extent leached outcrop-gossan assessment has become a lost art form, which considering its obvious value is a little perplexing. However, rather than launch into a tirade about the "old days" this is an attempt to represent and demystify some of the more useful field concepts. The text is designed to be of assistance to field geologists and prospectors, and does not qualify as an erudite rigorous academic tome. Hopefully solution chemists in particular will forgive some of the simplistic presentation.

Sincere acknowledgements are due to Willard (Bill) C. Lacy formerly Professor of Economic Geology at James Cook University, who greeted the returning bewildered youngster with a knowing smile and passed along much of his own extensive field experience.

Similarly several generations of students assisted with individual studies and subsequently despatched small parcels of earthy materials from around the globe. The latter caused considerable stress to various Australian customs officials.

*Roger G. Taylor*



|   |           |
|---|-----------|
| Preface .....   | VII       |
| <b>1 Introduction .....</b>   | <b>1</b>  |
| <b>2 Theoretical perspectives .....</b>   | <b>3</b>  |
| <b>3 Initial recognition .....</b>  | <b>9</b>  |
| 3.1 General aspects .....   | 9         |
| 3.2 Physical factors .....  | 9         |
| 3.2.1 Remoteness (limiting movement) .....  | 9         |
| 3.2.2 Concealment (limiting exposure) .....   | 10        |
| 3.3 Technical (advancing knowledge) .....   | 10        |
| 3.3.1 Changing concepts (geological reassessment) .....   | 10        |
| 3.3.2 New technology (scientific and technological evolution) .....                                     | 10        |
| 3.4 Sociological (people factors) .....   | 10        |
| 3.4.1 Access and risk barriers .....  | 10        |
| 3.4.2 Other opportunities .....   | 10        |
| <b>4 Broad scale – first impressions .....</b>  | <b>21</b> |
| 4.1 Size – shape .....  | 21        |
| 4.2 Quartz (textures and sulphide armouring) .....  | 21        |
| 4.2.1 Textures .....  | 21        |
| 4.2.2 Sulphide remnants .....   | 21        |
| 4.3 Limonite (composition, colour, source interpretation, host rock controls, and textural types) ..... | 22        |
| <b>5 Structure (layering and brecciation) .....</b>   | <b>29</b> |
| <b>6 Secondary minerals .....</b>   | <b>33</b> |
| 6.1 General aspects .....   | 33        |
| 6.2 Iron  |           |
| Goethite $\alpha\text{Fe}_3\text{O}(\text{OH})$ . Ferric oxyhydroxide.                                  |           |
| Haematite $\text{Fe}_2\text{O}_3$ . Iron oxide.   |           |
| Jarosite $\text{KFe}_3(\text{SO}_4)_2(\text{OH})$ . Potassium iron hydroxysulphate.                     |           |
| Melanterite $\text{FeSO}_4 \cdot 7\text{H}_2\text{O}$ . Hydrated iron sulphate.                         |           |
| Vivianite $\text{Fe}_3(\text{PO}_4)_2 \cdot 8\text{H}_2\text{O}$ . Hydrated iron phosphate. ....        | 34        |
| 6.3 Manganese   |           |
| “Manganese wad” and “Manganese oxides”, general terms.  |           |
| Psilomilane (“manganese oxides”, general term).   |           |
| Pyrolusite $\text{MnO}_2$ . Manganese oxide.  |           |
| Manganite $\text{MnO}(\text{OH})$ . Manganese oxyhydroxide.   |           |
| Neotocite $(\text{MnFeMg})\text{SiO}_3 \cdot \text{H}_2\text{O}$ . Hydrated iron silicate. ....         | 38        |

|        |  |    |
|--------|--|----|
| 6.4    | Copper .....   | 40 |
| 6.4.1  | General aspects .....  | 40 |
| 6.4.2  | Copper Cu. Native copper .....   | 42 |
| 6.4.3  | Copper pitch. Oxides/hydroxides of copper, silica, iron and manganese (mineral mixtures) .....   | 42 |
| 6.4.4  | Cuprite $\text{Cu}_2\text{O}$ . Red copper oxide (also variety chalcotrichite) .....   | 43 |
| 6.4.5  | Tenorite $\text{CuO}$ (also termed melaconite or black copper oxide) .....   | 43 |
| 6.4.6  | Malachite $\text{Cu}_2\text{CO}_3(\text{OH})_2$ . Copper carbonate (established usage, ignores hydroxyl input) .....   | 47 |
| 6.4.7  | Azurite $\text{Cu}_3(\text{CO}_3)_2(\text{OH})_2$ . Copper carbonate (established usage, ignores hydroxyl input) .....   | 47 |
| 6.4.8  | Chrysocolla $(\text{CuAl})_2\text{H}_2\text{Si}_2\text{O}_5 \cdot n(\text{H}_2\text{O})$ . Hydrated copper silicate .....  | 47 |
| 6.4.9  | Chalcanthite $\text{CaSO}_4 \cdot 5\text{H}_2\text{O}$ . Hydrated copper sulphide .....  | 47 |
| 6.4.10 | Atacamite $\text{Cu}_2\text{Cl}(\text{OH})_3$ . Copper hydroxychloride .....   | 47 |
| 6.4.11 | Brochantite $\text{CuSO}_4(\text{OH})_6$ . Copper hydroxysulphate .....  | 48 |
| 6.4.12 | Antlerite $\text{Cu}_3\text{SO}_4(\text{OH})_4$ . Copper hydroxysulphate .....   | 48 |
| 6.4.13 | Rare secondary copper minerals<br>Chalcosiderite $\text{Cu}(\text{Fe},\text{Al})_6(\text{PO}_4)_4 \cdot 4\text{H}_2\text{O}$ . Hydrated copper iron aluminium phosphate.<br>Dioptase $\text{CuSiO}_2(\text{OH})_2$ . Copper hydroxysilicate.<br>Linarite $\text{PbCuSO}_4(\text{OH})_6 \cdot \text{H}_2\text{O}$ . Hydrated lead copper sulphate.<br>Olivenite $\text{Cu}_2\text{AsO}_4\text{OH}$ . Copper hydroxyarsenate.<br>Pseudomalachite $(\text{Cu}_5\text{PO}_4)_2(\text{OH})_4$ . Copper hydroxyphosphate.<br>Turquoise $\text{CuAl}_6(\text{PO}_4)_4(\text{OH})_8 \cdot 4\text{H}_2\text{O}$ . Hydrated copper aluminium phosphate. .... | 48 |
| 6.4.14 | Supergene copper sulphides .....   | 49 |
| 6.5    | Lead .....   | 55 |
| 6.5.1  | General aspects .....  | 55 |
| 6.5.2  | Anglesite $\text{PbSO}_4$ . Lead sulphate .....  | 56 |
| 6.5.3  | Cerussite $\text{PbCO}_3$ . Lead carbonate .....   | 56 |
| 6.5.4  | Lead oxides<br>Massicot $\text{PbO}$ . Lead oxide<br>Litharge $\text{PbO}$ . Lead oxide<br>Minium $\text{Pb}_3\text{O}_4$ . Lead oxide .....   | 57 |
| 6.5.5  | Plumbojarosite $\text{PbFe}_6(\text{SO}_4)_4(\text{OH})_{12}$ . Lead/iron hydroxysulphate. ....  | 57 |
| 6.5.6  | Pyromorphite $\text{PbCl Pb}_4(\text{PO}_4)_3$ . Lead chlorophosphate and<br>Mimetite $\text{PbCl Pb}_4(\text{AsO}_4)_3$ , Lead chloroarsenate (members of a solid solution series) .....  | 57 |
| 6.5.7  | Rare secondary lead minerals .....   | 57 |
|        | Wulfenite $\text{PbMoO}_4$ . Lead molybdate<br>Crocoite $\text{PbCrO}_4$ . Lead chromate   |    |
| 6.6    | Zinc .....   | 62 |
| 6.6.1  | General aspects .....  | 62 |
| 6.6.2  | Smithsonite $\text{ZnCO}_3$ . Zinc carbonate .....   | 62 |
| 6.6.3  | Hemimorphite $\text{Zn}_4\text{S}_{12}\text{O}_7(\text{OH})_2 \cdot \text{H}_2\text{O}$ . Hydrated zinc silicate .....   | 63 |
| 6.6.4  | Hydrozincite $\text{Zn}_5(\text{CO}_3)_2(\text{OH})_6$ . Zinc hydroxycarbonate .....   | 63 |
| 6.6.5  | Zincian clays. Sauconite $\text{Na}_{0.3}(\text{Zn},\text{Mg})_3(\text{Si},\text{Al})_4\text{O}_{10}(\text{OH})_2 \cdot 4\text{H}_2\text{O}$ .....   | 63 |
| 6.6.6  | Rare secondary zinc minerals<br>Rosasite $(\text{Zn},\text{Cu})_2(\text{CO}_3)_2(\text{OH})_2$ . Aurichalcite $(\text{Zn},\text{Cu})_5(\text{CO}_3)_2(\text{OH})_6$ . Zinc copper hydroxycarbonates<br>Adamite $\text{Zn}_2\text{AsO}_4\text{OH}$ . Zinc hydroxyarsenate. Willemite $\text{Zn}_2\text{SiO}_4$ . Zinc silicate .....  | 63 |
| 6.7    | Nickel .....   | 68 |
| 6.7.1  | Garnierite $\text{Ni},\text{Mg}$ hydrosilicate (variable formula)<br>Gaspeite $(\text{Ni},\text{Mg},\text{Fe})\text{CO}_3$ . "Nickel" carbonate.<br>Annabergite $\text{Ni}_3(\text{AsO}_4)_2 \cdot \text{H}_2\text{O}$ . Hydrated nickel arsenate. ....  | 68 |

|          |   |            |
|----------|---|------------|
| 6.8      | Arsenic .....   | 68         |
| 6.8.1    | General aspects including scorodite $\text{Fe}^{3+}\text{AsO}_4 \cdot \text{H}_2\text{O}$ . Hydrated iron arsenate .....  | 68         |
| 6.9      | The ochres<br>Stibiconite $\text{Sb}_3\text{O}_6(\text{OH})$ . Antimony oxyhydroxide.<br>Bismuth ochre $\text{Bi}_2\text{O}_3$ ( $\pm$ impurities). Bismuth oxide.<br>Molybdic ochre $\text{Fe}_2(\text{MO}_4) \cdot n\text{H}_2\text{O}$ . Hydrated iron molybdate.<br>Tungstic ochre $\text{WO}_3 \cdot \text{H}_2\text{O}$ . Hydrated tungsten oxide (poorly defined composition). ..... | 71         |
| 6.10     | Secondary silver minerals .....   | 71         |
|          | Cerargyrite $\text{AgCl}$ . Silver chloride, and rare halides   |            |
| 6.11     | Uranium secondary minerals .....  | 74         |
| 6.11.1   | General aspects .....   | 74         |
| 6.11.2   | Uranium minerals .....  | 75         |
| <b>7</b> | <b>Boxworks and related features .....</b>  | <b>77</b>  |
| 7.1      | Introduction .....  | 77         |
| 7.2      | Development of cellular structures in leached outcrops .....  | 77         |
| 7.2.1    | Styles of ribbing .....   | 78         |
| 7.2.2    | The site of rib development .....   | 79         |
| 7.3      | Minerals .....  | 79         |
| 7.3.1    | Pyrite .....  | 79         |
| 7.3.2    | Pyrrhotite .....  | 85         |
| 7.3.3    | Chalcopyrite .....  | 85         |
| 7.3.4    | Sphalerite .....  | 87         |
| 7.3.5    | Galena .....  | 92         |
| 7.3.6    | Pentlandite/pyrrhotite (sulphide nickel assemblage) .....   | 95         |
| 7.3.7    | Arsenopyrite .....  | 97         |
| 7.3.8    | Carbonates .....  | 97         |
| 7.3.9    | Garnets .....   | 100        |
| 7.3.10   | Chalcocite .....  | 100        |
| 7.3.11   | Miscellaneous mineral boxworks/pseudomorphs and comments<br>(Molybdenite, cobaltite, fluorite, bornite, and magnetite) .....  | 102        |
| 7.4      | False gossan and related observations .....   | 104        |
| <b>8</b> | <b>Leached cappings in porphyry copper systems .....</b>  | <b>107</b> |
| 8.1      | General aspects .....   | 107        |
| 8.2      | Crackle/stockwork recognition .....   | 108        |
| 8.3      | Sulphide oxidation and supergene enrichment .....   | 113        |
| 8.4      | Field assessment of leached cappings .....  | 113        |
| 8.5      | Summary of procedures and examples .....  | 119        |
| 8.6      | Oxidised copper ores (“oxide zones”) .....  | 126        |
| <b>9</b> | <b>Concluding comments .....</b>  | <b>139</b> |
|          | <b>References .....</b>   | <b>141</b> |
|          | <b>Index .....</b>  | <b>143</b> |



# LIST OF FIGURES

## □ THEORETICAL PERSPECTIVES

|          |  |   |
|----------|--|---|
| Fig. 2.1 | General profile of oxidising ore. ....   | 6 |
| Fig. 2.2 | Simplified representation of oxidation profile (A) and general Eh/pH environment. .... | 8 |

## □ TYPES OF LEACHED CAPPINGS AND GOSSANOUS EXPOSURES

|           |   |    |
|-----------|---|----|
| Fig. 3.1  | Arroyo Amirillo, Sonora, Mexico. Limonite dominant ± clay, secondary minerals – conspicuous. ....   | 12 |
| Fig. 3.2  | Batacosa, Sonora Mexico. Limonite dominant ± clay, secondary minerals – conspicuous. ....   | 12 |
| Fig. 3.3  | Tabisco, Sonora, Mexico. Limonite dominant ± clay, secondary minerals – conspicuous. ....   | 12 |
| Fig. 3.4  | Yanque, Peru. Limonite dominant ± secondary minerals – conspicuous. ....  | 13 |
| Fig. 3.5  | Yanque, Peru. Limonite dominant ± clay, secondary minerals – conspicuous. ....  | 13 |
| Fig. 3.6  | Jabil, Yemen. Limonite dominant ± secondary minerals – conspicuous. ....  | 13 |
| Fig. 3.7  | Accha, Peru. Limonite dominant ± secondary minerals – conspicuous. ....   | 14 |
| Fig. 3.8  | Accha, Peru. Limonite dominant ± secondary minerals – conspicuous. ....   | 14 |
| Fig. 3.9  | Augouran, Iran. Limonite dominant ± secondary minerals – conspicuous. ....  | 14 |
| Fig. 3.10 | Trek prospect, British Columbia, Canada. Limonite dominant – conspicuous. ....  | 15 |
| Fig. 3.11 | McArthur River (H.Y.C.) Queensland, Australia.<br>Limonite dominant ± secondary minerals – conspicuous. ....                                      | 15 |
| Fig. 3.12 | McArthur River (H.Y.C.) Queensland, Australia.<br>Limonite dominant ± secondary minerals – conspicuous. ....                                      | 15 |
| Fig. 3.13 | Melon Patch prospect, Western Australia, Australia. Limonite dominant, inconspicuous. ....  | 16 |
| Fig. 3.14 | Jaguey, Sonora, Mexico. Limonite dominant with significant clay – conspicuous. ....   | 16 |
| Fig. 3.15 | Escondida Norte, Chile. Clay dominant ± limonite – conspicuous. ....  | 16 |
| Fig. 3.16 | Kerta district, West Java, Indonesia. Quartz dominant – hidden. ....  | 17 |
| Fig. 3.17 | Kerta district, West Java, Indonesia. Quartz dominant – hidden. ....  | 17 |
| Fig. 3.18 | Kerta district, West Java, Indonesia. Quartz – newly exposed. ....  | 17 |
| Fig. 3.19 | Kerta district, West Java, Indonesia. Quartz dominant – hidden. ....  | 18 |
| Fig. 3.20 | Pierena, Peru. Quartz dominant – conspicuous. ....  | 18 |
| Fig. 3.21 | Pierena, Peru. Quartz dominant – conspicuous. ....  | 18 |
| Fig. 3.22 | Mt Carlton-Silver Hills, Queensland, Australia.<br>Quartz dominant, minor limonite – concealed inconspicuous. ....                                | 19 |
| Fig. 3.23 | Mt Carlton-Silver Hills, Queensland, Australia.<br>Quartz dominant, minor limonite – concealed inconspicuous. ....                                | 19 |
| Fig. 3.24 | Mt Carlton-Herbert Creek East, Queensland, Australia.<br>Quartz dominant ± limonite ± secondary minerals – limited exposure – inconspicuous. .... | 19 |
| Fig. 3.25 | Oyu Tolgoi, Mongolia.<br>Clay dominant ± minor limonite ± secondary minerals – limited exposure – inconspicuous. ....                             | 20 |
| Fig. 3.26 | Oyu Tolgoi, Mongolia.<br>Clay dominant ± minor limonite ± secondary minerals – limited exposure – inconspicuous. ....                             | 20 |
| Fig. 3.27 | Century, Queensland, Australia.<br>Inconspicuous with no obvious limonite, clay, or secondary minerals. ....                                      | 20 |

## □ LIMONITE TERMINOLOGY

|          |   |    |
|----------|---|----|
| Fig. 4.1 | Mt Isa district, Queensland, Australia. Indigenous and fringing limonite. ....    | 25 |
| Fig. 4.2 | Escondida, Chile. Indigenous – Live limonite. ....                                | 25 |
| Fig. 4.3 | Toquepala, Peru. Indigenous – Live or relief limonite (see also Figure 4.2). .... | 25 |
| Fig. 4.4 | Location unknown. Indigenous limonite. ....                                       | 26 |

|                                       |   |    |
|---------------------------------------|---|----|
| Fig. 4.5                              | Collahuasi, Chile. Exotic or transported limonite. ....   | 26 |
| Fig. 4.6                              | Grasberg, Indonesia. Exotic limonite. ....  | 26 |
| <b>□ LIMONITE TYPES</b>               |   |    |
| Fig. 4.7                              | Location unknown. Botryoidal limonite. ....   | 27 |
| Fig. 4.8                              | Location unknown. Iridescent limonite. ....   | 27 |
| Fig. 4.9                              | Location unknown. Columnar limonite. ....   | 27 |
| <b>□ STRUCTURAL PRESERVATION</b>      |   |    |
| Fig. 5.1                              | Lady Loretta, Queensland, Australia. Structural preservation – layering. ....   | 30 |
| Fig. 5.2                              | Lady Loretta, Queensland, Australia. Structural preservation – layering. ....   | 30 |
| Fig. 5.3                              | Woodlawn-New South Wales, Australia. Structural preservation – layering. ....   | 30 |
| Fig. 5.4                              | Trek prospect, British Columbia, Canada. Structural preservation – breccia, shear fabric. ....  | 31 |
| Fig. 5.5                              | Isobella mine, Queensland, Australia. Structural preservation – breccia. ....   | 31 |
| <b>□ SECONDARY MINERALS</b>           |   |    |
| <b>□ IRON RICH SECONDARY MINERALS</b> |   |    |
| Fig. 6.1                              | Jarosite. ....  | 36 |
| Fig. 6.2                              | Haematite, goethitic limonite and jarosite. ....  | 36 |
| Fig. 6.3                              | Haematite and jarosite. ....  | 36 |
| Fig. 6.4                              | Melanterite. ....   | 37 |
| Fig. 6.5                              | Vivianite. ....   | 37 |
| <b>□ MANGANESE SECONDARY MINERALS</b> |   |    |
| Fig. 6.6                              | “Manganese oxide”. ....   | 39 |
| Fig. 6.7                              | “Manganese oxide”. ....   | 39 |
| <b>□ SECONDARY COPPER MINERALS</b>    |   |    |
| Fig. 6.8                              | Stability relations of some copper minerals at surface conditions and at low $f(\text{CO}_2)$ as a function of Eh and pH (Anderson, 1982). .... | 41 |
| Fig. 6.9                              | Native copper. ....   | 44 |
| Fig. 6.10                             | Native copper. ....   | 44 |
| Fig. 6.11                             | Pitch limonite. ....  | 44 |
| Fig. 6.12                             | Cuprite – tenorite (Copper oxide). ....   | 45 |
| Fig. 6.13                             | Cuprite (Copper oxide). ....  | 45 |
| Fig. 6.14                             | Cuprite (Copper oxide). ....  | 45 |
| Fig. 6.15                             | Chalcotrichite (Copper oxide). ....   | 46 |
| Fig. 6.16                             | Malachite and azurite (Copper carbonates). ....   | 46 |
| Fig. 6.17                             | Malachite (Copper carbonate). ....  | 46 |
| Fig. 6.18                             | Chrysocolla (Hydrated copper silicate). ....  | 50 |
| Fig. 6.19                             | Chrysocolla (Hydrated copper silicate). ....  | 50 |
| Fig. 6.20                             | Chalcanthite (Hydrated copper sulphate). ....   | 50 |
| Fig. 6.21                             | Atacamite (Copper hydroxychloride). ....  | 51 |
| Fig. 6.22                             | Brochantite (Copper hydroxysulphate). ....  | 51 |
| Fig. 6.23                             | Antlerite (Copper hydroxysulphate). ....  | 51 |
| Fig. 6.24                             | Dioptase (Copper hydroxysilicate). ....   | 52 |
| Fig. 6.25                             | Linarite (Hydrated lead copper sulphate). ....  | 52 |
| Fig. 6.26                             | Turquoise (Hydrated copper aluminium phosphate). ....   | 52 |

|           |  |    |
|-----------|--|----|
| Fig. 6.27 | Olivenite (Copper hydroxyarsenate).                        | 53 |
| Fig. 6.28 | Pseudomalachite (Copper hydroxyphosphate).                 | 53 |
| Fig. 6.29 | Chalcosiderite (Hydrated copper iron aluminium phosphate). | 53 |
| Fig. 6.30 | Chalcocite (Copper sulphide).                              | 54 |
| Fig. 6.31 | Chalcocite (Copper sulphide).                              | 54 |
| Fig. 6.32 | Chalcocite and covellite (Copper sulphide).                | 54 |

#### ▣ SECONDARY LEAD MINERALS

|           |   |    |
|-----------|---|----|
| Fig. 6.33 | Cerussite (Lead carbonate).                 | 58 |
| Fig. 6.34 | Cerussite (Lead carbonate).                 | 58 |
| Fig. 6.35 | Cerussite (Lead carbonate).                 | 58 |
| Fig. 6.36 | Anglesite (Lead sulphate).                  | 59 |
| Fig. 6.37 | Anglesite (Lead sulphate).                  | 59 |
| Fig. 6.38 | Galena, anglesite, massicot and minium.     | 59 |
| Fig. 6.39 | Massicot and minium (Lead oxides).          | 60 |
| Fig. 6.40 | Plumbojarosite (Lead iron hydroxysulphate). | 60 |
| Fig. 6.41 | Mimetite (Lead chloroarsenate).             | 60 |
| Fig. 6.42 | Pyromorphite (Lead chlorophosphate).        | 61 |
| Fig. 6.43 | Crocoite (Lead chromate).                   | 61 |
| Fig. 6.44 | Wulfenite (Lead molybdate).                 | 61 |

#### ▣ SECONDARY ZINC MINERALS

|           |  |    |
|-----------|--|----|
| Fig. 6.45 | Smithsonite (Zinc carbonate).                | 65 |
| Fig. 6.46 | Smithsonite (Zinc carbonate).                | 65 |
| Fig. 6.47 | Smithsonite (Zinc carbonate).                | 65 |
| Fig. 6.48 | Hemimorphite (Hydrated zinc silicate).       | 66 |
| Fig. 6.49 | Hydrozincite (Zinc hydroxycarbonate).        | 66 |
| Fig. 6.50 | Adamite (Zinc hydroxyarsenate).              | 66 |
| Fig. 6.51 | Aurichalcite (Zinc copper hydroxycarbonate). | 67 |
| Fig. 6.52 | Rosasite (Copper zinc hydroxycarbonate).     | 67 |
| Fig. 6.53 | Willemite (Zinc silicate).                   | 67 |

#### ▣ SECONDARY NICKEL, ARSENIC, ANTIMONY, MOLYBDENUM, BISMUTH, AND TUNGSTEN MINERALS

|           |  |    |
|-----------|--|----|
| Fig. 6.54 | Gaspeite (Nickel-iron-magnesium carbonate).  | 69 |
| Fig. 6.55 | Annabergite (Hydrated nickel arsenate).  | 69 |
| Fig. 6.56 | Garnierite ("Nickel-magnesium hydrosilicate").   | 69 |
| Fig. 6.57 | Scorodite (Hydrated iron arsenate).  | 70 |
| Fig. 6.58 | Erythrite (Hydrated cobalt arsenate).  | 70 |
| Fig. 6.59 | Cervantite (Stibiconite, Antimonic ochre – antimony oxide).                                      | 70 |
| Fig. 6.60 | Molybdcic ochre (Ferrimolybdite-hydrated iron molybdate).  | 72 |
| Fig. 6.61 | Bismuth ochre (bismuth oxide ± impurities).  | 72 |
| Fig. 6.62 | Tungstic ochre (Tungstic oxides ± impurities – also referred to as Tungstite or Ferritungstite). | 72 |

#### ▣ SECONDARY SILVER AND URANIUM MINERALS

|           |  |    |
|-----------|--|----|
| Fig. 6.63 | Cerargyrite (Horn silver-silver chloride).                     | 73 |
| Fig. 6.64 | Silver (Native silver).  | 73 |
| Fig. 6.65 | Carnotite (Hydrated potassium uranylvanadate).                 | 73 |
| Fig. 6.66 | Torbernite – Metatorbernite (Hydrated copper uranylphosphate). | 76 |

|           |  |    |
|-----------|--|----|
| Fig. 6.67 | Tyuyamunite – Carnotite and Uranospinite – Metauranospinite (Hydrated potassium and calcium uranylvanadate, plus hydrated calcium uranylarsenate). . . . . | 76 |
| Fig. 6.68 | Uranospinite – Metauranospirite (Hydrated uranylarsenate). . . . .   | 76 |

## □ BOXWORKS AND RELATED FEATURES

### □ PYRITE – BOXWORKS, PSEUDOMORPHS

|           |  |    |
|-----------|--|----|
| Fig. 7.1  | Pathways producing boxworks, in situ granular clusters, positive and negative pseudomorphs. . . . .            | 78 |
| Fig. 7.2  | Pyrite dominant leached capping and gossan. . . . .  | 81 |
| Fig. 7.3  | Pyrite – negative pseudomorphs. . . . .  | 81 |
| Fig. 7.4  | Pyrite – pseudomorphs. . . . .   | 81 |
| Fig. 7.5  | Photomicrographs of selected pyrite cellular developments. . . . .   | 82 |
| Fig. 7.6  | Negative ovoid cellular pyrite pseudomorphs in a quartz vein (with remnant pyrite – see Figure 7.5 A). . . . . | 82 |
| Fig. 7.7  | Pyrite gossan, cellular boxwork. . . . .   | 83 |
| Fig. 7.8  | Pyrite leached capping – gossan, cellular boxwork. . . . .   | 83 |
| Fig. 7.9  | Pyrite cellular sponge. . . . .  | 83 |
| Fig. 7.10 | Pyrite – cellular sponge boxwork. . . . .  | 84 |
| Fig. 7.11 | Pyrite – rectangular boxwork. . . . .  | 84 |
| Fig. 7.12 | Pyrite – remnant boxwork? . . . . .  | 84 |

### □ PYRRHOTITE SPONGES

|           |                                     |    |
|-----------|-------------------------------------|----|
| Fig. 7.13 | Pyrrhotite cellular sponge. . . . . | 86 |
| Fig. 7.14 | Pyrrhotite cellular sponge. . . . . | 86 |
| Fig. 7.15 | Pyrrhotite cellular sponge. . . . . | 86 |

### □ CHALCOPYRITE BOXWORKS

|           |                               |    |
|-----------|-------------------------------|----|
| Fig. 7.16 | Chalcopyrite boxwork. . . . . | 87 |
|-----------|-------------------------------|----|

### □ SPHALERITE BOXWORKS

|           |                                   |    |
|-----------|-----------------------------------|----|
| Fig. 7.17 | Sphalerite dissolution. . . . .   | 89 |
| Fig. 7.18 | Sphalerite replacement 1. . . . . | 89 |
| Fig. 7.19 | Sphalerite replacement 2. . . . . | 89 |
| Fig. 7.20 | Sphalerite boxwork. . . . .       | 90 |
| Fig. 7.21 | Sphalerite boxwork. . . . .       | 90 |
| Fig. 7.22 | Sphalerite boxwork. . . . .       | 90 |
| Fig. 7.23 | Sphalerite boxwork. . . . .       | 91 |
| Fig. 7.24 | Sphalerite boxwork? . . . . .     | 91 |

### □ LEAD GOSSANS – LEACHED CAPPINGS

|           |   |    |
|-----------|---|----|
| Fig. 7.25 | Galena-cerussite-massicot. . . . .            | 93 |
| Fig. 7.26 | Galena-cerussite-massicot-minium. . . . .     | 93 |
| Fig. 7.27 | Galena “gossan” – Surface expression. . . . . | 93 |
| Fig. 7.28 | Galena boxwork. . . . .                       | 94 |
| Fig. 7.29 | Galena boxwork. . . . .                       | 94 |
| Fig. 7.30 | Galena boxwork. . . . .                       | 94 |

### □ PENTLANDITE – PYRRHOTITE – NICKEL SULPHIDE ORES

|           |   |    |
|-----------|---|----|
| Fig. 7.31 | Nickel sulphide “gossan-ironstone”. . . . . | 96 |
| Fig. 7.32 | Nickel sulphide “gossan-ironstone”. . . . . | 96 |

|   |  |     |
|---|--|-----|
| Fig. 7.33   | Nickel sulphide “gossan-ironstone”   | 96  |
| Fig. 7.34   | Arsenopyrite fracture pattern  | 98  |
| Fig. 7.35   | Arsenopyrite – scorodite   | 98  |
| Fig. 7.36   | Arsenopyrite – scorodite boxwork   | 98  |
| <b>■ CARBONATE BOXWORKS</b>                                       |  |     |
| Fig. 7.37   | Siderite (carbonate) boxwork   | 99  |
| Fig. 7.38   | Siderite (carbonate) boxwork   | 99  |
| Fig. 7.39   | Carbonate boxwork  | 99  |
| <b>■ GARNET BOXWORKS AND PSEUDOMORPHS</b>                         |  |     |
| Fig. 7.40   | Garnet boxwork   | 101 |
| Fig. 7.41   | Garnet boxwork   | 101 |
| Fig. 7.42   | Garnet boxwork/pseudomorphs  | 101 |
| <b>■ MISCELLANEOUS BOXWORKS AND PSEUDOMORPHS</b>                  |  |     |
| <b>■ CHALCOCITE, COBALTITE, AND MOLYBDENITE</b>                   |  |     |
| Fig. 7.43   | Chalcocite   | 103 |
| Fig. 7.44   | Cobaltite  | 103 |
| Fig. 7.45   | Molybdenite  | 103 |
| <b>■ FALSE GOSSAN AND WEATHERING OF HOST ROCKS</b>                |  |     |
| Fig. 7.46   | False gossan – Serpentinite  | 105 |
| Fig. 7.47   | False gossan – Century mine area, Queensland, Australia  | 106 |
| Fig. 7.48   | False gossan – Olivine gabbro  | 106 |
| <b>■ PORPHYRY COPPER LEACHED CAPPINGS – HAEMATITE</b>             |  |     |
| Fig. 8.1  | Leached capping profile. Caujone porphyry copper, Peru   | 109 |
| Fig. 8.2  | Leached capping profile. Santa Rita porphyry copper, New Mexico, USA   | 109 |
| Fig. 8.3  | Leached capping profile. Ray porphyry copper, Arizona, USA   | 109 |
| Fig. 8.4  | Leached capping profile. Morenci porphyry copper, Arizona, USA   | 110 |
| Fig. 8.5  | Leached capping. San Manuel porphyry copper, Arizona, USA  | 110 |
| Fig. 8.6  | Leached capping. Morenci porphyry copper, Arizona, USA   | 110 |
| <b>■ PORPHYRY COPPER LEACHED CAPPINGS – “COPPER OXIDE ZONES”</b>  |  |     |
| Fig. 8.7  | Leached capping – oxidised copper style. El Abra porphyry copper, Chile  | 111 |
| Fig. 8.8  | Leached capping – oxidised copper style. Ray porphyry copper, Arizona, USA   | 111 |
| Fig. 8.9  | Leached capping – oxidised copper style. Escondida porphyry copper, Chile  | 111 |
| <b>■ PORPHYRY COPPER LEACHED CAPPINGS – JAROSITE AND GOETHITE</b> |  |     |
| Fig. 8.10   | Leached capping – jarositic ± minor goethite. Alumbrera porphyry copper, Argentina   | 112 |
| Fig. 8.11   | Leached capping – goethite/jarosite. Ujina, Chile  | 112 |
| <b>■ SUPERGENE ENRICHMENT</b>                                     |  |     |
| Fig. 8.12   | Supergene enrichment – polished sections   | 112 |
| <b>■ FIELD ASSESSMENT OF LEACHED CAPPINGS</b>                     |  |     |
| Fig. 8.13   | Graphic representation of logarithmic scale correlations between limonite mineralogy and original pyrite/chalcocite ratios in rocks prior to oxidation for non reactive gangue (argillic, advanced argillic, and phyllic alteration)(from Alpers and Brimhall, 1989) | 117 |

|   |   |     |
|---|---|-----|
| Fig. 8.14                                     | Model illustrating theoretical vertical zoning of supergene zoning effects shown overprinting on laterally zoned features of hypogene alteration and mineralogy of a cross section from an intrusive thermal centre into distal wall rocks (derived from Titley, 1995). | 118 |
| Fig. 8.15                                     | Limonite colours in relation to haematite – goethite – jarosite proportions.  | 119 |
| Fig. 8.16                                     | Escondida Norte, Chile. Crackle disseminated texture.   | 121 |
| Fig. 8.17                                     | Toquepala, Peru. Crackle disseminated texture.  | 121 |
| Fig. 8.18                                     | Toquepala, Peru. Crackle disseminated texture.  | 121 |
| Fig. 8.19                                     | Haematite dominant capping – after chalcocite.  | 122 |
| Fig. 8.20                                     | Haematite dominant capping – after chalcocite.  | 122 |
| Fig. 8.21                                     | Haematite dominant capping – after chalcocite.  | 122 |
| Fig. 8.22                                     | Goethite dominant leached capping.  | 123 |
| Fig. 8.23                                     | Goethite dominant leached capping.  | 123 |
| Fig. 8.24                                     | Goethite dominant leached capping.  | 123 |
| Fig. 8.25                                     | Jarosite dominant leached capping.  | 124 |
| Fig. 8.26                                     | Jarosite dominant leached capping.  | 124 |
| Fig. 8.27                                     | Jarosite dominant leached capping.  | 124 |
| Fig. 8.28                                     | Interpreted distribution and abundance of chalcocite in surface rocks prior to leaching with superimposed perimeter of underlying chalcocite ore. La Caridad, Sonora, Mexico (Saegart et al, 1974).   | 125 |
| Fig. 8.29                                     | Map showing leached capping of chalcocite and chalcopyrite derived limonite. Escondida, Chile (Ortiz, 1995).  | 125 |
| <b>■ OXIDISED COPPER ORES (“OXIDE ZONES”)</b> |   |     |
| Fig. 8.30                                     | Copper “oxide” zone in fault structure in tropical terrain.   | 129 |
| Fig. 8.31                                     | Major development of “Black oxide” – named from the extensive development of manganese oxides.  | 130 |
| Fig. 8.32                                     | Exotic copper oxide.  | 130 |
| Fig. 8.33                                     | Exotic copper oxide.  | 130 |
| Fig. 8.34                                     | Brochantite (Copper hydroxysulphate).   | 131 |
| Fig. 8.35                                     | Chrysocolla (Hydrated copper silicate).   | 131 |
| Fig. 8.36                                     | Atacamite (Copper hydroxychloride).   | 131 |
| Fig. 8.37                                     | Antlerite (Copper hydroxysulphate).   | 132 |
| Fig. 8.38                                     | Malachite (Copper carbonate).   | 132 |
| Fig. 8.39                                     | Escondida Norte. Lower supergene region.  | 133 |
| Fig. 8.40                                     | Escondida Norte. Mid to lower supergene region.   | 133 |
| Fig. 8.41                                     | Escondida Norte. Upper supergene region.  | 133 |
| Fig. 8.42                                     | Escondida Norte. Upper supergene region.  | 134 |
| Fig. 8.43                                     | Escondida Norte. Start of oxidised zone.  | 134 |
| Fig. 8.44                                     | Escondida Norte. Oxidised zone.   | 134 |
| Fig. 8.45                                     | Escondida Norte. Surficial region.  | 135 |
| Fig. 8.46                                     | Escondida Norte. Surface rock collected above known chalcocite zone.  | 135 |
| Fig. 8.47                                     | Escondida Norte. Other minerals in the local region. 1. Manganese oxide.  | 135 |
| Fig. 8.48                                     | Escondida Norte. Other minerals in the region. 2. Alunite? (Potassium aluminium hydroxysulphate).   | 136 |
| Fig. 8.49                                     | Oxidation profile at Grasberg Cu-Au mine, Indonesia.  | 136 |
| Fig. 8.50                                     | Grasberg primary ore. DDH 58, 251 m.  | 137 |
| Fig. 8.51                                     | Grasberg DDH 58, 152 m.   | 137 |
| Fig. 8.52                                     | Grasberg DDH 58, 80 m.  | 137 |
| Fig. 8.53                                     | Grasberg DDH 58, 50 m.  | 138 |
| Fig. 8.54                                     | Grasberg DDH 58, 9 m.   | 138 |

This text concentrates upon field observations concerning leached cappings and gossans, occurring as oxidised surface expressions of underlying ore zones.

Although the advent of modern multielement geochemical sampling and easier mechanical excavation assist considerably in subsurface interpretation, there are still many occasions where the first observation and recognition are made by the lone field geologist. New exposures continue to be found in remote and often difficult terrains, where “on the spot” skills are of prime importance.

In general terms the text has been arranged from the broad scale to the specific, and it should be realised that all scales provide valuable input for final interpretation. The topics covered include:

- Theoretical perspectives.
- Initial recognition.
- General field observations.
- Detailed field observations (secondary minerals, boxworks).
- Porphyry copper leached cappings.



This text is aimed at recognition, field procedures and interpretation of gossan-leached outcrops as they appear on the surface; however it is obviously useful for the observer to have a working concept of the factors controlling development.

The origin and nature of gossans / leached cappings have long been of interest to both the practical and scientific communities, and it is now well known that different sets of circumstances will result in different end products.

The gossan / leached capping formation process commences when ore assemblages and their associated wall rocks encounter the interface between the water table and the overlying surficial zone. This is in essence the transition from a reducing to an oxidising environment.

As the ore assemblages transition from the water table to surface via weathering, there are numerous factors which contribute to the final surface exposure.

The influences are a complex, interactive, combination of chemical, physical and kinetic effects (Blain and Andrew, 1977) and a short list of potential major inputs would include:

- The original mineral assemblages.
- The solubility of the individual minerals with respect to their stability fields.
- The acidity/alkalinity (pH) of the local groundwaters.
- Factors relating to oxygen availability and oxidation-potentials (Eh).
- Temperature.
- Factors relating to water availability, including:
  - Seasonal variation in water table levels.
  - Flow rates.
  - Local permeability.
  - Longer term effects relating to gradual climate change.
- Factors relating to tectonic activity including:
  - Uplift
  - Burial (via faulting).
- Factors relating to surficial modification:
  - Lateritisation.
  - Surface layer flooding via the precipitation of various combinations of quartz, iron oxides and carbonates (silcretes, ferricretes – ironstones – jaspers, calcretes).

Assessment of many of these variables is further complicated by uncertainty involving the actual processes involved. Two main lines of thought are current.

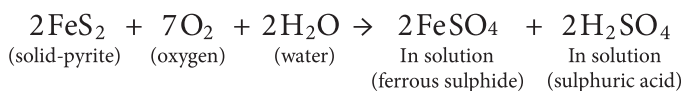
The first considers that as in normal weathering of silicate rocks, hydrolysis type reactions predominate. Near surface groundwaters set up hydrolytic reactions involving

the release and consumption of hydrogen ions and hydroxyl groups. The presence of sulphides results in the generation of sulphuric acid and/or ferric sulphate both of which are powerful oxidising agents.

This process of simple solution and oxidation chemistry to describe the reacting species, has recently (Thornber and Taylor, 1992) been augmented by suggestions that major sulphide orebodies will act as effective electronic conductors, such that the weathering results or is encouraged via electrochemical reactions between the sulphide conductor and the groundwater. This envisages an essentially corrosive process with anodic and cathodic controls (the sulphides represent large assemblages of galvanic cells). Recent studies concerning heap leaching of supergene copper ores have clearly established that sulphide oxidation will occur as an electrochemical process mediated by specific oxidising bacteria (Sillitoe, 2005).

Both mechanisms appear to be valid, with the electrochemical effect possibly being more influential in massive sulphide ore zones?

From a practical standpoint most observers would agree that the production of dilute sulphuric acid derived from the breakdown of pyrite (or less commonly pyrrhotite) is heavily implicated in the oxidation process. The proponents of the simple solution/oxidation process commonly represent the process as:



A leached cap is thus popularly viewed as the product of repeated and sustained immersion of the rocks within a dilute acid bath.

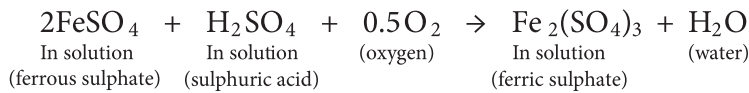
The acid effect is envisaged as taking large volumes of iron into solution which reprecipitates locally as “iron oxides”, and converts local wall rocks into various combinations of pale clays and iron oxides.

If the wall rocks are composed of iron poor aluminosilicates (feldspar dominant) low temperature clay components will probably dominate, with variable amounts of red-brown-orange “iron oxides” occurring as stains and precipitates along permeable zones such as cracks, joints and faults.

Conversely if the wall rocks are dominated by ferromagnesian components (biotite, amphibole, and pyroxene) the end result will be “iron oxide” dominant and distinctly more “rusty” in appearance. The general red/white effect obviously depends on the scale of the system, but within large scale disseminated sulphide stockwork and/or breccia systems can be at kilometre proportions.

Given that pyrite is by far the most abundant sulphide it is not surprisingly that leached outcrops are extremely common. In uncomplicated terms pyrite (or pyrrhotite) oxidation is the driving force and the resulting acid groundwater component is the dominant factor.

The pyritic system also generates a second major oxidising component in the form of ferric sulphate, which in combination with this acid is capable of effecting considerable sulphide dissolution to create metal sulphates in solution.



The materials taken into solution within the oxidising zone are available to form new compounds given favourable circumstances. In most cases these processes occur in, or closely adjacent to the original site of the leached capping. However, in other cases various elements may distribute quite widely via the local hydraulic systems.

The most conspicuous and widespread products are the “iron oxides” and “clay minerals” although dark “manganese oxides” often reach substantive proportions. (Most iron rich minerals contain manganese, easily released via oxidation).

Involvement of carbon dioxide via dissolution of carbonate or atmospheric contributions may result in new carbonates, and depending upon the original assemblages and local groundwater chemistry a wide range of oxides-hydroxides, silicates, sulphates, phosphates, chlorides and even vanadates may eventuate.

These new minerals are termed secondary minerals, and form either via direct precipitation (infill) or replacement (alteration). Metalliferous secondary minerals provide valuable clues concerning the underlying primary ore, although it should also be noted that a proportion of the released metal budget will also occur in trace amounts via complex absorption processes within both the “iron and manganese oxide” accumulations.

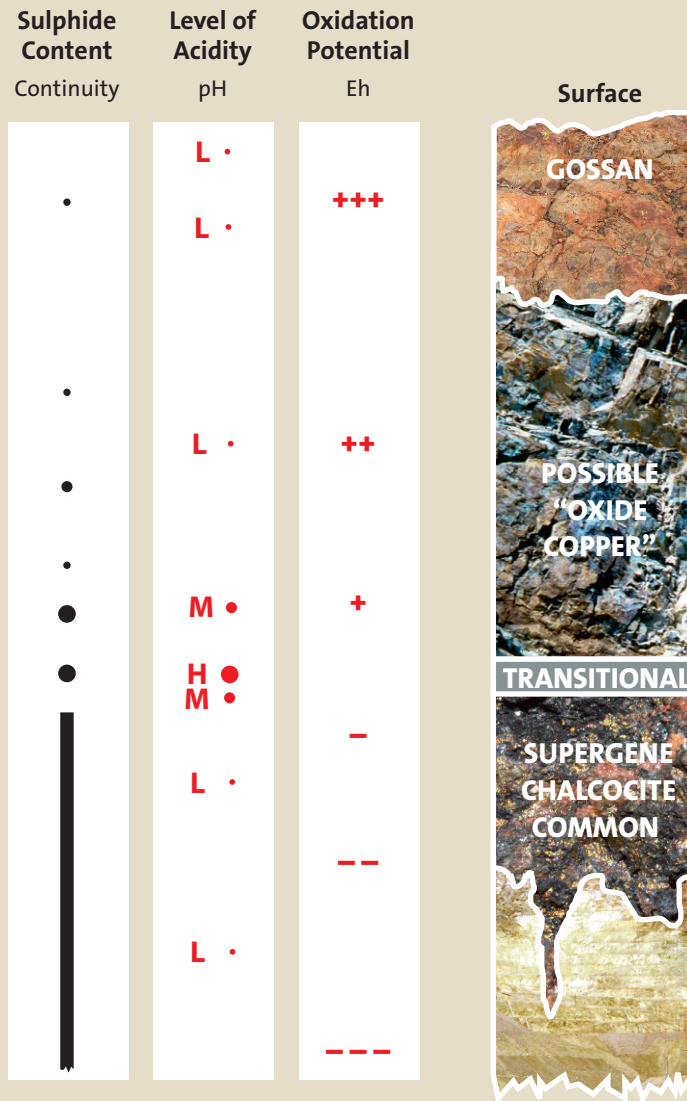
Leached cap development can also be influenced by processes operating just below the water table, where metal rich solutions percolating downwards from the oxidising region replace pre-existing sulphides (alteration) as conditions change from relatively acidic to relatively alkaline and oxygen potential reduces.

This process (supergene modification) is extremely common in copper assemblages, where supergene chalcocite±covellite replaces a wide range of primary sulphides resulting in a zone of enhanced copper values (supergene enrichment). A similar process occurs in sulphide nickel ores, where violerite±pyrite replaces pentlandite and pyrrhotite (Nickel et al, 1974 and Nickel et al, 1977).

Suggestions of supergene silver enrichment are common in the literature, but one of the prime examples has recently been questioned (Sillitoe, 2007, 2009).

From a leached cap point of view, supergene modification is of interest, as the mineral assemblage emerging into the oxidation zone has already been changed from the pristine (hypogene) condition.

The major features concerning the profile/development of an oxidising sulphide orebody are simplistically represented in [Figures 2.1](#) and [2.2](#)



• Low      L •      + Positive  
 • Moderate    M •      - Negative  
 • High      H •

**ZONE 1**

Surficial – leached capping zone. Total leaching.

**ZONE 2**

Major leaching – remnant sulphides may begin to become visible at lower depths.

Possible zone of major formation of metalliferous secondary minerals.

**WATER TABLE**

**ZONE 3**

Area of potential supergene sulphide formation. (Especially in copper systems).

**ZONE 4**

Primary (hypogene) ore assemblage. (Fresh sulphides).

Fig. 2.1 General profile of oxidising ore.

### ZONE 1

General character and points of interest.

- Widespread precipitation/alteration products forming surficial insoluble compounds – variable proportions of iron oxides/hydroxides, clay minerals, manganese oxides and silica.
- Textural preservation of major structural features is common (breccia, etc.) unless overprinted – flooded by late stage surficial products (ferricrete, silcrete, etc).
- Quartz veining preserved, – possible sulphide replicas/boxworks.
- Rare metalliferous secondary minerals.
- Quartz veining may encase/protect some small or original sulphides.

### ZONE 2

General character and points of interest.

- Similar to Zone 1, but with slightly less iron oxides/hydroxides, and increasing prospects of locating some partially oxidised sulphides with depth.
- In appropriate conditions secondary metalliferous minerals reach maximum concentrations in this zone, e.g. – “copper oxide” zones.
- Opportunity to observe transition zone at the water table/Zone 3 interface.
- Early stages of boxwork development often visible.

### WATER TABLE

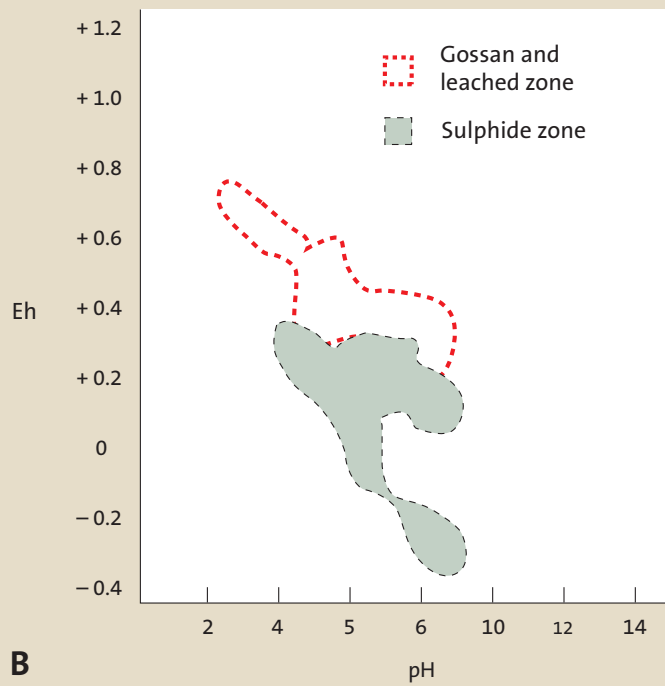
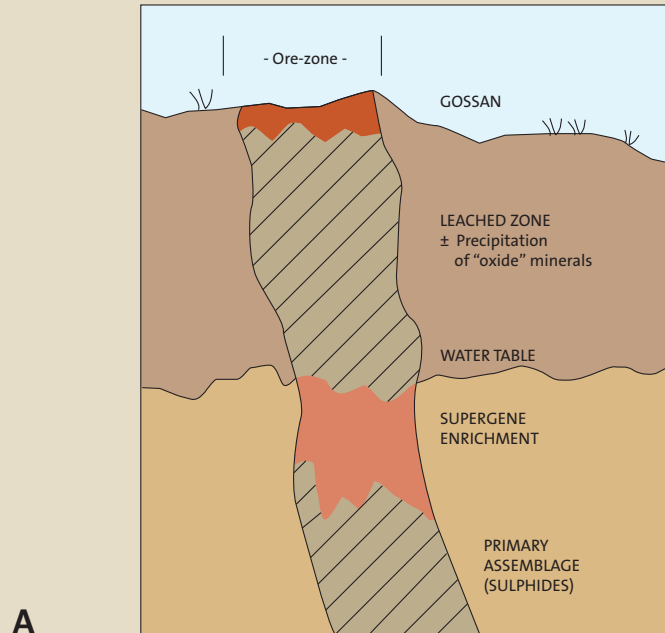
### ZONE 3

- Supergene enrichment (if present) ranges from moderate (immature) to major (mature).
- Primary sulphides usually present in lower regions.

### ZONE 4

- Primary ore textures – opportunity to see original textures.

Fig. 2.2 Simplified representation of oxidation profile (A) and general Eh/pH environment (B). (Data derived from Blain and Andrew 1977).



### 3.1 General aspects

The oxidation of sulphide rich ores usually results in conspicuous “rusty looking” exposures of red iron oxides which are variably referred to as gossans, leached cappings or ironstones. Gossan is the entrenched term, although given that there are also clay and quartz rich examples, leached cappings may be a better all embracing term.

Given a modicum of experience and good exposure it takes little expertise to recognise the leached-iron stained exposures. Suspicions are further aroused by the presence of a few secondary minerals (such as green copper products) and the frequent occurrence of vegetation reduction (kill zones) in response to acid groundwaters and toxic metalliferous input. Thus an occurrence of one or more of the following will promote further examination:

- Conspicuous concentrations of limonite (red-brown-orange iron oxides, [Figures 3.1–3.14](#)).
- Conspicuous occurrence of metalliferous secondary minerals ([Figures 3.5, 3.8, 3.12, 3.22, 3.26](#)).
- Conspicuous concentrations of quartz ( $\pm$  iron oxides), either in the form of alteration (vuggy silica of high sulphidation origin) or as obvious quartz veining. The latter survive to form boulders/fragments within residual soil cover ([Figures 3.15–3.24](#)).
- Occurrence of any of the above within local drainage systems. NB. Deep erosion may even contribute deeper profile materials, such as supergene enriched or primary sulphides.

Although early prospectors and modern geological exploration have located many of the early noticed gossanous exposures, it remains clear that there is still ample scope for new discoveries and/or reinterpretation of known exposures. Many new discoveries are well exposed as gossans/leached cappings. The twin porphyry copper occurrences of Escondida, and Escondida Norte (Chile) and the sulphide nickel occurrence at Voisey Bay (Canada) are good examples of very large unrecognised leached cappings.

There are many reasons why leached cappings remain unnoticed or only partially investigated. These include combinations of physical, technical, and sociological factors.

### 3.2 Physical factors

#### 3.2.1 Remoteness (limiting movement)

- Remote locations, with physically hostile conditions and limited population density ([Figures 3.10, 3.15, 3.25, 3.26](#)).

### 3.2.2 Concealment (limiting exposure)

- Major vegetation cover (Figures 3.17–3.19).
- Major shallow colluvium/eluvium as an erosional cover (Figures 3.25, 3.26).
- Major mature erosional surfaces with subdued topography ± development of surficial concealment overprints (laterite, silcrete, ferricrete, Figure 3.12).

## 3.3 Technical (advancing knowledge)

### 3.3.1 Changing concepts (geological reassessment)

- Development of new mineralisation models requiring re-evaluation of known mineral fields and greenfields prospecting (Figures 3.20–3.21)

### 3.3.2 New technology (scientific and technological evolution)

- Evolving geophysical/geochemical exploration techniques – linked to changing concepts.
- Metallurgical and improved mining techniques – linked to changing concepts (Figures 3.20–3.24).
- Presence of leached outcrops with unconventional expressions (e.g. low iron, Figures 3.23, 3.17).

## 3.4 Sociological (people factors)

### 3.4.1 Access and risk barriers

- New opportunities to explore with modern exploration techniques due to lowering of international access barriers, often combined with enticing changes of mining legislation, (Figures 3.25–3.26).

### 3.4.2 Other opportunities

- New access into areas where the local population is not attuned to mineral exploration – resulting in only minor prior exploration (Figures 3.16–3.21)

The continuing contribution via the presence of leached cappings towards exploration and ore discovery can be further appreciated via a short list of relevant mine developments over the last 13–14 years. It is stressed that this is indeed a short list, and many more examples could be included (Table 1).

**Table 1.1** A selection of recent discoveries where surficial leached cappings provided valuable clues to ultimate ore locations (1996–2009).

|   |  |
|---|--|
| 1966.<br>Kambalda, Australia<br>(Sulphide nickel).  | Initially located via a gossanous zone with nickel secondary minerals (gaspeite) in a well prospected gold field in Western Australia. First indication of a major nickel province. Sulphide nickel. Factors involved – changing geological concepts.  |
| 1981.<br>La Escondida, Chile<br>(Porphyry copper system – copper).  | Targeted province. Selected for drilling on the basis of extensive leached capping. Supergene enriched zone, below is well outlined by leached capping mineralogy. Escondida Norte subsequently located nearby (Figure 3.15). Factors involved – evolving geological concepts and changes in access – legislative regimes.   |
| 1983.<br>Pajingo, Australia<br>(Epithermal system – low sulphidation – gold).                                       | Target area selected by a single geologist, revealed a prominent quartz vein with bonanza gold values. The deposit (low sulphidation) system is located on the fringes of a well prospected goldfield – Charters Towers, Queensland. Factors involved – application of evolving geological concepts, applied to known mineral field.   |
| 1990.<br>Century, Australia<br>(stratabound, lead-zinc).  | Leached cap not recognised, due to low iron sphalerite. Discovered by “chance” drill hole aimed at different targets. Major stratabound lead-zinc deposit (Queensland). Factors involved – assessment of known mineralised area. New style of leached cap recognised retrospectively (Figure 3.27).  |
| 1993.<br>Voisey’s Bay, Canada<br>(sulphide nickel).   | Major gossan noted from helicopter reconnaissance trip. Sulphide nickel (Labrador) factors involved – prospecting in remote/hostile terrain.   |
| 1994.<br>Gosowong, Indonesia<br>(epithermal system – low sulphidation – gold).                                      | Targeted area, revealed stream exposures of gold bearing quartz veins. Epithermal system (Halmahera). Factors involved – favourable legislative regimes, improved geological concepts, heavily forested difficult terrain.   |
| 1996.<br>Oyu Tolgoi (Turquoise Hill)<br>(Porphyry copper and high sulphidation “epithermal” system – copper, gold). | Minor old working in Gobi desert. Scattered minor exposures interpreted as porphyry copper leached capping. Initial follows up located a high sulphidation zone. The major porphyry system (gold copper) was located many years later. Factors involved – favourable legislative regime, remote area, emerging geological concepts, exploration persistence with improved geological input (Figures 3.25– 3.26). |
| 1997.<br>Martabe, Indonesia<br>(Epithermal system high sulphidation – gold).  | Selected area, geochemical follow up revealed major leached exposures concealed in tropical jungle terrain. High sulphidation Au gold deposit (Sumatra). Factors involved – favourable legislative regime – emerging geological concepts, concealment in tropical vegetation.  |
| 2005.<br>Mt Carlton, Australia.<br>(Epithermal system – high sulphidation – gold).                                  | Targeted area – high grade zone located by discovery of small leached capping zone in light scrub. High sulphidation – AuAg ± Cu deposit (Queensland). Factors involved – reassessment of known area, recognition of unconventional low iron leached capping (Figures 3.22–3.26).  |

**Fig. 3.1** Limonite dominant  $\pm$  clay, secondary minerals – conspicuous.

The prominent limonitic gossan is part of the surface expression of a high sulphidation system, under exploration as a gold, silver, copper, lead and zinc prospect.

**Arroyo Amirillo, Sonora, Mexico.**

Photograph provided by A.P. Rovera.



**Fig. 3.2** Limonite dominant  $\pm$  clay, secondary minerals – conspicuous.

The very conspicuous red limonitic gossan is the surface exposure of a porphyry molybdenum system. Note the negative vegetation anomaly.

**Batacosa, Sonora Mexico.**

Photograph provided by A.P. Rovera.



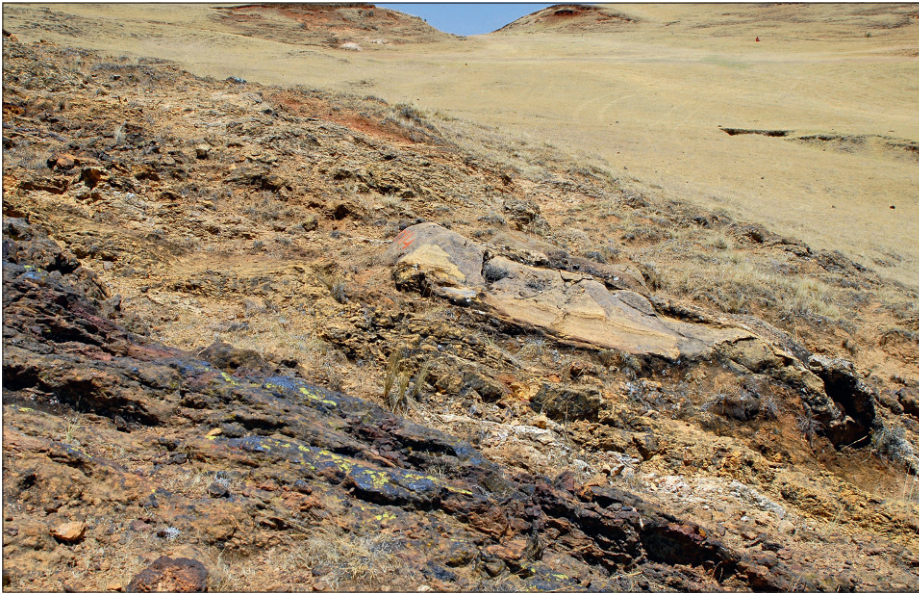
**Fig. 3.3** Limonite dominant  $\pm$  clay, secondary minerals – conspicuous.

Prominent ridge line with red-orange limonitic gossan  $\pm$  white clay. Surface expression of a low sulphidation epithermal gold-silver system.

**Tabisco, Sonora, Mexico.**

Photograph provided by A.P. Rovera.





**Fig. 3.4 Limonite dominant ± secondary minerals – conspicuous.**

Gossan composed of limonite and manganese oxides with significant lead and zinc assay values. The exposure represents the surface expression of a flat lying completely oxidised carbonate replacement style of lead zinc orebody. The zinc values relate to combinations of zinc carbonate (smithsonite) zinc silicate (hemimorphite) and zinc smectite (sauconite). The ore type is referred to as zinc-oxide or non sulphide zinc. (Hitzman et al 2003).

**Yanque, Peru.**  
Photograph provided by M. Boni.



**Fig. 3.5 Limonite dominant ± clay, secondary minerals – conspicuous.**

Close up of oxidising galena network with white lead carbonate (cerussite). Note general pale (goethite) colour of the exposure, possibly reflecting the carbonate source rock.

**Yanque, Peru.**  
Photograph provided by M. Boni.



**Fig. 3.6 Limonite dominant ± secondary minerals – conspicuous.**

Gossan composed of goethite (yellow-orange) manganese hydroxides (dark) zinc carbonate (smithsonite) and zinc silicate (hemimorphite). The materials represent oxidation of a Mississippi Valley style deposit and are variously referred to as non sulphide zinc ores or zinc-oxide deposits. The knobby texture suggests an original breccias texture?

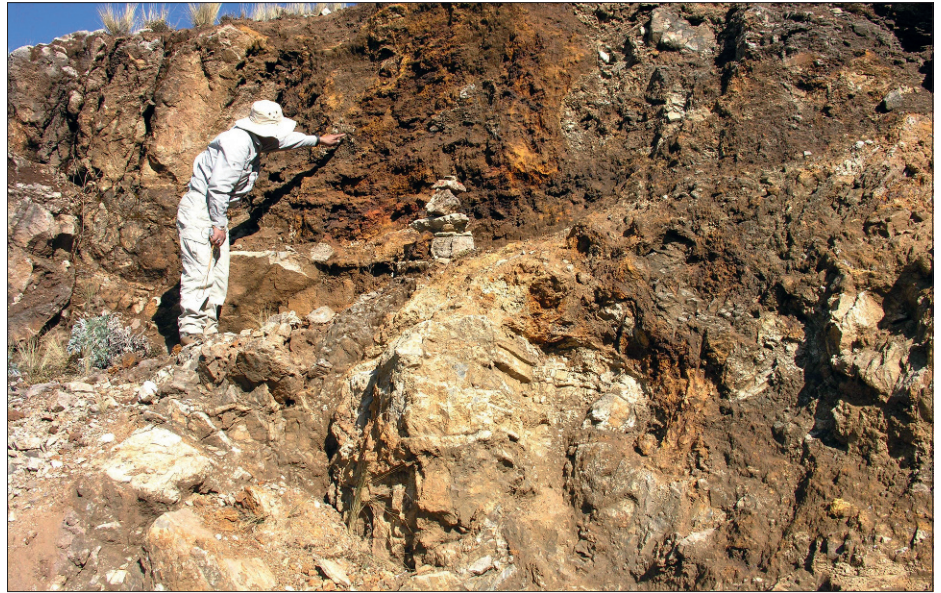
**Jabil, Yemen.**  
Photograph provided by M. Boni.

**Fig. 3.7 Limonite dominated  
± secondary minerals  
– conspicuous.**

A gossan profile composed of mixtures of goethite, haematite and manganese oxides. The Accha deposit is some 30km northeast of Yanque (Figures 3.4-3.5) and is a similar zinc-oxide style ore deposit derived by total oxidation of a carbonate replacement lead-zinc deposit. The ore is composed of zinc carbonate (smithsonite) and zinc silicate (hemimorphite) with minor zinc smectite (sauconite). Boni et al, 2009.

**Accha, Peru.**

Photograph provided by M. Boni.



**Fig. 3.8 Limonite dominated  
± secondary minerals  
– conspicuous.**

Close up of gossan (see Figure 3.7) composed of goethite, haematite and manganese oxides with conspicuous white crusts of zinc oxides (hydrozincite?).

**Accha, Peru.**

Photograph provided by M. Boni.



**Fig. 3.9 Limonite dominated  
± secondary minerals  
– conspicuous.**

Gossan composed of goethite (red), manganese oxides (dark) plus smithsonite/hemimorphite (not visible). The deposit is derived from the oxidation of a Mississippi Valley style lead-zinc occurrence.

**Augouran, Iran.**

Photograph provided by M. Boni.





**Fig. 3.10** Limonite dominated — conspicuous.

Although very visual the gossanous limonitic cliff face was only discovered in 2008. It illustrates that even easily observed gossans can elude observation in remote terrains. The exposure is of a breccia zone and regarded as a copper-gold–silver prospect of porphyry related style.

**Trek prospect, British Columbia, Canada.**

Photograph provided by S. Close.



**Fig. 3.11** Limonite dominated ± secondary minerals — conspicuous.

The linear zone of prominent limonitic material was located around 1955 in remote bushland on McArthur River station. The zone is slightly disturbed via trenching. The field party did not recognise its full importance as a major stratiform lead-zinc deposit despite the presence of hemimorphite (zinc silicate) at surface (Figure 3.12).

**McArthur River (H.Y.C.) Queensland, Australia.**

The deposit was initially named Heres Your Chance (H.Y.C.).



**Fig. 3.12** Limonite dominated ± secondary minerals — conspicuous.

Coarse grained white hemimorphite (zinc silicate) within limonitic gossan from the original surface exposure. The associated rock is oxidised/argillised siltstone and the original sulphide is composed of fine grained stratiform layers of pyrite, sphalerite, and galena. The white mineral was not identified initially and belated recognition of hemimorphite regenerated interest, leading to the discovery of the major zinc occurrence.

**McArthur River (H.Y.C.) Queensland, Australia.**

**Fig. 3.13 Limonite dominated – inconspicuous.**

Limonitic (ironstone) boulders and rubble scattered within spinnifex bushes. The low relief hinders physical vision. This remote small gossanous zone lies within a complex of pyroxenite, olivine gabbro, and troctolite host rocks – all obscured by deep weathering. Sampling yielded values of up to 0.45% nickel, 0.30% copper and 1.08 g/t gold.

**Melon patch prospect, Western Australia, Australia.**

Photograph provided by C.S. Rugless.



**Fig. 3.14 Limonite dominated with significant clay – conspicuous.**

Surface expression with limonitic, siliceous, and clay (white-mid distance) zones, representing a high sulphidation epithermal silver, lead zinc prospect. Note the relatively low relief of the clay rich sector.

**Jaguey, Sonora, Mexico.**

Photograph provided by A.P. Rovera.



**Fig. 3.15 Clay dominated ± limonite – conspicuous.**

The entire hill is a leached capping of a major porphyry copper deposit. The disseminated mineralisation (originally pyrite chalcopyrite and bornite) creates major leach effects causing argillic alteration, with relatively inconspicuous limonite staining. The clay alteration (white) is very noticeable along the vehicle tracks. The disseminated limonite effects are more visible at hand specimen level.

**Escondida Norte, Chile.**





**Fig. 3.16 Quartz dominant – hidden.** The photograph depicts the nature of rainforest terrains which conceal gossans and leached cappings in many regions of South East Asia and South America. This picture is from the Kerta region where low sulphidation gold veins were only recently recognised in the well populated terrain. A similar photograph could be shown for the recent Martabe high sulphidation discovery (Sumatra). In both cases the local populations are focused upon agriculture. Martabe showed up on a regional geochemical stream sediment survey (1997). A similar situation applies to several recent discoveries of iron-oxide copper – gold deposits in the Carajas region of Brazil.

**Kerta district, West Java, Indonesia.**  
Photograph provided by S. Prihatmoko.



**Fig. 3.17 Quartz dominant – hidden.**

Quartz boulders from low sulphidation epithermal veins occurring within a rubber plantation. The main sulphide content has been leached from the surficial material, although remnants may be shielded by quartz. Gold remains unaffected.

**Kerta district, West Java, Indonesia.**

Photograph provided by S. Prihatmoko.



**Fig. 3.18 Quartz – newly exposed.**

Boulders of low sulphidation epithermal quartz revealed via land clearing. Many show classic epithermal banded textures (see [Figure 3.19](#)).

**Kerta district, West Java, Indonesia.**

Photograph provided by S. Prihatmoko.

**Fig. 3.19 Quartz dominant – hidden.**

Surface profile of leached/ weathered quartz vein. Quartz is visible as grey soil coated particles adjacent to the green fern (lower mid section)

Inset illustrates classic epithermal layering within the drill core which is also visible in broken /slabbed surficial samples.

**Kerta district, West Java, Indonesia.**

Length of core 21 cm

See also [Figures 19](#) and [20](#).

Photograph provided by S. Prihatmoko.



**Fig. 3.20 Quartz dominant – conspicuous.**

Remnant occurrences of leached vuggy-silica capping within the Pierena high sulphidation epithermal gold-silver deposit. These remained undetected in the high mountains of north-central Peru, due to a combination of remoteness, political instability, and the geological emergence of a new model for the mineralisation type (see also [Figure 3.21](#)).

**Pierena, Peru.**

Photograph provided by D. Andrews.



**Fig. 3.21 Quartz dominant – conspicuous.**

Typical vuggy-silica at surface. The granular quartz with cavities is an alteration product of focused flow zones formed as part of the ore forming process. It survives at surface  $\pm$  minor limonite staining and insoluble gold grains, and is diagnostic of high sulphidation gold/silver environments.

**Pierena, Peru.**

Photograph provided by D. Andrews.

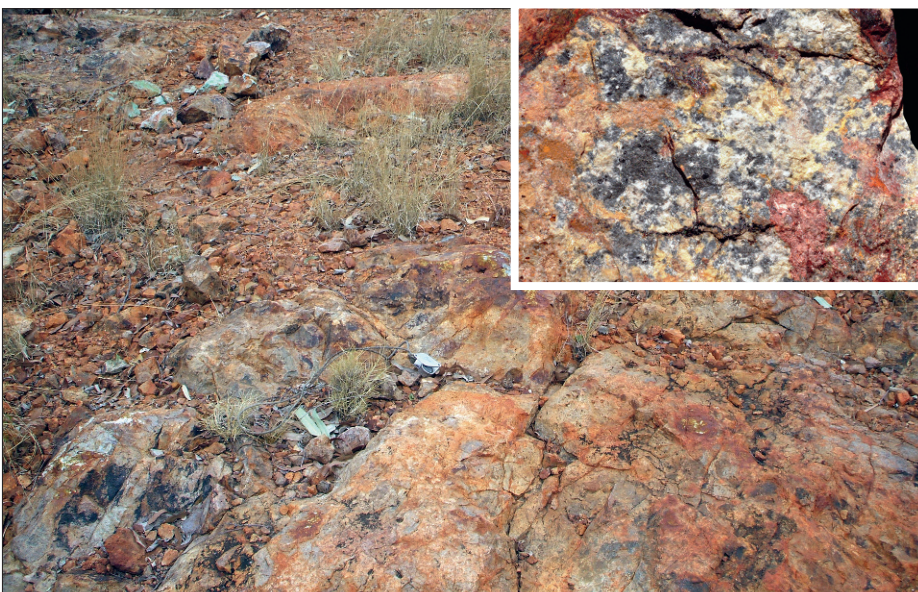




**Fig. 3.22 Quartz dominant, minor limonite – concealed inconspicuous.**  
The photograph illustrates the general nature of the terrain, which contains only one small significant leached capping exposure of the high grade silver – gold high sulphidation deposit. The discovery location lies some 100 metres beyond the dust plume rising from the drill rig to the right of the picture. The area had been previously prospected before the 2005 discovery.  
**Mt Carlton-Silver Hills, Queensland, Australia.**  
Photograph provided by S. Moore.



**Fig. 3.23 Quartz dominant, minor limonite – concealed inconspicuous.**  
The discovery exposure is concealed by low bushes, and can only be described as innocuous.  
The grey siliceous lichen covered rock was located by a senior field hand with prospecting experience – following up an anomalous soil sample. The weight of the sample and suspected fine dark sulphides aroused suspicions. A subsequent assay result yielded very high silver values. Note the problem of locating this exposure in the large area shown in [Figure 3.22](#) above.  
**Mt Carlton-Silver Hills, Queensland, Australia.**



**Fig. 3.24 Quartz dominant ± limonite ± secondary minerals – limited exposure – inconspicuous.**  
This limonitic exposure of silicified fragmental felsic volcanic is the limited surface expression of a low grade high sulphidation epithermal occurrence. Additional clues are provided by rare malachite and scorodite (iron arsenate), together with fine grained sulphides (pyrite enargite) encased in quartz (Inset – Width of frame 7.0 cm). Malachite samples (top left) await collection.  
**Mt Carlton-Herbert Creek East, Queensland, Australia.**

**Fig. 3.25 Clay dominant ± minor limonite ± secondary minerals – limited exposure inconspicuous.**

This photograph illustrates the general terrain and boulder style exposure of the Oyu Tolgoi system in the Gobi desert. A minor ancient surface scratching (Turquoise Hill) containing green copper secondary mineral (mostly malachite) led to further investigation in 1996. The minor copper showing led to the discovery of a high sulphidation copper system, and ultimately to the giant concealed porphyry copper gold deposit.

**Oyu Tolgoi, Mongolia.**



**Fig. 3.26 Clay dominant ± minor limonite ± secondary minerals – limited exposure inconspicuous.**

Malachite stained boulders at surface in the Gobi desert. This occurrence is part of the restricted surface signal, which reflects the giant Oyu Tolgoi porphyry copper-gold system.

**Oyu Tolgoi, Mongolia.**



**Fig. 3.27 Inconspicuous with no obvious limonite, clay, or secondary minerals.**

The giant stratabound zinc deposit was discovered in 1990, within a well prospected area, sporadically explored for around 100 years. The low iron sphalerite occurs in fine grained layer format with no significant pyrite. The weathering produces a completely innocuous surface result, resembling the general silty sediments of the region. The deposit was located via a somewhat inadvertent drill intercept, and the extensive surface exposures were only recognised subsequent to drilling. This picture shows the surface expression of a major ore horizon.

**Century, Queensland, Australia.**

Inset — Ore. Width of frame 6 cm.



## 4.1 Size – shape

The overall size and shape of any leached capping exposure is naturally of interest, and this in turn relates to geological context and anticipated deposit types. Broad scale knowledge of ore deposit styles is obviously an advantage. For instance:

Porphyry copper systems, epithermal lithocaps, and major breccia pipes commonly create kilometre-scale oxidised exposures (commonly with significant white/clay components), (Figures 3.1–3.3, 3.14–3.15, 3.20).

Exhalative-volcanogenic sulphide lenses tend to be exposed at surface as wide rusty iron-rich zones, with significant linear trends.

Dilatational veins and shear zones naturally form narrow linear zones (Figure 3.19) and can commonly be quickly put in contact via local knowledge (within a tin field, within a greenstone gold belt, etc.).

## 4.2 Quartz (textures and sulphide armouring)

### 4.2.1 Textures

A little geological knowledge concerning quartz textures is of considerable value, and in many cases with appropriate geological context, the leached capping can be easily categorised from the quartz style. Some obvious examples would include:

- Prominent multilayered crustiform textures in volcanic domains. Quartz dominant with little evidence of significant iron-rich sulphide leach cavities – these are hallmarks of many low-sulphidation epithermal veins (Figure 3.19).
- Major siliceous alteration with numerous cavities/vugs. Significant evidence of isolated sulphide zones via limonite development ± scorodite. This is the common expression of high-sulphidation epithermal styles, where early leaching and primary silicification, are overprinted by iron-arsenic-antimony-silver rich sulphides (pyrite, enargite, tetrahedrite) and subsequently oxidised (Figures 3.21–3.24).
- Veins containing massive textured white quartz which exhibit signs of pressure solution via stylonitic textures. Minor limonite development indicates low sulphide content. (The massive quartz results from recrystallisation under pressure). In appropriate slate belt terrains the quartz related textures are sufficient to type cast the vein as a possible gold-bearing structure.

### 4.2.2 Sulphide remnants

The second valuable component of quartz-rich leached cappings is the tendency for fine-grained sulphides encased in quartz to escape oxidation (Figure 3.24). This type of protective process is referred to as armouring.

It is always wise to break open 10–20 quartz specimens and then carefully inspect any small dark spots with a high power hand lens or microscope. This approach was used in mapping out pyrite-bornite-chalcopyrite zonation in the surficial leached capping at the giant El Salvador porphyry copper system in Chile (Gustafson and Hunt, 1975).

### 4.3 Limonite (composition, colour, source interpretation, host rock controls, and textural types)

An obvious early assessment action is to gain some impression of the amount of iron oxide present. The rusty iron capping is generally referred to via the generic “limonite”, and in simplistic term limonite content is a direct reflection of iron sulphides below (Figures 3.1–3.14). Iron-rich exposures can also relate to ferromagnesian or iron carbonate dominant protoliths via oxidation of amphiboles, pyroxenes, biotite, chlorite, siderite etc., although these are usually easily discerned via normal geological observation of local oxidation profiles (creeks, road cuttings, cliffs). The major contributors amongst the iron-rich sulphides are pyrite, pyrrothite and in some cases iron-rich sphalerite. Given that pyrite is by far the most commonly occurring sulphide, it always remains the first suspect.

There is no specific mineral called limonite, and the ferruginous material is somewhat variable in detailed composition. It is essentially a fine-grained mass of amorphous hydrated iron oxides, intermixed with other fine-grained components such as quartz (silica) and manganese oxides. The main iron oxides involved are haematite ( $\text{Fe}_2\text{O}_3$ ) and goethite ( $\alpha\text{Fe}^{3+}\text{O}(\text{OH})$ ) with very rare lepidocrocite ( $\text{FeO}(\text{OH})$ ).

The complex fine-grained (commonly siliceous) material may contain other fine grained additions such as jarosite ( $\text{KFe}_3(\text{SO}_4)_2(\text{OH})_6$ ), gypsum ( $\text{CaSO}_4$ ), alunite ( $\text{KAl}_3(\text{SO}_4)_2(\text{OH})_6$ ) and other relatively insoluble compounds such as scorodite ( $\text{FeAsO}_4 \cdot 2\text{H}_2\text{O}$ ) and metallic trace elements incorporated via adsorption onto the iron and manganese “oxides”.

The net result of all the above is to impart a wide range of colour variations to the exposures ranging from black through all shades of red and orange to yellow.

In theory a predominant reddish tinge favours excess haematite, and yellowish overtones favour goethite. However in practice this is a very unreliable criterion, with a wide range of colours commonly present within a single exposure. It is also wise to check superficial limonite colours by scratching them, or even grinding them to a fine powder. Some low pyrite, lead-zinc deposits tend towards the yellow end of the spectrum and are goethite dominant (Figures 3.4–3.5). However, it is reiterated that colour is not a reliable indicator of underlying mineral species.

Although colour is not a generally helpful criterion, it does become important in porphyry copper domains, where supergene chalcocite may evolve to dark brown/red/maroon haematite (see Section 8). Siderite seems to commonly oxidise to a distinctive deep brown colour, and within any individual region an experienced prospector/geologists may gain enough confidence to interpret some of the colour variations.

A further limonite feature worth both early and continuing inspection, concerns the interpreted origin in terms of source. Limonite which is fixed at the original sulphide

site is termed indigenous, whereas that fixed away from the dissolution site is termed exotic. Limonite that can be interpreted as coming from a nearby ex-sulphide source is termed fringing (Figure 30), (Blanchard, 1968). This near source fringing limonite was also called transported in an earlier publication (Blanchard, 1925). However with the passage of time the terms exotic and transported have become synonymous.

Indigenous limonite will thus mimic the original sulphide or at least survive as a partial filling within a developing cavity (Figures 4.1–4.5).

Exotic limonite is by far the most common, with rusty coloured materials staining the rocks (limonite fog) and/or precipitating along cracks and joints (Figures 4.5–4.9).

The concept has some value in the porphyry copper domains of southwestern USA, South America, and Australia where disseminated chalcocite grains may convert to limonitic/haematitic material in situ within low acid supergene/oxide domains (Figures 4.2, 4.3 and the later porphyry copper section).

In practice the indigenous/exotic distinction is commonly difficult to apply with respect to indigenous components. Most gossans are iron rich with abundant exotic limonite. This will both overprint indigenous components, and even more confusingly precipitate in leached cavities giving a superficially indigenous appearance. As a result the observer is often forced to make an unsatisfactory judgement call.

The in situ indigenous limonite concept is linked to the perceived neutralising power of the host rocks. In theory the transport of acid iron-rich fluids will be limited given rapidly neutralising gangue. Thus pyrite oxidising in a lime-rich sediment, may precipitate iron oxides more or less in situ.

Thus host rocks can be arranged in a general hierarchy from low to high neutralising effects.

- Inert – including sandstone or quartz, dominant, shale and hornfels.
- Slow neutralising – including felsic igneous rocks variably altered to clay, sericite and quartz.
- Moderate neutralising – including fresh igneous rocks or rocks with potassic alteration (secondary orthoclase and/or biotite). Mafic rocks are generally more reactive than felsic equivalents.
- Rapid neutralising – including limestone and other forms of carbonate rich rocks.

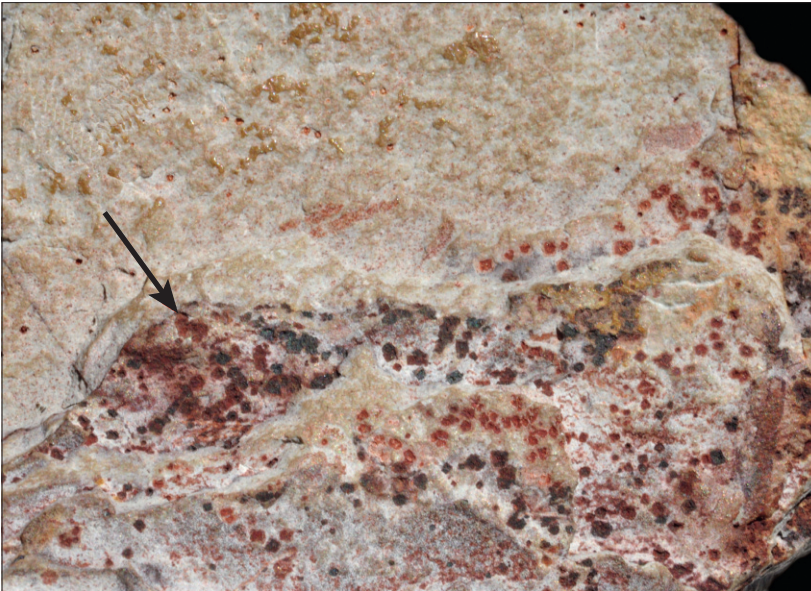
Limonite textures exhibit considerable variation and unfortunately there is no recognised formal nomenclature. Blanchard (1968) attempted some descriptive details and even discussed some possible differences between indigenous and exotic assemblages. Unfortunately there is considerably overlap and very few of the textures have any coherent diagnostic value. Without detailed classification supported by colour photography there remains some confusion, with the nodular limonite of one observer becoming the botryoidal limonite of another. A few terms are cautiously offered below.

|                    |   |
|--------------------|---|
| <i>Arborescent</i> | Linked granules as small branching clusters or knob-like projections of the granules. |
| <i>Botryoidal</i>  | Grape-like, small bubbles (Figures 4.7–4.8).  |

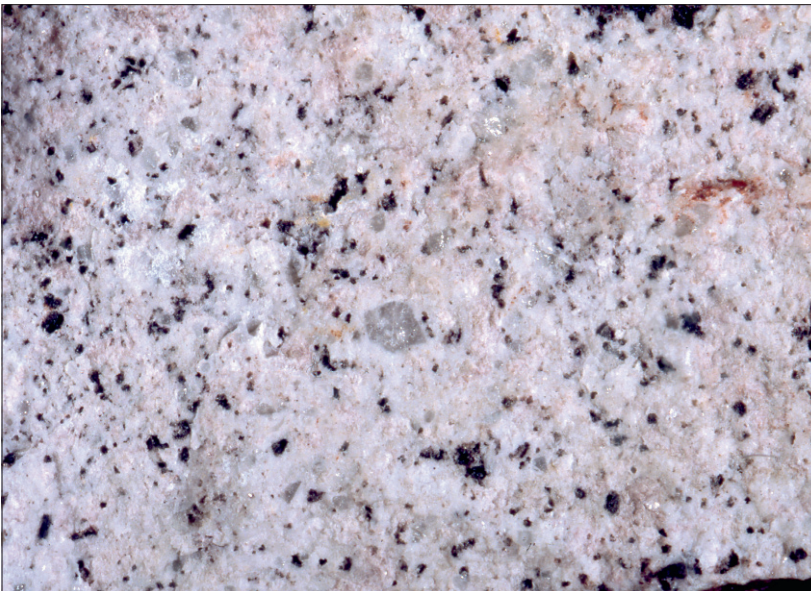
|                          |  |
|--------------------------|--|
| <i>Cellular</i>          | Boxwork styles (see Section 7).  |
| <i>Coagulated, Fused</i> | Granular style.  |
| <i>Columnar</i>          | Columns (Figure 4.9).  |
| <i>Concretionary</i>     | Concretions, similar to nodular or botryoidal.   |
| <i>Craggy</i>            | Clumped protuberances of granules (also called relief limonite, Figure 4.2).   |
| <i>Earthy</i>            | Powdery (similar to pulverulent).  |
| <i>Flaky</i>             | Flakes (sometimes referred to as flaky crusts) – these curl on drying out.   |
| <i>Flat</i>              | Smooth, paint-like.  |
| <i>Granular</i>          | Sugary – very common format (Figure 4.2).  |
| <i>Iridescent</i>        | Peacock colours (green, red, purple – also called turgite, Figure 4.8).  |
| <i>Mammillated</i>       | Mamillary, curved.   |
| <i>Live</i>              | Dark maroon indigenous limonite, interpreted as pseudomorphing supergene disseminated chalcocite in porphyry copper systems – characteristic colour, may show craggy or relief textures (Figures 4.2–4.3). |
| <i>Massive</i>           | No texture.  |
| <i>Nodular</i>           | Nodular, similar to botryoidal.  |
| <i>Pitch</i>             | Special term describing a varnished looking, deep red indigenous limonite, usually after chalcopyrite (Figure 6.11).   |
| <i>Pulverulent</i>       | Crumbly, earthy – very common format.  |
| <i>Caked</i>             | Caked (caked crusty) – clay rich limonite.   |
| <i>Relief</i>            | Sooty texture after sooty secondary chalcocite, see also craggy and relief. Commonly linked with live limonite in descriptive terms – relief-live limonite (Figures 4.1–4.2).                              |
| <i>Reniform</i>          | Kidney-shaped – similar to botryoidal.   |
| <i>Stalactitic</i>       | Stalactite-shaped.   |
| <i>Vitreous</i>          | Glassy.  |
| <i>Varnished</i>         | High sheen, desert varnish.  |

Very few of these have any genetic implications with the notable exceptions of:

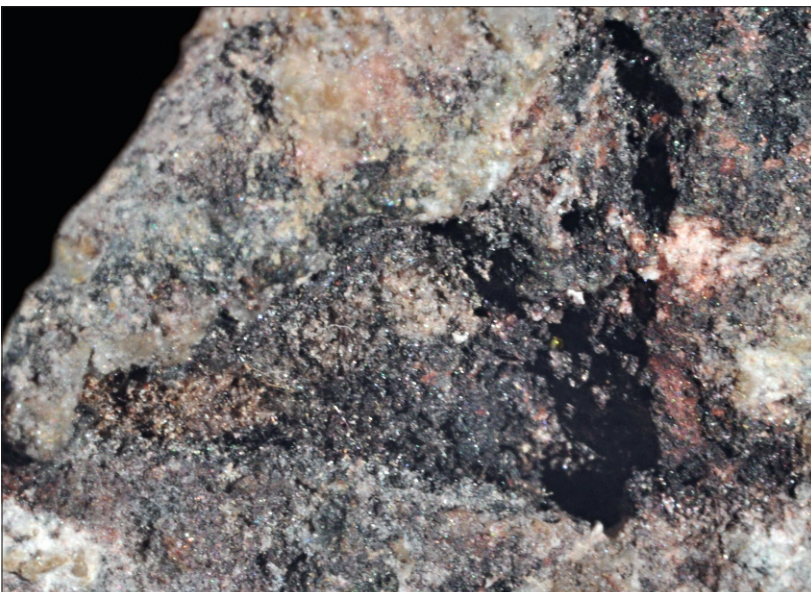
- Botryoidal – useful as an indication of exotic origin.
- Relief – live – *extremely* important indicator of probable subsurface supergene enrichment in porphyry copper systems.



**Fig. 4.1 Indigenous and fringing limonite.** Surface view of a fine layered (white) calcareous shale. The layer occupying the lower section of the picture contains abundant indigenous (in situ) limonite forming as pseudomorphs of pyrite crystals. Dark to reddish limonite is the end product. The large cluster (arrow) exhibits some diffuse red "fog" around (**fringing**) the ex-crystals, where iron has been transported, but quickly precipitated via interaction with the calcareous host. The latter is responsible for the rapid in situ pseudomorphic precipitation. **Mt Isa district, Queensland, Australia.** Width of frame 3.5 cm.



**Fig. 4.2 Indigenous – Live limonite.** The sample consists of quartz (grey) argillised feldspar (white) and numerous dark spots. It was originally fine-grained quartz feldspar porphyry with spots of pyrite and chalcopyrite. The latter were replaced by chalcocite and then later converted to in situ **maroon coloured (haematite dominant) limonite**. The live terminology is used to indicate the fact that an underlying supergene chalcocite zone is present. The indigenous character reflects a supergene rock emerging into the oxide zone with little or no pyrite remaining to produce major acid solutions. **Escondida, Chile.** Width of frame 3 cm.



**Fig. 4.3 Indigenous – Live or relief limonite (see also [Figure 4.2](#)).** Close up view of a large cavity containing dark **maroon live limonite**. The texture of the limonite reflects the original sooty texture of supergene chalcocite. The sooty chalcocite would have originally been chalcopyrite/pyrite (converted to chalcocite and then leached to leave pseudomorphic haematitic limonite). The term relief refers to the coarse sooty texture, where grains appear cemented together in small protuberances. A supergene chalcocite zone is indicated. **Toquepala, Peru.** Width of frame 2 cm.

**Figure 4.4 Indigenous limonite.**

Garnet crystals converted to, and pseudomorphed by limonite.

The in situ limonite is referred to as indigenous.

**Location unknown.**

Width of frame 5 cm.



**Figure 4.5 Exotic or transported limonite.**

The shattered porphyry provides an ideal environment for acidic fluids to traverse the rock mass, and precipitate copious orange limonite along the fracture surfaces. The limonite is derived via the dissolution of disseminated and veinlet style pyrite-chalcopyrite mineralisation. The terms exotic or transported are utilised to designate this type of externally derived limonitic material. The author prefers transported.

**Collahuasi, Chile.**

Photograph provided by D. Andrews.



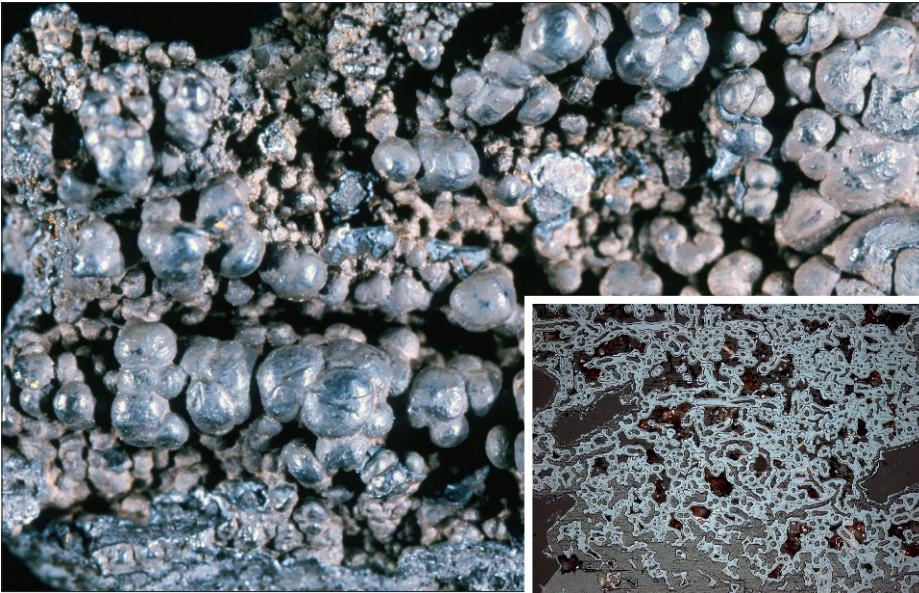
**Figure 4.6 Exotic limonite.**

The porphyritic rock has split open along an ex pyrite/chalcopyrite vein surface. Some vague cellular and/or small cavities (ex-sulphide?) are visible, but the main fracture is an intense development of fine orange/red rusty limonite staining. The majority of this is clearly not pseudomorphic after sulphides and would be regarded as of exotic or transported origin. The small cavities (cellular structures reflect the size of the sulphides at 1.0mm scales (or less). It is possible that a small proportion of limonite may be fringing?

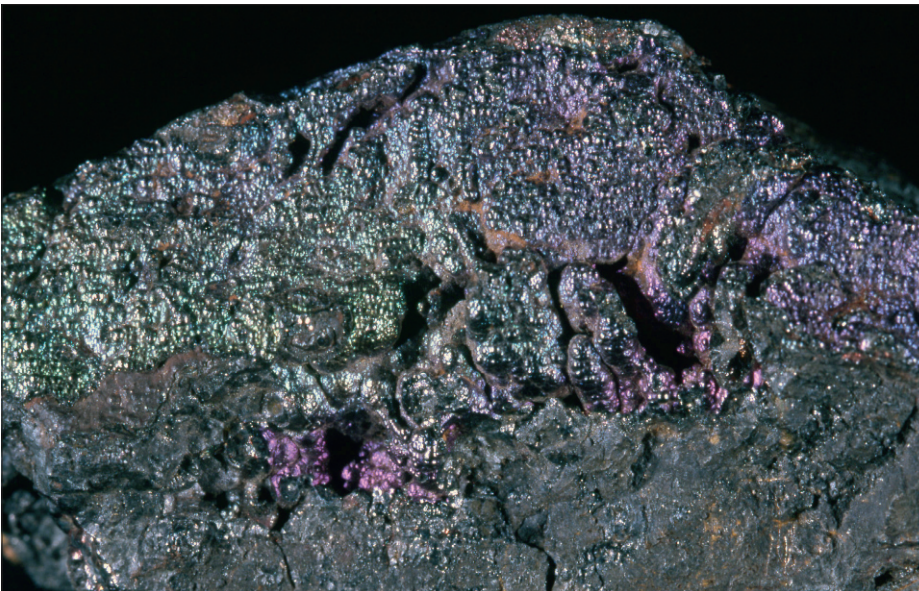
**Grasberg, Indonesia.**

Width of frame 11 cm.





**Figure 4.7 Botryoidal limonite.** This distinctive form is always indicative of transported/exotic limonite. The inset depicts botryoidal limonite in polished section (ordinary light) where it exhibits the characteristic globular texture.  
**Location unknown.**  
 Width of frame (botryoidal hand specimen) 6 cm.  
 Width of frame (polished section) 5.6 mm.



**Figure 4.8 Iridescent limonite.** This colourful form of limonite commonly causes confusion. The peacock colours are reminiscent of tarnishes on copper minerals (especially chalcopyrite). It is also referred to as turgite.  
**Location unknown.**  
 Width of frame 7 cm.



**Figure 4.9 Columnar limonite.** Tubular columnar features with some botryoidal overtones  
**Location unknown.**  
 Width of frame 6 cm.



It is particularly important to carefully observe and document the broad-scale textural features of leached exposures. Unfortunately this vital stage is commonly neglected in the haste to collect specimens for chemical analysis or microscopic examination. There is also a tendency to dismiss rusty or soft clay exposures as a textureless mess. This is only partially true, and in many cases features which are still present include, well developed layering, brecciation, irregular distribution of limonite types, and a simple description of the size and shape can be of great value. It is surprising how many features of the primary ore are reflected in the surface gossan awaiting recognition by astute observation. Layering within primary ores such as in volcanogenic or layer replacive sulphides is almost always preserved at outcrop, although it may be weakly developed, sporadically developed, or blurred via oxidation affects (Figures 5.1–5.3).

Much brecciation is either not recognised or dismissed as oxidation collapse, and numerous major and small scale breccia pipes are not initially recognised for this reason. Leached exposures are much more resistant to collapse and erosion than might be generally supposed. The insoluble oxide/silica combination commonly becomes much more resistant to weathering than the surrounding wall rocks. Hence siliceous/gossanous ridges and hills, where textural retention is common.

Failure to recognise the knobbly texture of breccia through either an iron oxide or clay mask is extremely common, and this problem has been treated at some length in a recent publication (Taylor, 2009).

The ability of surface gossan to faithfully reflect primary ore characteristics is well seen in many sulphide-rich tin systems. The kilometre-scale Siberia lode (Cu, Sn, Pb, Zn, As) system at Emuford in north Queensland is well-exposed, and the percentage of gossan versus quartz over the exposure illustrates clearly the percentage of sulphides versus gangue. It also illustrates the irregular-lensoid-patchy nature of the ore shoots (Kelly, 1976).

A further example of excellent textural preservation is given by the finely layered exposures of magnetite-fluorite skarns in the Mt Garnet region of North Queensland. These distinctively textured ores are locally termed “wrigglite”, and the texture is faithfully preserved at surface. It remained unnoticed throughout some seventy years of intense mining activity.

**Fig. 5.1 Structural preservation – layering.**

The surface exposure of this sediment-hosted deposit is highly iron stained, and retains a discernible layered format reflecting finely laminated layers of sulphide (pyrite, galena, and sphalerite) and fine dolomitic siltstone. These layers are readily visible upon breaking open exposures.

Figure 5.2 shows the reverse side of this specimen.

**Lady Loretta, Queensland, Australia.**

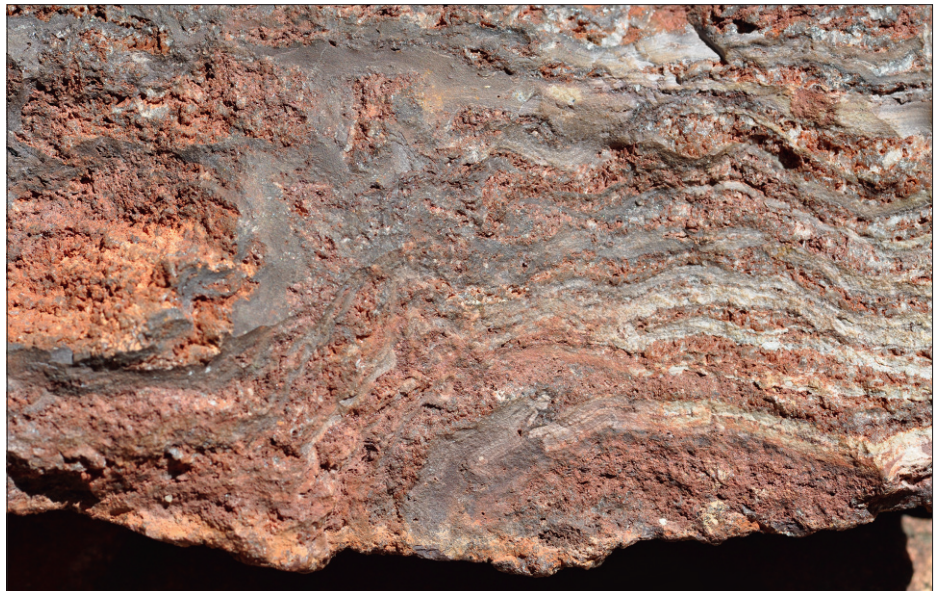
Width of frame 15 cm

**Fig. 5.2 Structural preservation – layering.**

The pale-white laminated layers are argillised versions of fine-grained dark dolomitic siltstones. The red iron-stained layers with a granular texture contain considerable cerussite (lead carbonate) and were originally galena rich, fine-grained sulphide layers.

**Lady Loretta, Queensland, Australia.**

Width of frame 15 cm.

**Fig. 5.3 Structural preservation – layering.**

The limonitic gossan exhibits both textural and colour variations, suggesting derivation from a variably textured iron-rich source. The original rock is composed of pyritic layers intercalated with dark shales. The volcanogenic deposit is a copper, lead, zinc, silver ore. The original sulphides are mostly fine-grained.

The inset shows primary pyrite-dominant ore – the layers run horizontal to the photograph – highlighted in white.

**Woodlawn – New South Wales, Australia.**

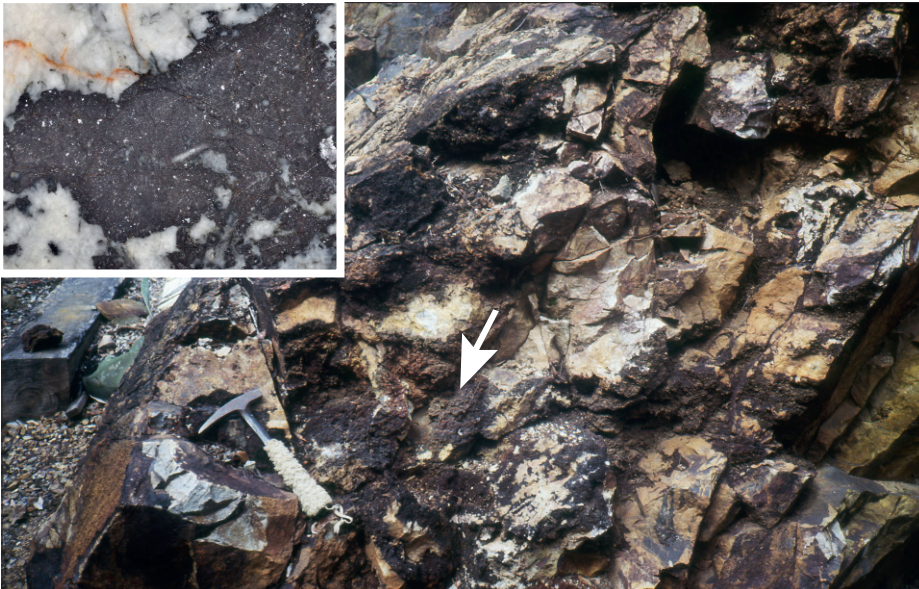
Width of frame (gossan) 9.5 cm.

Width of frame (inset) 8 cm.





**Fig. 5.4 Structural preservation – breccia, shear fabric.**  
 The limonitic gossan exposure is knobby with oriented fragments of various sizes, and reflects the underlying shear fabric.  
**Trek prospect, British Columbia, Canada.**  
 Photograph provided by S. Close.



**Fig. 5.5 Structural preservation – breccia.**  
 The gossan represents the surface exposure of a lead-zinc-silver deposit where brecciated sandstone/quartzite creates large cavities infilled with coarse-grained quartz, sphalerite, galena and minor chalcopyrite. The cavities are discernible at surface via quartz crystals heavily coated with transported limonite, derived from oxidation of iron-rich sphalerite. The cavities are dark red – brown (white arrow). Inset, quartz (white) – sphalerite (black).  
**Isobella mine, Queensland, Australia.**  
 Width of inset frame 6 cm.



## 6.1 General aspects

The various processes acting upon ore assemblages in the near surface environment result in the formation of new minerals either via replacement or precipitation. Within this context these are referred to as secondary minerals, and include new oxides, hydroxides, sulphates, carbonates, phosphates, silicates, native metals and even sulphides. These obviously provide valuable chemical clues concerning the subsurface primary (and supergene) assemblages, and the presence of secondary copper minerals automatically leads to suspicions of the most common copper sulphides such as chalcopyrite or bornite.

It is relatively uncommon for serious detailed searches of leached outcrops not to reveal some secondary minerals other than iron oxides. These are most vital clues and should always be sought with vigour. Considerable pounding open of rocks is recommended. Searching for secondary minerals in the surface environment is by no means simple, and although most geologists have little trouble in collecting the brightly coloured species, the less spectacular white-grey-buff specimens remain unnoticed. This is particularly true when they are fine-grained, and recognition is not assisted by the common coatings of iron oxides, and clays which obscure many of the secondary minerals. An in-depth knowledge of secondary minerals, their colours, shapes and typical associations is mandatory to any exploration geologist. Acquisition of this skill over a lifetime is a constant learning process, and an ability to work with a high power hand lens quickly becomes a reflex action. Not only is recognition of secondary minerals an essential attribute, but it is also important to have some conception of which secondary minerals are likely to survive the zone of oxidation and remain stable at surface. For instance it is rare to find aurichalcite or even zinc carbonate persisting to surface, whereas hemimorphite either in its original form or derived from the leaching of smithsonite is much more likely to persist. Hemimorphite was a major residual component in the McArthur River gossan ([Figure 3.12](#)). Scorodite (hydrated iron arsenate) and anglesite/cerussite (lead sulphate/carbonate) are similarly very persistent, although commonly obscured by iron oxides.

Given that there are literally hundreds of secondary minerals it would be impractical to cover them all here. Many are mineralogical curiosities which excite the mineral collector, but are unlikely to be encountered by the average exploration geologist. Similarly many are too fine-grained (especially clay-like formats) to be easily recognised. Given these constraints, the author has been selective, and this section attempts to illustrate the most common and useful examples. Similarly the photographs have been chosen to represent the most likely discovery format, rather than museum-style specimens.

In most cases only the critical identification criteria are given as it is not intended to write an academic mineralogical textbook, and many of the properties are of little or no value for field identification.

## 6.2 Iron

**Goethite  $\alpha\text{Fe}_3\text{O}(\text{OH})$ . Ferric oxyhydroxide.**

**Haematite  $\text{Fe}_2\text{O}_3$ . Iron oxide.**

**Jarosite  $\text{KFe}_3(\text{SO}_4)_2(\text{OH})$ . Potassium iron hydroxysulphate.**

**Melanterite  $\text{FeSO}_4 \cdot 7\text{H}_2\text{O}$ . Hydrated iron sulphate.**

**Vivianite  $\text{Fe}_3(\text{PO}_4)_2 \cdot 8\text{H}_2\text{O}$ . Hydrated iron phosphate.**

**(Figures 6.1–6.5).**

The most common and important iron-rich secondary minerals are the iron oxide/hydroxides – goethite and haematite, which are commonly linked to the potassium iron sulphate, jarosite.

Goethite and/or haematite form the basis of most rusty gossanous exposures, reflecting the breakdown of iron-rich components such as pyrite, pyrrhotite, iron-rich sphalerite, and related gangue minerals including chlorite, olivine, amphibole and pyroxene.

These are in fine-grained format, commonly associated with dark manganese oxides, fine grained silica and completely lacking in crystal format (best described as a ferruginous mass). As described previously the lack of obvious identification features has led to the generic term “limonite”. Scratching around with a hammer, checking general colours, or streak plate results, might lead to some feeling for haematite (red) or goethite (orange) rich. However, colour is commonly an unreliable indicator, and due caution is recommended. Both goethite and haematite are stable over a wide range of pH, and most of the end products are transported, precipitating along fractures, and staining the adjacent wall rocks. Further illustrations of ferruginous-gossanous outcrops are shown in the previous section.

Jarosite ( $\text{KFe}_3(\text{SO}_4)_2\text{OH}_6$ ) is a common associate of limonitic exposures and again occurs in fine-grained granular to fluffy formats, unlikely to be noticed by mineral collectors seeking cabinet specimens.

Like goethite and limonite it is extremely difficult to identify, and experienced geologists generally assume that the yellowish fine powdery – pulverulent – granular component of a leached capping may well contain jarosite – hence the term jarositic limonite is widely used.

Jarosite is taken to indicate highly acid fluid conditions (pH less than 3.0) within moderate to high oxidising situations. The potassium component is generally attributed to acid leaching of the wall rocks (K-feldspar?).

Within this acidic context, the occurrence of jarosite within kilometre-scale alteration/mineralisation systems is cautiously regarded with close attention. In many cases the occurrence of significant jarosite marks the outer area of the sulphide system, where pyrite occurs in excess of chalcopyrite. This in turn means that a highly enriched supergene blanket (chalcocite) is unlikely directly below the jarositic exposure.

Although of minor importance two other iron-rich secondary minerals are illustrated here. Vivianite ( $\text{Fe}_3(\text{PO}_4)_2 \cdot 8\text{H}_2\text{O}$ ) occurs both as a primary and secondary mineral. It is not common and is only included here as the spectacular dark blue colour attracts attention.

Melanterite ( $\text{FeSO}_4 \cdot 7\text{H}_2\text{O}$ ) is also included here. It is of rare occurrence in surficial gossans, but common in adits, old mine workings and oxidising pyritic drill core. It adopts a wide range of formats from stalactitic to the more common whiskery – fibrous style, and tends to oxidise/decompose on exposure to the atmosphere. Its main identifying feature is an horrendous metallic taste, best experienced by the utilisation of a field hand. It is included here as it is relatively common, although of no real consequence in gossan interpretation. Scorodite ( $\text{FeAsO}_4 \cdot 2\text{H}_2\text{O}$ ) is not treated here, but placed in the arsenic secondary mineral category (section 6.8).



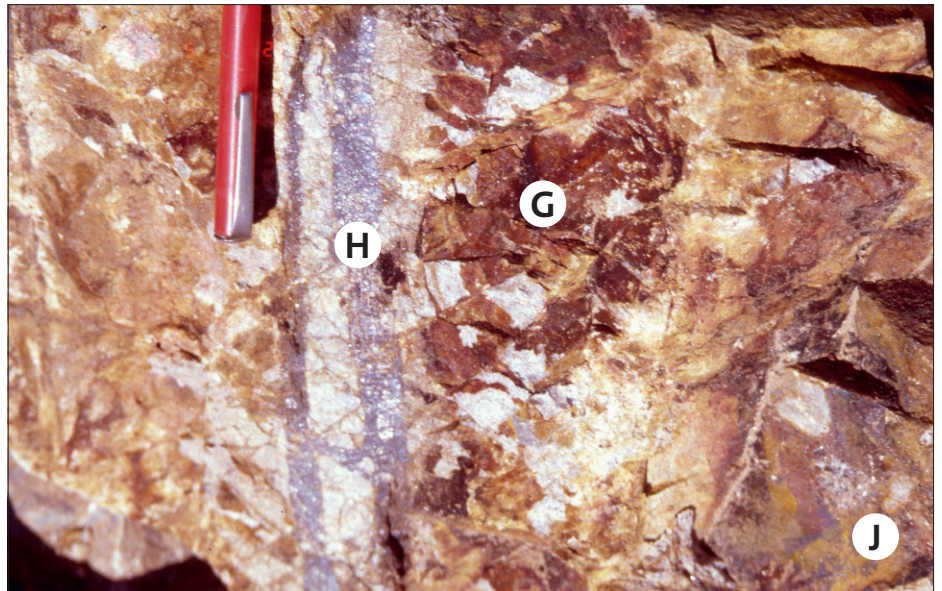
**Fig. 6.1 Jarosite.**

Fine-grained granular to clay-like, earthy. Suspected from yellow colour. Indicates a highly acid environment – probably via decomposition of iron-rich sulphide-pyrite? Transported – precipitating and staining rock. **Toughnut Mine, Arizona, USA.** Width of frame 4 cm.



**Fig. 6.2 Haematite, goethite limonite and jarosite.**

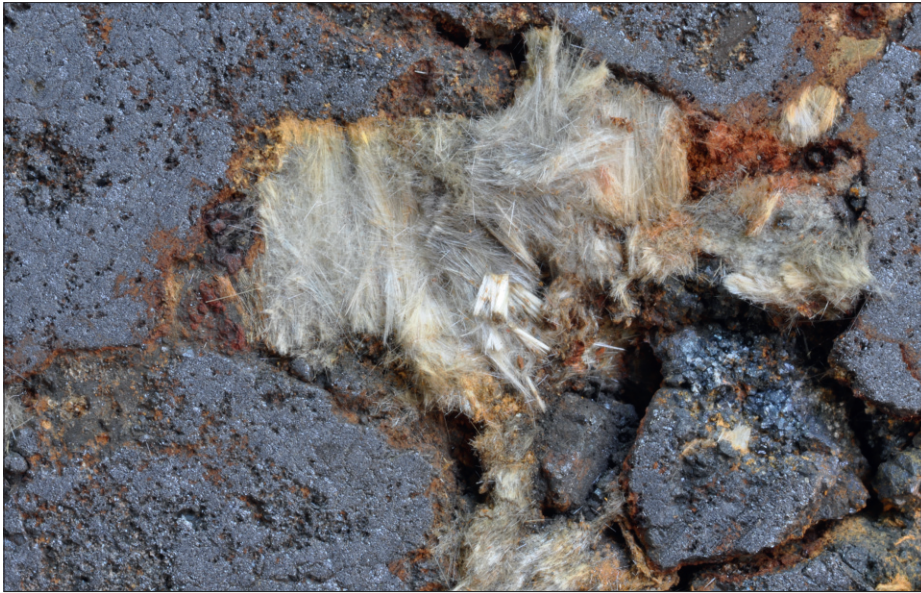
The maroon haematite (H) is ex-supergene chalcocite (Indigenous – Live limonite). The orange rusty components are transported – exotic goethitic limonite (G) merging into yellow tinged limonitic jarosite (J). **Morenci (porphyry copper), USA.** Specimen provided by D. Andrews.



**Fig. 6.3 Haematite and jarosite.**

Limonitic fragments – yellow jarositic (left) and maroon indigenous? Haematitic (right). **Ray (porphyry copper), USA.** Specimen provided by D. Andrews.





**Fig. 6.4 Melanterite.**  
Typical whisker-fibre format  
precipitating in cavity within  
magnetite.  
Width of frame 2 cm.



**Fig. 6.5 Vivianite.**  
Characteristic blue colour.  
NB It is possible that this par-  
ticular example is primary.  
**Grasberg (porphyry copper),  
Indonesia.**  
Width of frame 3 cm.

**6.3 Manganese.**  
**“Manganese wad” and “Manganese oxides”, general terms.**  
**Psilomilane (“manganese oxides”, general term).**  
**Pyrolusite  $\text{MnO}_2$ . Manganese oxide.**  
**Manganite  $\text{MnO (OH)}$ . Manganese oxyhydroxide.**  
**Neotcite  $(\text{MnFeMg}) \text{SiO}_3 \cdot \text{H}_2\text{O}$ . Hydrated iron silicate.**  
**(Figures 6.6–6.7).**

“Manganese wad” and “Manganese oxides” are general terms utilised to indicate black granular powdery to botryoidal manganese oxides. Psilomilane is also a general term commonly applied to more massive botryoidal mamillary styles of manganese oxides/hydroxides. It is also rarely used to indicate barium-rich manganese oxides/hydroxides.

Pyrolusite –  $\text{MnO}_2$ . This is most common major component of masses of “manganese oxides,” but cannot be positively identified in most exposures. Identification requires laboratory investigation.

Manganite –  $\text{MnO (OH)}$ . This is another common component of masses of “manganese oxides”. As with pyrolusite it cannot usually be positively identified in most exposures. Identification again requires laboratory investigation.

Neotcite –  $(\text{MnFeMg}) \text{SiO}_3 \cdot \text{H}_2\text{O}$ . Neotcite is a poorly defined substance, with no real field identification features other than being “manganese oxides”. The occurrence in spot formation seems common (Figure 6.7) and the tendency to contain copper visible by the rusty nail-hydrochloric test makes the compound of significance in porphyry copper terrains (see below).

Manganese is an extremely common component within gossaneous/leached capping zones usually occurring as dark, dull black amorphous powders, crusts and even botryoidal – reinform aggregates and columnar patches. The dark manganese is often intimately mixed with limonite and it is effectively impossible to identify the exact manganese minerals involved without a major research project and access to modern expensive equipment.

The author has never seen an identifiable crystal, and experienced observers will revert to terms such as manganese oxides, manganese wad for fine granular to sooty masses, or even psilomilane to more massive materials. These are all vague terms meant to indicate manganese oxides/hydroxides. They all have a dark streak or penknife scratch, and are commonly sooty, sticking as a fine dust to the fingers. The manganese oxides also have a tendency to form impressive fern like patterns along joint faces which can be mistaken by the unaware for plant fossils.

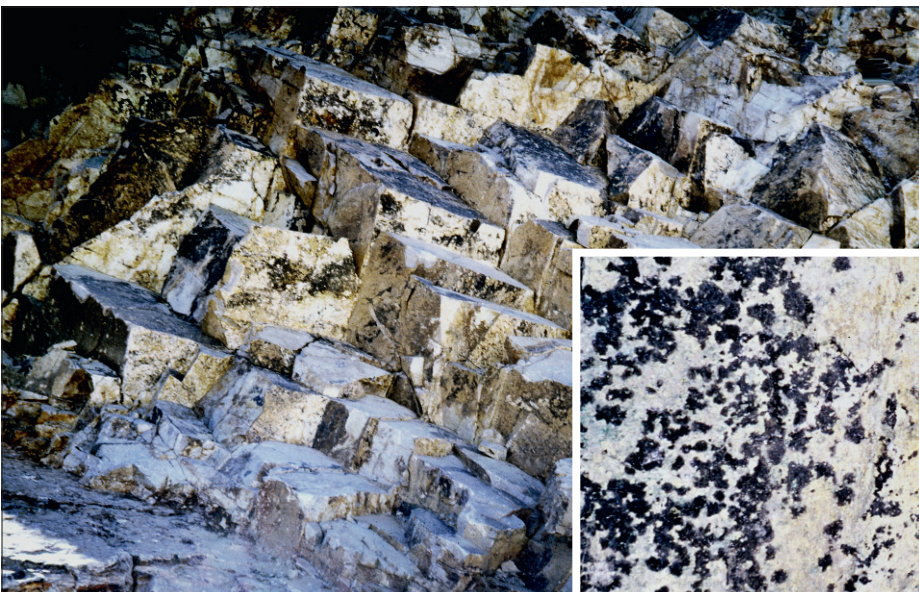
Manganese is present in a wide range of minerals usually in minute amounts (e.g. in iron-rich silicates) and easily taken into solution. This accounts for its widespread re-appearance as oxides and hydroxides. These can of course reach major proportions where manganese-rich primary minerals are involved such as rhodonite (silicate) or rhodochrosite (carbonate) and there are also major sedimentary manganese accumulations which may contribute to a major manganiferous capping.

“Manganese oxides” are well known sinks for trace amounts of other components, especially metals. Within this context “manganese oxides” on joints are well worth field testing for copper content. The test is conducted by treating with dilute hydrochloric acid, and contacting the solution with a rusty nail. The point of contact becomes coated with native copper. Although the author knows of no scientific data, porphyry copper prospectors regard neotocite as a major copper adsorber, and any “manganese oxide” coating responding is regarded as cupriferous neotocite. Neotocite has no well established field recognition features, although it does seem to favour a scattered spot style (Figure 6.7).



**Fig. 6.6** “Manganese oxide”. Solid botryoidal style, possibly pyrolusite? – although this cannot be established via visual inspection.

**Red Dog prospect, Ewan, Queensland, Australia.**  
Width of frame 5 cm.



**Fig. 6.7** “Manganese oxide”. Dark manganese oxide forming on joint faces. The close up (inset) exhibits manganese oxide occurring in a spotty format. This style is often tentatively called neotocite assuming it will respond to the rusty nail/hydrochloric acid test showing copper content (see text).

Width of inset frame 8 cm.  
**El Abra (porphyry copper) Chile.**  
Width of main frame about 6 m.

## 6.4 Copper (Figures 6.9–6.32)

### 6.4.1 General aspects

| Group      | Name                         | Formula   |
|------------|------------------------------|---|
| Element    | Copper (native copper)       | Cu  |
| Oxides     | Cuprite                      | $\text{Cu}_2\text{O}$   |
|            | Tenorite                     | CuO   |
|            | Chalcotrichite (hair copper) | CuO   |
| Carbonates | Malachite                    | $\text{Cu}_2\text{CO}_3(\text{OH})_2$   |
|            | Azurite                      | $\text{Cu}_3(\text{CO}_3)_2(\text{OH})_2$   |
| Sulphates  | Chalcanthite                 | $\text{CuSO}_4 \cdot 5\text{H}_2\text{O}$   |
|            | Brochantite                  | $\text{CuSO}_4(\text{OH})_6$  |
|            | Antlerite                    | $\text{Cu}_3\text{SO}_4(\text{OH})_4$   |
|            | Linarite                     | $\text{PbCuSO}_4(\text{OH})_6 \cdot \text{H}_2\text{O}$                               |
| Chlorides  | Atacamite                    | $\text{Cu}_2\text{Cl}(\text{OH})_3$   |
| Silicates  | Chrysocolla (mineraloid)     | $(\text{Cu}, \text{Al})_2\text{H}_2\text{Si}_2\text{O}_5 \cdot n(\text{H}_2\text{O})$ |
|            | Dioptase                     | $\text{CuSiO}_2(\text{OH})_2$   |
| Phosphates | Pseudomalachite              | $\text{Cu}_5(\text{PO}_4)_2(\text{OH})_4$   |
|            | Turquoise                    | $\text{CuAl}_6(\text{PO}_4)_4(\text{OH})_8 \cdot 4\text{H}_2\text{O}$                 |
|            | Chalcosiderite               | $\text{Cu}(\text{Fe}, \text{Al})_6(\text{OH}_4)_2 \cdot 4\text{H}_2\text{O}$          |
| Arsenates  | Olivenite                    | $\text{Cu}_2\text{AsO}_4\text{OH}$  |
| Sulphides  | Chalcocite                   | CuS   |
|            | Covellite                    | $\text{Cu}_2\text{S}$   |

The secondary copper minerals constitute one of the most abundant and conspicuous secondary mineral groupings, and with their predominately green-blue and red colours are easily noticed.

They generally result from the breakdown of common primary copper minerals such as chalcopyrite, bornite, chalcocite, and covellite or alternatively via the dissolution

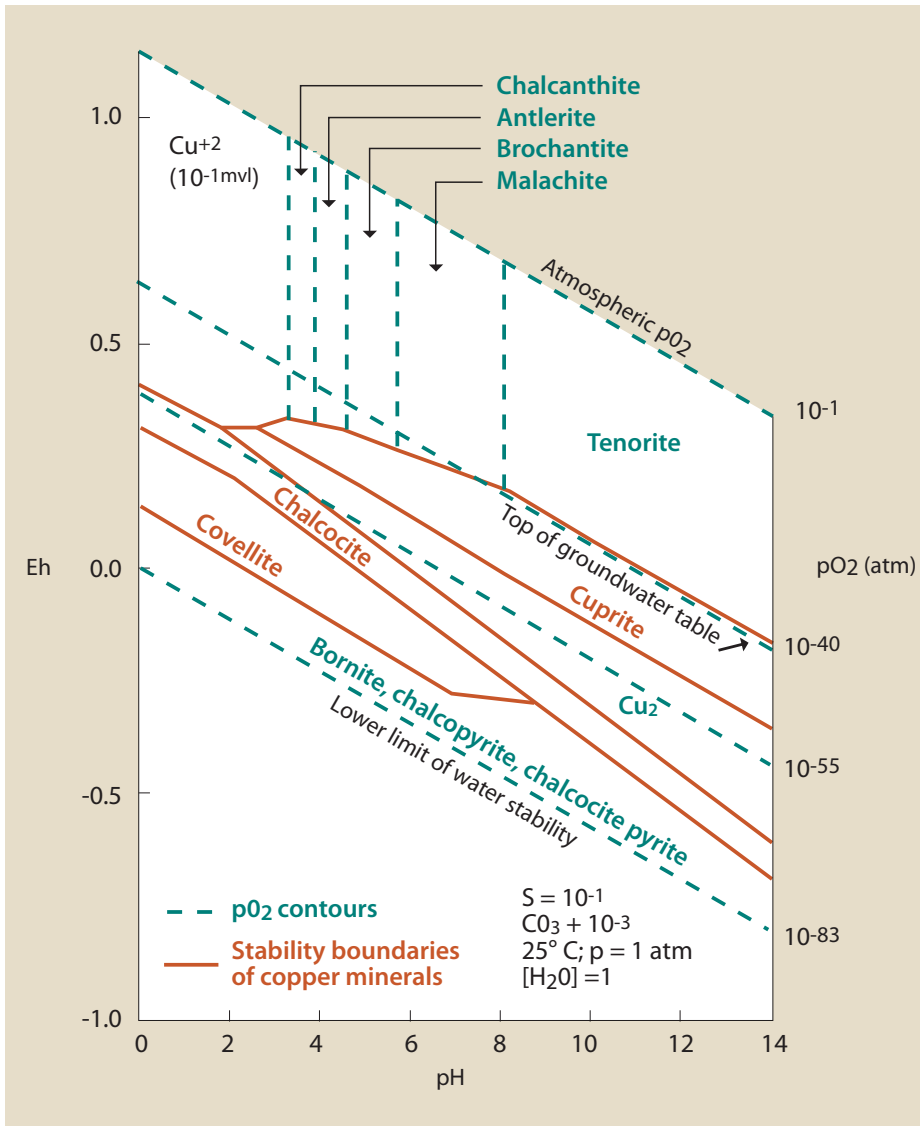


Fig. 6.8 Stability relations of some copper minerals at surface conditions and at low  $f(\text{CO}_2)$  as a function of Eh and pH (from Anderson 1982).

of secondary chalcocite/covellite formed as secondary enrichment materials around the water level. Given the common occurrence of one or more of these minerals in ore assemblages, numerous gossans/leached caps representing a wide range of deposit styles will develop copper secondary minerals. There is an industry saying amongst geologists that – “a little bit of copper goes a long way”.

There are a very large number of copper secondary minerals, reflecting the wide range of deposit types and more accurately the tendency of copper to combine with elements such as arsenic, and zinc to produce obscure arsenates, copper-zinc minerals, etc. Most of these are collector curiosities, and very few prospectors or geologists would know the full range. Fortunately the most common ones are usually present, and the list above has been especially selected to cover the most common species. It is also very useful to know that they tend to occur together, such that the discovery of one automatically leads to the suspicion that one of its common associates should be around. This reflects the fact that

the relevant minerals occur in a relatively tight cluster of pH/Eh conditions, with local groundwater compositions having sufficient components to form the relevant species (Figure 6.8). Thus cuprite, tenorite, native copper are common associates, along with a tendency to further oxidise to produce bright red haematitic limonite.

Supergene chalcocite will readily oxidise to cuprite, and cuprite in turn may further oxidise to tenorite. These reactions tend to occur in the deeper levels of gossan/leached cap profiles (see Figure 6.8).

Other common associates are malachite and chrysocolla, which usually precipitate at higher levels in the profile as infill products from permeating copper charged solutions. Malachite is probably the most common of all the copper minerals.

There are so many green copper minerals, that it is very difficult for both experienced and inexperienced observers to be fully confident of identification of small-scale specimens via direct observation. However it is a safe bet that a significant percentage of the green colours around copper gossans are malachite.

Although the standard pH-Eh diagram is set for certain conditions of temperature and fluid composition, it does provide a relatively robust guideline for precipitation conditions, and also explains the tendency for several minerals to occur together as conditions modify.

#### 6.4.2 Copper Cu.

##### Native copper (Figures 6.9–6.10).

Native copper can form both as a primary and secondary mineral. It is more common as a secondary product, and normally requires very little experience to recognise on account of its weight and conspicuous metallic shining copper sheen on broken examples. Specimens at surface tend to be coated with dark oxidation products, but the copper shown on broken surfaces is always spectacular.

The optimum conditions for formation are around pH 6–10, and Eh 0, (see Figure 6.8) and this environment is commonly present in the lower sections of gossan leached cap profiles, directly above the zone of supergene enrichment.

The end results are infill in character and vary enormously from irregular jagged slugs, through to arborescent sheets, and interesting wiry-filamentous shapes. Crystals are relatively common, often as dodecahedra. It is commonly associated with cuprite, and in many cases coated with films of malachite.

#### 6.4.3 Copper pitch (Figure 6.11). Oxides/ hydroxides of copper, silica, iron and manganese (mineral mixtures)

Copper pitch is a rather vaguely defined term, utilised to describe occurrences of a jet black to dark brown material with a conchoidal fracture and a reflectance similar to that of obsidian. It occurs mostly within arid copper rich terrains such as the southwest U.S. America (Arizona) and South America (Chile), and is essentially an amorphous mineraloid with a variable composition, involving oxides and hydroxides of copper, silica, iron and manganese. In the authors experience some occurrences

are ex-chalcopyrite, seemingly formed directly via surface exposure of chalcopyrite to surficial arid conditions. It is commonly associated with nearby copper secondary minerals, such as malachite.

#### **6.4.4 Cuprite $\text{Cu}_2\text{O}$ . Red copper oxide (also variety chalcotrichite) (Figures 6.12–6.14).**

Cuprite is a relatively common copper secondary minerals, and tends to form in the zone immediately above the supergene environment, where mildly favourable oxidising conditions and a pH range around 5–9 encourage precipitation. It is thus relatively rare in surficial outcrops, and more likely to be found in shallow prospecting shafts and their related dumps.

It occurs in a variety of formats, ranging from attractive vitreous red equant crystals (commonly as octahedra or dodecahedra) to less conspicuous dark reddish-grey fine-grained metallic lumps. The latter are commonly partially “coated” with later developments of the dark copper oxide (tenorite)  $\pm$  fine malachite and/or reddish haematite grains/crystals (Figure 6.12). These reflect further oxidation in a slightly higher Eh environment, at variable pH and groundwater compositional regimes. At least some of the fine-grained cuprite forms via direct oxidation (alteration) of secondary chalcocite.

Cuprite is easily recognised by the combination of weight, colour and the association with other copper secondary minerals (especially, malachite and/or chrysocolla).

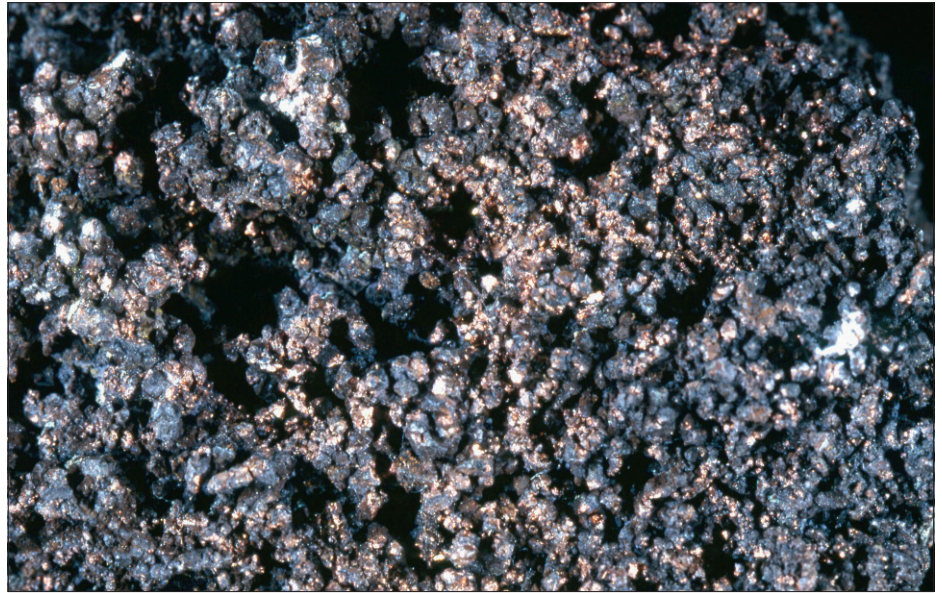
In some regions (e.g. Cloncurry, Australia) the occurrence of an extremely red variety known as chalcotrichite (also  $\text{Cu}_2\text{O}$ ) in either fibrous or earthy formats provides extremely striking red copper colours. The very fine fibrous clusters are sometimes referred to as hair copper (Figure 6.15).

#### **6.4.5 Tenorite $\text{CuO}$ (also termed melaconite or black copper oxide).**

Tenorite usually forms as a fine black sooty powder and more rarely in massive fine-grained lumps where the term melaconite is favoured.

As might be anticipated fine black powder like substances are common in gossans, especially where manganese oxides are abundant. Positive identification is not feasible in the field, although tenorite might be strongly suspected when black powders coat cuprite, together with other obvious signs of major copper secondary minerals (malachite, chrysocolla).

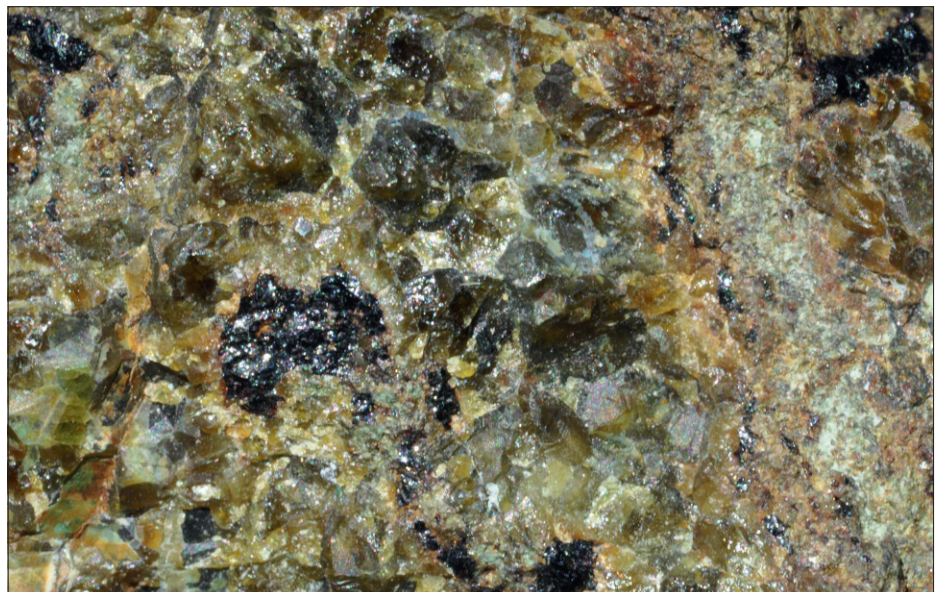
**Fig. 6.9 Native copper.**  
Numerous small equant  
crystals  
(dodecahedra-infill texture).  
Sometimes referred to as mossy  
texture.  
**Locality unknown.**  
Width of frame 2 cm

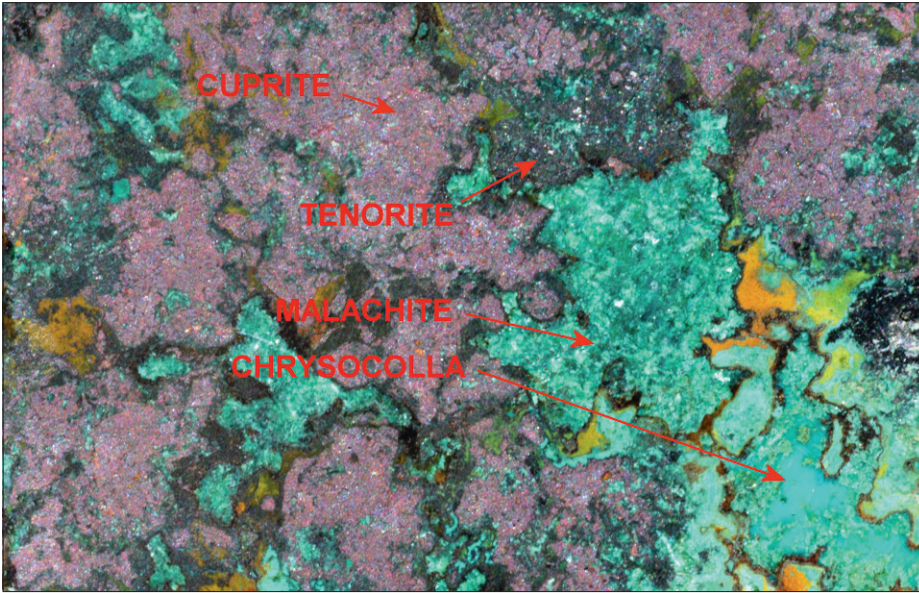


**Fig. 6.10 Native copper.**  
Infill cavity within grey metallic  
cuprite.  
**Locality unknown.**  
Width of frame 2 cm.



**Fig. 6.11 Pitch limonite.**  
Deep red brown oxidation  
product of chalcopryite?  
With conchoidal fracture and  
resinous lustre.  
Encased in green garnet–skarn.  
**Pukakaka district, Peru.**  
Width of frame 2 cm.

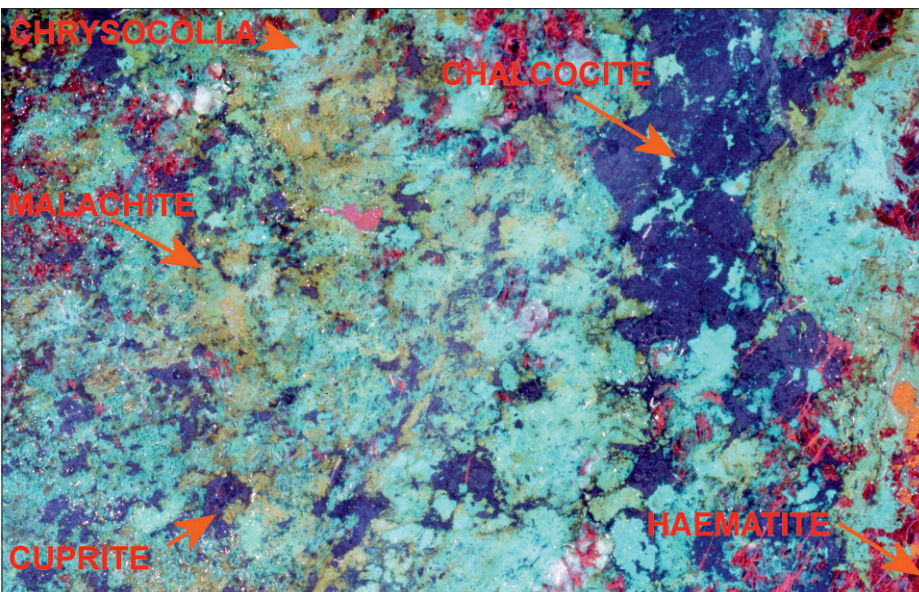




**Fig. 6.12** Cuprite-tenorite (Copper oxide). Maroon coloured cuprite with rims and partial coatings of tenorite (black). Cavities infilled with malachite (dull green) and chrysocolla (emerald green). Cloncurry region, Australia. Width of frame 4.5 cm.



**Fig. 6.13** Cuprite (Copper oxide). Well formed, deep red – black crystals precipitating in a cavity. Red Dome copper gold mine, Chillagoe, Queensland, Australia. Width of frame 5 cm.



**Fig. 6.14** Cuprite (Copper oxide). An instructive photograph showing supergene chalcocite (originally in a chalcopyrite? vein) – being replaced – pseudomorphed by fine-grained cuprite (note the subtle colour change). As oxidation progresses malachite – chrysocolla precipitate in evolving spaces and stain? (alter) the wall rocks. Finally the cuprite is partly removed and/or? altered to red haematite (indigenous). Mt Surprise district, Queensland, Australia. Width of frame 10 cm.



**Fig. 6.15 Chalcotrichite (Copper oxide).**

A variety of cuprite with rich red colouration occurring in both powder-like formats and as fine fibres (inset).

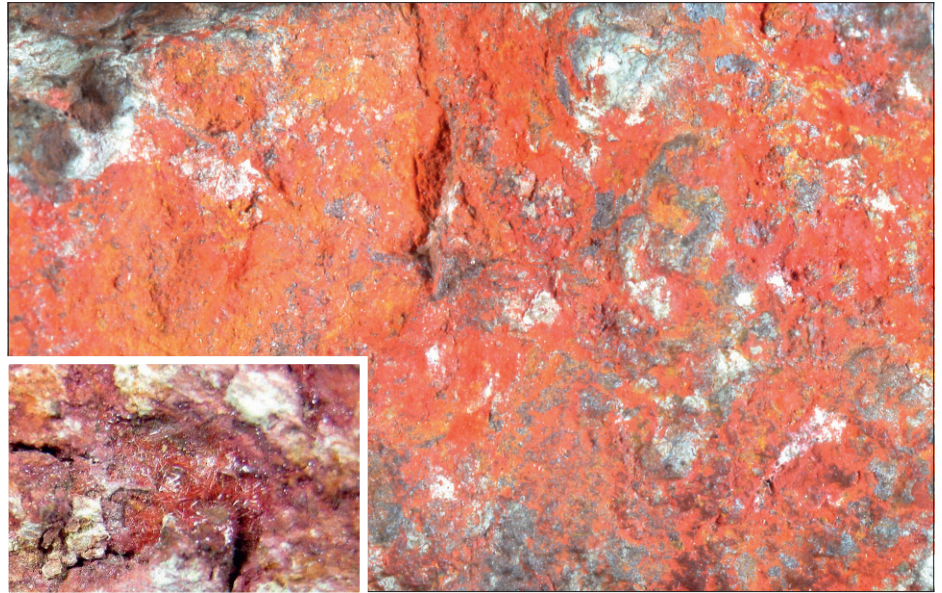
**Location (Powder format) – Cloncurry district, Queensland, Australia.**

Width of frame 8 cm.

**Location (Fibrous format) – (“Hair copper”) Ray Mine, Arizona, USA.**

Width of frame 2 cm.

Inset photograph provided by H. Huehne



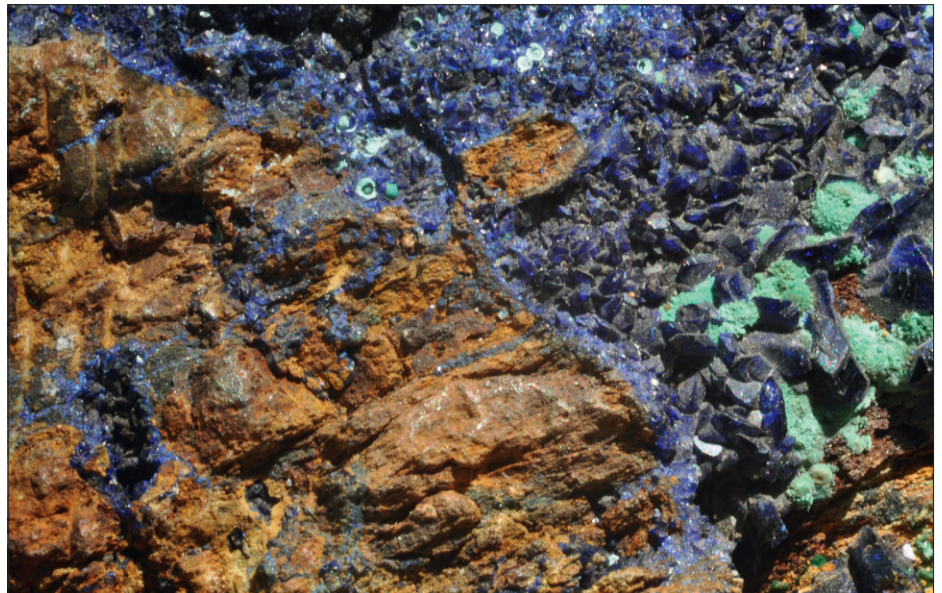
**Fig. 6.16 Malachite and azurite (Copper carbonates).**

Malachite (green) granular nodules precipitating on prismatic (wedge shapes) azurite crystals (deep blue).

The overall format is an infill vein.

**Bisbee, Arizona, USA.**

Width of frame 5 cm.



**Fig. 6.17 Malachite (Copper carbonate).**

Finely layered crustiform.

Botryoidal at the larger scale.

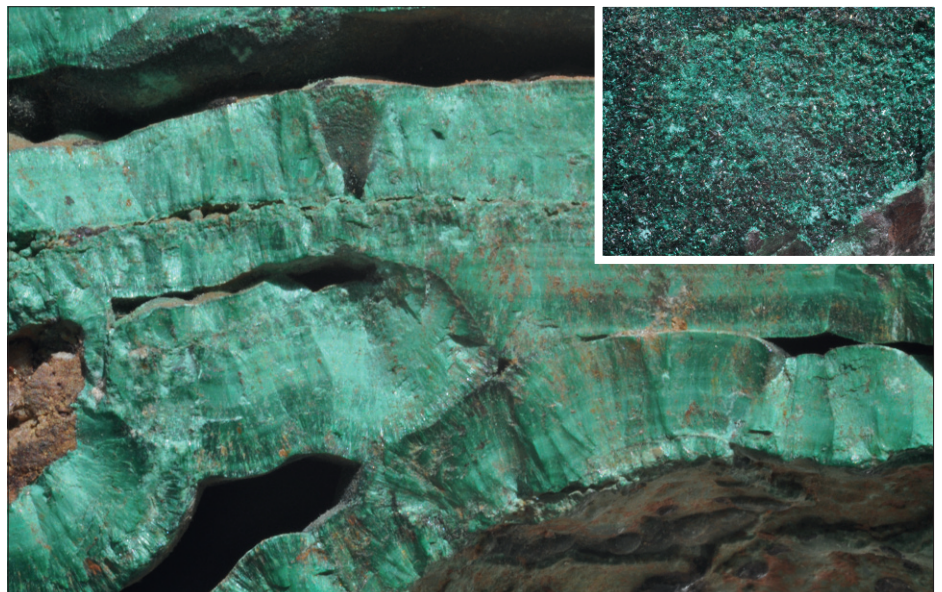
The inset shows typical fine prismatic malachite crystals ranging from dark to blue green in colour.

**Location (botryoidal) – Warren district, Arizona, USA.**

Width of frame 6.5 cm.

**Location (crystals) Unknown.**

Width of frame 4 cm.



**6.4.6 Malachite  $\text{Cu}_2\text{CO}_3(\text{OH})_2$ . Copper carbonate (established usage ignores hydroxyl input) (Figures 6.12, 6.14, 6.16–6.17).**

Malachite occurs in a wide variety of formats. Green “stains” are the most common, although fibrous, acicular, botryoidal, mamillary and more rarely stalactitic forms are well-represented. Crystals are rare and prismatic. The colours can vary from a pale to a deep green. As might be anticipated malachite is common in limestone/carbonate terrains, and commonly forms over a wide area, such that it is not always directly over the subsurface deposit, again the maxim that “a little bit of copper goes a long way” is worth recalling. Common associated minerals are cuprite, tenorite, chrysocolla and azurite.

**6.4.7 Azurite  $\text{Cu}_3(\text{CO}_3)_2(\text{OH})_2$ . Copper carbonate (established usage ignores hydroxyl input) (Figure 6.16).**

Azurite is far less abundant than the green carbonate (malachite) but equally conspicuous with an azure blue colour. It is common as “stains”, but has many different habits including massive, nodular and stalactitic. Crystals are prismatic commonly bladed with wedge-shaped terminations. Azurite colours tend to fade slightly over time when exposed to the light. The common associated minerals are malachite and cuprite.

**6.4.8 Chrysocolla  $(\text{CuAl})_2\text{H}_2\text{Si}_2\text{O}_5 \cdot n(\text{H}_2\text{O})$ . Hydrated copper silicate (Figure 6.18–6.19).**

Chrysocolla along with azurite and malachite are the big three most commonly occurring green/blue copper minerals. They form in similar slightly alkaline pH ranges. Chrysocolla is instantly recognised via the characteristic glassy blue-green colour, which is valued as a semi-precious gemstone. It has a variety of habits ranging from massive to globular and botryoidal, although crystals are unknown. The composition is also slightly variable and it is best regarded as a mineraloid. It occurs mostly as an infill mineral, although alteration styles also occur. It should also be noted that in the super arid zones of the Atacama region, chrysocolla is usually strongly associated with malachite, brochantite, antlerite and atacamite.

**6.4.9 Chalcantite  $\text{CaSO}_4 \cdot 5\text{H}_2\text{O}$ . Hydrated copper sulphide (Figure 6.20).**

Chalcantite is relatively rare in gossanous zones, as it is water soluble. However, as with minerals such as atacamite and brochantite, it is much more common in arid environments. The colour and metallic taste are usually sufficient for identification.

**6.4.10 Atacamite  $\text{Cu}_2\text{Cl}(\text{OH})_3$ . Copper hydroxychloride (Figure 6.21).**

Atacamite is unstable in fresh meteoric water, and thus in most circumstances is an unlikely discovery in surficial exposures. However, it is abundant in some regions, forming a major constituent of the supergene oxide zones in many of the copper deposits located in the Atacama desert in northern Chile (e.g. Chiquicamata, Escondida, Mantos Blancas, Radomiro Tomic and Spence).

Atacamite is a dark green mineral forming fine-grained cryptocrystalline aggregates and visible crystals, occurring as infill within veins, cracks and also as corrosion coatings

on preexisting copper minerals. Crystals are usually rather small with prismatic or equant habits, which are difficult to identify in the field. The striated faces on larger crystals are occasionally helpful, but it is easily confused with its dimorph paratacamite  $(\text{CuZn})_2\text{Cl}(\text{OH})_3$ , as well as its common associates brochantite, and antlerite. Gypsum is another closely associated mineral.

Atacamite requires saline solutions for its formation and a hyperarid climate for preservation. Its mode of formation has been the subject of considerable recent research (Reich et al, 2008) and gypsum saturated copper-bearing ground waters are the prime candidates derived either by evaporation of meteoric water, or pumping of deeper-seated basinal brines via locally active fault systems. Very recent formation is recorded (Reich et al, 2008) via the formation of atacamite coatings on miner's boots left underground in the early 1900s.

#### 6.4.11 Brochantite $\text{CuSO}_4(\text{OH})_6$ . Copper hydroxysulphate (Figure 6.22)

Brochantite is similar to atacamite in that it can form in prolific amounts within supergene oxide zones in hyperarid climates. It is commonly a major associate of atacamite, with the pair forming the bulk of oxide ore at locations such as Spence in the Atacama desert of northern Chile. The mineral is emerald green in colour and ranges from fine granular forms to prismatic or acicular crystals. It is usually present as infill, is effectively indistinguishable from antlerite (see below) and fine-grained atacamite.

#### 6.4.12 Antlerite $\text{Cu}_3\text{SO}_4(\text{OH})_4$ . Copper hydroxysulphate (Figure 6.23)

As indicated above, atacamite is so similar to brochantite in both colour and habit, that hand specimen differentiation is effectively impossible. They are also common associates in the supergene oxide zones of northern Chile, and antlerite is allegedly of rare occurrence. However, checking of brochantite zones at Chiquicamata revealed substantial antlerite. Despite the name, the mineral bears no resemblance to antlers, but is named from original discovery at the Antler mine, in Arizona, USA. Atacamite, brochantite and antlerite are sometimes referred to as the desert minerals.

#### 6.4.13 Rare secondary copper minerals

- Chalcocyanite  $\text{Cu}(\text{Fe},\text{Al})_6(\text{OH})_2 \cdot 4\text{H}_2\text{O}$ . Hydrated copper aluminium phosphate (Figure 6.29).
- Dioptase  $\text{CuSiO}_2(\text{OH})_2$ . Copper hydroxysilicate (Figure 6.24).
- Linarite  $\text{PbCuSO}_4(\text{OH})_6 \cdot \text{H}_2\text{O}$ . Hydrated lead copper sulphate. (Figure 6.25).
- Olivenite  $\text{Cu}_2\text{AsO}_4\text{OH}$ . Copper hydroxyarsenate (Figure 6.27).
- Pseudomalachite  $(\text{Cu}_5\text{PO}_4)_2(\text{OH})_4$ . Copper hydroxyphosphate (Figure 6.28).
- Turquoise  $\text{CuAl}_6(\text{PO}_4)_4(\text{OH})_8 \cdot 4\text{H}_2\text{O}$ . Hydrated copper aluminium phosphate (Figure 6.26).

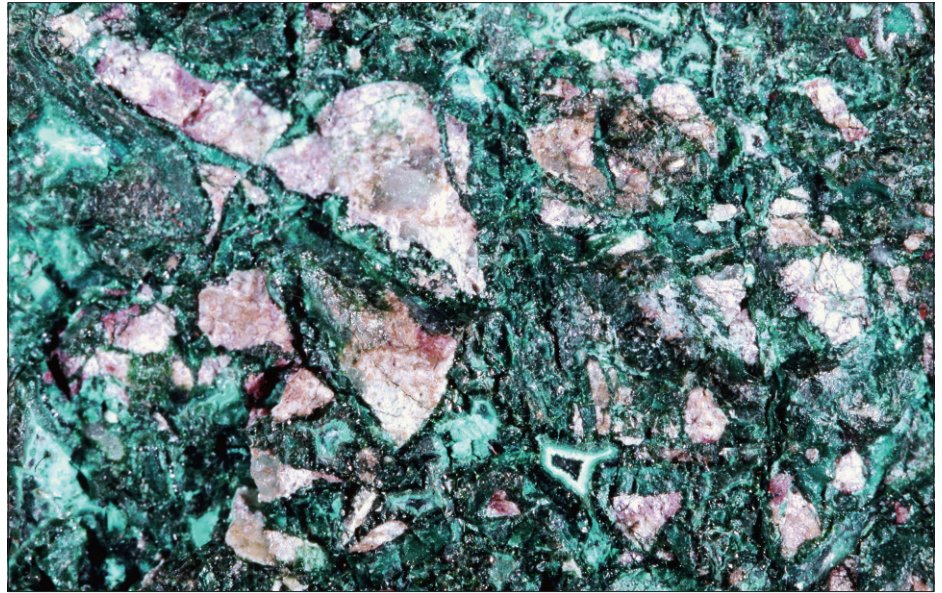
As previously mentioned the list of copper-bearing secondary minerals is extremely long, and most of these exhibit blue or green colours. It is very difficult to be familiar with all of the permutations and the main minerals listed above (malachite, azurite, chrysocolla along with the oxides) will usually be sufficient to characterise the gossan/leached capping as being copper-related. Similarly, even an unidentified green/blue mineral would suggest copper, arsenic or possibly nickel origins, which would at least be of some value, taken in context. A few of the rarer minerals are pictured here.

#### 6.4.14 Supergene copper sulphides (Figures 6.30–6.32)

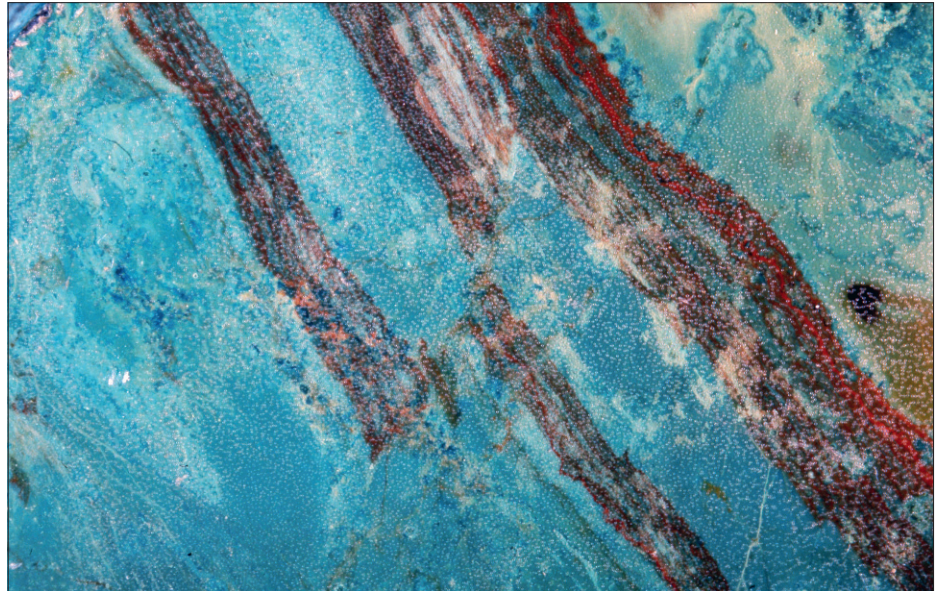
The major supergene sulphides (chalcocite  $\text{Cu}_2\text{S}$ , and covellite  $\text{CuS}$ ) are rarely seen at surface, forming via replacive processes immediately below water table level. They are usually fine-grained dark black/blue and although chalcocite is of more common occurrence, it is very common to find the two intermixed. The fine-grained nature may render visual distinction impossible. The supergene process is covered more extensively later in this book, as it has implications for both boxwork development and limonite compositions in porphyry copper systems. Chalcocite and covellite are however common on mine dumps, as they formed attractive high value copper ores for early small-scale miners. Chalcocite and covellite can also form as primary minerals.



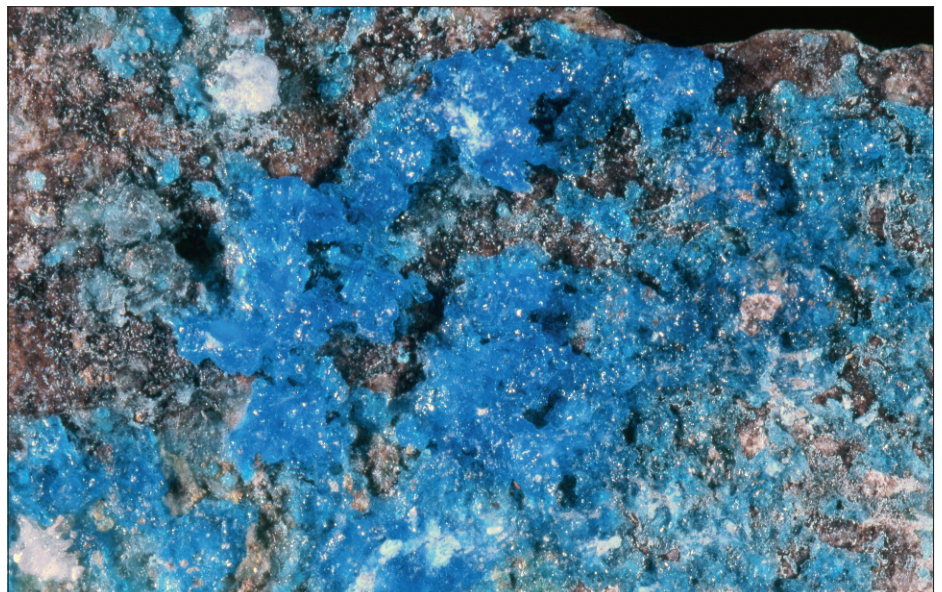
**Fig. 6.18 Chrysocolla (Hydrated copper silicate).** Cryptocrystalline semi-botryoidal infill in breccia cavities and staining (alteration of wall rocks). The blue-green colours usually provide a clear distinction from the green colours of malachite. **Miami mining district, Arizona, USA.** Width of frame 6 cm.

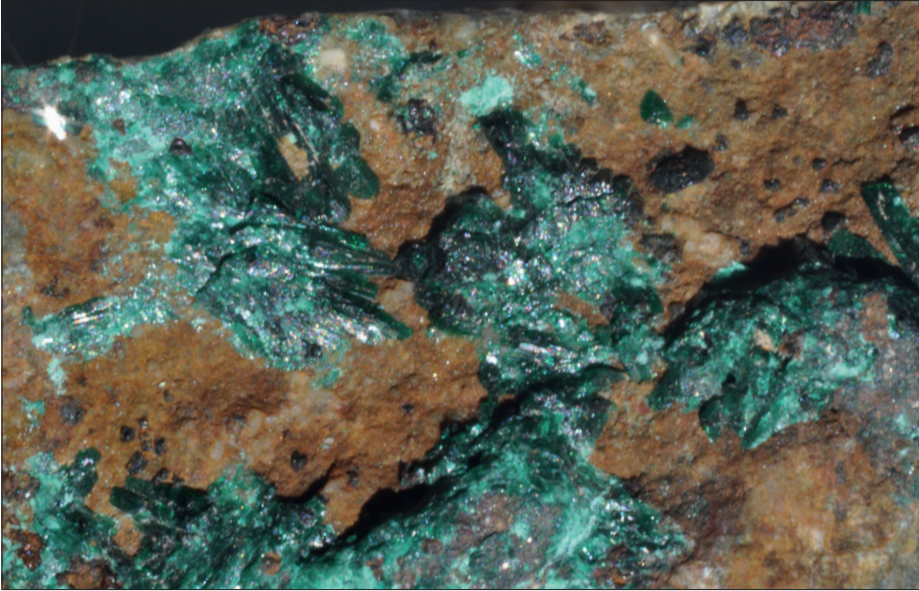


**Fig. 6.19 Chrysocolla (Hydrated copper silicate).** Fine-grained blue-green chrysocolla replacing clay-rich sediments. **Locality unknown.** Width of frame 8 cm.



**Fig. 6.20 Chalcantite (Hydrated copper sulphate).** Chalcantite readily dissolves in water and hence is rare in leached capping and gossans. However it is common in the ultra dry regimes of some desert regions (especially the Atacama region of Chile, which is also a major copper province). The characteristic colour and tendency to form prismatic to tabular crystals are the main identifying characteristics, together with a metallic taste. The substance is poisonous if ingested in any quantity. **Escondida mine, Chile.** Width of frame 6 cm.





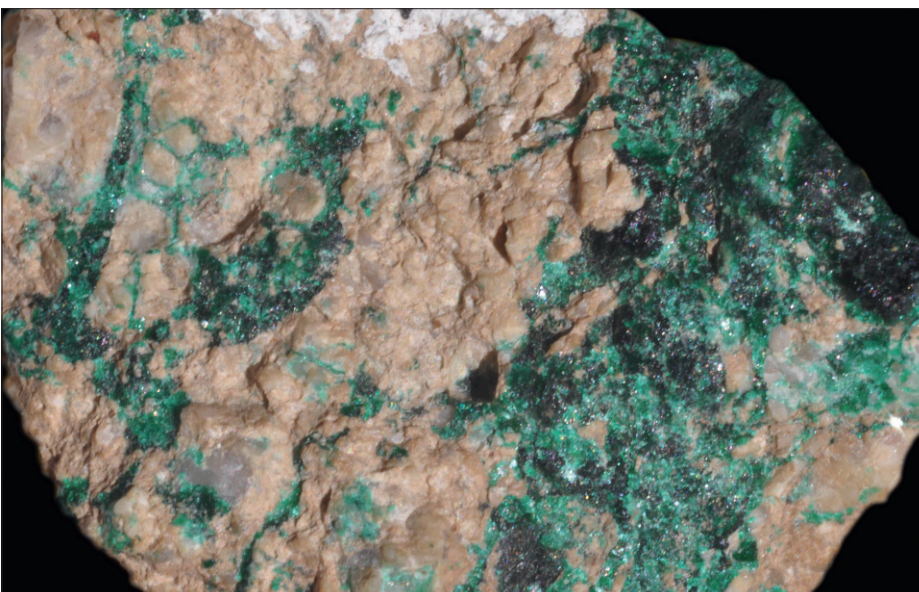
**Fig. 6.21 Atacamite (Copper hydroxychloride).** Although rare in general the mineral is common in the hyperarid Atacama region of northern Chile. It commonly forms a significant percentage of supergene copper oxide ore zones, and can be very difficult to distinguish from its common associates brochantite and antlerite. A striation on the crystal faces is helpful on larger prismatic specimens. Unstable in water.

**Mantos Blancos, Chile.**  
Width of frame 4 cm.



**Fig. 6.22 Brochantite (Copper hydroxysulphate).** Acicular rosettes nucleating on fine-grained quartz. The mineral is similar to atacamite, in that it favours arid climates. It can also occur in darker more prismatic habits, where it becomes very difficult to distinguish from antlerite, atacamite or even malachite.

**Mt Oxide, Queensland, Australia.**  
Width of frame 5 cm.



**Fig. 6.23 Antlerite (Copper hydroxysulphate).** Veins with infill crystals. This crystal format is also common in brochantite. The common format, similar colours and typically fine-grained nature, renders visual distinction from brochantite impossible.

**Chiquicamata, Chile.**  
Width of frame 3 cm.



**Fig. 6.24 Dioptase (Copper hydroxysilicate).**

Dioptase is extremely rare and the author has never seen any in a surficial gossan-leached capping. It is included here to complete the range of green copper colours.

Dioptase is a minor gemstone, and its sub-adamantine lustre augments the dark blue-green emerald colours. The colour alone is sufficient for positive identification. It tends to occur in desert regions.

**Location unknown.**

Width of frame 4 cm.



**Fig. 6.25 Linarite (Hydrated lead copper sulphate).**

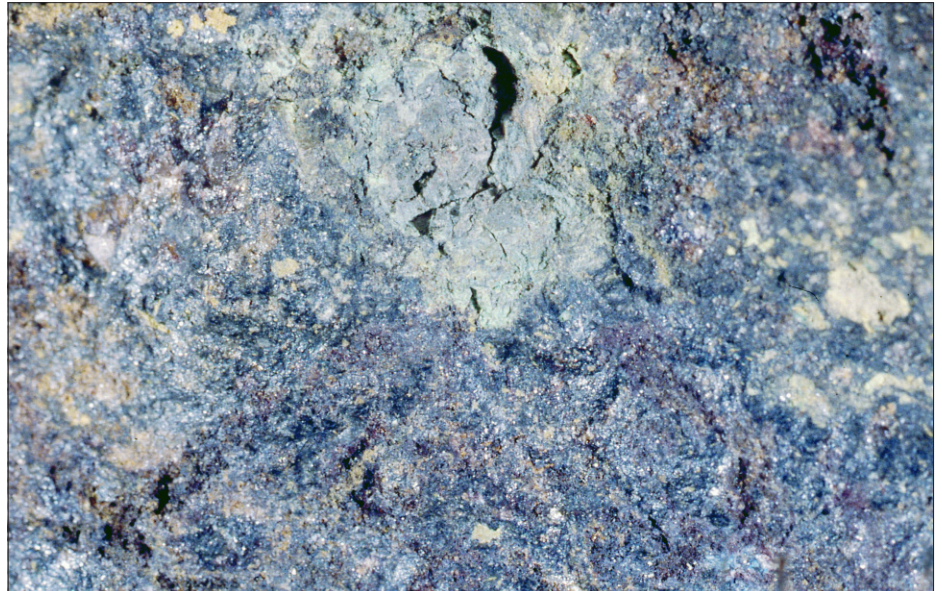
This rare mineral is included to remind the reader that there are a host of minor rare copper minerals with red, green and blue colours.

This particular specimen is a little dark in colour. The normal azure blue examples are much coveted by rare mineral collectors.

Despite many years of gossan examination, the author has only seen one field example.

**Cloncurry region, Queensland, Australia.**

Width of frame 5 cm.



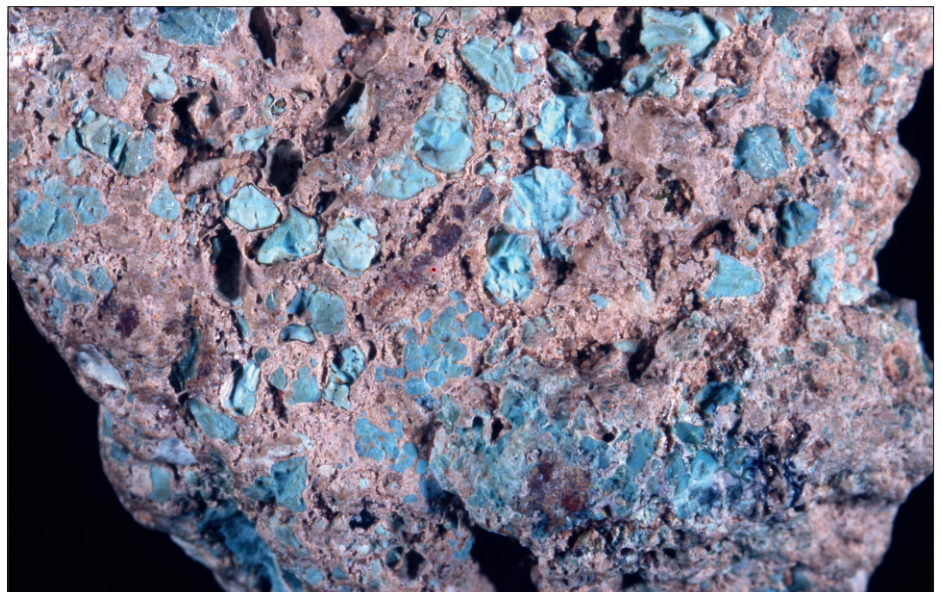
**Fig. 6.26 Turquoise (Hydrated copper aluminium phosphate).**

Turquoise is a semiprecious gemstone which is relatively rare. It occurs as a cryptocrystalline mineral, usually in arid regions, with a wide variation in colour (white, blue-green to sky blue).

It occurs as infill within veins and cavities, in and around oxidising copper deposits.

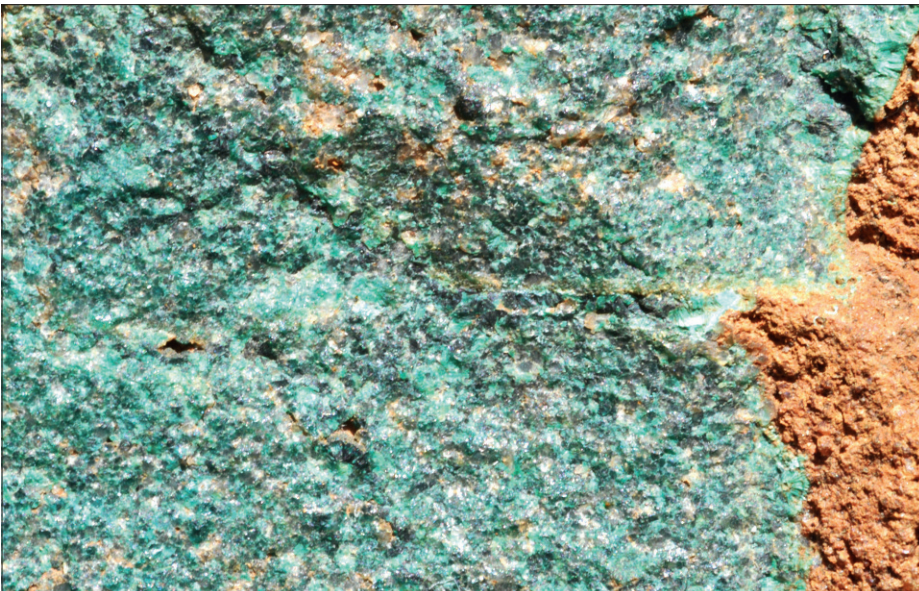
**Location unknown.**

Width of frame 4 cm.

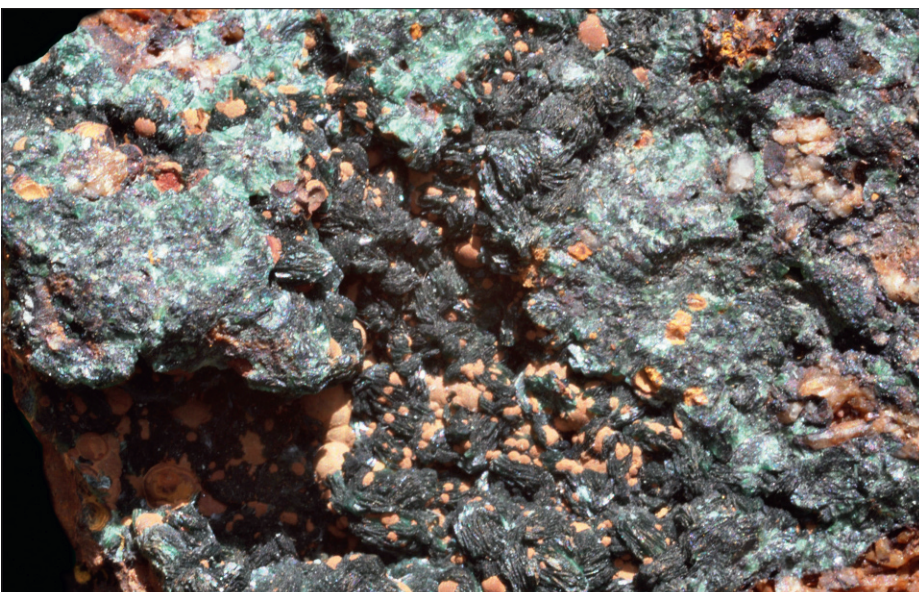




**Fig. 6.27 Olivinite (Copper hydroxyarsenate).** This specimen has been included as a further reminder that there are numerous rare green coloured copper minerals. It is impossible/impractical to become familiar with all of them. For instance olivinite is isostructural with libethenite (copper hydroxyphosphate) and adamite (zinc hydroxyarsenate) which also may exhibit similar green colours. The green colour here would arouse copper or arsenic suspicions regarding these scattered prismatic crystals.  
**United North Australia mine, Herberton, Queensland, Australia.**  
Width of frame 3 cm.



**Fig. 6.28 Pseudomalachite (Copper hydroxiphosphate).** The name reflects the ability of this phosphate mineral to resemble malachite. It even has similar botryoidal and prismatic shapes. Fortunately it is rare and even when misidentified is still indicating nearby copper. There are also two green very rare polymorphs (ludjibaite and reichenbachite)  
**Mt Kelly, Mt Isa district, Queensland, Australia.**  
Width of frame 3 cm.



**Fig. 6.29 Chalcosiderite (Hydrated copper iron aluminium phosphate).** A final example to illustrate the large number of green copper-bearing minerals. This phosphate is very rare.  
**Laurdum, Greece.**  
Width of frame 3 cm.

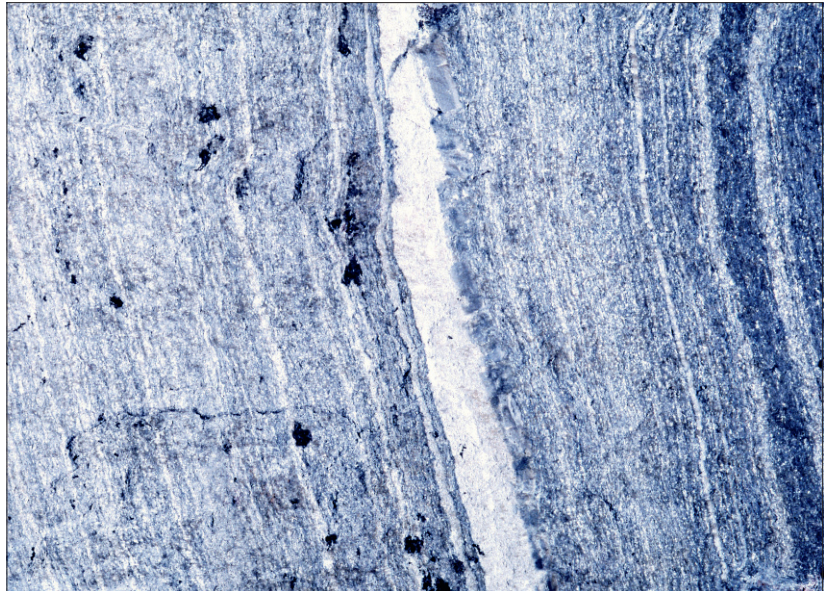
**Fig. 6.30 Chalcocite (Copper sulphide).**

It is important to understand the supergene process as it may play a major role in the surficial end-product. Supergene chalcocite forms via the replacement of preexisting sulphides. It rarely survives to reach the surface gossan-leached capping zones. It may convert to cuprite, or alternatively to red haematite. The cuprite may then alter to haematite. Copper is released into solution and may reprecipitate as secondary "oxide zone" minerals.

The dark spots here were originally pyrite in fine-grained carbonaceous shale.

**Location unknown.**

Width of frame 8cm.

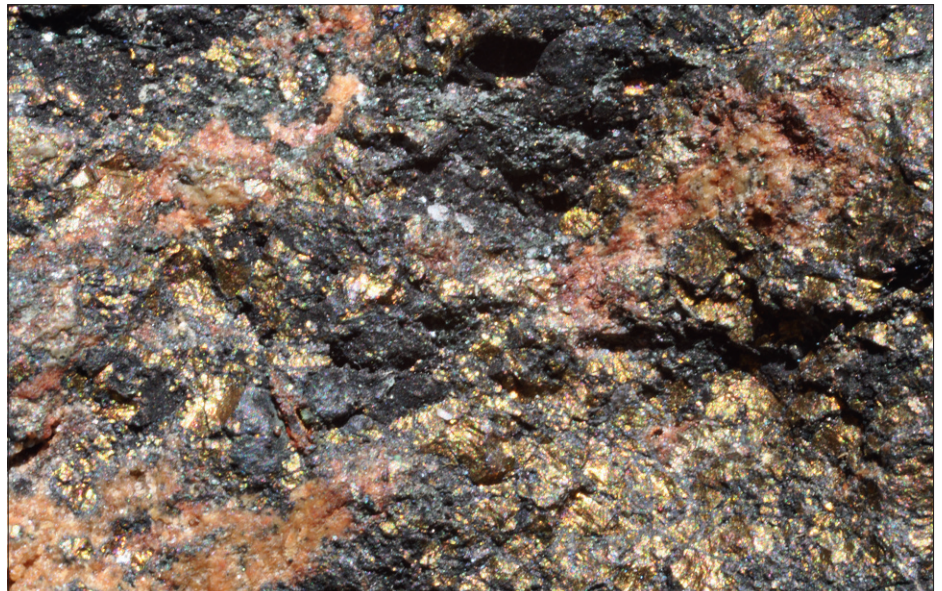


**Fig. 6.31 Chalcocite (Copper sulphide).**

Chalcocite dark matt black-blue replacing (altering) chalcopyrite. The process produces very fine-grained alteration products which may take on a sooty appearance. The end result here would be massive fine-grained chalcocite.

**Location unknown.**

Width of frame 4 cm.

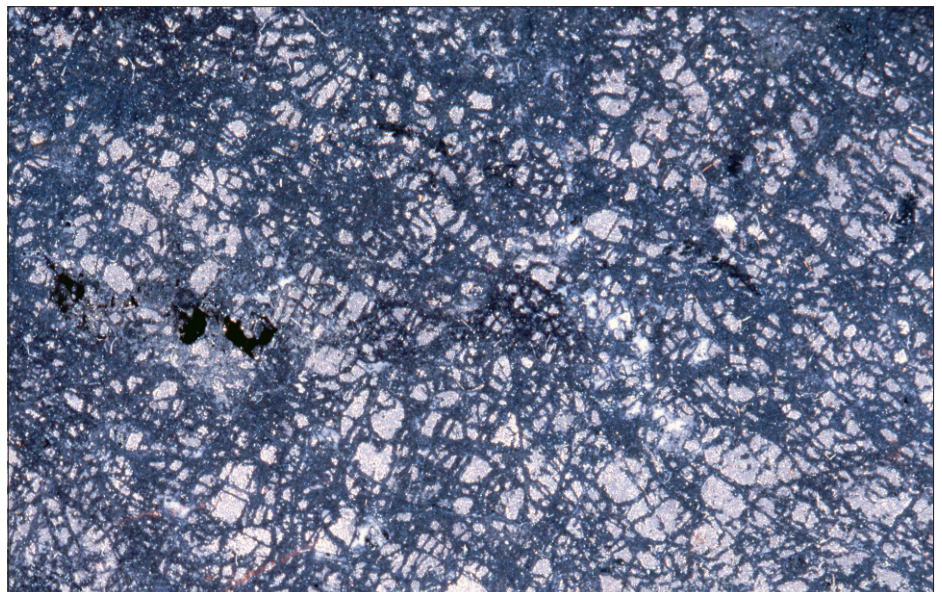


**Fig. 6.32 Chalcocite and covellite (Copper sulphide).**

Chalcocite and covellite replacing arsenopyrite. The alteration-replacement process forms a combination of very fine-grained chalcocite and covellite, which cannot be individually identified by the naked eye. The strong blue tinge here could suggest a high proportion of covellite but is not diagnostic.

**United North Australia-Balgammon mine, Herberton, Queensland, Australia.**

Width of frame 6 cm.



## 6.5 Lead (Figures 6.33–6.44)

### 6.5.1 General aspects

| Group     | Name           | Formula  |
|-----------|----------------|--|
|           | Litharge       | PbO  |
| Oxides    | Minium         | Pb <sub>3</sub> O <sub>4</sub>                                       |
|           | Massicot       | PbO  |
| Carbonate | Cerussite      | PbCO <sub>3</sub>  |
| Sulphates | Anglesite      | PbSO <sub>4</sub>  |
|           | Plumbojarosite | PbFe <sub>6</sub> (SO <sub>4</sub> ) <sub>4</sub> (OH) <sub>12</sub> |
| Arsenates | Mimetite       | PbClPb <sub>4</sub> (AsO <sub>4</sub> ) <sub>3</sub>                 |
|           | Pyromorphite   | PbClPb <sub>4</sub> (PO <sub>4</sub> ) <sub>3</sub>                  |
| Molybdate | Wulfenite      | PbMoO <sub>4</sub>   |
| Chromate  | Crocoite       | PbCrO <sub>4</sub>   |

The most common secondary lead minerals are anglesite (lead sulphate), cerussite (lead carbonate) and the various oxides (massicot, minium, and litharge). Their production and abundance ultimately relate back to the presence of galena in the primary ore. There are numerous ore types which contain galena, all of which contain different mineral associations and different grain sizes within a wide range of geological environments. These include:

- Skarns.
- Carbonate replacements.
- Mississippi Valley styles.
- Large-scale stratabound deposits of debated origin including Broken Hill types, Mt Isa relatives, and volcanogenic ores.
- Numerous veins relating to epithermal (especially intermediate-sulphidation) systems and also veins peripheral to porphyry copper, tin and other magmatic connected systems.

It is noted that many of the above link to carbonate-related environments, and that mineralogical types range from pyrite-rich to pyrite-poor with most having a strong connection to zinc concentrations in the form of sphalerite. Environments such as

McArthur River are noted for fine-grained sulphides, whilst skarns and Mississippi Valley types are typically coarse-grained.

### 6.5.2 Anglesite $\text{PbSO}_4$ . Lead sulphate (Figures 6.36–6.38).

Anglesite tends to be the favoured product in regimes with low pH and high  $\text{SO}_4^{2-}$ , a situation which is favoured by high pyrite in the system and production of acid conditions around the water table level.

Anglesite is common in oxidising lead-rich systems, occurring as small white grey prismatic crystals and earthy masses. The mineral is isomorphous with barytes and literally occurs in scores of different formats. Crystals tend to have bright high lustre faces. The author would confess to continual problems of differentiating small transparent crystals of cerussite v anglesite.

Anglesite commonly replaces galena via a rim alteration process, resulting in concentric layers of anglesite. This precipitates at low pH conditions, and is relatively insoluble. This fine-grained rim of insoluble material may eventually protect the galena from further oxidation, and is probably the reason why galena is commonly found as residual cores within concentrically layered anglesite. The process is referred to as the armoring of galena (Reichert, 2009). The anglesite shells alter to massicot and then red lead oxides approaching surface probably via direct exposure to oxygen. The anglesite shells may also contain/alter? to cerussite.

### 6.5.3 Cerussite $\text{PbCO}_3$ . Lead carbonate (Figures 6.33–6.35).

In contrast to anglesite, cerussite formation is favoured within domains of higher pH (5–7), and is particularly abundant in carbonate dominant terrains. Like anglesite it may form in a wide range of formats from an almost unnoticeable fine granular style to spectacularly reticulate crystalline prismatic (matchstick) forms. Cerussite is mostly colourless to white-grey, and like anglesite is characterised by being soft and also heavy when in bulk formats.

The granular format is the most common, appearing as fine-grained translucent grains forming as a direct replacement/alteration of galena. A coarse sugar-like texture is the usual end result. It is also suspected to replace anglesite (Reichert, et al, 2008).

Cerussite also occurs as infill, which is usually coarser-grained filling open fractures and cavities. The “matchstick” style format is much admired, although the small transparent platy style is very innocuous and commonly overlooked when only one or two small (gypsum-like) crystals are present.

Cerussite and galena are known to coexist with non-oxidised zinc sulphides, and local galvanic coupling has been suggested as an alternative mode of formation (Szczeuba and Sawlowicz, 2009).

**6.5.4 Lead oxides (Figures 6.36, 6.38–6.39).**

**Massicot PbO. Lead oxide. Litharge PbO. Lead oxide.  
Minium Pb<sub>3</sub>O<sub>4</sub>. Lead oxide.**

These three minerals are best treated as a group. Massicot is extremely common in and around lead gossans. It seems to form mostly as a direct replacement of anglesite and/or granular cerussite. The result is fine grained yellow to orange, sugary/crumblly material commonly tinged with red. Some occurrences are earthy, heavy, granular lumps. Massicot commonly converts directly into red/orange materials (pseudomorphing the granular massicot formats) which are mixtures of red lead oxides ± limonite. It is rarely possible to distinguish litharge from minium and in the field yellow and red lead oxides are probably the best terms to utilise. Most of the red is dull coloured and primarily minium. Crystals of minium and litharge (the dimorph of massicot) are extremely rare, and the author has yet to find one in the field. The yellow/red/orange lead colours are however very common and easily confused with jarosite, haematite, limonite tones. However, the granular textures and ovoid clustering (see later boxwork sector) may arouse strong suspicions.

**6.5.5 Plumbojarosite PbFe<sub>6</sub>(SO<sub>4</sub>)<sub>4</sub>(OH)<sub>12</sub>. Lead/iron hydroxysulphate (Figure 6.40).**

This fine-grained yellow substance is present in many lead gossans. It is unfortunately indistinguishable from the yellow lead oxide and identification always requires laboratory backup for positive recognition. The term “yellow lead” products is a safe option.

**6.5.6 Pyromorphite PbCl Pb<sub>4</sub>(PO<sub>4</sub>)<sub>3</sub>. Lead chlorophosphate (Figure 6.42) and Mimetite PbCl Pb<sub>4</sub>(AsO<sub>4</sub>)<sub>3</sub>, Lead chloroarsenate (Figure 6.41).**

These two minerals form part of a solid solution series which also includes the extremely rare red vanadate (vanadinite). Both minerals commonly occur as infill crystalline products easily identified via their hexagonal prism shapes, with blunt hexagonal ends, and curving barrel-like formats.

Their colours range from shades of pale green, through yellow – orange to brown. Although colour is not diagnostic the phosphate-rich end-members tend to be green, with browner colours favouring mimetite.

**6.5.7 Rare secondary lead minerals.**

**Wulfenite PbMoO<sub>4</sub>. Lead molybdate (Figure 6.44).  
Crocoite PbCrO<sub>4</sub>. Lead chromate (Figure 6.45).**

Both of these minerals are exceptionally rare and only included here as their bright red-orange crystal colours attract attention in specific localities. Crocoite forms prismatic bright red crystals and wulfenite commonly presents as orange thin tabular plates.



**Fig. 6.33 Cerussite (Lead carbonate).**

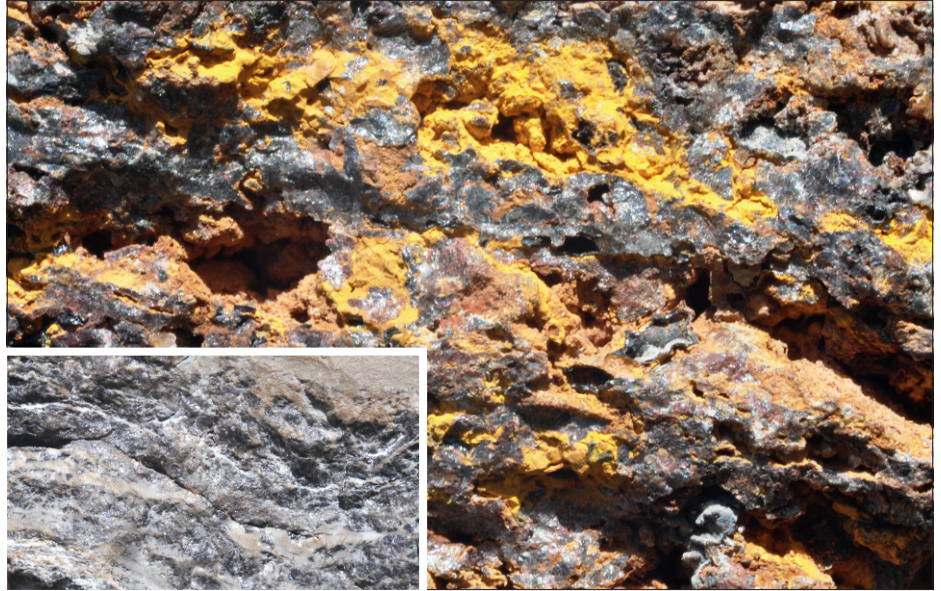
Granular fine-grained grey cerussite ( $\pm$  anglesite?) – The vitreous lustre is prominent, reflecting an original package of fine-grained galena and calcareous shale. Surface sample.

**Mt Isa, Queensland, Australia.**

Width of frame 4 cm.

The inset shows the same situation some metres below the surface.

Width of frame 4 cm.



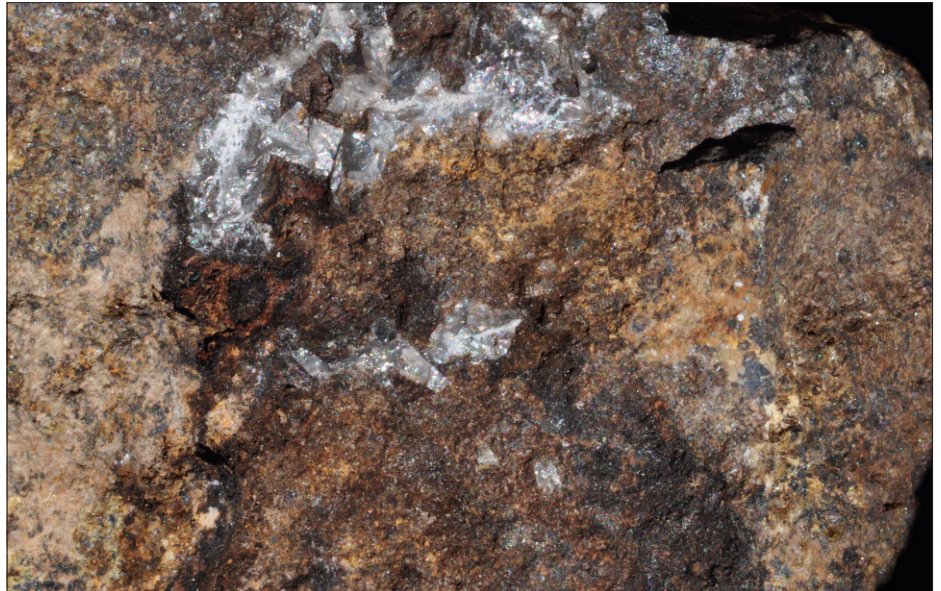
**Fig. 6.34 Cerussite (Lead carbonate).**

Inconspicuous small clear crystals with a high vitreous lustre. Easily scratched due to low hardness.

This is a common format and easy to overlook when only a few crystals are available in iron-stained gossan.

**Mt Isa, Queensland, Australia.**

Width of frame 2.5 cm.



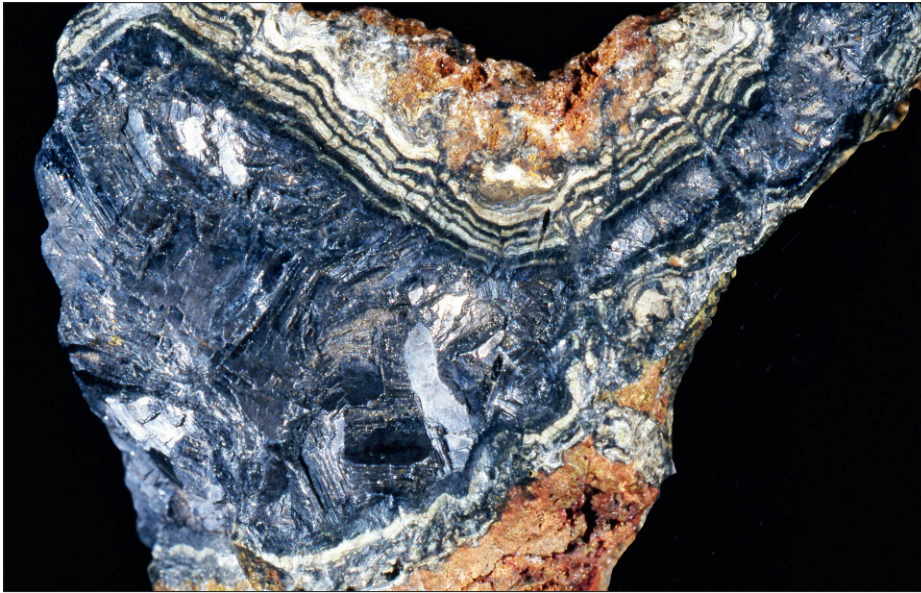
**Fig. 6.35 Cerussite (Lead carbonate).**

Instantly recognizable from the matchstick-like format, with a strong vitreous lustre. These crystals have precipitated on transported botryoidal limonite.

**Location unknown.**

Width of frame 4.5 cm.





**Fig. 6.36 Anglesite (Lead sulphate).**  
Layers of anglesite forming via replacement /alteration of galena (centre). The rhythmic pattern suggests regular changes in conditions. The reddish outer coating is composed of iron-stained lead oxides.  
**Location unknown.**  
Width of frame 7 cm.



**Fig. 6.37 Anglesite (Lead sulphate).**  
A cut slab showing remnants of galena (grey with dark border zones) being progressively replaced by layers of anglesite. The galena is sometimes referred to as armoured (protected from further oxidation, whilst progressing up profile – explaining residual galena found in some surface exposures). However in this case the materials have moved below a water table level, allowing the formation of supergene chalcocite covellite (dark alteration rim on galena – see top of frame)  
**Location unknown.**  
Width of frame 6 cm.



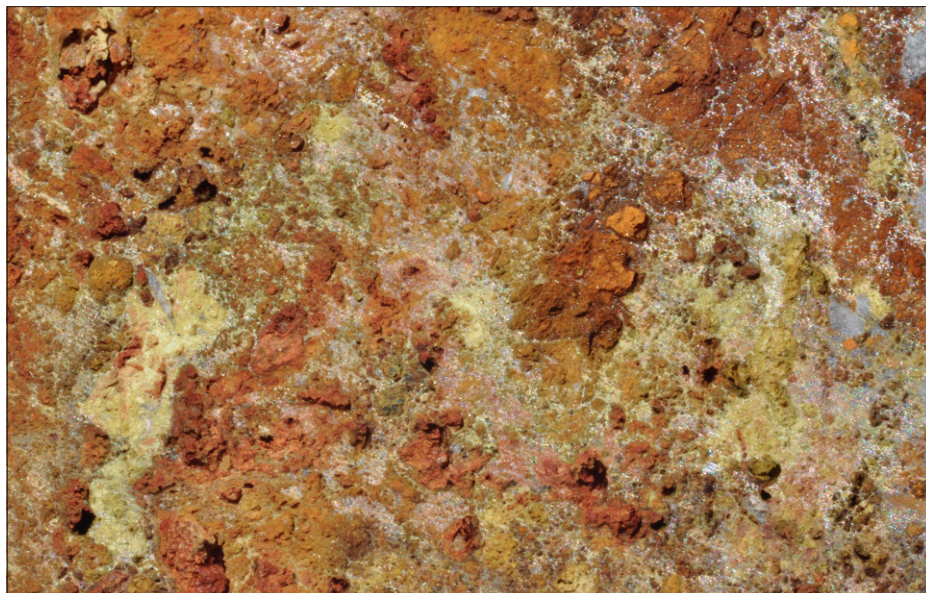
**Fig. 6.38 Galena, anglesite, massicot and minium.**  
Galena (dark grey – centre) surrounded by replacive cerussite (paler grey-glassy). The original cerussite layers (see [Figures 6.37–6.38](#)) are replaced by massicot (yellow) at near surface levels, and finally at surface the massicot is replaced by minium (red).  
**Argentine district, Queensland, Australia.**  
Width of frame 3.5 cm.

**Fig. 6.39** Massicot and minium (Lead oxides).

Complete oxidation of in situ galena (see [Figures 6.36–6.38](#)) to the yellow and red lead oxides. The red-orange colours are essentially minium  $\pm$  iron oxides, derived from the very near-surface oxidation of massicot (yellow). Fresh galena remnants can be found upon breaking open some gossan exposures. There are several yellow lead powdery products (see below) and laboratory work is required for positive identification.

**Argentine district, Queensland, Australia.**

Width of frame 5 cm.

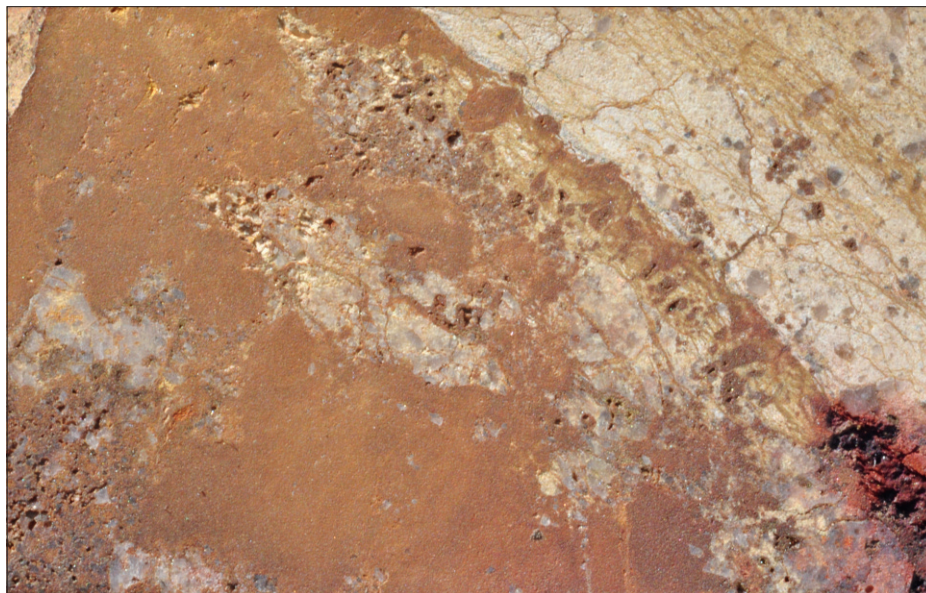


**Fig. 6.40** Plumbojarosite (Lead iron hydroxysulphate).

Plumbojarosite occurs as a yellow-orange earthy powder and as such is not distinctive enough to be identified with any certainty in the field. It is essentially similar to massicot, jarosite and some other lead compounds. The best that can be done is to mentally register the possibility of lead in the system and suspect galena as the source. Plumbojarosite is isomorphous with jarosite.

**Reward copper mine, Charters Towers, Queensland, Australia.**

Width of frame 5 cm.



**Fig. 6.41** Mimetite (Lead chloroarsenate).

Mimetite is the arsenic end-member of the pyromorphite (lead chlorophosphate) series. Good crystals are common for the series, with characteristic curved barrel-shaped forms. The colours are variable from shades of brown to green. In general the green shades indicate the pyromorphite end-members, although distinction via colour is unreliable. There is also a rare red vanadium end member-vanadinite.

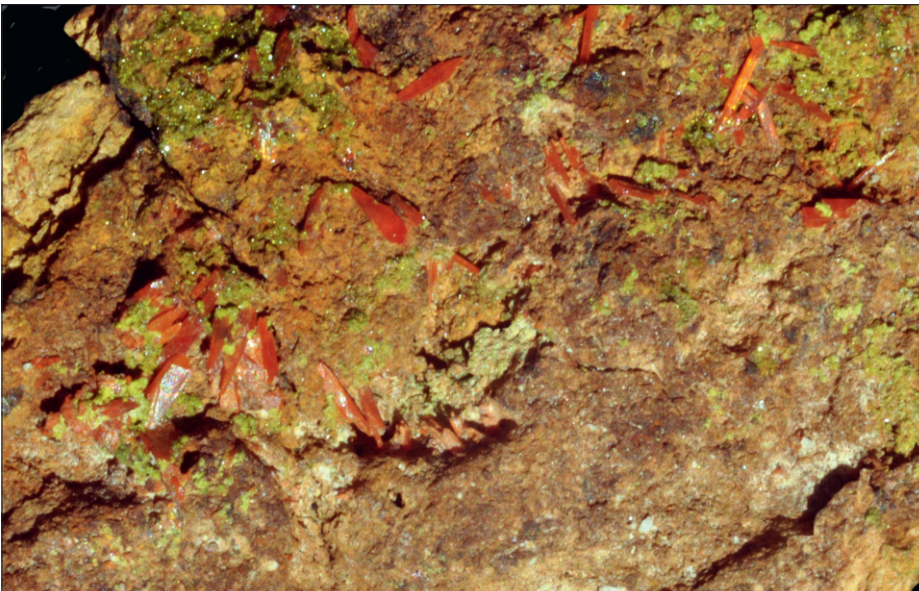
**Location unknown.**

Width of frame 6.5 cm.





**Fig. 6.42 Pyromorphite (Lead chlorophosphate).** Classic barrel-shaped crystals, which are characteristic of the pyromorphite-mimetite-vanadinite series (see also [Figure 6.41](#)). **Location unknown.** Width of frame 4 cm.



**Fig. 6.43 Crocoite (Lead chromate).** A very rare but very striking red prismatic mineral. The associated green mineral is probably pyromorphite. **Platts prospect, Dundas, Tasmania, Australia.** Width of frame 6 cm.



**Fig. 6.44 Wulfenite (Lead molybdate).** Another very rare lead mineral. **Ruggles Mine, New Hampshire, USA.** Width of frame 5 cm.

## 6.6 Zinc (Figures 6.45–6.53)

### 6.6.1 General aspects

| Element       | Name         | Formula  |
|---------------|--------------|--|
| Carbonates    | Smithsonite  | ZnCO <sub>3</sub>  |
|               | Hydrozincite | Zn <sub>5</sub> (CO <sub>3</sub> ) <sub>2</sub> (OH) <sub>6</sub>  |
|               | Rosasite     | (Cu,Zn) <sub>2</sub> CO <sub>3</sub> (OH) <sub>2</sub>   |
|               | Aurichalcite | (Zn,Cu) <sub>6</sub> (CO <sub>3</sub> ) <sub>2</sub> (OH) <sub>6</sub>   |
| Silicates     | Hemimorphite | (Zn) <sub>4</sub> Si <sub>2</sub> O <sub>7</sub> (OH) <sub>2</sub> · 2H <sub>2</sub> O                         |
|               | Willemite    | Zn <sub>2</sub> SiO <sub>4</sub>   |
| Zinc smectite | Sauconite    | Na <sub>0.3</sub> (Zn,Mg) <sub>3</sub> (SiAl) <sub>4</sub> O <sub>10</sub> OH <sub>2</sub> · 4H <sub>2</sub> O |
| Arsenate      | Adamite      | Zn <sub>2</sub> AsO <sub>4</sub> OH  |

Zinc secondary minerals are particularly common in carbonate-rich terrains, where deposits referred to as non-sulphide zinc deposits are composed almost entirely of zinc secondary minerals (Hitzman et al, 2003). The commonly occurring minerals (listed below) are smithsonite (zinc carbonate), hemimorphite (hydrous zinc silicate), hydrozincite (hydrous zinc carbonate) and various zinc-rich clays such as sauconite (zinc smectite). The “zinc oxide” deposits contain varying proportions of these minerals representing varying degrees of supergene (oxide) enrichment and with advancing metallurgical techniques have become of minor recent commercial interest.

Several of their gossanous exposures are shown in Figures 3.4–3.9, and in terms of secondary minerals it is quite common for all of the above minerals to occur in one exposure, or even within a single hand specimen. Some excellent reviews of “zinc oxide” deposit styles are available, and essentially initially acid oxidising fluids quickly take zinc into solution and it may be fixed locally as “zinc oxides” either around the site of sphalerite dissolution via interaction with carbonate host rocks, or alternatively transported some distance away before depositing via both replacive and infilling processes (Balassone et al, 2008, Reichert, 2009, Hitzman et al, 2003, Reichert and Borg, 2007).

### 6.6.2 Smithsonite ZnCO<sub>3</sub> . Zinc carbonate (Figures 6.45–6.47).

Smithsonite along with hemimorphite and hydrozincite is stable under intermediate to high pH values buffered by carbonate rocks. It is by far the most commonly occurring of the zinc secondary minerals and is renowned for its somewhat bewildering array of crystal habits and wide variations in colour. The colours range from colourless to pastel shades of buff, brown and pale green. The crystal habits are poorly understood ranging from the extremely common concretionary-botryoidal, colloform-crustiform

formats, to a wide range of crystal shapes. It is not uncommon to find 3–5 generations of smithsonite in one deposit, ranging from rhombohedral, scalenohedral, subhedral, granular (rice grain smithsonite) to botryoidal. Smithsonite is usually present as infill, although it does replace both sphalerite and carbonate host rocks.

**6.6.3 Hemimorphite  $Zn_4S_{12}O_7(OH)_2 \cdot H_2O$ .  
Hydrated zinc silicate (Figure 6.48).**

Hemimorphite is a very common associate of smithsonite implying a considerable overlap of depositional conditions. It seems especially common where some opaline/cryptocrystalline siliceous wall-rocks are involved.

Hemimorphite derives its name from the hemimorphic development of its crystal faces (crystals can be terminated by different faces). Its common radiating/cockscorn fan-like format is very distinctive, but hemimorphite ranges from massive, through granular, to botryoidal/reniform. Colours range from colourless to white, blue and pale green. It is considerably less soluble in near-surface acid conditions than smithsonite and once formed will persist to surface in various iron-rich gossans (see Figure 3.12, McArthur River).

**6.6.4 Hydrozincite  $Zn_5(CO_3)_2(OH)_6$ . Zinc hydroxycarbonate (Figure 6.49).**

Hydrozincite is also a common associate of the “zinc oxide” assemblages and is usually found as late-stage white massive, earthy, powdery aggregates and encrustations on smithsonite and/or hemimorphite. It also occurs prolifically on some old mine dumps as a white coating (zinc bloom) on sphalerite.

Hydrozincite occupies a similar medium to high pH field as smithsonite. Smithsonite is considered to require relatively high  $PCO_2$  conditions ( $>10^{1.41}$  atm) in excess of atmospheric  $CO_2$  partial pressures created by neutralisation of the oxidising solutions by carbonate host rocks, whereas hydrozincite precipitation is favoured at close to atmospheric pressures. Hydrozincite forms both as an infill and replacive mineral.

**6.6.5 Zincian clays. Sauconite  $Na_{0.3}(Zn,Mg)_3(SiAl)_4O_{10}(OH)_2 \cdot 4H_2O$   
(Figure 3.7).**

There are several ill-defined smectite style clays containing zinc. Sauconite seems the most common, occurring as a reddish-brown-yellow clay. It is not identifiable without detailed laboratory follow up. Given the problems with this group of clays, the general term zincian clay is best applied tentively to field situations.

**6.6.6 Rare secondary zinc minerals.**

**Rosasite  $(Zn,Cu)_2(CO_3)(OH)_2$ . Aurichalcite  $(Zn,Cu)_5(CO_3)_2(OH)_6$ . Zinc copper hydroxycarbonates**

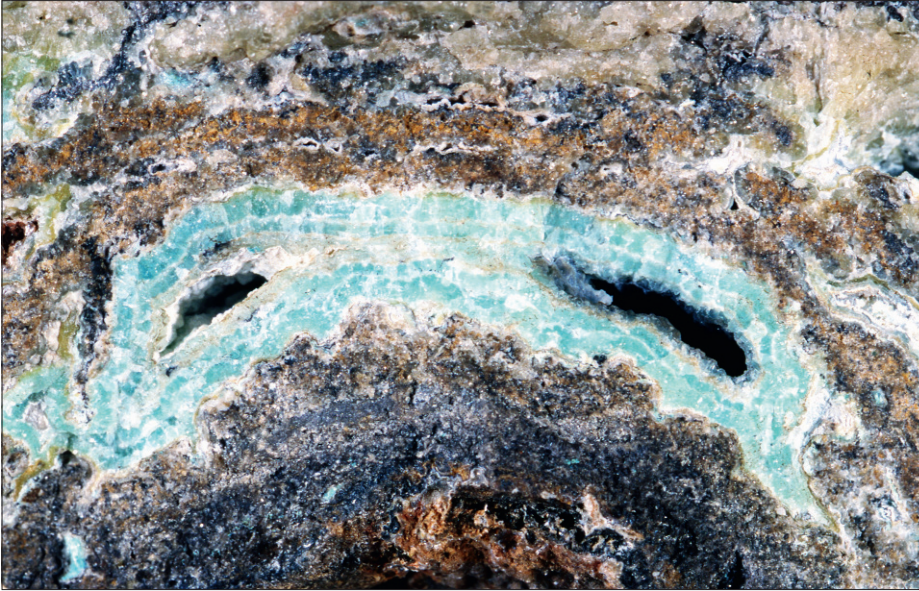
**Adamite  $Zn_2AsO_4OH$ . Zinc hydroxyarsenate.**

**Willemite  $Zn_2SiO_4$ . Zinc silicate**

- Rosasite  $(Zn,Cu)_2(CO_3)(OH)_2$  and Aurichalcite  $(Zn,Cu)_5(CO_3)_2(OH)_6$  are zinc copper hydroxycarbonates (Figures 94–95) and deserve inclusion here, as although rare they commonly occur with the trio, smithsonite-hemimorphite-hydrozincite as spectacularly coloured encrustations.

Rosasite is blue-green, usually found as a fibrous mineral in globular aggregates. Aurichalcite tends to be in prismatic or spherical aggregates with a sky-blue colour attracting immediate attention.

- Adamite  $Zn_2 AsO_4 OH$ . Zinc hydroxyarsenate (Figure 6.50). Adamite is isomorphous with olivenite, and also occurs with smithsonite and hemimorphite. It may also associate with scorodite (iron arsenate). It forms wedge-shaped prisms, commonly grouping in clusters, or even botryoidal formats. It is mostly colourless and very difficult to visually recognise with any confidence.
- Willemite  $Zn_2 SiO_4$ . Zinc silicate (Figure 6.53). Willemite is a rare zinc mineral which occurs both as a primary and secondary mineral. It is colourless to white, but can crystallise in many shades, ranging from green through light blue to burgundy red or mahogany. The author has never located any willemite within a gossanous assemblage. The famous mine-scale occurrence at Beltana in South Australia was discovered via surficial occurrence of concretionary-botryoidal to massive lumps occurring at surface. This occurrence was considered supergene originally, but identified as probably primary upon excavation (Groves et al, 2003).



**Fig. 6.45** Smithsonite (Zinc carbonate).

This photograph illustrates many of the extremely variable pastel colours of smithsonite. The entire plate contains successive infilling layers of botryoidal smithsonite, ranging through shades of grey and brown, to the very common green. The late encrusting white mineral is hydrozincite (a late zinc hydroxycarbonate – see text).

**Location unknown.**  
Width of frame 8 cm.



**Fig. 6.46** Smithsonite (Zinc carbonate).

Typical botryoidal texture with the very common pale green colour.

**Location unknown.**  
Width of frame 2 cm.



**Fig. 6.47** Smithsonite (Zinc carbonate).

Rare crystal format.

**Location unknown.**  
Width of frame 2 cm.



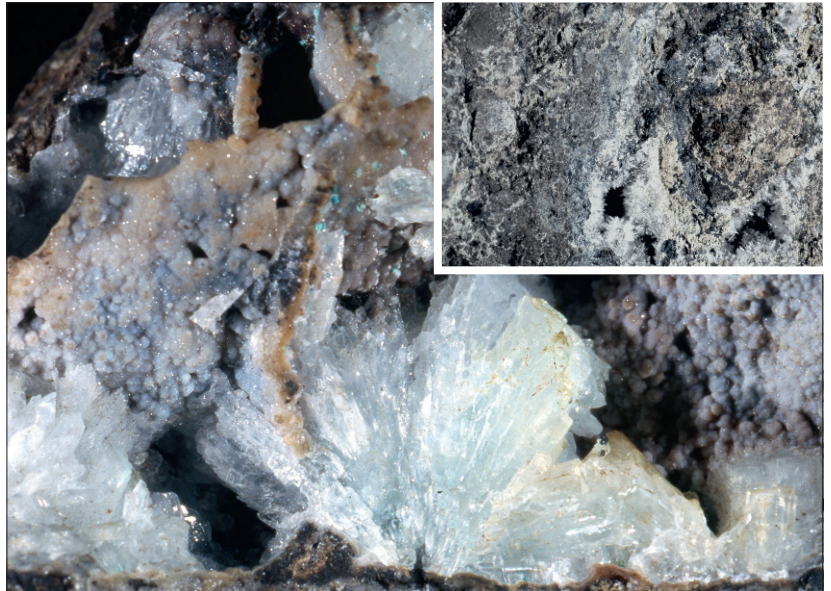
**Fig. 6.48 Hemimorphite (Hydrated zinc silicate).**

Hemimorphite takes on a range of habits, but is usually recognised by its propensity to form fan-like clusters (colourless to pale green). It is commonly associated with both smithsonite, seen here as botryoidal grains, and white hydrozincite. It is relatively insoluble. (see [Figure 3.12](#)). The crystals are commonly very small, as depicted in the inset (see bottom right corner for a very typical occurrence).

**Location**—Muldiva, Queensland, Australia.  
Width of frame 4.5 cm.

**Inset:**—Yanque, Chile.

Width of frame 1.5 cm. (see [Figure 3.4](#)).

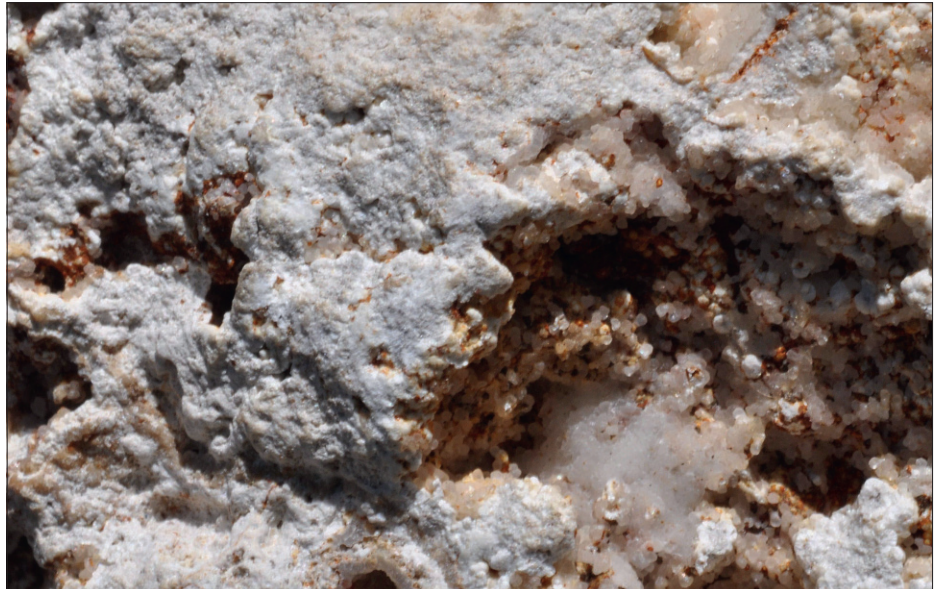


**Fig. 6.49 Hydrozincite (Zinc hydroxycarbonate).**

White powdery coatings are the most common format, encrusting either hemimorphite or smithsonite. Hydrozincite is also commonly seen coating sphalerite on mine dumps (zinc bloom).

**Rabl Karuten, Austria.**

Width of frame 3 cm.



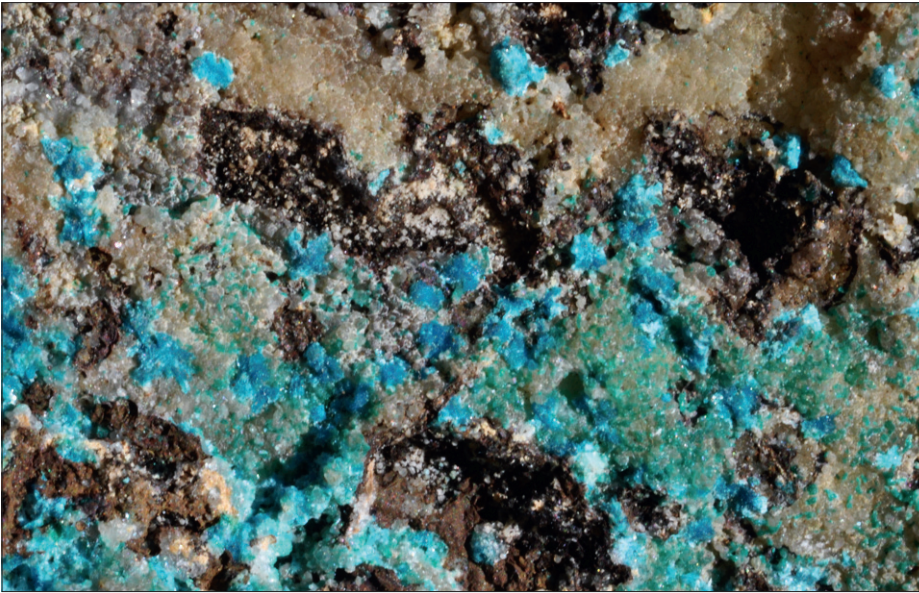
**Fig. 6.50 Adamite (Zinc hydroxyarsenate).**

Adamite occurs in association with smithsonite and hemimorphite as a rare mineral. It can be conspicuous via yellow or lime green colours, but mostly inconspicuous as shown here by the colourless crystals. It might be suspected if more common arsenic minerals such as scorodite are located, together with lead secondary minerals (i.e. an inferred lead-zinc-arsenic association).

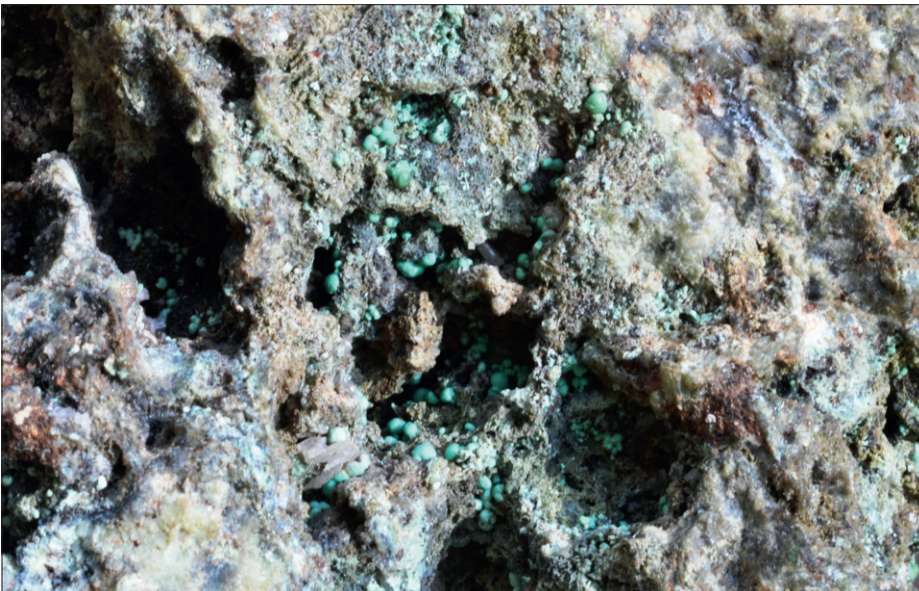
**Location unknown.**

Width of frame 3.5 cm.

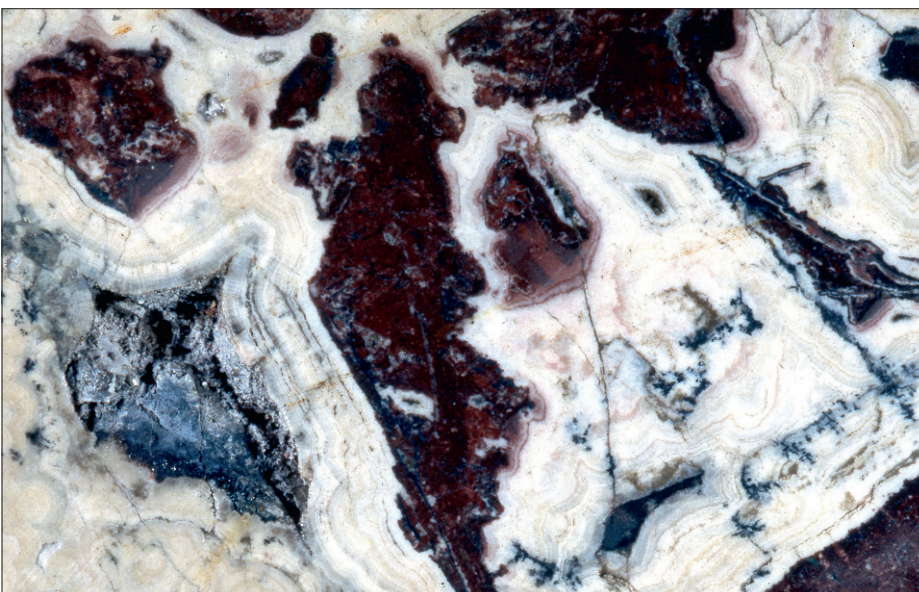




**Fig. 6.51 Aurichalcite (Zinc copper hydroxycarbonate).** Aurichalcite is easily recognised via its colour and close association with other zinc minerals such as smithsonite, hemimorphite, hydrozincite and rosasite. It tends to form in short fibrous clusters. **Location unknown.** Width of frame 4.5 cm.



**Fig. 6.52 Rosasite (Copper zinc hydroxycarbonate).** Like aurichalcite, rosasite is easily recognised when in globular format via its colour and association with smithsonite, hemimorphite, hydrozincite and aurichalcite. **Ewan district, Queensland, Australia.** Width of frame 2 cm.



**Fig. 6.53 Willemite (Zinc silicate).** Willemite occurs both as a supergene and primary mineral with a wide range of both colour and format. This concretionary botryoidal form was found at surface as a heavy rock, indicating the site of a mineable zinc occurrence. The deposit is now considered to be a primary willemite occurrence (insoluble in near surface environs). **Beltana, South Australia, Australia.** Width of frame 6 cm.

## 6.7 Nickel (Figures 6.54–6.56)

### 6.7.1 Garnierite, Gaspeite, and Annabergite

| Group     | Name        | Formula   |
|-----------|-------------|---|
| Silicate  | Garnierite  | Ni,Mg hydrosilicate (variable formula)  |
| Carbonate | Gaspeite    | (Ni,Mg,Fe) CO <sub>3</sub><br>“Nickel carbonate”  |
| Arsenate  | Annabergite | Ni <sub>3</sub> (As <sub>2</sub> O <sub>7</sub> ) <sub>2</sub> · H <sub>2</sub> O<br>Hydrated nickel arsenate |

The nickel secondary minerals are very helpful in assessing gossanous exposures in that they are mostly apple green and very visual.

Most weathered ultramafic rocks, especially when lateritic will develop infill veins, cavities and infilled by green nickel compounds. These are essentially silicates with variable amounts of nickel and magnesium which are collectively called “garnierite”. They do not reflect sulphide nickel ore, but the high trace nickel content of ultramafic rocks. Under lateritic conditions there is a possibility of lateritic nickel ore developing lower in the profile. Sulphide nickel ores tend to produce masses of iron (limonite) with rare nickel secondary minerals.

Gaspeite (nickel carbonate) is common in the West Australian nickel province, where despite its very obvious apple green colours was not recognised as a nickel sulphide indicator until 1964. The area had been well-prospected for gold, but the presence of a whole nickel province remained unknown.

Annabergite is also rather conspicuous and seems to be more commonly associated with Ni-Cu-Ag ores.

## 6.8 Arsenic (Figures 6.27, 6.41, 6.50, 6.55, 6.57–6.58, 6.67–6.68)

### 6.8.1 General aspects including scorodite Fe<sub>3</sub>AsO<sub>4</sub> · H<sub>2</sub>O. Hydrated iron arsenate

Arsenic containing secondary minerals are relatively common within gossans and leached cappings reflecting the underlying presence of arsenopyrite or alternatively arsenic-rich minerals associated with high-sulphidation deposits (eg. enargite).

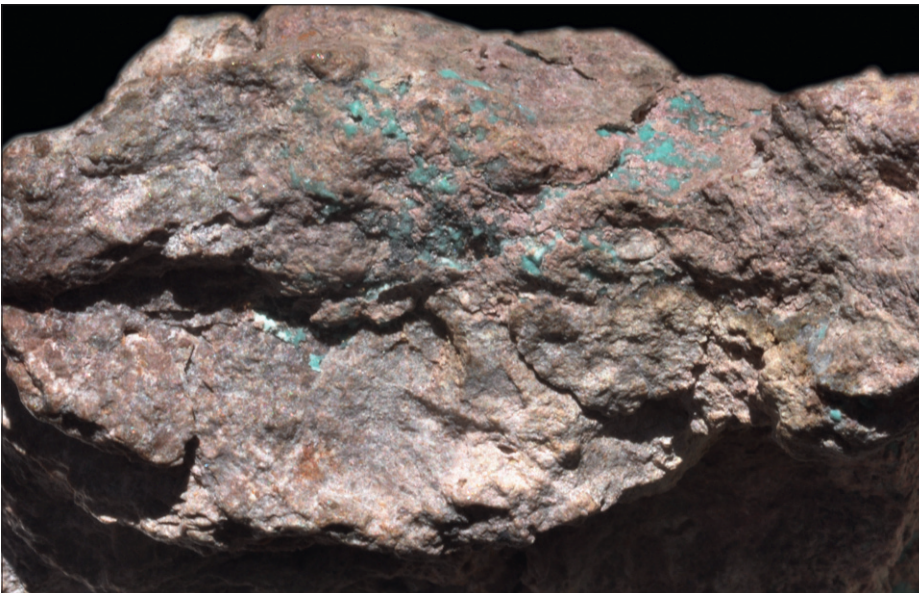
The various minerals are usually rare within individual exposures, forming as arsenates in combination with a wide range of other metals (Fe, Cu, Pb, Zn, Ni, Co). Many of these are illustrated in this text under the headings of the individual metals (Figures 6.27, 6.41, 6.50, 6.55, 6.57–6.58, and 6.67–6.68). The most prolific arsenic secondary mineral is scorodite (hydrated iron arsenate), which is characterised by the pale green colour and granular arborescent texture (Figure 6.57).



**Fig. 6.54 Gaspeite (Nickel-iron-magnesium carbonate).** This distinctive apple green mineral is of common occurrence within the siliceous ferruginous gossans of the sulphide nickel deposits of Western Australia. Despite the conspicuous colour, the significance of this mineral as a nickel indicator was not appreciated until the discovery of Kambalda in 1964. The mineral usually occurs as infill veins.

**Kambalda, Western Australia, Australia.**

Width of frame 6 cm.



**Fig. 6.55 Annabergite (Hydrated nickel arsenate).**

This relatively scattered powdery encrustation is noticeable via the bright green colour (nickel bloom). It is usually an oxidation product derived from niccolite (Nickel arsenide).

Common in specific localities with nickel arsenic associations, such as the Kupferschiefer in Germany and the Sudbury region, Ontario, Canada.

**No locality given.**

Width of frame 6 cm.



**Fig. 6.56 Garnierite ("Nickel-magnesium hydrosilicate").**

Many green veins, encrustations, and stains occur in and around weathered lateritic ultramafic rocks. They are of variable composition and given the generic name of garnierite. (Ni-bearing magnesium layer silicates).

**Noumea, New Caledonia.**

Width of frame 5 cm.

**Fig. 6.57 Scorodite (Hydrated iron arsenate).**

A very common mineral usually derived from arsenopyrite via direct oxidation, such that scorodite marks the original arsenopyrite position. The colour and fine granular texture is characteristic. The grains commonly appear to be stuck together in a texture termed arborescent by Blanchard (1968). The insoluble scorodite may convert to brown "limonite" at the surface interface.

**UNA mine, Watsonville, Queensland, Australia.**  
Width of frame 4 cm.



**Fig. 6.58 Erythrite (Hydrated cobalt arsenate).**

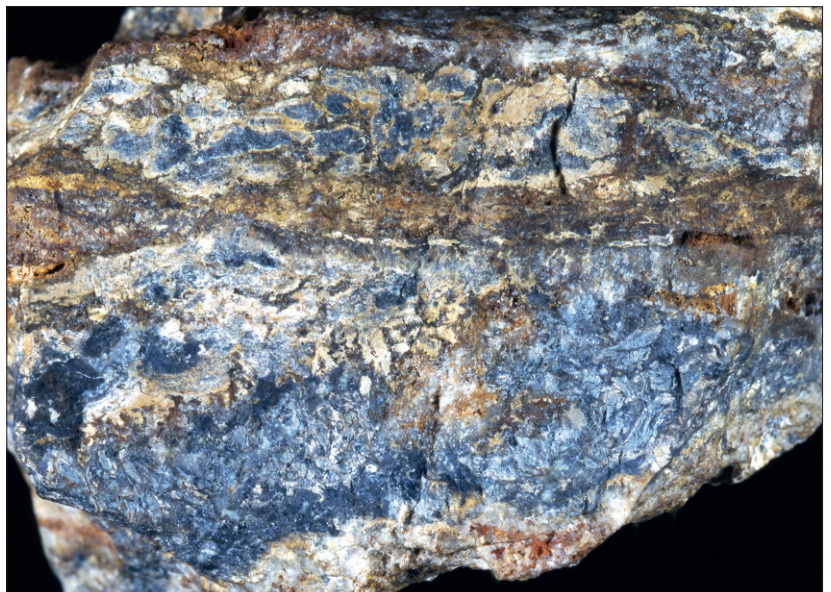
This mineral presents no recognition problems, with the crimson colour being very characteristic. Stellate aggregates are well-displayed on this specimen. Erythrite commonly forms via oxidation of cobalt-nickel-arsenic-silver deposits as in the Cobalt region of Ontario, Canada.

**Mt Cobalt, Queensland, Australia.**  
Width of frame 6.5 cm.



**Fig. 6.59 Stibiconite (Antimonic ochre, antimony oxide).**

Stibnite ( $Sb_2S_3$ ) oxidises directly to become replaced by a pale creamy – buff, fine-grained to massive “oxide” coating. This occurs at the surface (atmospheric) and varies from a thin coating, to total pseudomorphic replacement. Normally the first hammer blow, or a quick surface inspection, will reveal “fresh” metallic grey stibnite (lower sector of the accompanying plate). The author is not totally clear how this mineral differs visually from similar textured coatings of cervantite ( $Sb_2O_4$ ) and tends to use the terms interchangeably **Dimbulah district, Queensland, Australia.**  
Width of frame 8 cm.



## 6.9 The ochres

**Stibiconite**  $\text{Sb}_3\text{O}_6(\text{OH})$ . Antimony oxyhydroxide.

**Bismuth ochre**  $\text{Bi}_2\text{O}_3$  ( $\pm$  impurities). Bismuth oxide.

**Molybdic ochre**  $\text{Fe}_2(\text{MO}_4) \cdot n\text{H}_2\text{O}$ . Hydrated iron molybdate.

**Tungstic ochre**  $\text{WO}_3 \cdot \text{H}_2\text{O}$  (Figures 6.59–6.62)

| Composition                      | Name                                      | Formula   |
|----------------------------------|---|---|
| Antimony oxyhydroxide            | Stibiconite                               | $\text{Sb}_3\text{O}_6(\text{OH})$                      |
| Bismuth oxide                    | Bismuth ochre                             | $\text{Bi}_2\text{O}_3$ ( $\pm$ impurities)             |
| Arsenate Hydrated iron molybdate | Molybdic ochre, Ferrimolybdite, Molybdite | $\text{Fe}_2(\text{MO}_4) \cdot n\text{H}_2\text{O}$    |
| Hydrated tungstic oxide          | Tungstic ochre, Tungstite                 | $\text{WO}_3 \cdot \text{H}_2\text{O}$ (poorly defined) |

The term is utilised here to group a set of secondary minerals which are essentially oxides forming as thin crusts, actually coating the primary mineral. They seem to be a result of prolonged surface exposure, and are only of minor importance in a prospecting sense. In most cases the primary mineral is easily located as a relatively insoluble product at surface (molybdenite, wolframite, native bismuth, stibnite). In many cases the minerals are further protected, in that they tend to occur in quartz veins and are armoured from meteoric oxidising fluids.

## 6.10 Secondary silver minerals.

**Cerargyrite**  $\text{AgCl}$ . Silver chloride and rare halides

(Figures 6.63–6.64)

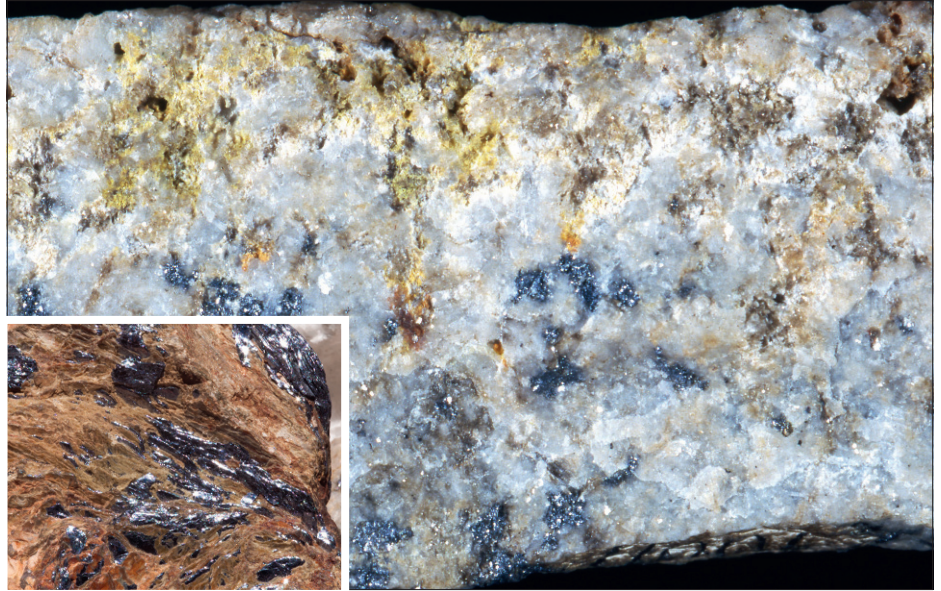
Despite several generations of textbooks indicating supergene silver enrichment, this process has recently been re-examined (Sillitoe, 2009) and considerable doubt expressed as to its effectiveness.

However, silver is well-documented as concentrating within the oxidised ore zone, where it appears as silver halides, argentojarosite, argentian plumbojarosite, and argentian beudandite and within manganese oxide concentrations.

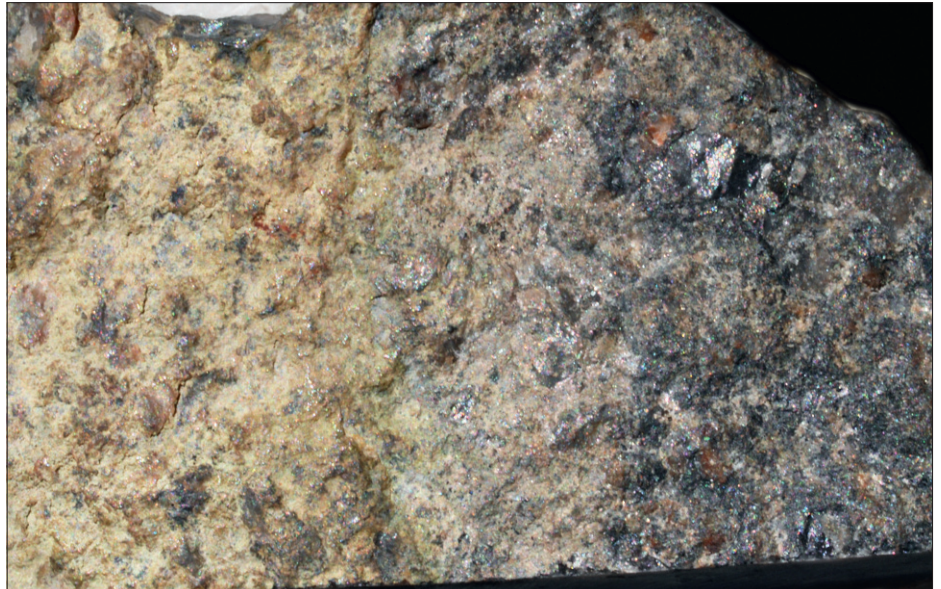
The silver halides are chlorargyrite (cerargyrite)  $\text{AgCl}$ , embolite,  $\text{Ag}(\text{ClBr})$  bromargyrite,  $\text{AgBr}$ , iodargyrite ( $\text{AgI}$ ) and rodembolite,  $\text{Ag}(\text{ClBrI})$ . Cerargyrite is the most common and is commonly referred to as “horn silver” (Figure 6.63). Native silver is also commonly reported, usually lower in the profile than the halides (Figure 6.64) and is famed for its wiry and fern-like habits.

Although the conditions causing the halides to precipitate are still being debated, it would appear that silver is relatively easily fixed in well-developed oxidised zones, with mostly insoluble products preventing further dissolution and transport to the supergene regime.

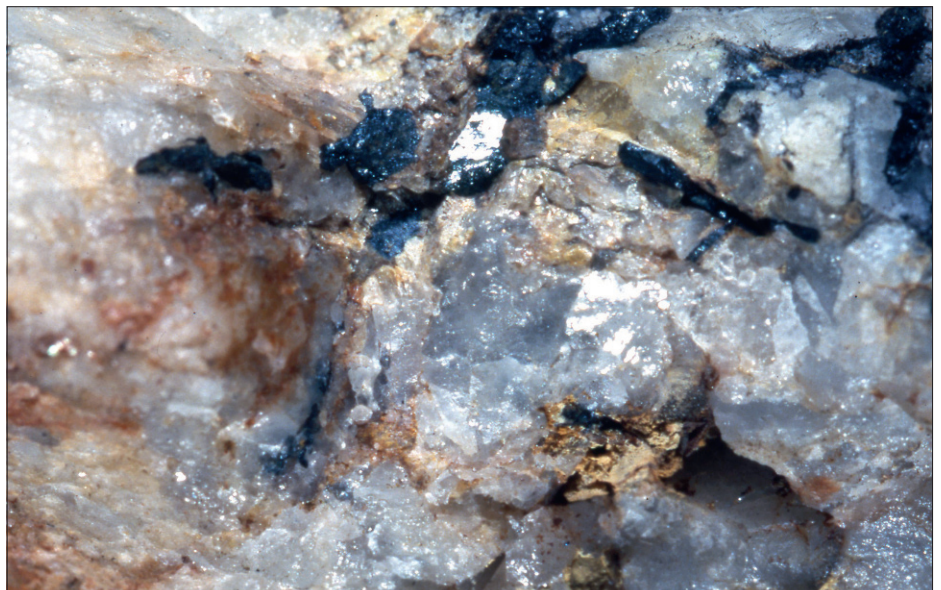
**Fig. 6.60 Molybdic ochre (Ferrimolybdite-hydrated iron molybdate).**  
Powdery-earthy, pale yellow encrustations forming directly from molybdenite. Usually only a few centimetres away from (or directly linked to) fresh molybdenite (metallic on the accompanying plates).  
**Main plate – Ewan district, Queensland Australia.**  
**Inset, location unknown.**  
Width of main frame 5 cm.  
Inset 4 cm.



**Fig. 6.61 Bismuth ochre (bismuth oxide  $\pm$  impurities).**  
Yellow powder (left), surficial occurrence characteristically within centimetres of native bismuth (metallic grains to the right).  
**Location unknown.**  
Width of frame 5 cm.



**Fig. 6.62 Tungstic ochre (Tungstic oxides  $\pm$  impurities—also referred to as Tungstite or Ferritungstite).**  
Yellow–yellow red coating—smears (pale on slide) occurring both on, and adjacent to wolframite (dark metallic).  
**Location unknown.**  
Width of frame 3 cm.





**Fig. 6.63 Cerargyrite (Horn silver-silver chloride).**

A relatively rare mineral, generally massive with horn like colours (left).

The mineral is sectile, heavy, and commonly occurs as heavy pale grains in panned concentrates in silver-rich terrains.

**Herberton, Queensland, Australia.**

Width of frame 4.5 cm.



**Fig. 6.64 Silver (Native silver).**

Native silver occurs as both a primary and secondary mineral. It has several habits ranging from arborescent through wiry to massive. The format here is as small silver grains filling a cavity. The identification of the dark mineral at the cavity edge is uncertain, probably chalcocite?

**Mt Oxide, Queensland, Australia.**

Width of frame 4 cm.



**Fig. 6.65 Carnotite (Hydrated potassium uranylvanadate).**

Fine-grained yellow powder. This format is very common in uranium minerals and visual identification is normally not possible. For instance autunite-metaautunite (hydrated calcium uranylphosphate) like carnotite are relatively common minerals usually occurring as a yellow powder. Despite visual identification problems yellow-green smears and powders are always worth checking via laboratory or field detecting radiation equipment.

**South Dakota, USA.**

Width of frame 6 cm.

## 6.11 Uranium secondary minerals (Figures 6.65–6.68)

### 6.11.1 General aspects

The uranium secondary minerals are both a source of delight and frustration to the exploration geologist or prospector. The positive side is that they are relatively easy to recognise with their yellow to yellow-green colours. The frustrating side is that there are scores of them and they are impossible to identify as specific uranium minerals without recourse to laboratory techniques. Many of them are also unstable when exposed to the atmosphere, and the prefix meta is applied adding to the long list of names. For instance autunite ( $\text{Ca}(\text{UO}_2)_2(\text{PO}_4)_2 \cdot 10\text{--}12 \text{H}_2\text{O}$ ) dehydrates to become metaautunite ( $\text{Ca}(\text{UO}_2)_2(\text{PO}_4)_2 \cdot 2\text{--}6 \text{H}_2\text{O}$ ) when exposed to the atmosphere. This is a pseudomorphic process which is not readily amenable to perception in the field.

The plethora of minerals forming mostly as fine encrustations and powders results from the ability of uranium species to form simple and complex, oxides, hydroxides, arsenates, phosphates, carbonates, silicates, vanadates as well as incorporating elements such as fluorine, molybdenum and even tungsten into their structure.

In the authors experience only torbernite ( $\text{Cu}(\text{UO}_2)_2(\text{PO}_4)_2 \cdot 10 \text{H}_2\text{O}$ ) with its green mica-like appearance is easily suspected in the field circumstance, although it is probably actually metatorbernite at surface ( $\text{Cu}(\text{UO}_2)_2(\text{PO}_4)_2 \cdot 8\text{--}12 \text{H}_2\text{O}$ ). In reality even this field identification requires laboratory follow-up.

Uranium cappings vary from extremely obvious with plenty of yellow-green colours in powdery format, to extremely subtle (Ben Lomond, Queensland, Australia) where the surface expression is restricted to pale lemon powders along narrow joint/vein exposures. Naturally serious uranium prospectors will probably be equipped with geophysical equipment to detect radiation, and in this sense mineral identification may be a secondary problem.

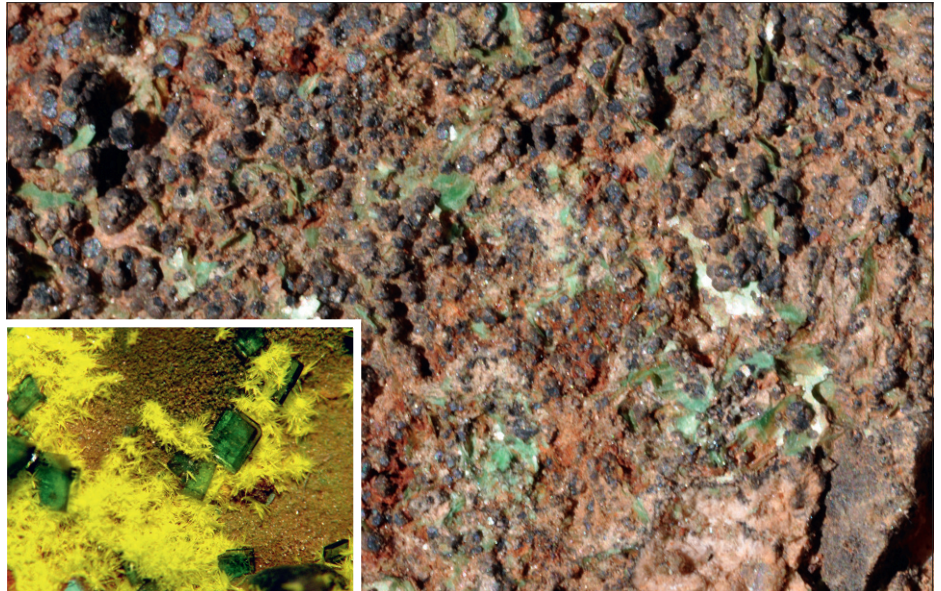
Given the identification problems only a few of the many uranium secondary minerals are illustrated here.

## 6.11.2 Uranium minerals

| Name             | Formula  | Composition                       |
|------------------|--|-----------------------------------|
| Autunite         | $\text{Ca}(\text{UO}_2)_2(\text{PO}_4)_2 \cdot 10\text{--}12\text{H}_2\text{O}$        | Hydrated calcium uranylphosphate  |
| Metaautunite     | $\text{Ca}(\text{UO}_2)_2(\text{PO}_4)_2 \cdot 2\text{--}6\text{H}_2\text{O}$          | Hydrated calcium uranylphosphate  |
| Carnotite        | $\text{K}_2(\text{UO}_2)_2(\text{VO}_4)_2 \cdot 1\text{--}3\text{H}_2\text{O}$         | Hydrated potassium uranylvanadate |
| Tyuyamite        | $\text{Ca}(\text{UO}_2)_2(\text{V}_2\text{O}_8)_2 \cdot 5\text{--}8\text{H}_2\text{O}$ | Hydrated calcium uranylvanadate   |
| Metatyuyamite    | $\text{Ca}(\text{UO}_2)_2(\text{V}_2\text{O}_8)_2 \cdot 3\text{H}_2\text{O}$           | Hydrated calcium uranylvanadate   |
| Schoepite        | $(\text{UO}_2)_8\text{O}_2(\text{OH})_{12} \cdot 12\text{H}_2\text{O}$                 | Uranyl hydroxide                  |
| Metaschoepite    | $\text{UO}_3 \cdot 1\text{--}2\text{H}_2\text{O}$                                      | Uranyl hydroxide                  |
| Torbernite       | $\text{Cu}(\text{UO}_2)_2(\text{PO}_4)_2 \cdot 10\text{H}_2\text{O}$                   | Hydrated copper uranylphosphate   |
| Metatorbernite   | $\text{Cu}(\text{UO}_2)_2(\text{PO}_4)_2 \cdot 8\text{--}12\text{H}_2\text{O}$         | Hydrated copper uranylphosphate   |
| Uranospinite     | $\text{Cu}(\text{UO}_2)_2(\text{AsO}_4)_2 \cdot 10\text{H}_2\text{O}$                  | Hydrated uranylphosphate          |
| Metauranospinite | $\text{Cu}(\text{UO}_2)_2(\text{AsO}_4)_2 \cdot 2\text{--}8\text{H}_2\text{O}$         | Hydrated uranylphosphate          |

**Fig. 6.66 Torbernite-Metatorbernite (Hydrated copper uranylphosphate).** Bright green micaceous crystals, with reflective surfaces always have a strong possibility of being torbernite or the dehydrated pseudomorph metatorbernite. However laboratory work is required to support the field identification.  
**Mt Painter, South Australia, Australia.**

Width of frame 5.5 cm.  
Inset – torbernite crystal (green) and schoepite-meteshoepite (yellow)-uranyl hydroxide. Width of frame – about 2 cm.  
**Mosonoi mine, Kolwezi, Shaba (Katanga), Congo.**  
Photograph provided by P. Schumacher



**Fig. 6.67 Tyuyamunite-Carnotite and Uranospinite-Metauranospinite.** (Hydrated potassium and calcium uranylvanadate, plus hydrated calcium uranylarsenate). The pale yellow-white powder is the tyuyamunite-carnotite mix and the green crystals are the uranospinite (bottom right). Neither can be identified with certainty without laboratory support. Pale yellow powders are common in secondary uranium minerals (Figure 6.65).  
**Koongarra Prospect, Northern Territory, Australia.**  
Width of frame 3 cm.



**Fig. 6.68 Uranospinite-Metauranospirite.** (Hydrated uranylarsenate). Typical pale green tabular crystals. However, the colour and shapes do not provide enough criteria for positive field identification. Nonetheless a uranium mineral would be suspected.  
**Koongarra Prospect, Northern Territory, Australia.**  
Width of frame 3 cm.



## 7.1 Introduction

Boxwork or cellular “limonite” structures are pictured in many textbooks and every practicing geologist has the feeling that they should be able to interpret these textures. Obviously to pick up a leached outcrop and pronounce its original valuable mineral content, would be a distinct advantage.

However, boxworks/cellular limonites can develop from a variety of sources and are very difficult to approach with any confidence. At the outset it should be stated that visible boxworks are relatively rare, and in practice form only a small part of leached outcrop skills. The overall textures within the leached outcrop, combined with secondary mineral content and geochemical signature, will generally give quicker and more positive clues than the rarer and commonly more obscure boxwork style structures. Also within the modern exploration context most leached outcrop problems can be quickly resolved via backhoes, bulldozers, shallow drilling or even portable XRF analysers.

Nonetheless, the author has experienced numerous remote field occasions where knowledge of boxwork development has proved very useful and would certainly encourage young professionals to acquire a good grounding in the basics of boxwork/cellular limonite developments.

## 7.2 Development of cellular structures in leached outcrops (Figure 7.1)

Cellular structures popularly termed boxworks develop in any circumstance where fluids penetrate along rock or mineral discontinuities and precipitate minerals (infill or alteration) as narrow ribs which ultimately survive the weathering process. In other words they are the insoluble component left when the host has been removed reflecting the original crack pattern.










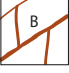



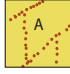







The channelways include grain boundaries, cleavages, micro-fractures at the individual grain scale and rock fracture patterns at the larger scale.

A common misunderstanding is an appreciation that most boxworks reflect the fracture pattern of a rock mass and do not represent individual minerals. It takes some time to realise that the search for diagnostic mineral boxworks must occur at a scale appropriate for the individual mineral concerned. If the original rock is a fine-grained massive sulphide, the observer is unlikely to see any boxwork at eye level scale. A boxwork developing in this circumstance will reflect the breaking pattern of the sulphide rock. Similarly large-scale boxwork structures commonly develop in rocks which have nothing to do with mineralisation (serpentinite, carbonate). Fortunately these are usually easy to decipher in the field context as the host rock is usually directly adjacent.

### 7.2.1 Styles of ribbing

The components of the boxwork are generally referred to as ribs, and need very careful inspection. As mentioned above it is very important to ascertain the scale of viewing and to only deal with sets of ribs which seem to belong to one original source. Most boxworks are composed of sets of ribs at different scales (coarse rib patterns versus finer) and it is usually prudent to mentally isolate all those of the same scale and note their pattern.

**Fig. 7.1 Pathways producing boxworks, in situ granular clusters and positive and negative pseudomorphs**  
 NB. All Pathways may become flooded (overprinted) by surficial processes – infilled by transported limonite/silica products (cherts and/or ironstones may result).

| COMMON PATHWAYS         | HYOGENE  | SUPERGENE   | WATER TABLE (FLUCUATING)  | OXIDE ZONE  | LEACHED CAP GOSSAN ZONE  | COMMENT  |
|-------------------------|--|---|---|---|--|--|
| 1. DISSOLUTION          | <br>Original Sulphide   | <br>Original Sulphide<br>Dissolution |   | <br>Cavity     | <br>Negative pseudomorph | Most common pathway especially if via pyrite, sphalerite or pyrrhotite. Acid attack in lower oxide zone creates cavities which may reflect mineral shapes (negative pseudo-morphs). Major dissolution may occur in carbonate hosts, creating space for infill oxides. Especially zinc minerals via sphalerite dissolution. |
| 2. SUPERGENE ENRICHMENT | <br>Original Sulphide  | <br>Supergene Enrichment            |   | Change of Chalcocite<br>Covelite  |  | Original mineralogy changed at supergene zone. Chalcocite covellite formation common. Upward changes important in porphyry copper systems (see text Section 8).  |
| 3. BOXWORK FORMATION    | <br>Original Sulphide | <br>Original Sulphide              |  | <br>Ribbing  |                        | (A) Ribbing development commences at water table (B) Remnant sulphide leached in oxide zone giving boxwork (C) boxwork at surface affected by weathering may crumble, or become partially removed.   |
| 4. IN SITU RESIDUES     | <br>Original Sulphide | <br>Original Sulphide              |  | <br>Grains   |                        | (A) Ribs form as insoluble secondary minerals. ± rim replacement. (B) Process continues in oxide zone creating a granular mass. (C) Crumbling/ weathering of granular mass at surface ± further oxidation.<br><br>Examples<br>Galena → Anglesite/Cerussite → Lead Oxides<br>Arsenopyrite → Scorodite → Limonite            |
| 5. PSEUDO-MORPHISM      | <br>Original Sulphide | <br>Original Sulphide              |  | <br>Limonite |                        | Especially in carbonate-rich hosts – rapid acid neutralisation may produce pseudomorphs (A, B, C) especially after pyrite.   |

The composition of ribbing varies enormously and although most are combinations of silica and/or iron oxides this is certainly not true in the case of galena or arsenopyrite where the ribs contain major components of secondary minerals such as cerussite or scorodite. Smithsonite also forms a major rib component in many carbonate/lead-zinc boxwork developments.

### 7.2.2 The site of rib development (Figure 7.1)

Another popular misconception is that the rib development in leached outcrops is part of the immediate surface weathering process. This is true in some instances, but in most cases the main stage of rib development occurs around the water table level, becomes arrested as the mineral emerges into a higher level, and only becomes exposed as the remainder of the mineral is removed by the oxidation process.

Many boxworks actually reach peak development immediately above the water table in the zone of high acid generation. The intense acid leaching removes the mineral (usually sulphides) leaving the insoluble ribbing.

A further problem is encountered in that a good boxwork development in the middle to upper profile is also a zone of major permeability and quite commonly the boxwork becomes infilled by later precipitation (flooded). This is very common in old profiles subjected to lateritic development, and/or saline groundwaters with the net result that the boxwork and leached outcrop generally becomes a mass of silica and/or iron and manganese oxides (chert, jasperoidal siliceous ironstone).

In some instances, near surface weathering may actually differentially start to exhume a flooded boxwork.

Obviously there are many difficulties for both the experienced and inexperienced geologist. A good approach within a new region is to forget the theory and to work diligently on old mine dumps. The early prospectors often stopped digging at the water table, and the dumps usually contain an excellent profile of leached outcrop development. It is much easier to start with the known ore and work upwards to see what actually happens to each component. The most valuable specimens are half-half which clearly show the origin of a particular boxwork. This can then be applied on a regional basis. The process cannot be recommended strongly enough and is the only way to develop an expertise for leached outcrops in a particular district. It should form an early phase in any localised exploration programme.

## 7.3 Minerals

### 7.3.1 Pyrite (Figures 7.1–7.12)

Pyrite is by far the most common sulphide mineral, and its presence can be suspected in most gossan/leached cap exposures. It commonly forms cellular/boxwork structures. Pyrite is readily taken into solution in highly acid oxidising environments, with the iron component ultimately reprecipitated as exotic iron oxides (Figures 4.5–4.9). Indeed any exposure containing large amounts of rusty-orange-yellow exotic iron oxides, is automatically suspected as being pyrite-rich. This is normally accompanied by intense clay (acid leach) development within aluminosilicate wall works (argillisation).

Pyrite occurs in a wide variety of formats including:

*Isolated crystals.*

*Small crystals occurring as a pyrite mass.*

*Fine-grained massive pyrite with no easily visible crystals.*

The most common response is for the mineral to dissolve and leave behind a cavity which might become the site for the precipitation of “limonite infill” (iron oxides  $\pm$  silica) and where the cavity reflects the shape of the original crystals (mostly rounded dodecahedra, and more rarely cubes). Even within a large reasonably coarse grained granular mass, it is normally possible to observe the leached ovoid/cubic outlines (especially on edge zones where crystals tend to become isolated (Figures 7.1, 7.4, 7.6–7.10, 7.12). In rare instances a neutralising wall rock (carbonate-rich shale) may cause precipitation of iron oxides at the site of dissolution to form pyrite pseudomorphs (Figure 4.1 and 7.3).

Visible boxworks occur mostly from massive fine grained pyrite, or clumps of coarse-grained pyrite crystals. The latter tend to leach out and create sponge-like structures (pyrite sponges) whilst the former may develop very thin silica  $\pm$  iron oxide ribs reflecting the crack pattern of the pyrite lump (Figures 7.9–7.11).

Unfortunately the crack pattern of pyrite is completely random (not cleavage-controlled) and as such the boxwork pattern exhibits no particular geometry. The beginner is advised to look at crack patterns developed in pristine pyrite masses to observe the range of complex patterns. In general rectangular shapes are produced, but obviously all options are open. The writer has never been sure at what stage the siliceous ribs develop (water table level or higher?).

Given that there is no characteristic boxwork for the more rectangular styles, positive identification is scientifically doubtful and in most instances the source of such boxworks is interpretive or retrospective as partially developed specimens become available. Fortunately many pyritic associations are also in silica-dominant rocks and pyrite can be found preserved in silica high in the profile. The silica armour protects isolated patches from the acid/oxidising fluids.



**Fig. 7.2 Pyrite – dominant leached capping and gossan.** This style of exposure comes under immediate suspicion as involving pyrite. The extensive clay alteration and abundant transported limonitic iron oxides in major and minor vein formats, suggest major acid production. This in turn suggests major input from the most common sulphide-pyrite (Pyrrhotite is a far less likely option). Detailed examination would follow looking for pyrite cellular evidence.  
**Batu Hijau, Indonesia.**  
Width of frame 10 m.



**Fig. 7.3 Pyrite – negative pseudomorphs.** Cube shaped cavities reflect the complete removal of pyrite. The low neutralising environment of a quartz-rich host rock discourages precipitation of indigenous limonite (see [Figure 7.4](#), below).  
**Location unknown.**  
Width of frame 4 cm.



**Fig. 7.4 Pyrite – pseudomorphs.** In-situ conversion of pyrite to limonite. The host rock is calcareous with strong neutralisation effects causing formation of indigenous limonite. At some localities such as the Caruso mine in the central Harts Range in the Northern Territory Australia, these may weather out and are locally called “devil’s dice”. See also [Figure 4.1](#).  
**Location unknown.**  
Width of frame 5 cm.

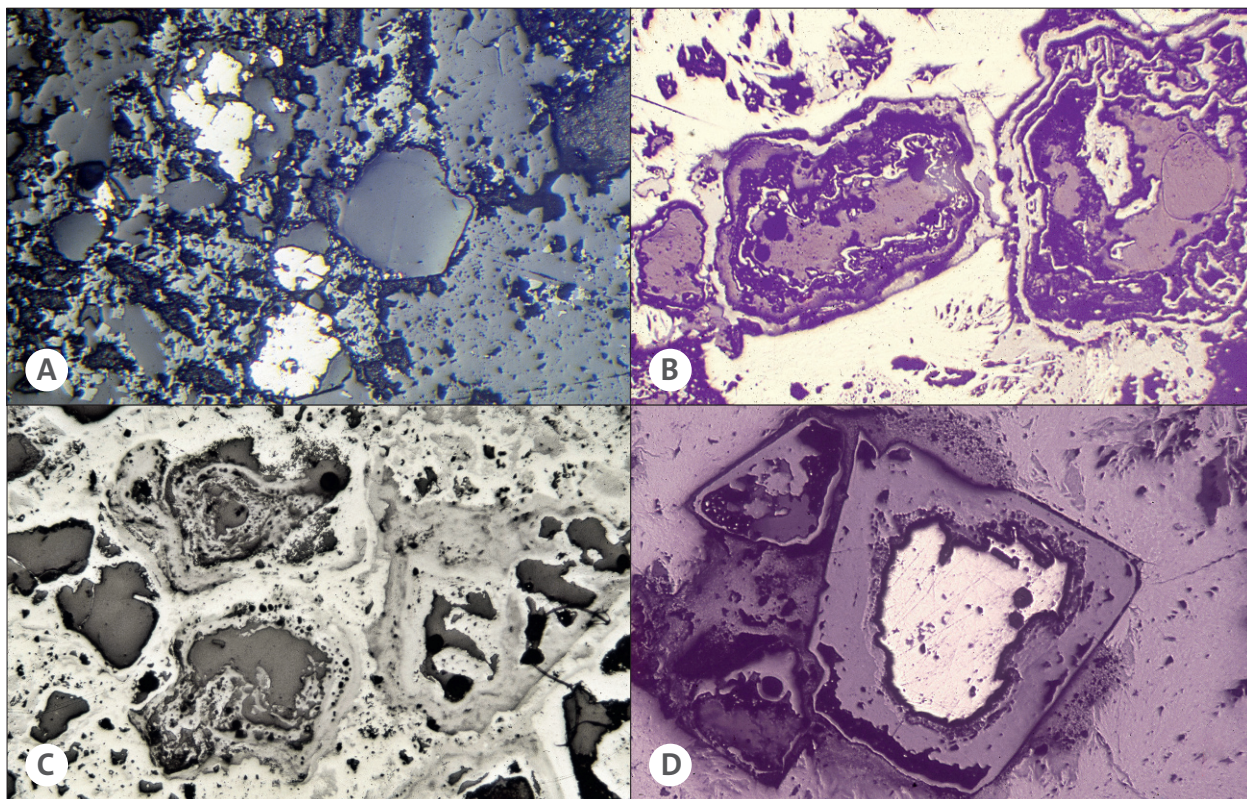
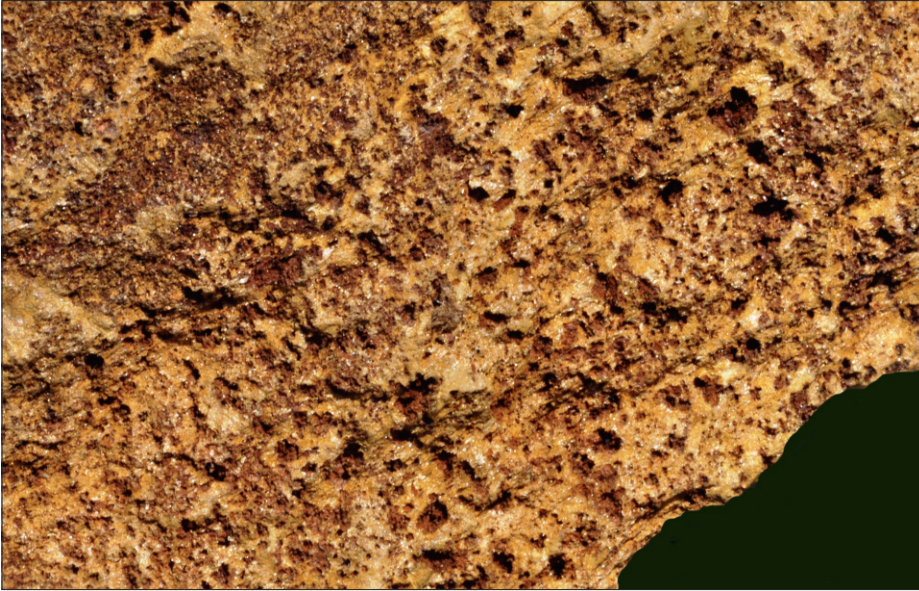


Fig. 7.5 Photomicrographs of selected pyrite cellular developments. Note the shapes.

- A Pyrite (pale) dissolution – empty cavity.  
Sweeney's prospect, Zeehan, Tasmania, Australia.  
Width of frame 5.6mm.
- B Ex-pyrite cavities (dark) with concentric limonite boxwork rinds.  
Location unknown.  
Width of frame 1.4 mm.
- C Ex-pyrite cavities (dark) with slightly more disordered limonite rinds.  
Location unknown.  
Width of frame 1.4 mm.
- D Pyrite (pale) dissolution – thick walled limonite cell or pseudomorph.  
Location unknown.  
Width of frame 1.4 mm.

Fig. 7.6 Negative ovoid cellular pyrite pseudomorphs in a quartz vein, with remnant pyrite (see Figure 7.5 A).  
Home Hill district, Queensland, Australia.  
Width of frame 10 cm.





**Fig. 7.7** Pyrite gossan, cellular boxwork.

Disseminated pyrite oxidised to form ovoid cellular pseudomorphic shapes. The cavities are partially lined with limonite (similar to [Figures 7.5 B, C](#)). Identification is an interpretation relying on the common dodecahedral (rounded) shape plus abundant iron oxide). The host rock is micaceous schist.

**Woodlawn, NSW, Australia.**  
Width of frame 5 cm.

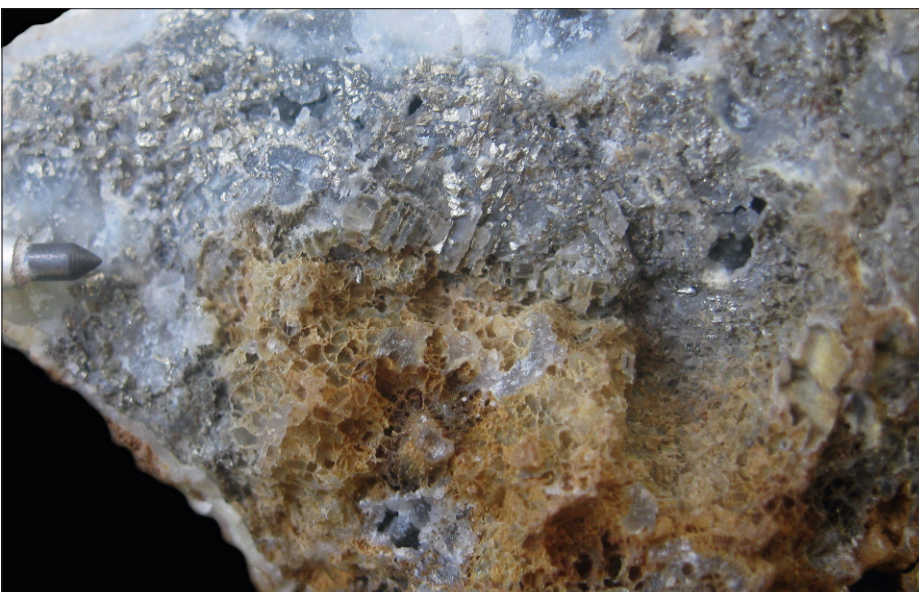


**Fig. 7.8** Pyrite leached capping. Dark quartz veins with boxwork.

The boxwork has many hints of ovoid cells (thick-walled), see [Figure 7.5 D](#).

The ovoid shapes, adjacent iron staining (suggesting an iron-rich mineral) and clay-altered wall rocks all implicate pyrite as the most likely original sulphide. From a quartz-pyrite-gold stockwork.

**Cenesis prospect, Atacama region, Chile.**  
Width of frame 6 cm.



**Fig. 7.9** Pyrite cellular sponge.

An excellent example of thin-walled cellular boxwork sponge showing all stages of development from granular pyrite to empty cells. The cell walls are siliceous, and this thin-walled webbing is very common in pyrite-derived sponges. Note also the ovoid shapes and delicate cross ribs within some of the cells. Quartz vein with pyrite.

**Kerta region, Indonesia.**  
Width of frame 4 cm.  
Photograph provided by R. Gosse.

**Fig. 7.10 Pyrite – cellular sponge boxwork.**

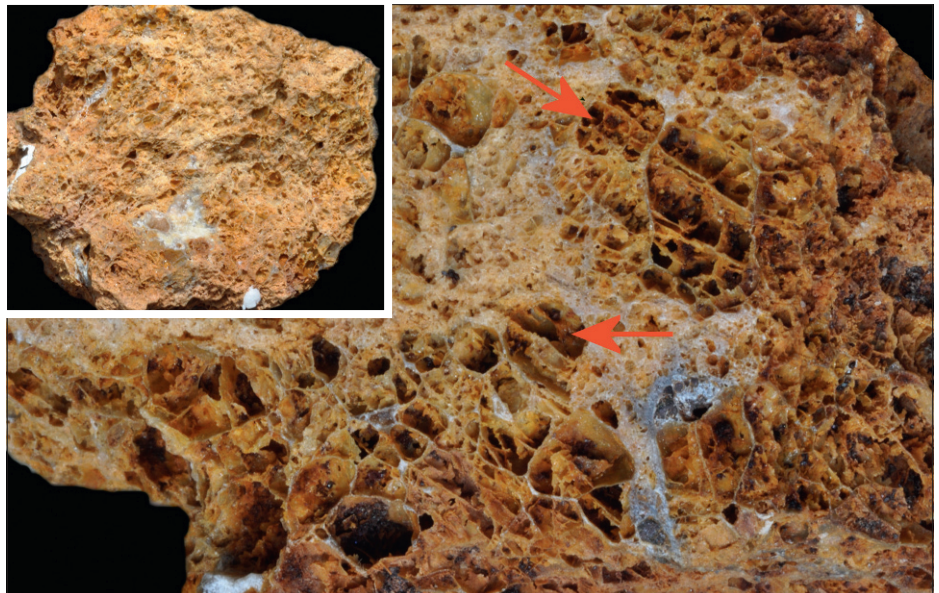
Very good example of a cellular pyrite sponge boxwork derived from coarse-grained pyrite (see also [Figure 7.9](#)).

The term sponge comes from the shape (inset) and the light weight, delicate, thin walled webwork. Identification utilises these characteristics, along with colour and recognition of ovoid negative pseudomorphs (arrows and [Figure 7.5](#)).

Individual pyrite grains also develop finer internal septa reflecting cracks in the original grain (main frame).

**Location unknown.**

Width of frame 6 cm.

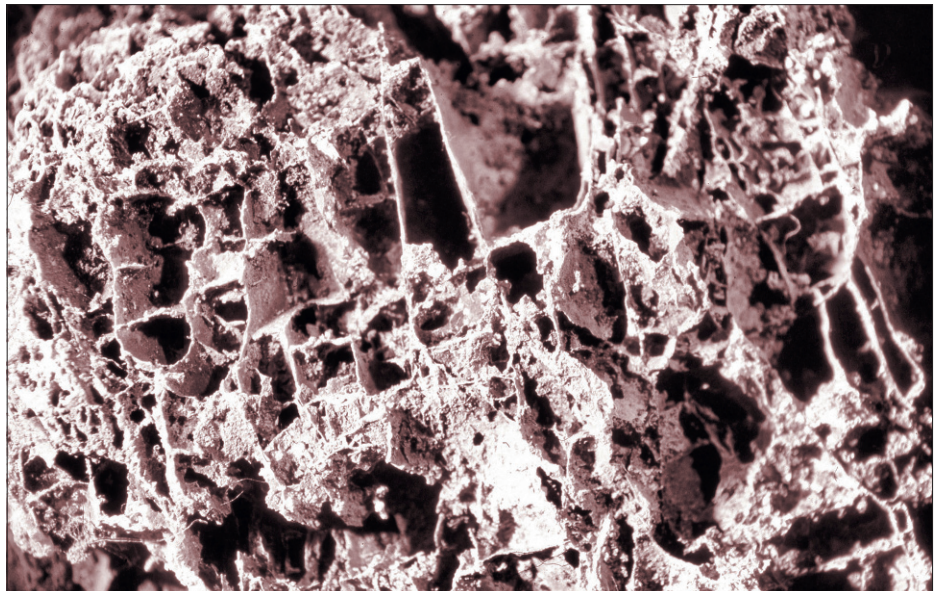


**Fig. 7.11 Pyrite – rectangular boxwork.**

This form of boxwork is completely different to sponge styles and less common. The original rock is extremely fine-grained sulphide (micron-scale) as in many volcanogenic deposits. The thin-walled sponge simply reflects the fracture pattern of the fine-grained mass, and has nothing to do with individual grains. Interpretation clues are the delicate cell walls and local features such as layering, and major signs of acid attack (transported limonites and clay altered wall-rocks).

**Mount Molloy copper mine, Queensland Australia.**

Width of frame 6 cm.

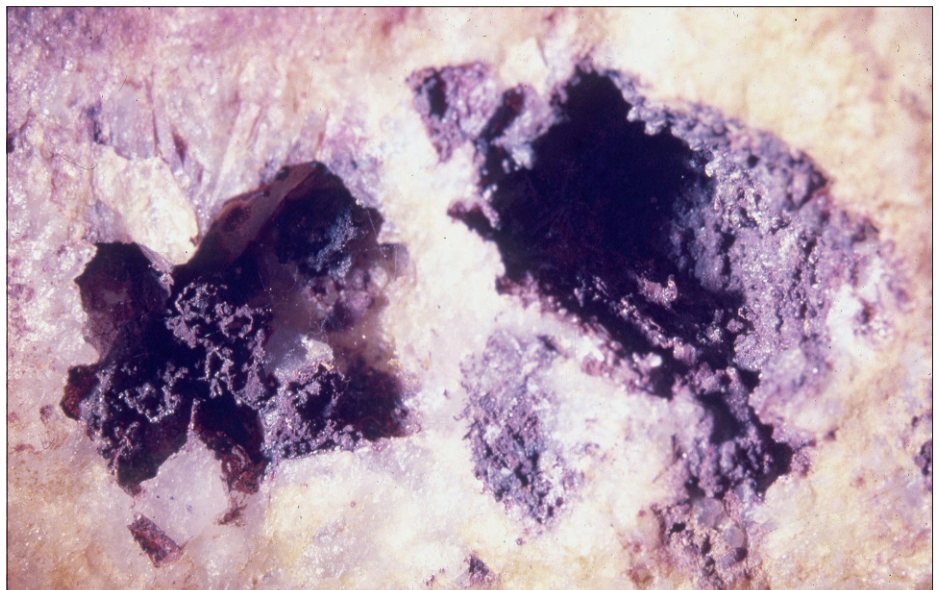


**Fig. 7.12 Pyrite – remnant boxwork?**

This plate illustrates a common problem. Is the limonite in this obvious pyrite negative pseudomorph indigenous or transported? The pattern to the left looks like frail boxwork remnant (see above), possibly coated with limonite. The granular botryoidal coating to the right, looks like botryoidal transported infill? A rather loose provisional interpretation will result.

**Location unknown.**

Width of frame 3 cm.



### 7.3.2 Pyrrhotite

Pyrrhotite with its non-stoichiometric composition ( $\text{Fe}_{(1-x)}\text{S}$ ) is very unstable and oxidises very easily and rapidly. Given this, it is not surprising that pyrrhotite boxworks are very rare. The general visual surficial result is a large amount of transported/exotic iron oxide particularly in botryoidal format (Figures 7.13–7.15). This is commonly directly over the main ore zone or immediately adjacent, in spongy formats, with the adjacent wall-rocks argillised via major acid fluid attack.

The second reason which prevents development of visual boxwork is that most pyrrhotite is in massive format with grain sizes of micron scales. With this fine grain size any potential boxwork is unlikely to be visible, unless its reflecting the fracture pattern of the massive format.

Despite this some authors record visible and/or microscopic cellular textures (Blanchard, 1968), sub parallel reticulate delicate ribbing (Blanchard, 1968, Blain and Andrew, 1977 – microscopic) and some unusual hieroglyphic shapes (Blain and Andrew, 1977 – microscopic). It could be possible, that many of these are actually exotic/transported textures?

### 7.3.3 Chalcopyrite

Chalcopyrite is very susceptible to replacement by chalcocite and/or covellite in the zone just below the water table (supergene enrichment). Given that most systems contain enough pyrite/pyrrhotite to easily produce the conditions required for this process, chalcopyrite very rarely survives the passage upwards into the oxide zone (Figure 6.31).

In the rare cases where a visual boxwork forms there seem to be two main end-products, both of which have angular patterns.

- Rectangular cell patterns with closely spaced thin parallel walls. These contain rare cross cell walls at around  $95\text{--}100^\circ$ . The parallel tram track ribs extend to embrace several, individual cells. The reasons for this pattern remain obscure, and the author has not succeeded in finding a visual example in the field. However, both Blanchard (1968) and Blain and Andrew (1977) illustrate examples. The latter at microscope level.

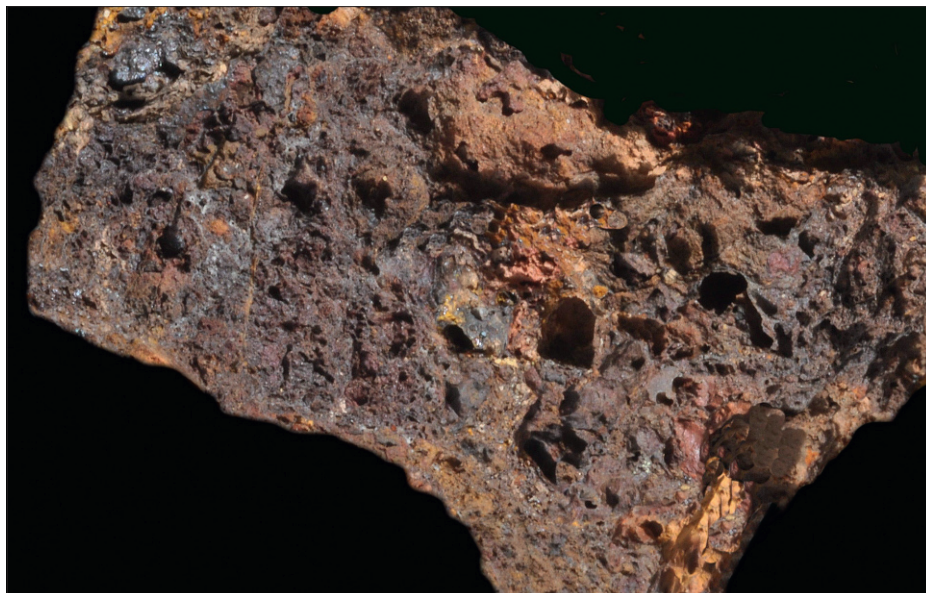
The example shown in Figure 7.16 (Inset C) derives from an old photograph (hence poor reproduction) donated by W.C. Lacy from the Arizona porphyry copper district.

- Thick-walled maroon coloured boxwork forming quadrilateral ( $\pm$  triangular) shapes (Figures 7.16 ABC). These are commonly associated with red limonite and malachite. These are well-represented in the Cloncurry iron oxide copper-gold deposits, Queensland, Australia. It is always worth remembering that chalcopyrite is by far the most common copper sulphide, followed by bornite as a poor second. In this context secondary green copper minerals most likely indicate chalcopyrite! It is also worth noting that there are hints of the parallel tram line ribbing in the thick-walled boxworks.

**Fig. 7.13** Pyrrhotite cellular sponge.

This specimen from a surface exposure illustrates the bubbly iron-dominant format of a sponge-style gossan, developing directly over a pyrrhotite zone. It remains unclear whether this is an exotic mass or a true boxwork. The writer would favour the former owing to the amount of botryoidal limonite. It is however representative of many surface gossans over pyrrhotite (See below)

**Siberia Lode, Emuford, Queensland, Australia.**  
Width of frame 6 cm.

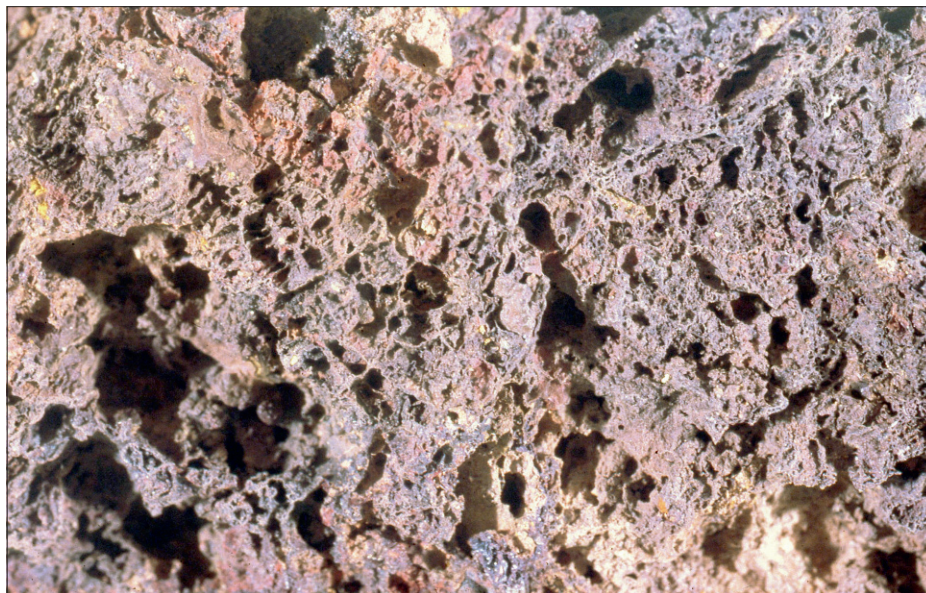


**Fig. 7.14** Pyrrhotite cellular sponge.

This cut surface of a limonite mass developed over pyrrhotite dominant ore, reveals a cellular texture reminiscent of botryoidal limonite. This texture has been nominated as pyrrhotite boxwork (Blanchard, 1968). The author is doubtful of this interpretation preferring to think of it as a mass of rapidly precipitated botryoidal limonite (transported, but forming close to source).

**United North Australia mine, Herberton, Queensland, Australia.**

Width of frame 6 cm.

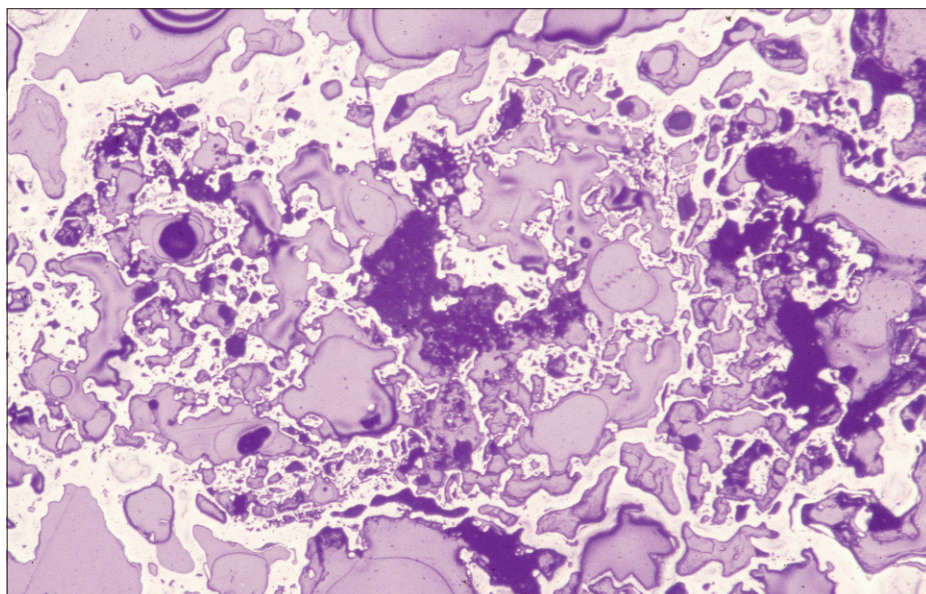


**Fig. 7.15** Pyrrhotite cellular sponge.

Polished section of the above specimen. Note the very irregular limonite (white) pattern, similar to botryoidal limonite (Figure 4.7).

**United North Australia mine, Herberton, Queensland, Australia.**

Width of frame 2.8 mm.



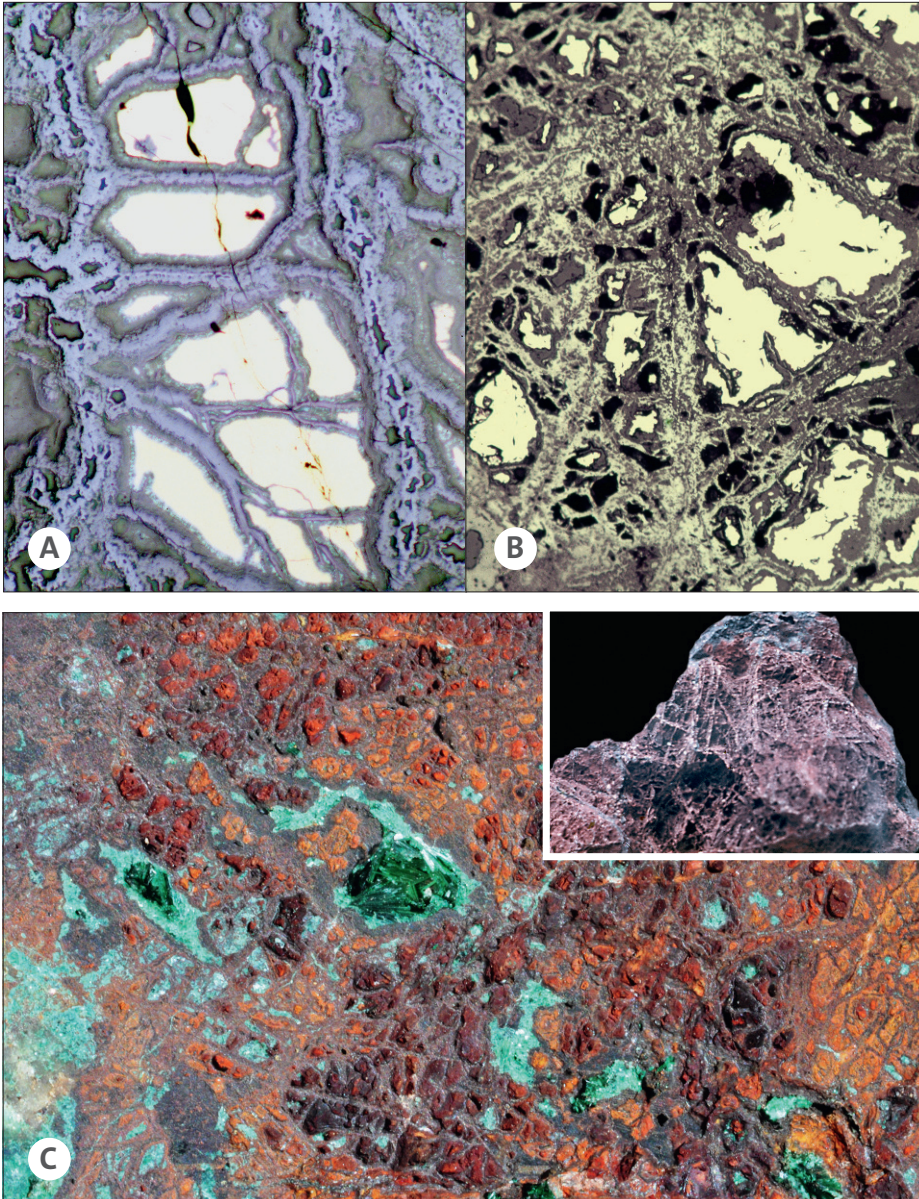


Fig. 7.16 Polished sections illustrating the typical fracture pattern of chalcopyrite (pale), and thick cell wall development (A) followed by dissolution and cavity development (black) (B) Note triangular and quadrilateral cell shapes. Cloncurry district, Queensland, Australia. Width of frames 4.5 mm.

**Development of boxwork.**  
 In this case (C) the situation shown above (A, B) has progressed. Rib development ceases. Chalcopyrite converts to orange blebs of limonite. The orange kernels are removed (erosion?) and a characteristic quadrilateral-triangular boxwork emerges with thick maroon cell walls. Late malachite. The inset shows a thin walled version with a more-parallel rib development (see text)  
**Main frame – Mighty Atom mine, Kjabbi, Queensland, Australia.**  
 Width of frame 5 cm.  
**Inset – from S.W., USA.**  
 Width of frame 1 cm

### 7.3.4 Sphalerite

Visible sphalerite boxworks are exceptionally rare. This is a direct reflection of a combination of factors (Figures 7.2, 7.17–7.19).

- (a) Sphalerite is extremely susceptible to acid attack and quickly goes into solution. This is encouraged by the perfect octahedral cleavage, twinning, and a propensity for sphalerite to be effectively “non-stoichiometric”. The net result is a cavity. If the sphalerite is iron-rich, there may be a considerable amount of exotic limonite in the region, and zinc is readily taken into limonitic-clay mineral-manganese oxide systems (Figure 7.17).

- (b) Sphalerite is also extremely susceptible to supergene replacement and in high copper environments converts to chalcocite/covellite at the supergene zone (Figure 7.19).
- (c) In most environments sphalerite has a pyrite association and is hence readily exposed to acid attack. In carbonate environments sphalerite may be protected from acid attack, but is extremely easily converted to carbonates (smithsonite) in the oxide zone. In some instances major early smithsonite ribbing may develop (Figures 7.19, 7.21).

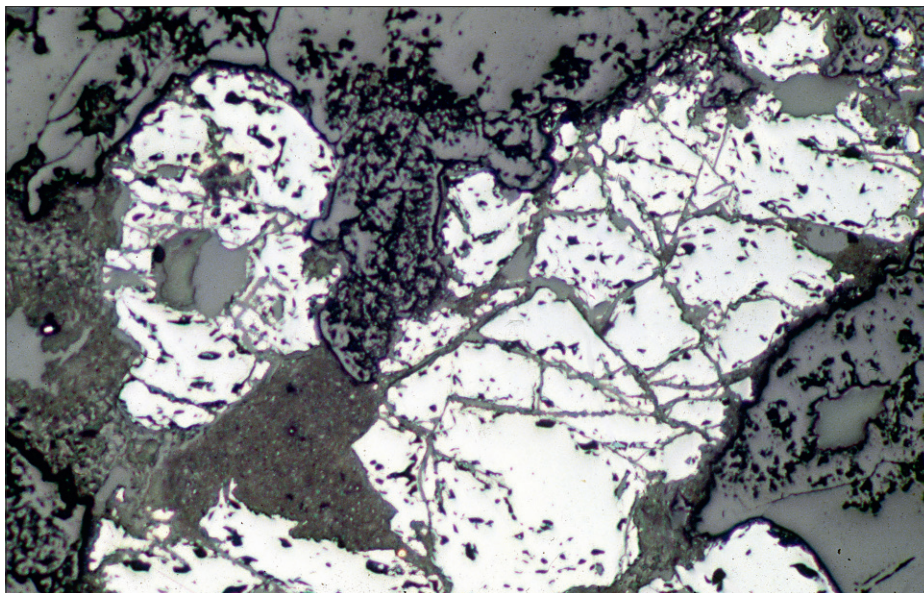
However, despite the many problems, sphalerite boxworks do occur in situations where silica or silica  $\pm$  iron oxide has managed to precipitate within the cleavage/crack network at an early stage. In most cases this occurs as a very fine delicate ribbing which is commonly partially developed or has become broken owing to its fragile nature (7.20–7.22).

The sphalerite crack/fracture pattern is very characteristic and typified by distinctive low acute angle intersections (Figures 7.17–7.22). Although not visually common, the boxwork is commonly well-developed in finer-grained ores, and can be seen microscopically within the ovoid sphalerite grains/crystals (Figure 7.20).

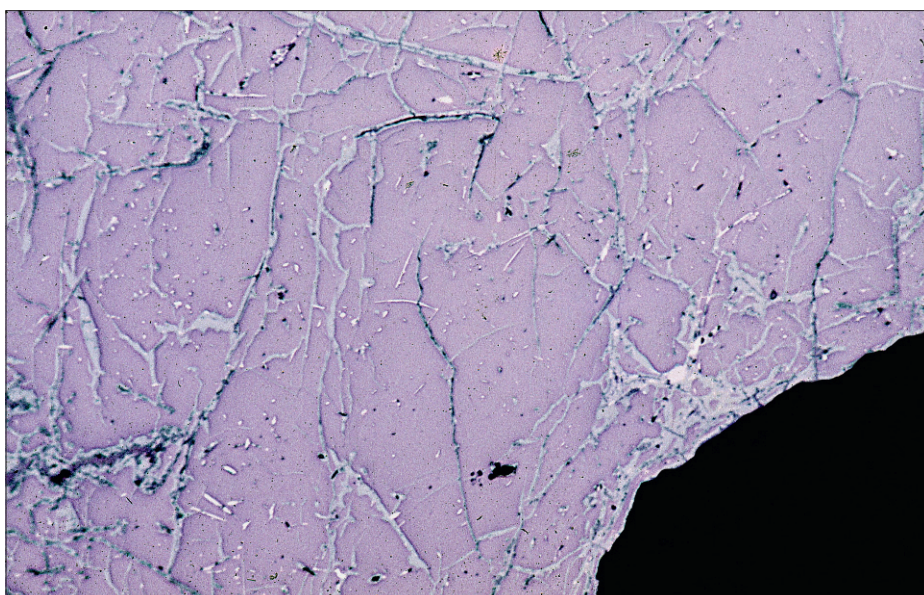
With a lack of boxworks and secondary minerals sphalerite is commonly difficult to detect in aluminosilicate wall-rocks. Carbonate wall-rocks may develop some “oxide” minerals (smithsonite, hemimorphite) which provide valuable clues.

Fortunately the vast majority of sphalerite is accompanied by galena, and it is usually a safe assumption to automatically add sphalerite to a prominent insoluble assemblage of lead secondary minerals (cerussite, anglesite, “lead oxides”).

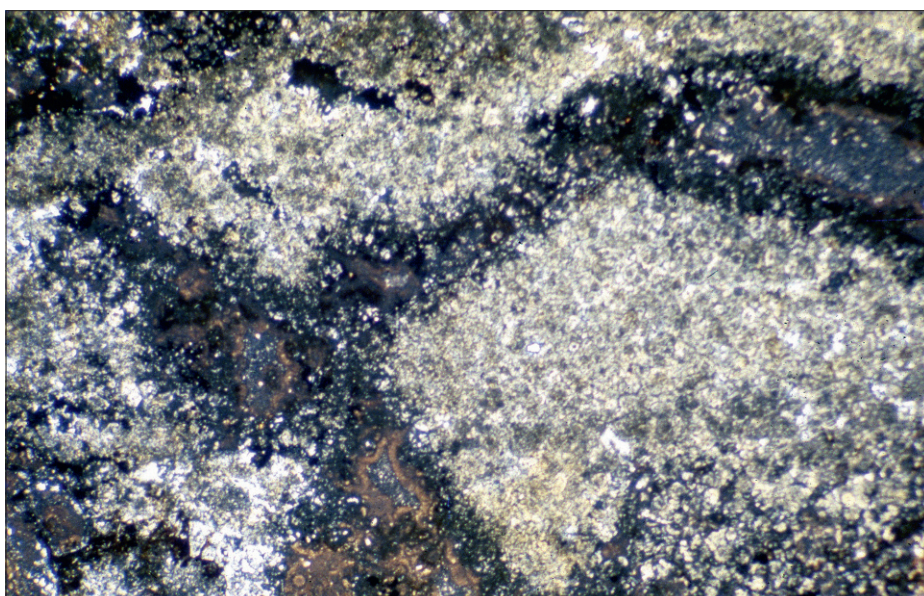
The giant Century zinc deposit provides an interesting example illustrating problems. Here the absence of galena and pyrite and low-iron sphalerite combine to give almost no indication of the underlying 10–15% zinc mineralisation (Figure 3.27).



**Fig. 7.17 Sphalerite dissolution.**  
The normal fate of sphalerite in acid environments is to dissolve. Here the sphalerite (pale in polished section) is being removed via fluids entering along the 111 cleavage planes (dark cracks). NOTE THE ACUTE ANGLED FRACTURE PATTERN. **Sweeny's prospect, Zeehan, Tasmania, Australia.** Width of frame 5.6 mm.

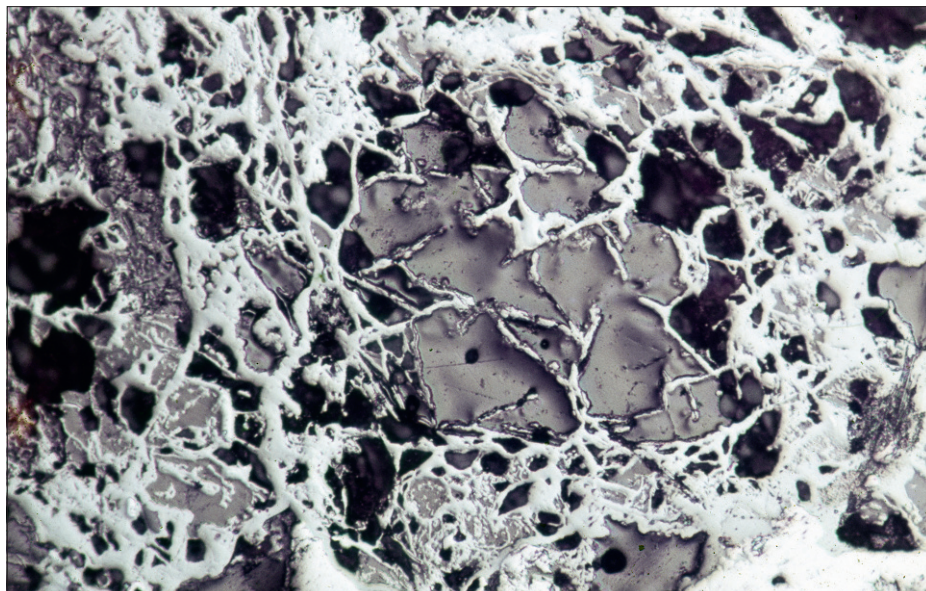


**Fig. 7.18 Sphalerite replacement 1.**  
A second very common fate of sphalerite is to be totally replaced by supergene chalcocite/covellite. This polished section shows the start of the process with blue chalcocite forming along the various fracture surfaces including 111 cleavage planes. NOTE THE ACUTE ANGLE INTERSECTION PATTERN (BOTTOM-MIDDLE). **Location unknown.** Width of frame 5.6 mm.



**Fig. 7.19 Sphalerite replacement 2.**  
Sphalerite surviving the supergene and upper water table zone (mostly in carbonate environments) may be replaced by secondary zinc minerals in the oxide zone. This thin section illustrates a granular dark smithsonite? alteration, of pale brown sphalerite, as well as some smithsonite (darker brown colloform) precipitating in a dissolution gap. **Location unknown.** Width of frame 6 mm.

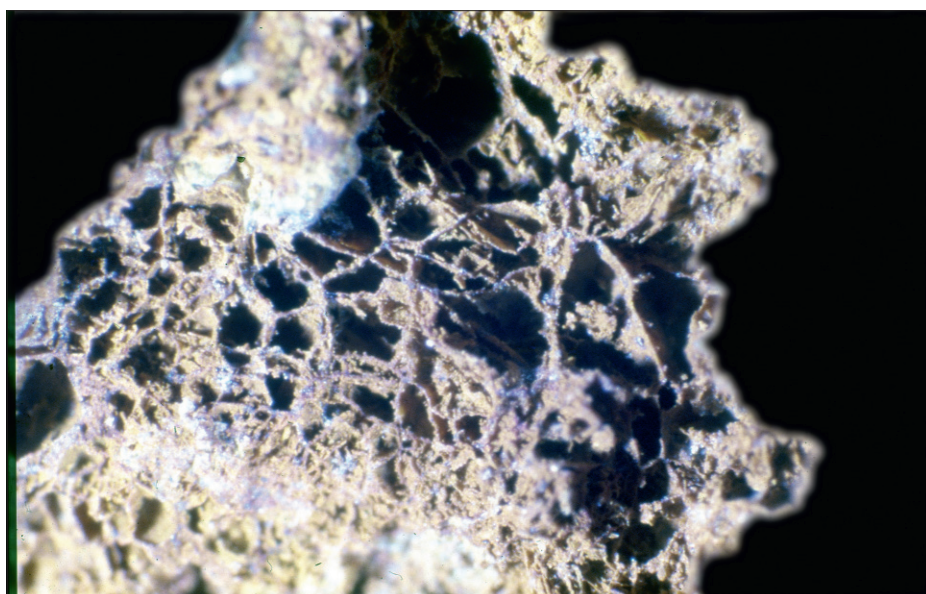
**Fig. 7.20 Sphalerite boxwork.** Sphalerite boxworks are exceedingly rare, with dissolution and chalcocite (or smithsonite) replacement eliminating the sulphide well prior to surface. This polished section displays an excellent pattern of sphalerite boxwork (central grain-white thin cell walls) Note the characteristic low angle intercepts of the septa (see [Figures 7.16–7.17](#)). **Unknown location.** Width of frame 5.6 mm.

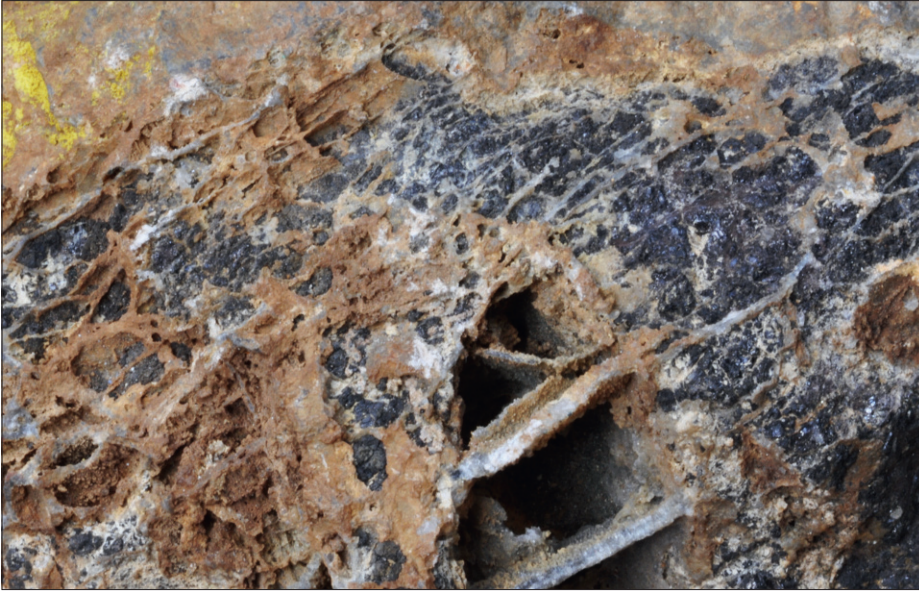


**Fig. 7.21 Sphalerite boxwork.** Ribs of smithsonite? coated with small crystals of botryoidal smithsonite. The latter flood/obscure the main boxwork structure (see below). The identities of the blue and yellow minerals are uncertain (Specimen no longer available). **Ban Ban Springs, Queensland, Australia.** Width of frame 6 cm.



**Fig. 7.22 Sphalerite boxwork.** An exceptionally rare example of a visible sphalerite boxwork. The sample comes from a sector of the same deposit as in [Figure 7.17](#), but with less flooding. Compare the rib pattern with [Figures 7.17–7.18](#), and [7.20](#). The frail ribbing with low angle intercepts is sometimes referred to as a cornflake texture. **Ban Ban Springs, Queensland, Australia.** Width of frame 2 cm.





**Fig. 7.23 Sphalerite boxwork.** This developing boxwork is a little unusual in that the ribs are actually primary quartz “veining” in broken sphalerite. Later sphalerite (black) removal via acid attack creates a boxwork with acute angles reflecting the 111 cleavage intercepts. The characteristic acute angles are best seen in the fine white quartz stringers to the mid and upper right. **Locality unknown.** Width of frame 7 cm.



**Fig. 7.24 Complex ribbing.** The large-scale ribbing (centre left-white tinged) exhibits a good low angle intercept (arrow.) This is repeated at smaller scales. The host rock is limestone. The ribs are suspected as being smithsonite and there are minute hemimorphite crystals partially coating the ribs. The combined features strongly suggest an original large sphalerite mass. **Evelyn lead zinc prospect, Northern Territory, Australia.** Width of frame 11 cm.

### 7.3.5 Galena

Contrary to geological intuition galena does not form boxwork structures that resemble a stack of hollow cubes resembling a dolls house and reflecting perfect cleavage.

Galena is relatively insoluble and is not easily dissolved and transported away from its original position, but effectively oxidises in-situ to anglesite/cerussite which later converts into massicot and minimum (yellow-red iron oxides), (Figures 6.38–6.39). Large masses of coarse-grained galena commonly convert to anglesite near the water table, with the anglesite forming as concentric/ring ovoid structures within the mass, with no apparent regard for the cleavage or crystal shapes (Figures 6.36–6.38). This process is not well understood, but is a very common first response to oxidation. The remaining central galena converts to granular cerussite presumably slightly higher in the profile. It is not clear whether or not the initial anglesite rim is always present.

The granular cerussite conversion is actually an alteration process which commences along the cleavage (Figure 7.25), but quickly spreads out and appears to continue developing throughout the profile in a granular/sinter-like format. At the immediate surface it converts to yellow-red lead oxides (Figures 7.25–7.26). The granular cerussite is actually a form of ultra-thick ribbing and commonly appears as a large sugary-sinter, like zone forming lacy rib patterns. The net result is an extremely characteristic texture of thick sugary ribs which may occupy 60–80% of the original galena site, with no obvious set pattern (Figures 7.27–7.30).

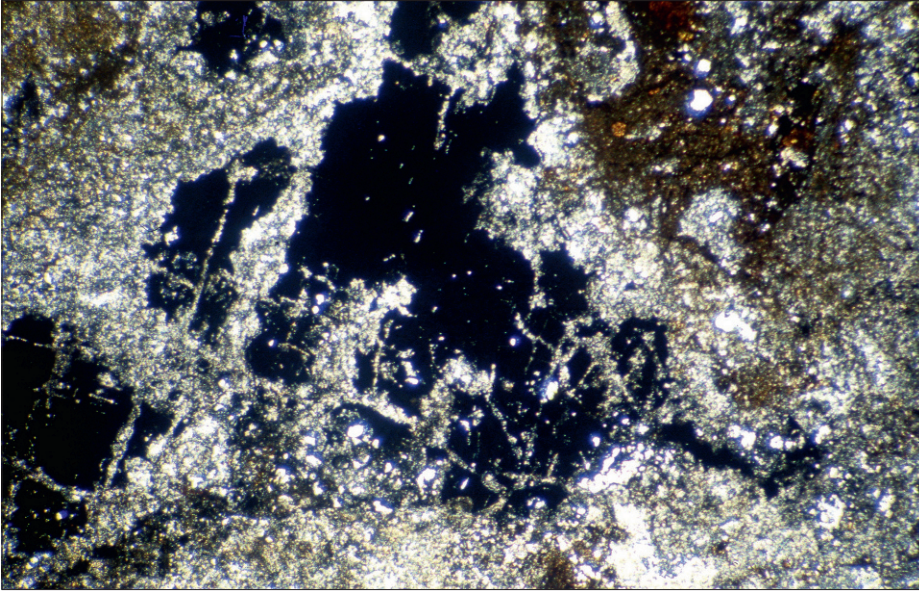
The galena percentage is easily deduced from the mineralogy of the ribbing, although in many cases ribbing is a misleading term for the irregularly shaped masses of cerussite.

In rare cases mechanical weathering may remove some of the granular texture and expose ribs where cubic boxworks are visible (alternatively central galena may dissolve? Figures 7.29–7.30). The granular cerussite can be difficult to recognise as it is fine-grained, in places semi-converted to lead oxides and stained with limonite and/or green arsenical components.

In some instances the converted central core zone of an original anglesite rim, seems to weather preferentially leaving small crater-like cavities (Figure 7.27).

In reality most gossanous exposures of galena-rich deposits are easily recognised via the secondary lead minerals and/or kernels of unoxidised galena.

Recognition of probable primary galena also triggers a search for hints of the commonly associated sphalerite.



**Fig. 7.25 Galena-cerussite-massicot.**

A thin section showing galena (black) being replaced by granular cerussite (lead carbonate) via fractures and cleavages.

The cerussite alters to massicot (lead oxide-orange, top right (see [Figures 7.38](#) and [7.26](#)).

**Locality unknown.**

Width of frame 5.6 mm.

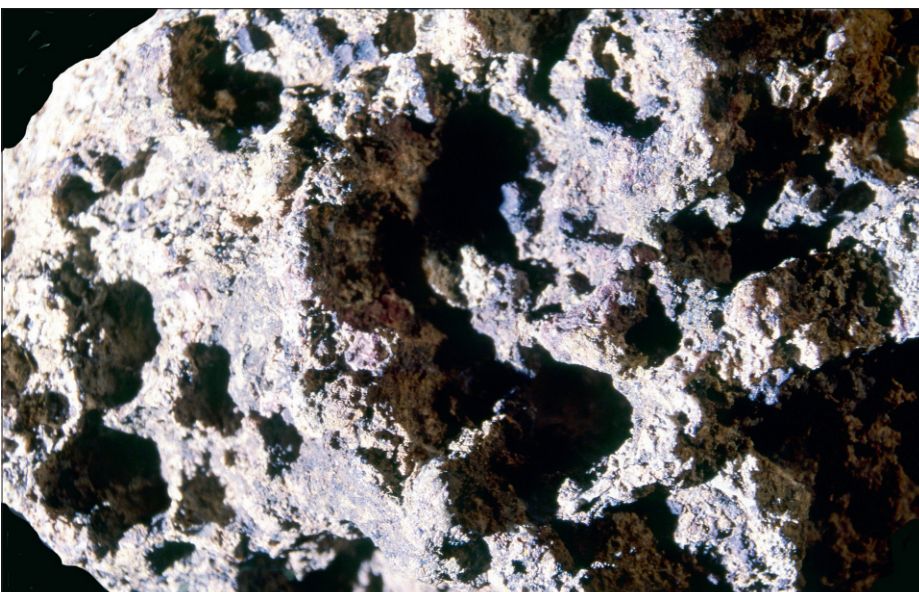


**Fig. 7.26 Galena-cerussite-massicot-minium.**

Galena residual kernels-remnant central galena (as above) converts to coarse granular cerussite. This is susceptible to removal via mechanical erosion at surface. The surrounding shells of early cerussite (± anglesite) convert to massicot (yellow) which in turn converts to "minium" (orange-red). See also [Figures 7.37](#)–[7.38](#).

**Argentine district, Queensland, Australia.**

Width of frame 6 cm



**Fig. 7.27 Galena "gossan" – Surface expression.**

Leached capping –eroded version of [Figure 7.26](#). Circular cavities in granular massicot/cerussite, where softer? or less compact central core materials have been removed via mechanical weathering. Galena residuals are located within centimetres, and quickly revealed via lusty hammer blows!

**Sorby Hills, Northern Territory, Australia.**

Width of frame 7 cm

**Fig. 7.28 Galena boxwork.** A central galena kernel as in [Figures 7.25–7.26](#), having converted to cerussite ribs and grains, is now undergoing minor surficial erosion to produce a “floral” pattern. The outer shell contains considerable yellow–green massicot. The colour here is a little greener than usual? Once again remnant galena kernels can be found nearby, and there are no serious problems in interpreting galena in the deposit.

**Locality unknown.**

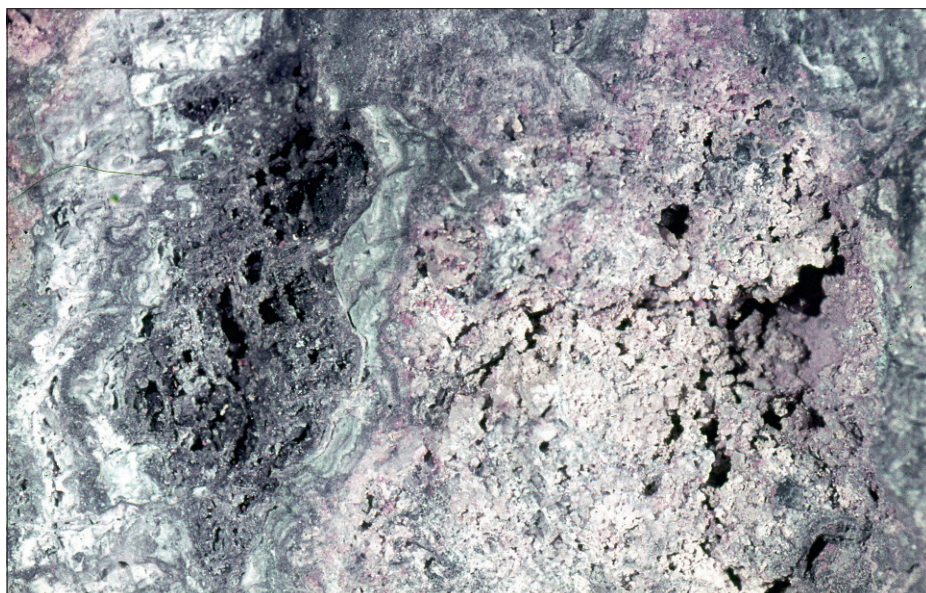
Width of frame 2.5 cm.



**Fig. 7.29 Galena boxwork.** An exceptionally rare example of “cubic” boxwork (left) emerging via erosion of an original central ex galena core-kernel subsequently replaced by granular cerussite (see [Figures 7.26–7.28](#)). Possibly the initially formed cerussite ribs formed a more coherent mass than the later granular product? The weathered outer shell of “massicot” is well seen to the right.

**Locality unknown.**

Width of frame 6 cm.



**Fig. 7.30 Galena boxwork.** Close up of the interior of a cavity which was once a kernel zone similar to [Figure 7.28](#). Despite the almost total erosion of the granular cerussite, a thin remnant lines the walls and displays an impressive cube like pattern. It is stressed that this cleavage pattern is very unusual with examples like [Figures 7.26](#) and [7.28](#) being the norm.

The identity of the minute green minerals is unknown (rosasite suspected)

**Locality unknown.**

Width of frame 3 cm.



### 7.3.6 Pentlandite/pyrrhotite (sulphide nickel assemblage)

Although pentlandite is not a common mineral, it becomes important in the recognition of nickel-sulphide ores in association with pyrrhotite. Gossans of this original assemblage are relatively common in Western Australia where they occur as silica flooded red-brown chert-jasper reflecting the lateritic/arid surface developed over long time periods. They are also referred to as ironstones (Figures 7.31–7.33).

The hard/brittle exposures may be associated with some development of nickel, secondary minerals, particularly the striking apple green/yellow nickel iron-magnesium carbonate (gaspeite). Less obviously the siliceous mass replaces the ferruginous gossan in a pseudomorphic fashion, such that many textures are recognisable. A good rock saw is highly recommended. Textures preserved include visible differences between ex-host rocks and sulphides, enabling recognition of breccia, sulphide layering and even different sulphide types (Figures 7.31–7.33).

The latter require microscopic treatment. At microscope level the classic fracture (parting) pattern of pentlandite is often recognisable, despite the fact that it has been converted successively to violarite, iron oxides and silica. Each conversion is texturally retentive and whilst not exactly a boxwork structure, has been extensively used in West Australia in the discrimination of nickel sulphide-rich derived jaspers from other ironstones. Utilised in conjunction with geochemical dispersion, petrology becomes a powerful discriminatory tool (Nickel et al, 1974, and Nickel et al, 1978).

**Fig. 7.31** Nickel sulphide “gossan-ironstone”.

The “gossan” is now composed almost entirely of silica with minor green nickel? minerals in late cavities. However this cut surface reveals textural variations. The darker patches (for example top left) are interpreted as ex –rock fragments, surrounded by paler ex –sulphide materials (pyrrhotite –pentlandite).The breccia may be a matrix style ore where deformed sulphides have disrupted the wall rocks? Petrology may detect remnant sulphide textures.

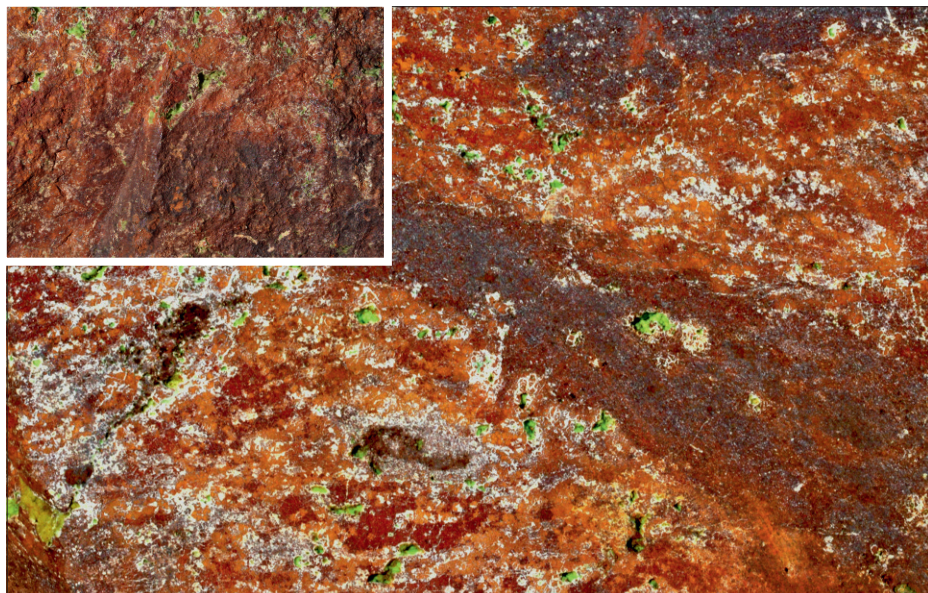
**Widgee 3 orebody, Widgeewooltha, Western Australia, Australia.**  
Width of frame, 8 cm.



**Fig. 7.32** Nickel sulphide “gossan-ironstone”.

Siliceous jasperoidal alteration of original ferruginous gossan with minor later gaspeite in cavities. The texture suggests dark ex-rock fragments in a paler ex –sulphide (pentlandite-pyrrhotite) matrix .The inset (4 cm) illustrates the surficial uncut surface.

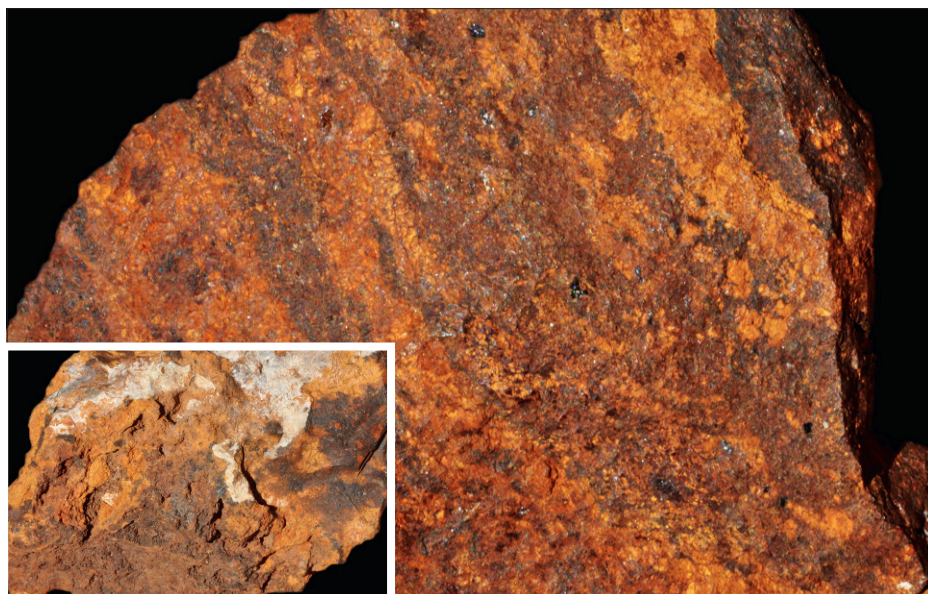
**Otter mine, Kambalda, Western Australia, Australia.**  
Width of frame, 9 cm.



**Fig. 7.33** Nickel sulphide “gossan-ironstone”.

Siliceous jasperoidal ironstone with textural indications suggesting layered sulphides (orange) with darker wall rocks (see above, [Figures 7.31–7.32](#)). The main frame is a broken surface and the inset (4 cm) is the surface expression.

**Kambalda mine, Kambalda, Western Australia, Australia.**  
Width of frame 5 cm.



### 7.3.7 Arsenopyrite

Arsenopyrite is the most common arsenic bearing mineral (Figure 7.34) and is the only one which occurs in sizable enough amounts to produce visible leached outcrop products. Most of the other arsenic bearing minerals occur as fine grained sulphosalts, which are almost impossible to identify even in their pristine state.

Arsenopyrite behaves very similarly to galena, reflecting a generally insoluble character. Similarly to sphalerite and chalcopyrite it is very susceptible to covellite/chalcocite conversion at the supergene zone (Figure 6.32). However, it also occurs in many copper poor associations, and hence survives to enter the oxide zone. Arsenopyrite has a characteristic rhomboidal crack pattern (Figure 7.35) and this controls the development of ribbing. The ribs develop via an alteration process, which converts arsenopyrite to scorodite (hydrated iron arsenate, Figures 6.57, 7.34–7.35). This quickly spreads from the original points of access, and the net result is a fine grained granular mass of scorodite. On rare occasions, some vague rib structure may be visible. Minor leaching of the scorodite mass occurs at surface (conversion to limonite) but for the most part the mass is effectively featureless and in many ways resembles the granular cerussite end product of galena.

Fortunately scorodite is easily recognised via its pale (arsenic) green colour and the characteristic granular texture. It is not entirely clear how the granular mass develops into a spongy format, but the scorodite is essentially marking the original arsenopyrite site. On many occasions grains form upon grains to give a complex arborescent pattern.

Scorodite also forms as a breakdown product of other arsenic rich sulphides such as enargite and other related minerals in high sulphidation mineral assemblages. These are usually fine grained and the replacive process forms isolated granular cluster of scorodite, rather than the large masses that may develop from “massive” arsenopyrite concentrations.

### 7.3.8 Carbonates

Carbonates are very common associates of mineralisation. In many cases these are iron rich (siderite, ankerite, ferruginous dolomite) which can form significant gossanous exposures and occasionally boxwork structures (Figures 7.37–7.38).

Siderite normally oxidises to a characteristic rich brown chocolate coloured limonite, although other paler colours are recorded (yellow to grey-grown). The net result can be a major gossanous exposure in iron rich carbonate rocks. Siliceous ribbing is a common development, which ranges from random in format, to rare examples of ribbing forming pseudomorphic rhombohedral cleavage patterns. The materials are often coarsely cellular.

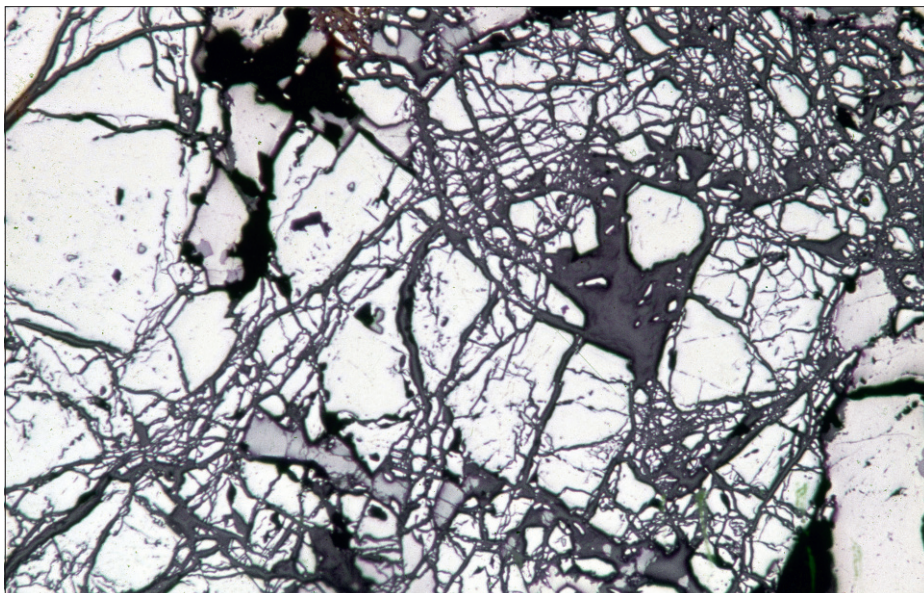
Siderite crystals may be replaced by indigenous limonite to form perfect chocolate brown pseudomorphs, which upon further oxidation may become finely cellular and display some characteristic cleavage patterns (Figure 7.38 and 7.38 inset).

Carbonates in general are easily dissolved, but despite this, there are many instances where thin “silica” ribbing develops via alteration (both supergene, and hypogene) where subsequent dissolution leaves excellent boxworks (Figures 7.39). There is often a problem of scale, and it is important to conduct hand lens inspection with some concept of potential grain size.

**Fig. 7.34 Arsenopyrite (fracture pattern).**

The polished section (right) shows the typical fracture pattern of arsenopyrite (pale) which is essentially random here, although there is a hint of quadrilateral elements.

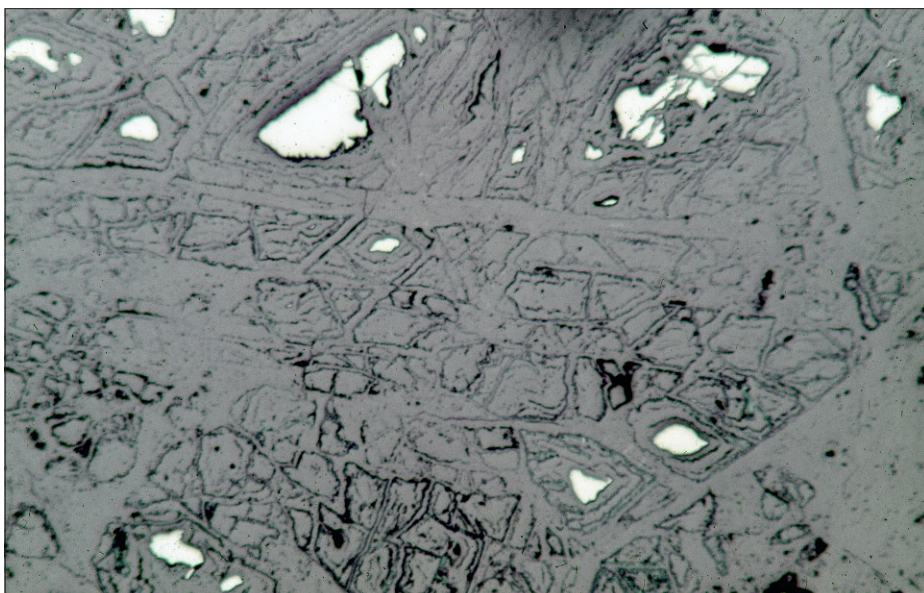
**Location unknown.**  
Width of frame 5.6 mm.



**Fig. 7.35 Arsenopyrite-Scorodite.**

Arsenopyrite is very susceptible to supergene replacement via chalcocite /covellite (Figure 6.32). However, if it survives passage through the water table zone it is often replaced directly in the oxide zone by generations of scorodite (hydrous iron arsenate). This is well seen in the adjacent polished section which is essentially all scorodite (grey), plus an unidentified black substance. Some pale arsenopyrite remnants are present.

**Location unknown.**  
Width of frame 5.6 mm.

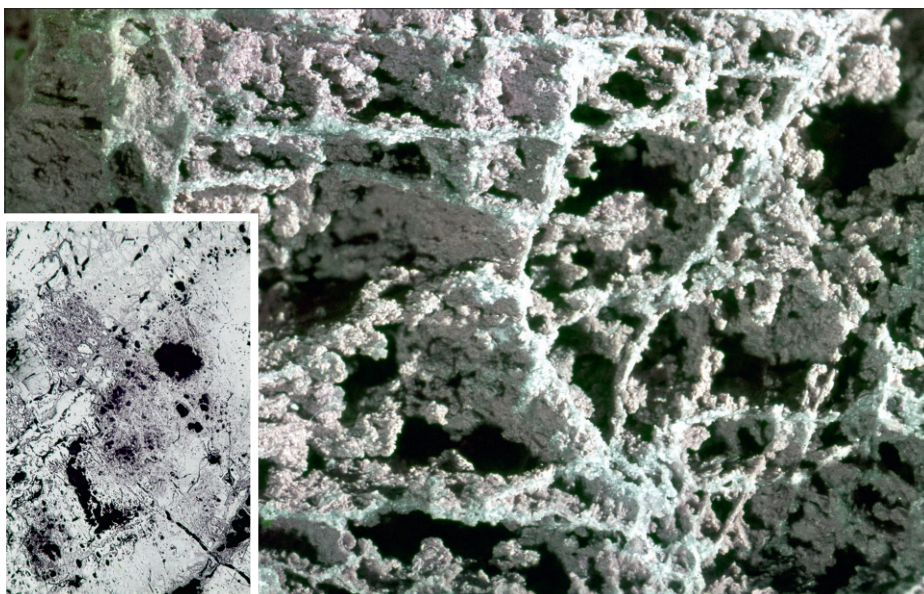


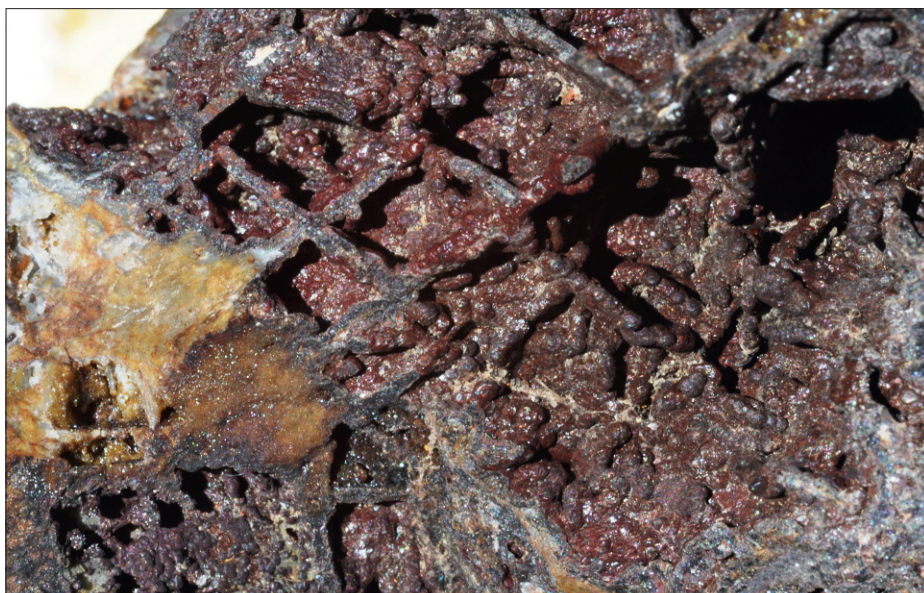
**Fig. 7.36 Arsenopyrite-scandite boxwork.**

The inset picture of a polished section, illustrates generational replacement of scorodite (grey to white) with initial coarse ribbing.

Length of frame 5.6 mm. The main frame illustrates the common end product of coarse scorodite ribbing (defining cells) encrusted with granular scorodite. It is not entirely clear how the open spaces are formed (arsenopyrite dissolution?). See also Figure 6.57.

**Location unknown.**  
Width of frame 5 cm.





**Fig. 7.37 Siderite (carbonate) boxwork.**

Prominent coarse rhombohedral ribbing emerging from an oxidised mass of siderite. The brown colour is common, presumably reflecting the original iron content now appearing as iron rich silica. The glassy reflective granules attached to the ribs are probably also quartz, and it is not clear whether they are transported or indigenous. However it is a common feature suggesting an indigenous process.

**Locality unknown.**  
Width of frame 3.5 cm.



**Fig. 7.38 Siderite (carbonate) boxwork.**

Siderite frequently oxidises in a pseudomorphic manner to chocolate coloured limonite, with further weathering bringing out some rhombohedral boxwork. The emerging boxwork is well shown in the main frame (width of frame 5 cm).

The inset contains good examples of pseudomorphed wedge shaped crystals (arrows) and some boxwork developing. (Main frame and inset).

**Mt Wright gold mine, Ravenswood, Queensland, Australia.**

Width of frame 1.5 cm



**Fig. 7.39 Carbonate boxwork.**

A perfect carbonate boxwork with distinctive delicate rhombohedral ribbing. Less well developed examples are also present. It is not clear whether or not the holes are ex carbonate?

**Location unknown.**  
Width of frame 1.5 cm.

### 7.3.9 Garnets

Garnet boxworks and pseudomorphs are relatively common, especially in and around skarn rich environments (Figures 7.40–7.42). Garnet characteristically forms ovoid rhombohedral crystals, usually occurring as a granular mass at millimetre grain sizes. The crystals tend to convert to limonite (usually pale orange) and are hence present as pseudomorphs. They are often a little difficult to see in fine grained formats, but are easily visible in larger crystals.

In thin sections the crystal outlines, tend to be hollow with very delicate ribbing resembling the petals of a flower. This is rarely seen in hand specimens, but the general effect is to produce an extremely lightweight end product. The crystal shapes are the main identifying feature.

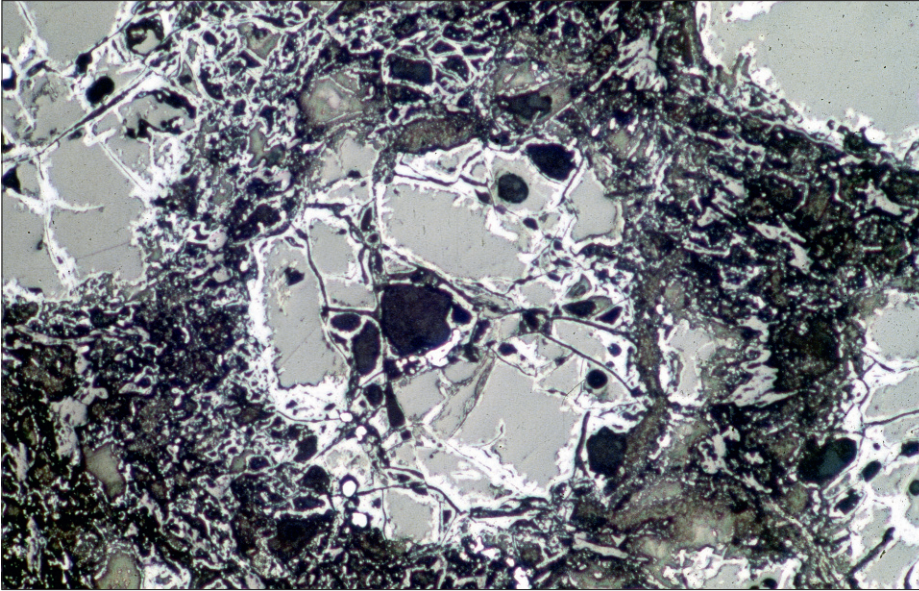
#### 7.3.10 Chalcocite (Figure 7.43)

Chalcocite forms both as a primary and supergene mineral. In the latter case it is usually fine grained and replacive of a preexisting sulphide.

The behaviour of primary chalcocite which occurs in both massive formats remains undocumented and the author has been unsuccessful in observing either the breakdown process or any indications of boxwork formation.

Secondary/supergene chalcocite may convert to cuprite, and/or maroon coloured haematitic limonite and this process is discussed later in the context of leached cap assessment in porphyry coppers (see also indigenous limonite (Figures 4.1–4.4).

Cellular boxworks representing chalcocite derived from granular chalcopyrite/pyrite clusters, have been rarely observed (Blanchard, 1968), but only as a leached section representing the above along an open fracture. The author has also noted this format at Escondida, where it is presumed to be a leached maroon haematite patch, derived from a granular pyrite/chalcopyrite mix, where original cell walls are emerging? (Figure 7.43).



**Fig. 7.40 Garnet boxwork.** Polished section showing ovoid garnet outlines. With the cavities (pale grey) rimmed, and containing delicate limonite ribs (white). The overall patterns resemble a flower, and the outlines reflect dodecahedral garnet crystals. **Tommy Burns tin mine, Sunnymount, Queensland, Australia.** Width of frame 5.6 cm.



**Fig. 7.41 Garnet boxwork.** Garnet pseudomorphs and developing boxwork in magnetite. Note easily recognisable rounded dodecahedral shapes. **Gillian tin prospect, Mt Garnet, Queensland, Australia.** Width of frame 7 cm.



**Fig. 7.42 Garnet boxwork/pseudomorphs.** The inset shows a dark gossanous skarn zone adjacent to an argillised diatreme. **Santa Rita copper mine, New Mexico, USA.** Photograph provided by D. Andrews. The main frame illustrates a very typical low iron granular garnet gossan, characterised by the pale limonite, closely spaced pseudomorphs, and very light weight. The garnets are fine granular about the size of the arrowhead, which is pointing at a particularly obvious garnet pseudomorph. In section the garnets are as shown in **Figure 7.40** (essentially hollow) – hence the very light weight. **Location unknown.** Width of frame 6.5 cm.

### 7.3.11 Miscellaneous mineral boxworks/pseudomorphs and comments (Molybdenite, cobaltite, fluorite, bornite and magnetite, Figures 7.44–7.45)

- *Molybdenite* (Figure 7.45). Molybdenite is very resistant to weathering, but has been recorded as being completely dissolved, leaving bladed-flaky negative pseudomorphs.
- *Cobaltite* (Figure 7.44). Boxworks of cobaltite have not been reported, but pseudomorphs of the cubic crystals occur at Mt Cobalt, Cloncurry, Queensland associated with conspicuous erythrite.
- *Fluorite*. Fluorite occasionally dissolves, leaving perfect negative cube shaped pseudomorphs.
- *Bornite*. The author has not observed the bornite weathering process. It usually converts to chalcocite/covellite at the supergene zone. However, Blanchard reports bornite derived boxworks as reflecting the curved primary crystal faces to give a unique spherically triangular configuration (Blanchard, 1968).
- *Magnetite*. Magnetite is common in many ores, and fortunately is very resistant to weathering. It does not form visible boxworks and in most cases retains both its crystal form and magnetism. Under extreme conditions it may partially convert to red limonite and beneath a microscope may exhibit replacive zonal and parting textures. In areas of the Atacama region, Chile it can be replaced totally by red haematitic limonite.

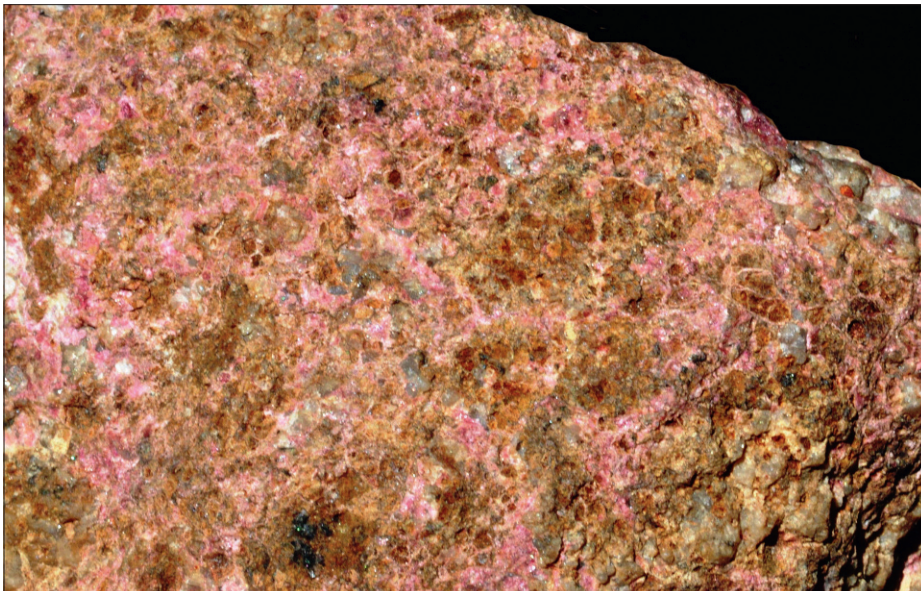


**Fig. 7.43 Chalcocite.**

A very rare boxwork where small ovoid rim structures (cellular ribs) have developed around grains clusters of ovoid chalcocite grains. These are derived from original clusters of pyrite-chalcocite (arrows) via total supergene replacement. The ribs seem to be emerging from haematitic limonite (red scratches) which is the normal surficial end product. It is suggested that this is a leached version of live limonite (indigenous maroon haematite) derived from chalcocite (Figures 4.2–4.4).

The latter occurs within centimetres of this locality in disseminated format. This specimen comes from a prominent through going joint surface, which would allow extra late acid water flow? Blanchard (1968) reports a similar cellular boxwork. **Escondida, Chile.**

Width of frame 5 cm.

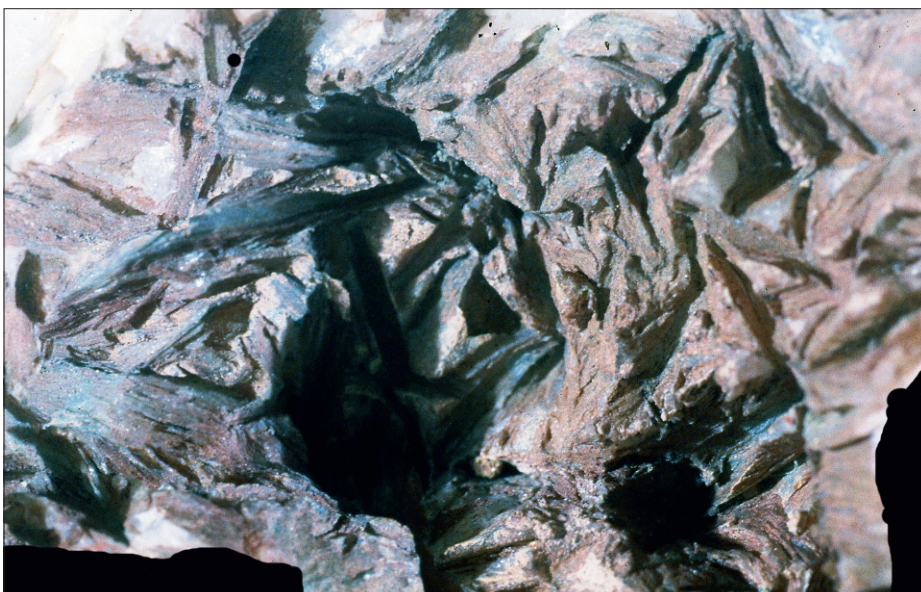


**Fig. 7.44 Cobaltite.**

Ovoid-cubic pseudomorphs of cobaltite (orange limonite), overprinted by crimson erythrite (hydrated cobalt arsenate) on a joint surface. The observer is unlikely to miss the cobalt signal!

**Mt Cobalt, Cloncurry, Queensland, Australia.**

Width of frame 5 cm.



**Fig. 7.45 Molybdenite.**

Negative pseudomorphs of molybdenite blades in a quartz vein.

**Ravenswood district, Queensland, Australia.**

Width of frame 5 cm.

## 7.4 False gossan and related observations (Figures 7.46–7.48)

Limonitic/ferruginous exposures are not limited to underlying sulphide related ore zones, and there are numerous circumstances where the observer is forced to ponder upon probable origin.

Ordinary rocks with high iron contents will easily yield ferruginous surface products, especially in tropical climates. Ultramafic rocks are very susceptible to such end products (Figure 7.46 and 7.48). However, in most cases a quick check on the local conditions and weathering profiles will quickly resolve this type of problem (lateritic profiles, deep weathering, etc).

Surface detrital ferruginous duricrusts can also create problems and promote such thoughts as “Is this isolated fragmental rock a remnant of an original ferricrite or oxidised mineralised breccia?”

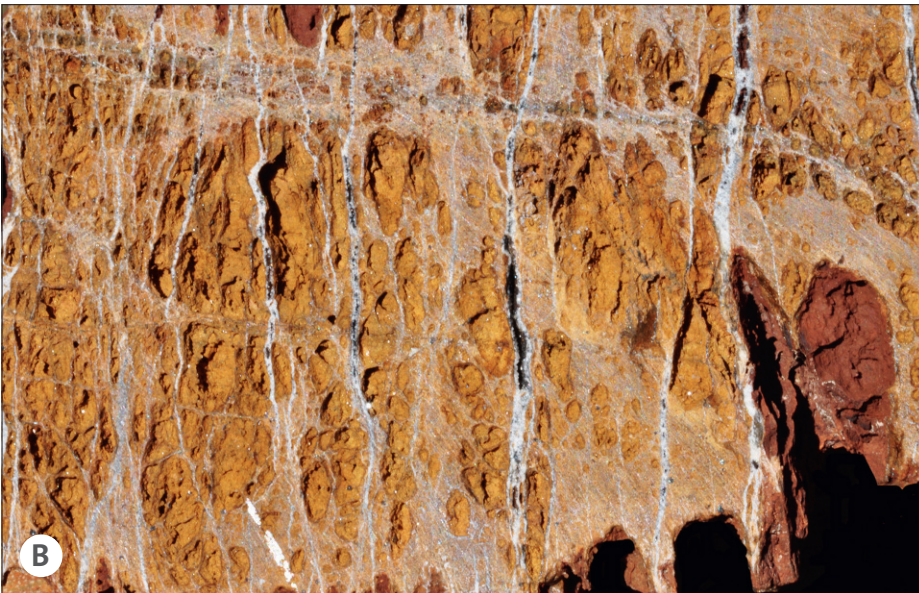
Again in most cases some further examination of the exposure and local environs will normally resolve the problem. Most false gossans are full of transported/exotic limonite and manganese oxides, with little sign of boxworks, relevant secondary minerals, and often contain mixed fragments suggesting surficial origins. Many of these carry interesting metal values due to adsorption factors relating to limonite/manganese oxides. Particular problems occur in the rare case where some of the detritus is actually “real gossan” incorporated into the weathering mass!

The Century case provides an interesting example of “catch 22” involving “false gossan” with one particular exposure contributing enormously to the non recognition of the major Century deposit for some 100 years (Figure 7.47).

The relevant outcrop occurs in very isolated terrain and is very conspicuous, attracting the attention of any passing prospector. It is clearly surficial ferruginous and interpreted as some type of remnant coarse fragmental ferricrite. Botryoidal limonite is abundant; with prolific manganese oxides. Assay values yield very high zinc values, but this was not considered significant as there are known lead-zinc veins in the district.

It now appears that the values were significant, in the context that the main stratiform ore zone is exposed only a few hundred metres away from the large ferruginous boulder. Discovery was via a somewhat fortuitous drill intercept, and the exposure had remained unnoticed with the low iron sphalerite not producing significant limonite.

Even more problems are encountered when the ferruginous materials are present as siliceous jasperoidal materials. These can represent genuine hypogene siliceous alteration with mild surficial oxidation, silicified gossan, or surficial alteration of regional (or even local origin) of non sulphide materials. The field procedures are relatively restricted, and amount to establishing the geological context, and collecting a suite of specimens. The latter will be available for slabbing to collect relevant structural and textural information, and also for petrological and/or geochemical data if required. Large samples for slabbing are recommended. It is rare in these circumstances to find useful secondary minerals, although green nickel compounds are relatively common in the hard red jasperoidal surface exposures of sulphide nickel deposits in Western Australia (Figures 7.31–7.33). This really comes down to a common sense approach. The geological setting is obviously of prime value in establishing potential deposit types (sulphide nickel v volcanogenic exhalative).



**Fig. 7.46 False gossan – Serpentine.**  
 The three plates illustrate the progressive replacement of a leached serpentinite rock with prominent garnierite veining, to form a surficial limonite dominant replica. The final product is coarse celled, and in the field all stages of development are easily observed.  
 The specimens come from 1 m depth (A) 4 cm depth (B) and the surface (C).  
**Greenvale, Queensland, Australia.**  
 Width of frames 8 cm.

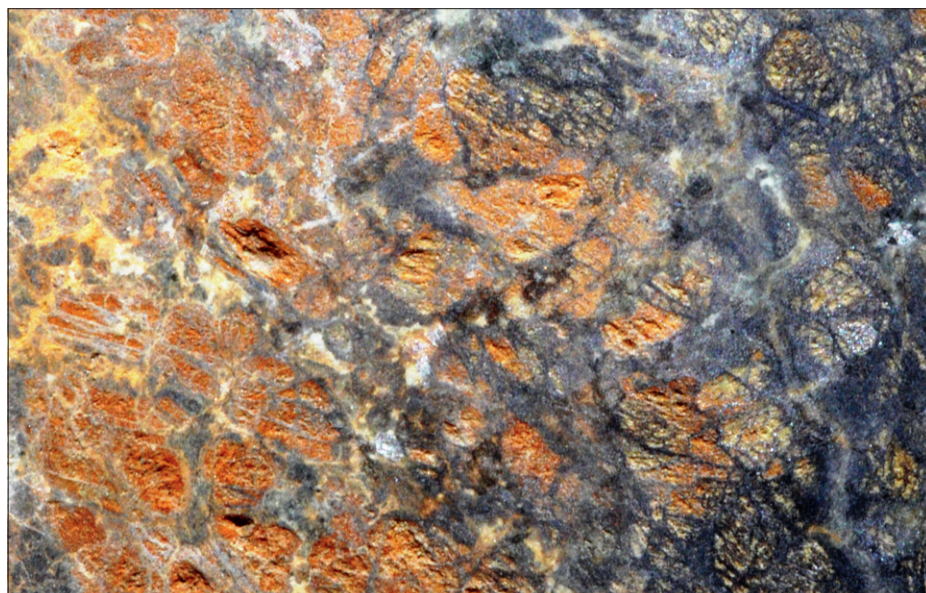
**Fig. 7.47 False gossan – Century mine area, Queensland, Australia.**

This conspicuous ferruginous cemented rubble boulder occurs within a few hundred metres of the real leached cap exposure of the giant stratiform Century zinc deposit. It is visible for kilometres and always attracted geological and prospector attention. It contains numerous lumps of exotic botryoidal limonite and manganese oxides, and is of detrital surface origin. It does however contain strongly anomalous zinc values. These were not regarded as significant as there are zinc veins in the general region. [Figure 3.27](#) shows the actual ore zone exposure, which is not ferruginous, reflecting the low iron content of the sphalerite ore. The exposure is being admired by Dr Grahame Broadbent.



**Fig. 7.48 False gossan – Olivine gabbro.**

Ovoid limonite pseudomorphs resulting from the weathering of the igneous rock. Dark silica alteration to the right. Minor investigation quickly reveals the situation. Many iron rich minerals quickly oxidise to form ferruginous surface limonite. Chlorite is another common example often forming red limonitic gossan. **Carajas region, Brazil.** Width of frame 5 cm.



## 8.1 General aspects

The large scale leached cappings involved with porphyry copper systems have long attracted attention both in terms of discovery and general assessment. Within this context it is useful to understand the main characteristics of porphyry copper systems. Fortunately the prevalence of open cut mining provides excellent exposures extending from hypogene environments through to the surface and the profiles have been well studied (Sillitoe, 2005, [Figures 8.1–8.11](#)).

The textures and mineralisation styles involved with porphyry copper systems vary enormously, and the sulphides tend to occur as disseminated alteration sulphides and/or vein style sulphides in minute to major scale veins ([Figures 8.16–8.18](#)). These may be widely distributed or focussed in sets. Intrusive breccias complicate the picture in many cases, with mineralisation occurring as matrix alteration and/or as infill between pre-existing fragments. This range in style and contingent surficial recognition is an integral part of prospect assessment, and is not easy to delineate within the typically acid-leached clay altered exposures.

However, even with all the complexity attributed to leached outcrops, the best and absolutely critical field guide is an ability to recognise the basic structural architecture of the system from the outcropping (or drill core) materials. A porphyry system is very unlikely to exceed economic constraints unless the channelways controlling mineralisation are sufficiently focussed to allow either major hypogene or subsequent supergene concentration. This is usually easily seen by rapid examination of available field and drill core materials. Exploration personnel should constantly be aware that from hundreds of occurrences only a handful develop into mines. In most cases secondary enrichment is the vital factor, providing an enriched near surface zone of copper concentration.

- Disseminated (alteration) sulphides.
- Complex networks-stockworks of crackle style veins, microveins linked to the disseminated material, generally exhibiting a broad scale distribution ([Figures 8.16–8.18](#)).
- Oriented styles of dense fracturing, such as sheeted veins, which in combination with the above form systems where small areas contain extremely high grades (Grasberg style).
- Major breccia systems of various types associated with the crackle/broken rock styles mentioned above. Occasionally a porphyry system is almost entirely composed of intrusive breccia pipes.

All of the above may occur within a porphyry style host rock setting, or within country rocks (metasediments, andesites and carbonate rich sequences). The latter are usually skarn dominated. It can quickly be appreciated that the well established, easy to

understand model of the classic San Manuel system, with a relatively uniform structural (crackle) style, well developed annular alteration zones, neatly systematic distribution of ore grade and uniform host rocks, is not necessarily the porphyry copper system that any particular exploration discovery is dealing with.

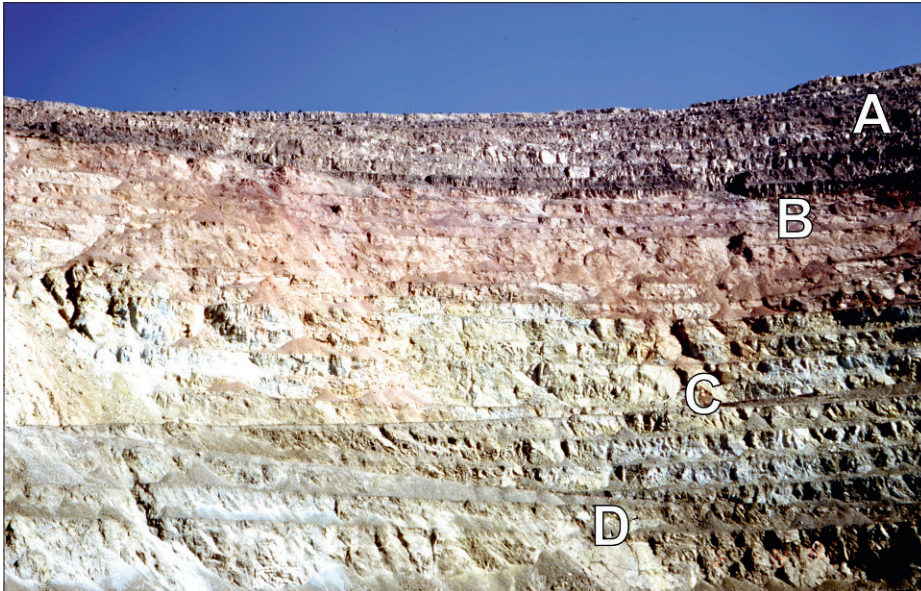
## 8.2 Crackle/stockwork recognition

Despite the previous section describing potential variations, it remains true that the vast majority of porphyry systems are essentially controlled by variations of the overprinted crackle theme. Several generations of widespread “shattering” form a multiple overprinting system, channelling and depositing ore and ore related fluids. The actual end result can obviously vary from relatively uniform fracture density, to irregular spacing where oriented fault systems focus fracture density. However, regardless of the pattern, it is the fracture density which is the most critical feature. Most experienced observers/consultants stress this as a major priority given that they are working within a crackle style system as opposed to a major breccia.

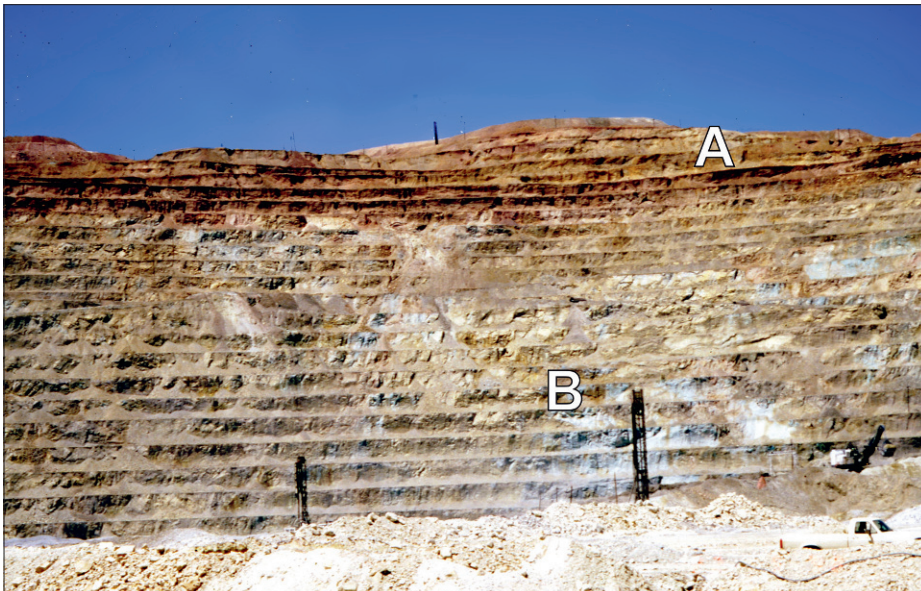
Fortunately surface weathering/leaching enhances vision of shatter/crackle fault broken rock systems, with iron staining picking out both the patterns and density for easy assessment.

Systems of evaluation (measuring) are not easy to devise and that developed by Titley et al (1986) at Sierrita-Esperanza is a popular choice. This can be adjusted to suit the purpose but values of fracture abundance are determined from measurements of the total fracture lengths divided by the outcrop area within which the lengths were measured. The Sierrita-Esperanza exercise demonstrates a general truth that fracture density relates directly to ore centres.

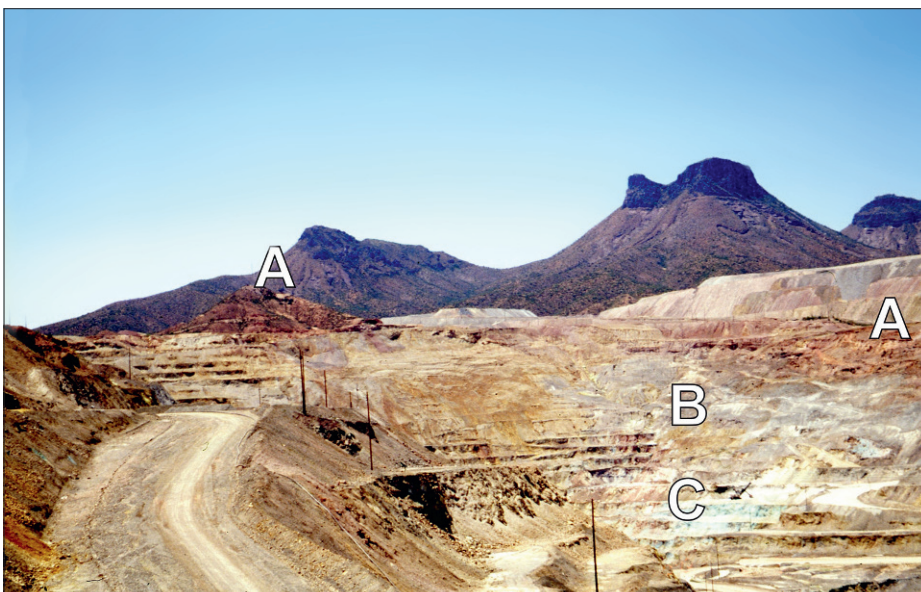
The method is perhaps a little tedious for everyday use, but is easily converted into semi-qualitative use with simple mapping divisions of high-low-medium. However, it is important to use a relatively consistent surface area measure for working semi quantitatively. The approach is very strongly recommended in both surface outcrop/drill logging practise.



**Fig. 8.1 Leached capping profile.**  
A late ignimbrite layer (A) overlies the leached cap profile. The red upper zone (B) is the haematitic leached capping of a former chalcocite enriched supergene blanket. It is underlain by a mixture of both jarositic and goethitic limonite (C), which passes downwards into grey supergene chalcocite ore (D).  
**Cajujone porphyry copper, Peru.**  
Photograph provided by D. Andrews.



**Fig. 8.2 Leached capping profile.**  
Orange red haematite rich zone (A) passing down into grey supergene "chalcocite" zone (B).  
**Santa Rita porphyry copper, New Mexico, USA.**  
Photograph provided by D. Andrews.



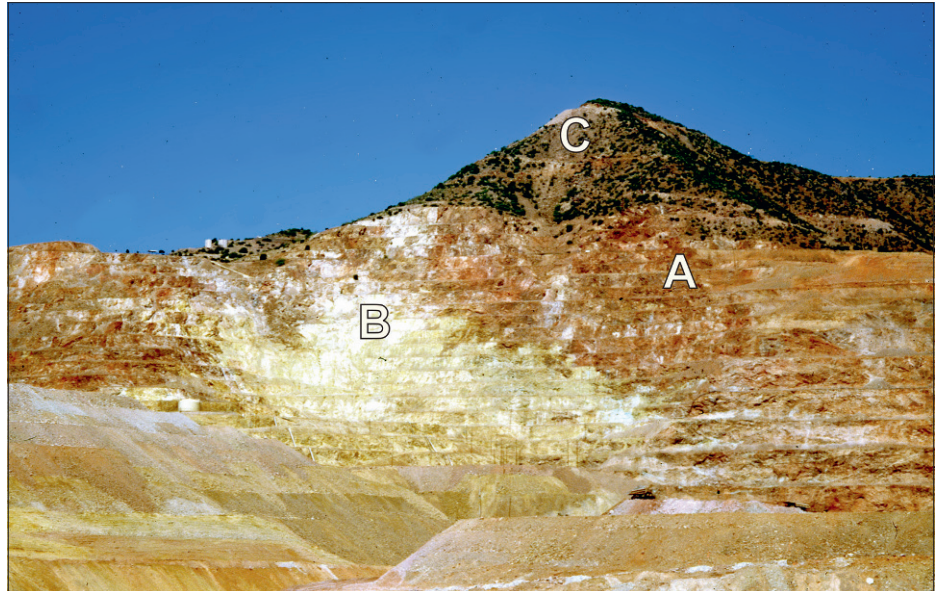
**Fig. 8.3 Leached capping profile.**  
The original exposure is preserved in the hill (A-left) and the haematitic capping is seen in the pit (A-right). The main supergene enriched chalcocite zone (B) contains an area of oxide copper ore (green-C). Note the term "oxide copper" is used very loosely in the porphyry copper world, usually describing malachite, chrysocholla and brochantite in variable proportions. Ray is unusual in that the host rock is schist, as opposed to porphyry.  
**Ray porphyry copper, Arizona, USA.**  
Photograph provided by D. Andrews.

**Fig. 8.4 Leached capping profile.**

Red haematitic leached capping (A) flanking a core of yellow-white jarositic porphyry (B) overlain by (C) goethitic capping across an older oxidised zone.

**Morenci porphyry copper, Arizona, USA.**

Photograph provided by D. Andrews.



**Fig. 8.5 Surface exposure of the famous San Manuel ore deposit.**

The exposure is a weathered breccia zone with maroon coloured indigenous limonite, denoting an ex-chalcocite supergene enrichment zone. Leached capping.

**San Manuel porphyry copper, Arizona, USA.**

Photograph provided by D. Andrews.

Width of frame 3 m.



**Fig. 8.6 Abundant red haematitic limonite.**

Maroon colour-capping representing an ex-supergene "chalcocite" zone.

Leached capping.

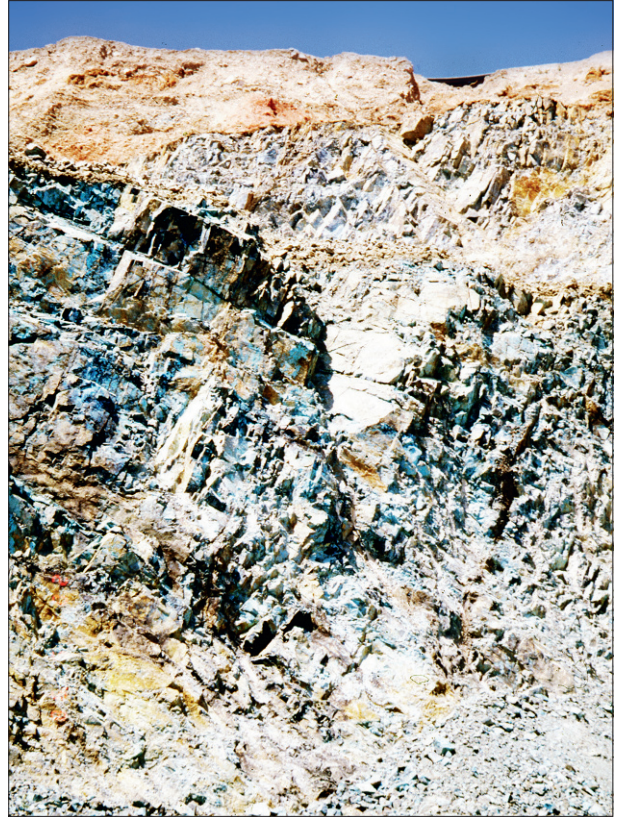
**Morenci porphyry copper, Arizona, USA.**

Photograph provided by D. Andrews.

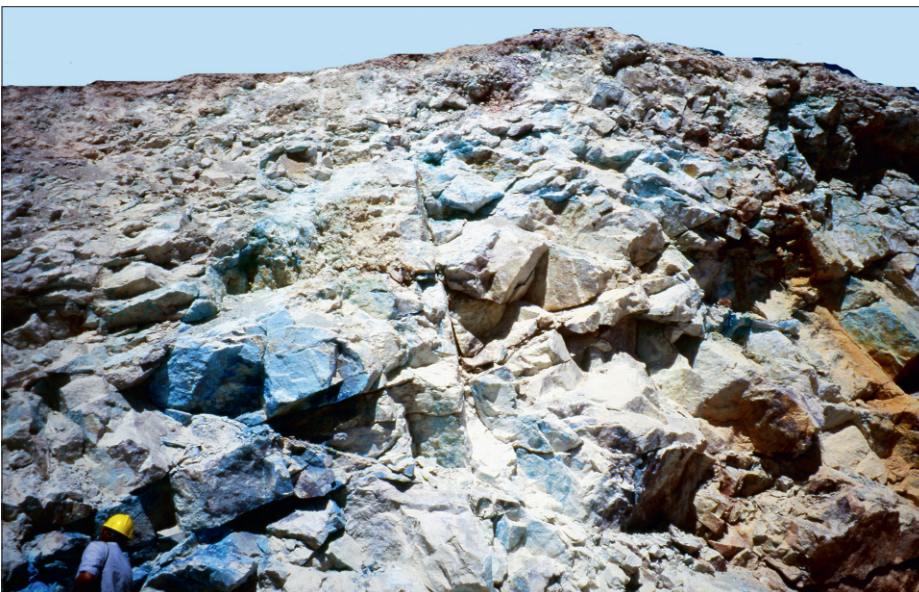




**Fig. 8.7 Leached capping – oxidised copper style.**  
 The El Abra surface exposure covers an area of about one square kilometre where green copper oxidation minerals are abundant. The central zone is predominately chrysocholla ± atacamite, pseudomalachite, antlerite and brochantite (see [Figures 6.18–6.23](#) and [6.28](#)). As can be seen here these are late features, largely infill dominated – fracture controlled. Subsequent fracturing contains transported rusty goethitic limonite. The host rocks are potassic altered, argillised, intermediate composition porphyries.  
**El Abra porphyry copper, Chile.**  
 Photograph provided by D. Andrews.



**Fig. 8.8 Leached capping – oxidised copper style.**  
 Zone of green oxidation copper minerals (chrysocholla, malachite?) forming well below surface, note upper haematite zone.  
**Ray porphyry copper, Arizona, USA.**  
 Photograph provided by D. Andrews.



**Fig. 8.9 Leached capping– oxidised copper style.**  
 Section of green-blue copper oxide within the pit composed of brochantite, atacamite, antlerite and chrysocholla ± minor chalcantite. The green-blue copper minerals here are not as well represented at surface, but occur in the upper to mid profile in selected regions. They range from a few metres to 200 m thick, assaying from 0.2–1.5% Cu.  
**Escondida porphyry copper, Chile.**  
 Photograph provided by D. Andrews.

**Fig. 8.10 Leached capping – jarositic ± minor goethite.**

This system has no supergene enrichment and the primary ore (white lower pit) is chalcopyrite dominant with minor pyrite + biotite and magnetite. The host porphyry is potassically altered. Insufficient acid is generated to produce significant chalcocite, but enough to cause argillic alteration. Major yellow jarosite occurs in the surficial regions.

**Alumbraera porphyry copper, Argentina.**

Photograph provided by D. Andrews.



**Fig. 8.11 Leached capping – goethite/jarosite.**

Surface exposure of an originally pyrite rich quartz sericite zone, now converted to goethite ± jarosite and clay. Note rusty limonite stains where rocks have fractured along veins. Exposures of this nature eventually focused exploration on the major ore zone with some geophysical input.

**Ujina, Chile.**

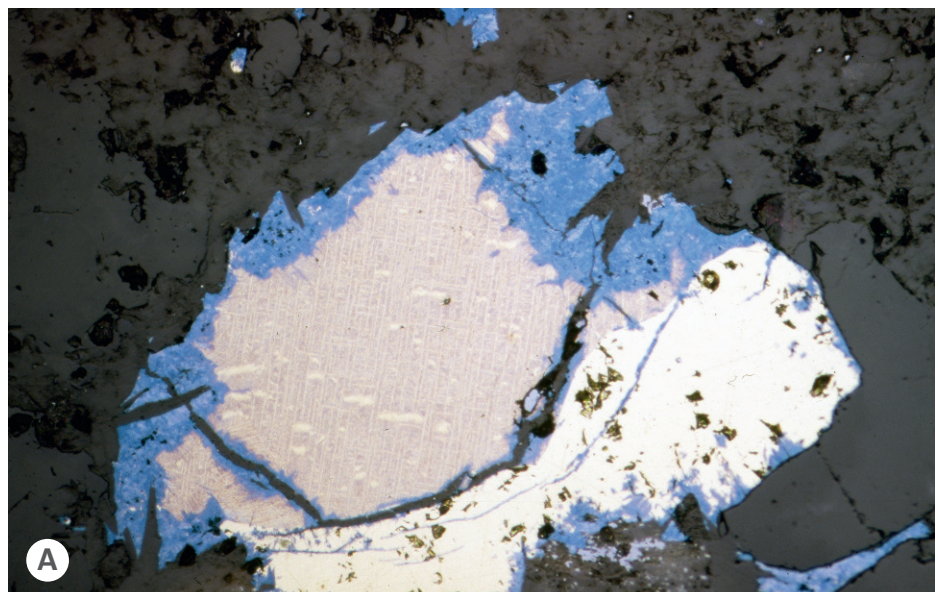
Photograph provided by D. Andrews.



**Fig. 8.12 A Supergene enrichment – polished sections.** Bornite (pink) and chalcopyrite (yellow) with rim and fracture controlled replacement by chalcocite (blue). The beginning of enrichment is seen here.

When the primary copper minerals are replaced, the process then replaces the associated pyrite (see overpage) **Specimen from Escondida Norte, Chile.**

Width of frame 2.4 mm.





**Fig. 8.12 B** Supergene enrichment – polished sections. Advanced chalcocite development replacing pyrite. At this stage the profile would be referred to as mature. When replacement is minor the enrichment is called immature. **Specimen from Escondida Norte, Chile.** Width of frame 5.6 mm.

### 8.3 Sulphide oxidation and supergene enrichment

Sulphide oxidation is a complex process and still a subject of research with special reference to metallurgical perspectives. The major operating factors are considered to involve solution chemistry and electrochemical processes catalysed by bacteria. Oxidation via direct exposure to the atmosphere is another very minor contributor.

The main action occurs in the surficial vadose zone and capillary fringe above the water table and in detail relates to permeability controls probably down to the nano scale involving oxygen and water. The net result in porphyry copper systems is that copper is taken into solution and remains in solution at  $\text{pH} < 5.5$ , descending into the hypogene domain to cause major enrichment at the general water level.

It should be noted that if the solutions are at higher pH levels, copper may precipitate utilising one of the available anions in the groundwater (hydroxyl, carbonate, chloride) derived from sulphide dissolution (sulphate, arsenate) or extracted from the host rocks (silicate, phosphate, carbonate). In this case little or no copper may reach the hypogene materials to form a “chalcocite” supergene zone.

Porphyry copper systems typically contain variable amounts of pyrite  $\pm$  chalcopyrite/bornite. In terms of supergene enrichment the copper minerals are quick to convert to chalcocite  $\pm$  covellite, whilst pyrite is relatively immune at the early stages of the process. Nonetheless given sufficient time and acid supply via oxidising pyrite, the descending copper solutions will completely replace the pyrite. At this point the supergene blanket is conventionally termed mature. Early or intermediate stage conversions are termed immature (Figure 8.12 A, B)

### 8.4 Field assessment of leached cappings

The porphyry copper leached cappings can be loosely divided into either limonitic or oxide copper dominant (Figures 8.1–8.11). The limonitic species are more common and

can be further examined in terms of haematite, goethite, jarosite proportions (Figures 8.13–8.15). Surficial assessment can be approached in a variety of ways all of which have value, and can be utilised in combination.

### Approach No 1

Megascopic field assessment. This has been mentioned above, and should be considered as the priority approach. It involves examination of the leached exposures from a channelway/structural control perspective. Given that the leached exposures will have retained the primary structural control features, the first approach should be to determine whether or not the system is dominated by widespread crackle (stockworking – Figures 8.16–8.17), focussed veining stockworking or brecciation (intrusive breccia, etc). In some instances it will be a combination situation with intrusive style breccias being common in porphyry systems. At this early style investigation of the density of fracturing and/or fluid ingress via breccia matrices become the prime focus, as ultimately the grade of the system relates directly to the focussing or intensity of focussing controlling fluid access. Although surface exposures/drill cores may be dominated by surficial clay alteration, the access system is usually well represented via limonite distribution.

### Approach No. 2

Estimation of the volume percent of acid forming sulphides. Given that supergene enrichment and primary sulphide grades are very much a function of sulphide content, it is usually helpful to acquire some estimate of the original volume percent of primary acid forming sulphides (AFS). This can be approached in the crackle/disseminated style systems via utilisation of petrology style percentage composition estimators (visual volume percent mineral estimators – charts/circles). This is actually much more difficult to do with any precision than it sounds. Firstly the charts are not really designed to resemble realistic porphyry copper veinlet/disseminated spot alteration. Secondly the observer is trying to distinguish genuine primary features (ex-veins, spots – now holes or limonite occupied cavities) within a sea of limonitic overprinting (indigenous v transported). Many cavities are pin head size and there can be problems in deciding what is an appropriate original cavity verses an acid leach hole in clay altered host rocks. Estimates are difficult at low sulphide density, where the rocks tend to be fresher. Thirdly observation is not always easy in the highly weathered surficial rocks and granular limonite has a habit of weathering out.

However, despite the problems a relatively unsophisticated and necessarily slightly messy approach will generally distinguish high/low/medium divisions and in many ways makes the observer focus upon the structural control scenario so important in approach No 1. Answers should fall in within the 0.1–8.0% ranges.

It is probably not a task for someone without prior experience or conceptual realisation of just how a primary porphyry copper ore might look.

### Approach No 3

Assessment of the mineralogy, texture and abundance of leached capping “limonitic minerals” (haematite, goethite, jarosite – Figures 4.1–4.9, 6.1–6.3) in relation to underlying sulphide assemblages (Figures 8.13–8.27).

This approach is popular and although bordering on an art form has enjoyed considerable success over the years, particularly in evaluating the position and nature of supergene blankets (Sillitoe, 2005).

It has reasonable validity in sectors of southwestern USA, South America (especially Chile) and parts of Australia where particular climatic conditions have operated.

The technique requires an ability to distinguish between indigenous and transported limonite (Figures 4.1–4.9, Table 8.1) where indigenous limonite is considered to be limonite occupying former sulphide sites, and transported/exotic limonite as representing iron that has clearly moved from its original source and is now precipitated in fractures, or as general iron staining (including jarosite).

Original supergene blankets are frequently exposed at surfaces as oxidised remnants via erosion and/or uplift. Given that chalcocite oxidises to haematite rather than goethite the end products are relatively easy to recognise via the maroon colours of the largely indigenous sulphides. This can be utilised for both reconnaissance exploration and later more detailed evaluation.

The factors controlling haematite formation as opposed to goethite remain unclear (Alpers and Brimhall, 1989).

Original chalcopyrite/pyrite ratios become reflected by the ultimate chalcocite/pyrite ratios within a well developed supergene blanket, and the oxidised equivalents produce haematite-goethite-jarosite combinations which vary systematically with changing chalcocite/pyrite ratios (Figures 172–174).

This general picture can be seen from Table 8.1, originally produced by Loghry (1972) for southwestern USA situations, and modified slightly by Alpers and Brimhall (1989) for their classic study at Escondida in Chile. Figure 8.13 also reproduced from Alpers and Brimhall (1989) eloquently illustrates the limonite ratio and indigenous v transported concepts in Table 8.1.

The Loghry model was developed reflecting considerable experience from many workers in the southwestern USA porphyry domains, where zonal arrangements of chalcopyrite ± bornite and pyrite are common in the primary ores.

A popular model combining data from several southwestern USA deposits (Titley 1982, Titley and Marozas 1995) depicts sulphides arranged as a series of shells, around a barren central porphyry centre.

This conceptual picture (Figure 8.14) has an inner zone at the porphyry fringes where chalcopyrite exceeds pyrite, moving to a large central zone where pyrite dominates, grading to an outer pyrite fringe. Maximum sulphide contents of up to 10% occur in the central shell, where a non reactive sericite alteration, maximum fracture density, and a favourable pyrite/chalcopyrite balance results in maximum development of a supergene chalcocite zone. The optimum balance for maximum supergene enrichment is suggested as around 4.5:1 pyrite/chalcopyrite.

Table 8.1 Textures and relative abundances of limonites formed from various initial ratios of pyrite/chalcocite (after Loghry, 1972).

| Slow neutralisers<br>phyllic, argillic or<br>advanced argillic<br>alteration |                      | Indigenous limonites <sup>1</sup>                          | Relative abundance |             |  | Moderate<br>neutralisers<br>potassic, propylitic<br>or weak phyllic<br>alteration |              |
|--|----------------------|--|--------------------|-------------|--|---|--------------|
| $X_{Cu}$ <sup>2</sup>  | (py/cc) <sub>α</sub> |  | Indigenous         | Transported | Transported<br>limonites <sup>1</sup>                  |   |              |
| <sup>3</sup>   | 1:2.8+               | None   |                    |             | None   | 1:2.5+  | <sup>3</sup> |
| 1.23   | 1:2.5                | H; fragile, <i>relief</i> , fine<br>cellular               | 10                 | 0           | H; none or rare  | 1:2.0   | 1.16         |
| 1.16   | 1:2                  |  |                    |             |  | 1:1.5   | 1.06         |
| 1.06   | 1:1.5                |  | 9                  | 1           |  | 1:1   | 0.92         |
| 0.92   | 1:1                  | H; <i>relief</i> , hard cellular                           | 8                  | 2           | H; <i>fringing</i>                                     | 1.5:1   | 0.75         |
| 0.75   | 1.5:1                | H; relief, hard cellular,<br><i>rare botryoidal</i>        | 7                  | 3           | H; fringing, exotic<br>(in fractures)                  | 2:1   | 0.64         |
| 0.64   | 2:1                  | H ≅ G; <i>botryoidal</i> , hard<br>cellular, relief        | 6                  | 4           | H > G (> J);<br>fringing, exotic,<br>rarely iridescent | 3:1   | 0.49         |
| 0.49   | 3:1                  | H > G;<br><i>botryoidal</i> , hard<br>compact, rare relief | 5                  | 5           | H > G (> J);<br>fringing, exotic,<br>rarely iridescent | 4:1   | 0.40         |
| 0.40   | 4:1                  | H ≅ G;<br><i>nodular</i> , hard<br>compact, vitreous, flat | 4                  | 6           | G > H (≅ J);<br>iridescent                             | 5:1   | 0.33         |
| 0.33   | 5:1                  | G > H  | 3                  | 7           | J ≅ G > H  |   |              |
| 0.25   | 7:1                  | (G + J) > H  | 2                  | 8           | J > G > H  |   |              |
| 0.20   | 10:1                 | G + J  | 1                  | 9           | J > G  |   |              |
| < 0.10   | > 20:1               | None   | 0                  | 10          | J  |   |              |

<sup>1</sup> G = goethite, H = haematite, J = jarosite; italics indicate diagnostic haematite textures

<sup>2</sup>  $X_{Cu}$  = multiplication factor equal to percent copper per volume percent indigenous limonite ( $V_{α}$ ); based on copper content and specific gravity of sulphides (from Loghry, 1972)

<sup>3</sup> Insufficient acid for complete leaching; produces abundant copper oxides and hydroxysulfates

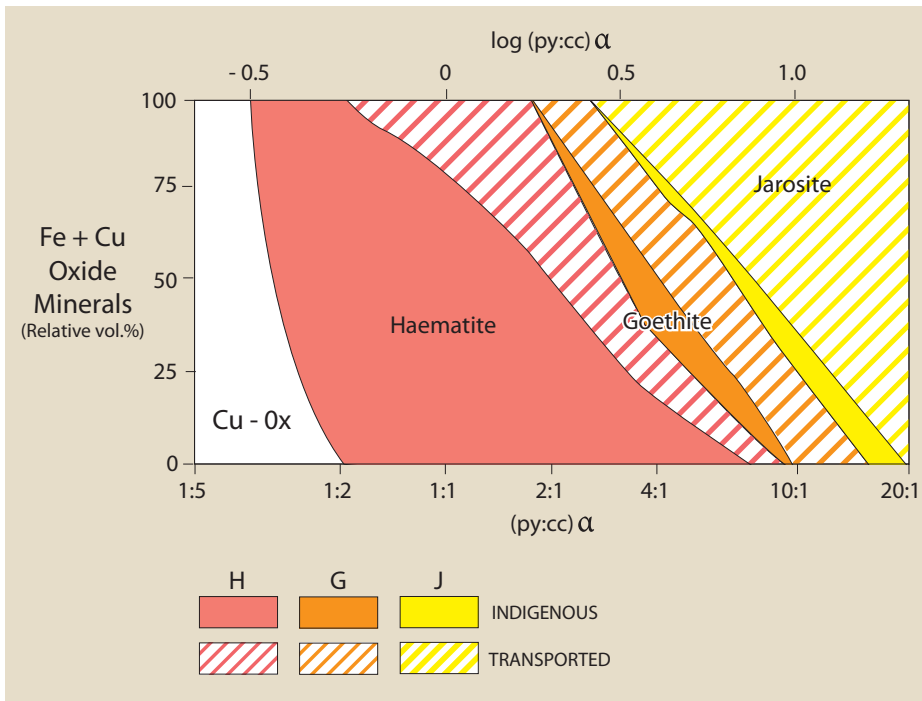


Fig. 8.13 Graphic representation of logarithmic scale correlations between limonite mineralogy and original pyrite/chalcocite ratios in rocks prior to oxidation for non reactive gangue (argillic, advanced argillic, and phyllic alteration) (from Alpers and Brimhall, 1989).

The southwestern states model (Figure 8.14) still has useful conceptual value, but as new discoveries have occurred during the subsequent 25–30 years, it now needs to be applied with caution.

Many systems lack an obvious central barren porphyritic core zone (e.g. Escondida) whilst others are confused by the presence of overprinting copper rich high sulphidation systems (Escondida, Escondida Norte and Chiquicamata – Chile). The giant Grasberg system in Irian Jaya is even more divergent with the copper being contained in late stage semi parallel stockwork of sulphide only veinlets and is neither disseminated in the classic southwestern USA sense, nor inherently associated with sericitic alteration. At Alumbrera (Argentina), the chalcopyrite/bornite stage is associated with the zone of potassic alteration and no supergene blanket has formed, due to low pyrite contents. Observers utilising the Loghry style approach should also take into account the host and host rock alteration in terms of their ability to neutralise acids. Sericite (phyllic) and advanced argillic systems have little or no effect, whereas potassic and propylitic zones are moderately neutralising. The system is also not designed for carbonate host rocks (see Table 8.1).

This might all sound a little complex and daunting to the beginner, but in reality the maroon haematite colours and yellow overtones of the jarositic and members are relatively easy to recognise and visual impressions during early exploration are quickly achieved (Figures 8.16–8.27).

The most sought after discovery is any sign of a preexisting chalcocite blanket, now in oxidised surficial format (Figures 8.28–8.29). The maroon coloured “relief or live” limonite (haematite dominant) is a very distinctive colour, and found occupying the tiny ovoid holes once represented by chalcopyrite or pyrite alteration grains. Ex-infill veinlets are often easier to see, as the rocks break open along them, exposing maroon chalcocite ovoid replicas (Figures 4.2–4.3, 8.19–8.21).

As might be expected chalcopyrite boxworks are effectively absent, as all chalcopyrite will have been converted to chalcocite prior to oxidation.

Detailed limonite mapping is often employed and is usually accompanied by some form of total sulphide estimation (Approach No 2).

Limonite mapping involves the utilisation of specially prepared “limonite colour charts” (Figure 173) depicting the colours resulting from various proportions of haematite, goethite and jarosite.

Munsell soil colour charts can also be utilised once a set of standards has been prepared.

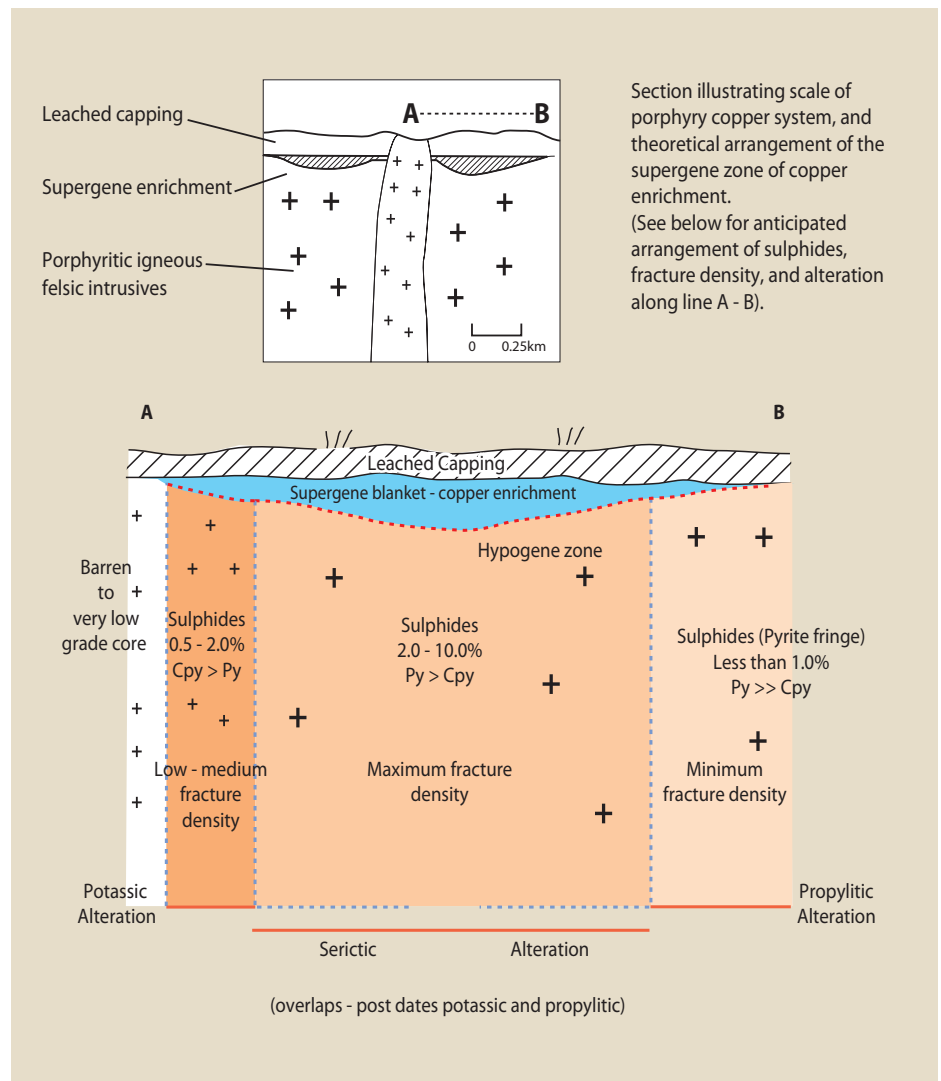
In the field it is very important to dry scratch the relevant limonites when recording colour, as many exposed surfaces show false colours via desert weathering, lichens and general surficial contamination (usually darker).

**Fig. 8.14 Porphyry Copper Intrusion Centred Model – General Features.**

Model illustrating theoretical vertical zoning of supergene zoning effects shown overprinting on laterally zoned features of hypogene alteration and mineralogy of a cross section from an intrusive thermal centre into distal wall rocks.

**NB.** This is derived from generalisations concerning the classic southwestern USA systems, and is a simplified version of that presented by Titley 1982, and Titley and Marozas, 1995 (Sulphides in volume%). The model envisages an annular shell-like arrangement, with a central porphyry surrounded by shells of changing sulphide density, chalcopyrite/pyrite ratios, fracture density, and wall rock alteration (within porphyritic igneous host rocks). Optimum conditions for maximum supergene development are considered to be around 4.5:1 pyrite/chalcopyrite.

**NB.** The model should be applied with appropriate geological consideration (see text).



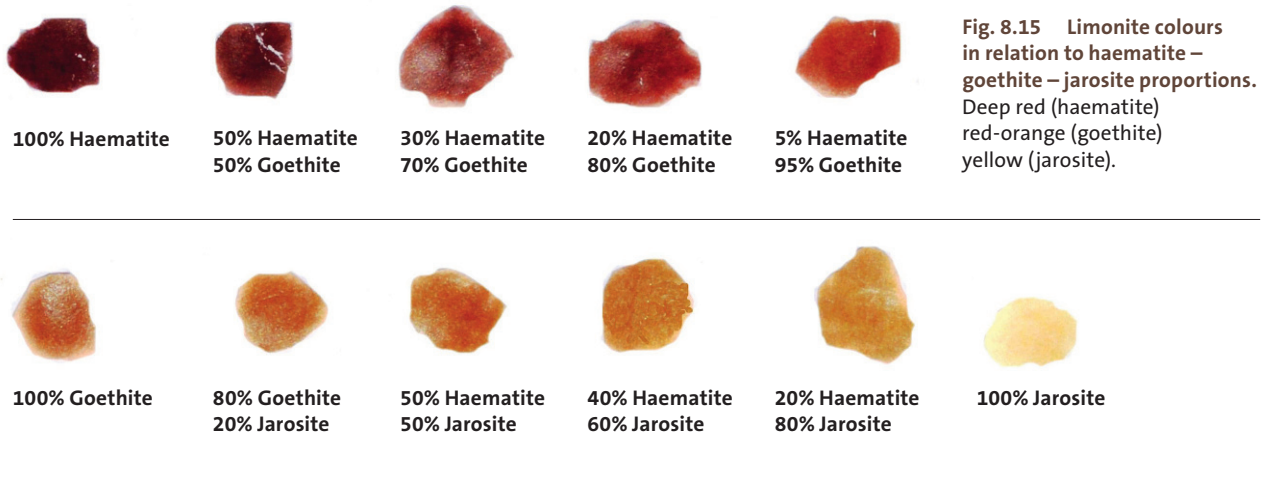


Fig. 8.15 Limonite colours in relation to haematite – goethite – jarosite proportions. Deep red (haematite) red-orange (goethite) yellow (jarosite).

#### Approach No 4

A further approach utilised most successfully at El Salvador in Chile (Gustafson and Hunt 1975) is to conduct a petrographic examination of all quartz veins to establish the presence (if any) and composition of any sulphides which may have escaped the supergene and/or oxidation process (armoured by quartz). This is obviously not a field technique and requires detailed and time consuming petrographic work.

## 8.5 Summary of procedures and examples

In summary there are a range of procedures available which should be utilised in combination, and assessment is dictated by factors which include general exploration policy towards leached cappings, exposure and expertise available. However, if exploration detects leached porphyry style exposures, there is much to be gained from careful inspection. It is recognised that detailed leached cap assessment requires expertise and considered interpretation. However, there are general basics which should be within any exploration geologists repertoire, these include:

Broad scale parameters.

- Structural context of channelways (crackle, breccia etc).
- Fracture density.
- General amount (percentage) of acid forming sulphide.
- General distribution of goethite rich material versus jarosite.
- General distribution of clay rich versus clay poor zones (kaolin).

Detailed parameters.

- Recognition of potential chalcocite zones via recognition of haematitic relief/live limonite

The combination of the above usually goes a long way in original assessment, and as work proceeds may acquire increasing significance in targeting exploration and focussing drill

site selection. Obviously other exploration parameters will be operational to add to the picture, such as mapping, geochemical surveys and appropriate geophysics. Viewed in this context, the known field skills are an extremely useful exploration parameter and still have a major role to play in preliminary and continuing assessment of porphyry coppers (Rivera et al, 2009).

There have been a few instances where significant copper has been located below goethite/jarosite only leached outcrops (i.e., haematite poor – with no sign of chalcocite residuals). However this is to be expected in early cycle situations or in erosional situations where upper blanket remnants may have been rapidly removed.

However, where mature chalcocite profiles have intersected the surface, their oxidation products have played a major role in guiding exploration.

Two examples serve to illustrate the situation. The first at La Caridad, Mexico (Figure 8.28) would clearly act as a drill target signal. The haematite zone does not cover the entire subsurface chalcocite zone, but certainly guides the explorer.

The second example is even more relevant (Figure 8.29). The leached capping map at Escondida, Chile (Ortiz, 1995) did in fact point to the ore zone, and had it been followed up earlier would have focussed the exploration team in the right place considerably earlier in the exploration history. The initial field results for Escondida were followed up by the most well controlled scientific study of arid zone leached capping geology which is highly recommended reading for interested geologists (Alpers and Brimhall, 1989). The mineralogy, textures and relative abundance of supergene limonite minerals (haematite, goethite and jarosite) were used to reconstruct the former ratio of pyrite to chalcopyrite to chalcocite and the pre-oxidation copper grade based upon empirical limonite-sulphide correlation supported by quantitative limonite mapping.

The author has personally conducted reconnaissance investigations at the nearby Escondida Norte (Figure 3.15), and as expected the “live limonite” occurrences are sufficiently well developed to illustrate the general value of this approach.

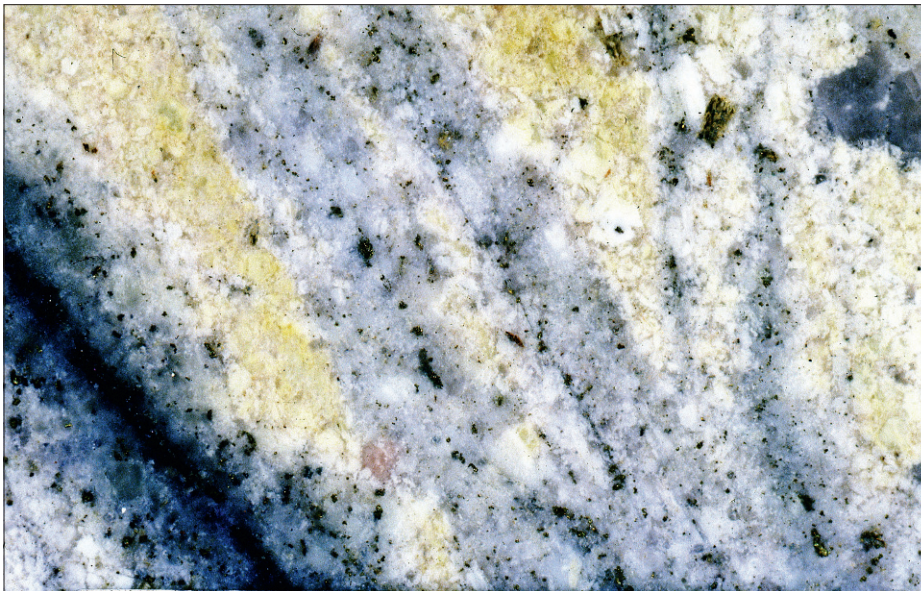


**Fig. 8.16** Transition from chalcocite supergene enrichment zone (white-grey) to haematite altered oxide zone (red).

Note the abundance of small crack-like stockwork veinlets in the upper sector, many of which have pale grey sericite – quartz  $\pm$  sulphide alteration-infill.

**Escondida Norte, Chile.**

Width of frame about 1 m.



**Fig. 8.17** Typical stockwork texture. The argillised porphyry (cream-white) is cut by small veins and cracks (dark) with halos of sericite-silica –sulphide (phyllic) alteration (grey).

The veinlets contain sulphide infill (dark).

Both the alteration sulphide spots and infill grains would have been mixtures of chalcopyrite and pyrite, now converted to chalcocite. Minor amounts of sulphide remain (yellow) which are pyrite (see [Figure 8.12 A–B](#)).

**Toquepala, Peru.**

Width of frame 2.5 cm (Cut slab).



**Fig. 8.18** Close up of an infill veinlet of quartz and sulphides (yellow and black) with an alteration halo of grey silica sericite (phyllic) alteration. The host rock is argillised porphyry. The dark sulphide is chalcocite forming as an alteration of chalcopyrite, and the yellow is unaltered pyrite (see [Figure 8.12 A–B](#)). This is an example of incomplete supergene chalcocite alteration –sometimes referred to as immature.

Note also the tiny sulphide alteration spots in the halo are also converted to chalcocite.

**Toquepala, Peru.**

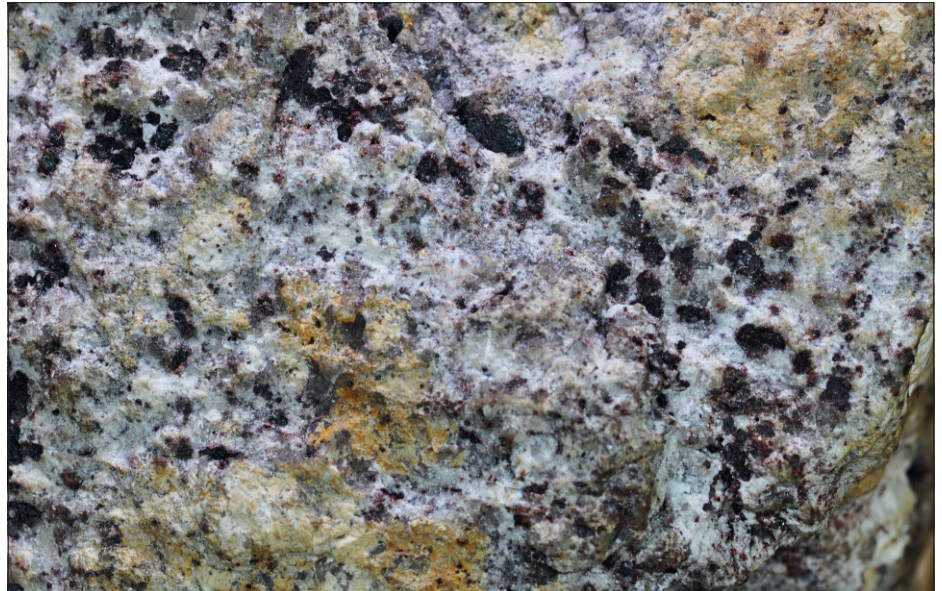
Width of frame 2 cm (Uncut rough surface).

**Fig. 8.19** Haematite dominant capping – after chalcocite.

The dark maroon ovoid spots represent ex-chalcocite sites. The cavities contain prominent indigenous maroon coloured limonite (live limonite after chalcocite – see [Figures 4.2–4.3](#) and [Table 8.1](#)). They were originally sulphide sites (chalcopyrite pyrite) with sericite alteration halos (see [Figures 8.16–8.17](#)).

**Locality unknown.**

Width of frame 3 cm.



**Fig. 8.20** Haematite dominant capping – after chalcocite.

Dark maroon indigenous haematite filling or partially filling cavities—classic live limonite derived from chalcocite.

The chalcocite replaced original chalcopyrite /pyrite occupying these sites.

**Coulston, Queensland, Australia.**

Width of frame 3.5 cm.



**Fig. 8.21** Haematite dominant capping – after chalcocite.

Several rocks, breaking open along original sulphide veinlets where the sulphides (chalcopyrite/pyrite) have been successively converted to chalcocite and then maroon coloured haematite (see haematite cappings above and [Figures 8.1–8.6](#)).

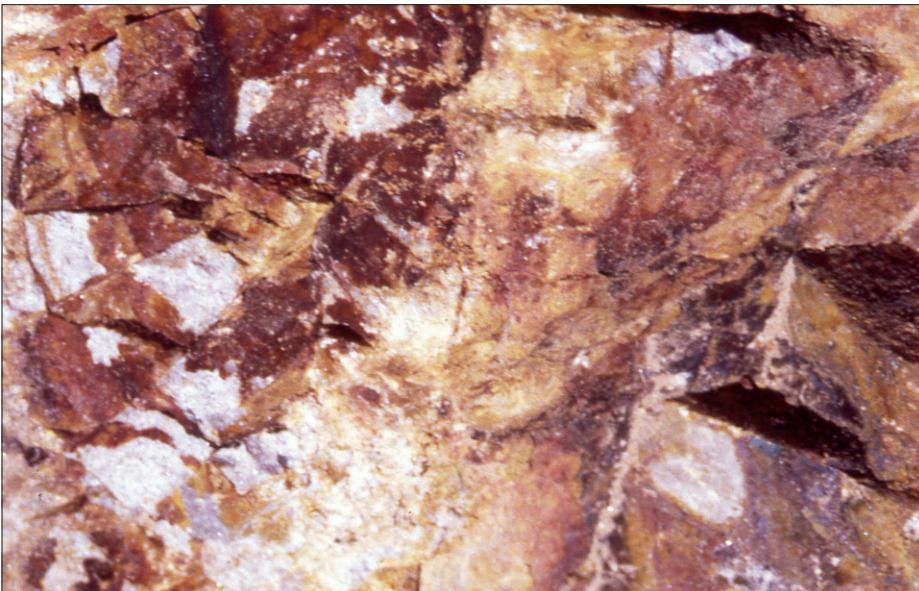
**Santa Rita, New Mexico, USA.**

Width of frame 200 cm.





**Fig. 8.22** Goethite dominant leached capping. Note the red-orange goethite colours in comparison with [Figures 8.19–8.20](#), showing the maroon colours of haematite dominant situations. The cavities are less full or even empty which coincides with an increase in transported limonite (see [Table 8.1](#)). The latter is showing up as precipitation along joints and fractures (bottom right hand corner and in tiny cracks (see also [Figure 8.15](#)). **Location unknown.** Width of frame 4.5 cm.



**Fig. 8.23** Goethite dominant leached capping. A range of goethite (red-orange to orange) colours occurring as transported limonite coating joint surfaces. The rock would also be inspected more closely and disseminated materials also assessed as above ([Table 8.1](#)). **Morenci, Arizona, USA.** Width of frame 1 m.



**Fig. 8.24** Goethite dominant leached capping. Broken surface with abundant orange coloured transported limonite (goethite). Both this and adjacent disseminated styles would be assessed in terms of limonite styles and composition ([Table 8.1](#) and [Figure 8.15](#)). Original sulphide density would also be estimated –see text. **Locality unknown.** Width of frame 3 cm.

**Fig. 8.25 Jarosite dominant leached capping.**

Argillic altered breccia (white kaolinised fragments) with jarosite coated joint faces (yellow tinged). The combination is taken to represent acid conditions relating to original dominant pyrite content. The darker materials are probably manganese oxides?

**Morenci, Arizona, USA.**

Width of frame 8 cm.



**Fig. 8.26 Jarosite dominant leached capping.**

Argillic altered host porphyry with jarosite dominant (orange-yellow) transported limonite precipitating along the fractures. The colours and limonite style would suggest original pyrite dominance (see [Table 8.1](#) and [Figure 8.15](#)).

**Toquepala, Peru.**

Width of frame 24 cm.



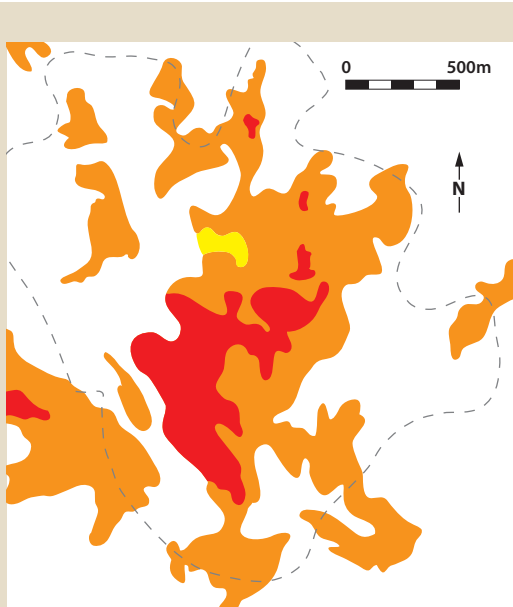
**Fig. 8.27 Jarosite dominant leached capping.**

Orange-brown-yellow jarositic limonite precipitating on a joint surface in argillised porphyry. Indication of pyrite rich domain (see also [Figures 6.1, 8.15, 8.25–8.26](#) and [Table 8.1](#)).

**Toquepala, Peru.**

Width of frame 6 cm.





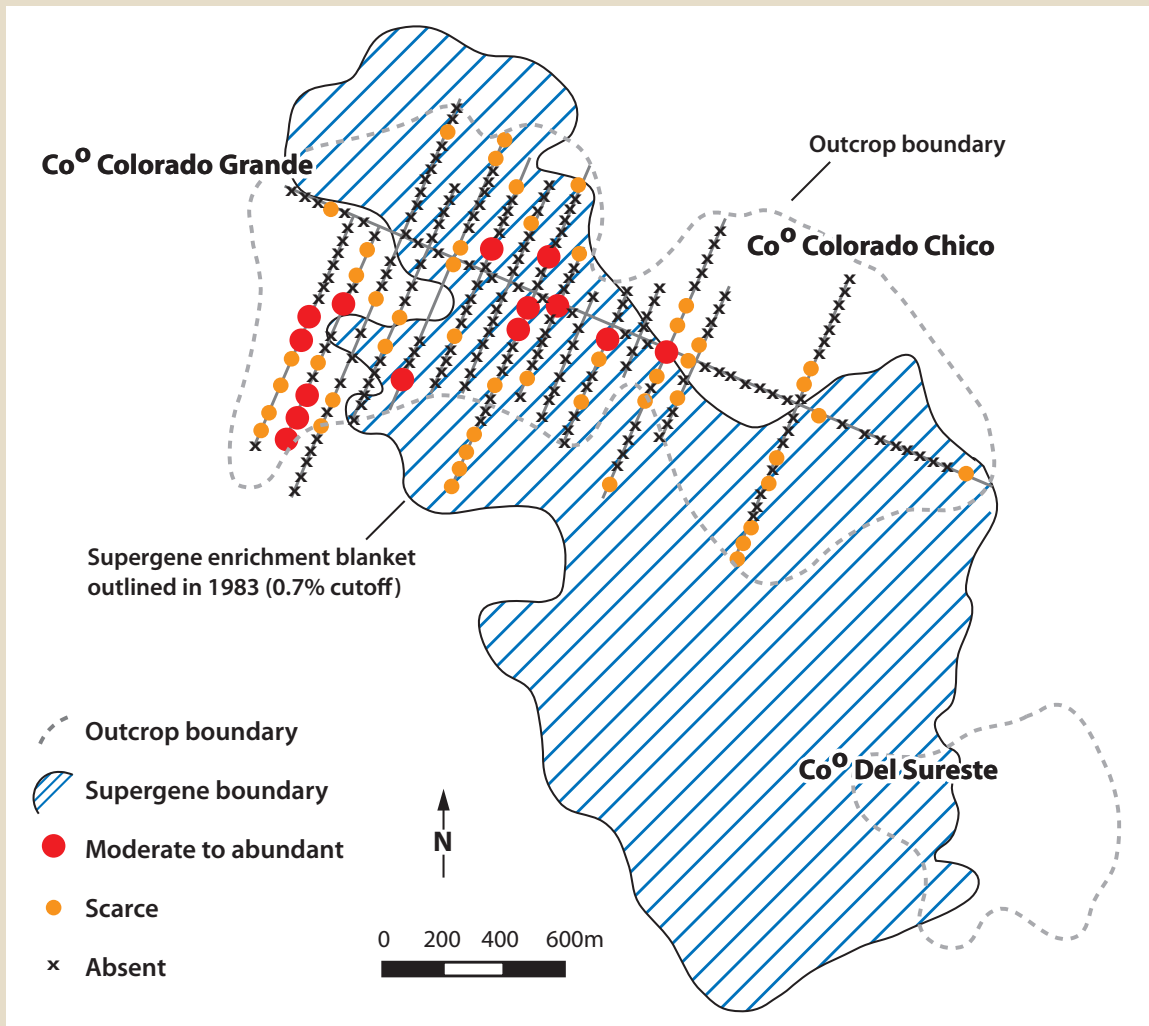
- Strong (haematite)
- Moderate (goethite)
- Weak to nil (jarosite)
- Extent of economic chalcocite enrichment

**Fig. 8.28** Map showing interpreted distribution and abundance in surface rocks prior to the leaching with superimposed perimeter of underlying chalcocite ore (Saegert et al; 1974). **La Caridad, Mexico.**

Limonite Capping as characterised by haematite, goethite, and jarosite dominance. Although the haematite rich material only pinpoints one third of the main underlying chalcocite zone, it still serves as a valuable initial drill focus.

**Fig. 8.29** Map showing leached capping and abundance of chalcocite and chalcopyrite derived limonite (live limonite – maroon coloured – see [Figures 4.2, 4.3, and 8.19–8.21](#)). Modified from Ortiz, 1995. **La Escondida, Chile.**

Note excellent general correlation with enrichment blanket where surface exposure is available.



**Co<sup>o</sup> Colorado Grande**


Outcrop boundary

**Co<sup>o</sup> Colorado Chico**

Supergene enrichment blanket outlined in 1983 (0.7% cutoff)

**Co<sup>o</sup> Del Sureste**

 Outcrop boundary

 Supergene boundary

● Moderate to abundant

● Scarce

x Absent

0 200 400 600m

## 8.6 Oxidised copper ores (“oxide zones”)

The term “oxide zone” is widely employed in porphyry copper parlance to describe oxidised copper ores composed of green copper minerals ± manganese oxides (Figures 8.7–8.9, 8.23–8.38). Major occurrences of the latter are similarly referred to as “black oxide zones” (Figure 8.31). The prime economic occurrences of these are in the Atacama super arid region of northern Chile where combinations of malachite, brochantite, and antlerite are common constituents (Figures 6.12, 6.14, 6.16, 6.17–6.19, 6.21–6.22, and 8.34–8.38).

In terms of leached cappings “oxide zones” present very few problems concerning recognition at surface with the dominant green copper minerals catching the eye (often chrysocolla dominant).

The main groupings of oxidised copper zones (Sillitoe, 2005) are:

- Copper oxides underlain by primary (hypogene) ore with little or no supergene enrichment (see Grasberg overview, later in this section. Figures 8.49–8.54).
- Copper oxides underlain by supergene enrichment (Escondida Norte, Figures 8.39–8.48).
- Copper oxides of strongly transported, exotic origin (Figures 8.32–8.33).

Oxide zones within porphyry systems may develop at several points within the system, and do not necessarily develop surface expressions. In fact within the central Andes region, they commonly occur at depth, intervening as lensoid zones between oxidised and hypogene/or enriched zones (Figures 8.39–8.49). Conversely in some deposits with low ratios of copper sulphide to pyrite, copper oxide zones may extend from primary ore zones to surface. The El Abra deposit in Chile extends for some 800 m in full vertical extent (Figure 8.7) embracing some 90–300 m of oxide zone.

The “oxide” minerals are mostly of transported origin, precipitating as infill in veins and cavities with minor replacement of clays in the associated argillic altered host rocks. The common minerals, malachite, brochantite, antlerite and atacamite occupy stability fields in the pH zones of around 4–8 (Figure 6.8).

Sillitoe (2005) provides an excellent overview of the oxide zones within northern Chile and observes that the assemblages differ slightly reflecting oxidising conditions: As might be anticipated the hydroxysulphate dominant styles imply oxidation of local pyrite bearing supergene styles.

Occurrences of the arsenate minerals such as conichalcite and chenevixite tend to signal the presence of enargite and hence overprinting high sulphidation systems.

The green oxide zones may grade laterally or internally to black oxide zones in an irregular zonation style (Chavez, 2000).

A list of copper related supergene – oxide minerals is given in Table 2, (derived from Sillitoe, 2005). It is reasonably comprehensive but many other minerals are recorded in minor amounts (Chavez, 2000).

The exotic copper oxide deposits result from acid copper rich solutions travelling laterally away from the oxidising porphyry copper centre. They ultimately precipitate with the favoured location frequently occupying coarse gravels at the base of local

| Oxidised zones (essentially in situ)  | Dominant copper minerals (variable ratios)                                      | Less common copper minerals   |
|---|---|---|
| <b>1. Near neutral to alkaline conditions (low pyrite available), failure to develop major supergene enrichment</b> | Chrysocolla<br>Atacamite<br>Malachite   | Copper bearing limonite, neotocite, copper clays with minor tenorite, paramelaconite, pitch limonite, copper wad and copper pitch, plus occasional locations with copper phosphate and arsenate minerals. |
| <b>2. Acid conditions</b>   | Copper hydroxysulphates (brochantite, antlerite)                                | Chrysocholla, atacamite, malachite, copper pitch, neotocite ± other minor species.  |
| <b>3. Very acid conditions</b>  | Copper hydroxysulphates (brochantite, antlerite)<br>chalcantite, króhukite.     | –   |
| <b>Exotic copper zones (Palaeochannel styles)</b>   | Chrysocolla, atacamite, copper wad, copper pitch (± gypsum and opaline silica). | –   |

surficial sequences (Figure 8.32). In some instances the gravels may contain mineralised porphyry fragments. This palaeochannel style is especially well developed in the super arid zones of the Atacama region, producing such rich deposits as the famous Exotica at Chiquicamata (Figure 8.33). Palaeochannel oxide style deposits have been located up to some 6–8 km distant from their potential source (Munchmeyer, 1996).

Copper minerals are precipitated when pregnant copper bearing ore solutions chemistry becomes in excess of around pH 5.5. Black oxide zones are common in peripheral regions, although many pass into limonitic domains.

**Table 8.2** Principal copper oxide supergene minerals in oxidised porphyry copper systems, northern Chile. (Derived from Sillitoe, 2005).

| Mineral                               | Formula  | Abundance                                | Figure                       |
|---------------------------------------|--|--|------------------------------|
| Chrysocolla <sup>1</sup>              | $(\text{Cu,Al})_2\text{H}_2\text{Si}_2\text{O}_5 \cdot n(\text{H}_2\text{O})$  | Ubiquitous                               | 6.14, 6.18, 6.19, 8.35       |
| Malachite                             | $\text{Cu}_2\text{CO}_3(\text{OH})_2$  | Abundant                                 | 6.14, 6.16, 6.17, 7.16, 8.38 |
| Azurite                               | $\text{Cu}_3(\text{CO}_3)_2(\text{OH})_2$                                      | Uncommon                                 | 6.16                         |
| Antlerite                             | $\text{Cu}_3(\text{SO}_4)_4(\text{OH})_4$                                      | Common                                   | 6.23, 8.37                   |
| Brochantite                           | $\text{CuSO}_4(\text{OH})_6$   | Abundant                                 | 6.22, 8.34                   |
| Chalcanthite                          | $\text{CuSO}_4 \cdot 5\text{H}_2\text{O}$                                      | Uncommon                                 | 6.20                         |
| Króhnikite                            | $\text{Na}_2\text{Cu}(\text{SO}_4) \cdot 2\text{H}_2\text{O}$                  | Very uncommon                            | –                            |
| Atacamite/paratacamite/clinoatacamite | $\text{Cu}_2\text{Cl}(\text{OH})_3$  | Abundant                                 | 6.21, 8.36                   |
| Pseudomalachite                       | $\text{Cu}_5(\text{PO}_4)_2(\text{OH})_4$                                      | Uncommon                                 | 6.28                         |
| Liebethenite                          | $\text{Cu}_2\text{PO}_4(\text{OH})$  | Very uncommon                            | –                            |
| Sampleite                             | $(\text{Na,Ca,Cu})_5(\text{PO}_4)_4\text{Cl} \cdot 5\text{H}_2\text{O}$        | Very uncommon                            | –                            |
| Turquoise                             | $\text{CuAl}_6(\text{PO}_4)_4(\text{OH})_8 \cdot 4\text{H}_2\text{O}$          | Uncommon                                 | 6.26                         |
| Conichalcite                          | $\text{CuCa}(\text{AsO}_4)\text{OH}$   | Very uncommon                            | –                            |
| Chenevixite                           | $\text{Cu}_2\text{Fe}_2(\text{AsO}_4)_2(\text{OH})_4 \cdot \text{H}_2\text{O}$ | Very uncommon                            | –                            |
| Cuprite                               | $\text{Cu}_2\text{O}$  | Uncommon                                 | 6.12–6.15                    |
| Tenorite                              | $\text{CuO}$   | Uncommon                                 | 6.12                         |
| Paramelaconite                        | $\text{Cu}_4\text{O}_3$  | Uncommon                                 | –                            |
| Pitch limonite                        | $\alpha - (\text{Fe,Cu})\text{O}(\text{OH})$                                   | Common                                   | 6.11                         |
| Crednerite                            | $\text{CuMnO}_2$   | Uncommon                                 | –                            |
| Copper wad <sup>2</sup>               | Cu bearing Mn oxyhydroxide + other phases                                      | Abundant (especially in exotic deposits) | 8.47                         |
| Copper pitch (black chrysocolla)      | $(\text{Cu,Fe,Mn})_2\text{H}_2\text{S}_{12}\text{O}_5(\text{OH})_4$            | Common                                   | –                            |
| Neotocite <sup>1,2</sup>              | $(\text{Cu,Mn,Fe})\text{SiO}_2 \cdot \text{H}_2\text{O}$                       | Abundant                                 | 6.7, 8.31                    |
| Copper clays <sup>2</sup>             | Smectite or kaolinite with sorbed Cu or intergrown chrysocolla                 | Abundant                                 | 6.19                         |

<sup>1</sup> Mineraloid, <sup>2</sup> Mineral mixture

Although rare, exotic copper zones are recorded in humid environs, e.g. Boyugo, Philippines (Braxton et al, 2009).

Most of the “oxide copper” zones currently undergoing commercial extraction stem from the arid zones of South America with lesser contributions from southwestern USA and Australia.

Porphyry copper profiles from the humid environs (Philippines, Indonesia) rarely exhibit significant leached capping or oxide zone profiles (Braxton et al, 2009), although there are spectacular exceptions such as Boyongan. The latter is concealed beneath volcanic derived sediments, which include fragments from the porphyry. Weathering of these into the local creeks provided the initial clues, which enabled exploration to focus on the source zone. To the surprise of the industry, drilling established a buried cuprite dominant oxide zone some 600 m in thickness. This is composed of irregularly distributed zones dominated by neotocite (Figure 6.7), malachite, azurite, cuprite (with major chalcotrichite, Figure 6.15) and native copper (Figures 6.9–6.10), (relatively high redox conditions).

Supergene depth, chalcocite development is minimal. This assemblage is far more difficult to treat than the hydroxysulphate species of the central Andes.

Most of the humid climate leached caps are minimal depth and oxide zones are in the 30–70 m range with malachite as the main surficial mineral. Given their relatively young age, and humid weathering conditions many have only minor supergene enrichment zones, and the leached capping assessment techniques applied in the arid zones are not applicable. However, there are exceptions with Ok Tedi; Papua New Guinea containing a 300 m leached capping. Each system needs to be assessed separately. The Grasberg system provides a good case history (Figures 8.49–8.54), where expectations of a low grade leached cap or oxide system proved correct, but primary grades of copper and gold proved spectacularly high. There is no real way of predicting primary grades from the surficial outcrops, and low grade expectations almost prevented discovery. Similarly at Batu Hijau (Indonesia), the primary grades allow economic extraction and are not easily apparent from the surficial exposures.



**Fig. 8.30** Copper “oxide” zone in fault structure in tropical terrain.

Green malachite precipitating in the upper sector of the vadose zone (see also Figures 8.7–8.9).

**Batu Hijau, Indonesia.**

Width of frame about 20 m.

**Fig. 8.31** Major development of “Black oxide” – named from the extensive development of manganese oxides.

The latter often contain copper (see neotcite [Figure 6.7](#)). Large clumps of sooty manganese precipitates are referred to as manganese or copper wad. Individual manganese minerals cannot be distinguished without recourse to laboratory techniques. The manganese here coats joint surfaces.

**El Abra, Chile.**

Width of frame 5 m.



**Fig. 8.32** Exotic copper oxide.

Green copper minerals cementing alluvial wash.

This type of copper development is virtually restricted to the arid desert regions of the Atacama region, and represents copper originally derived from a nearby porphyry system. The copper minerals are typically mixtures of chrysocholla, atacamite copper wad, and copper pitch.

**Huiniquintipa, Chile.**



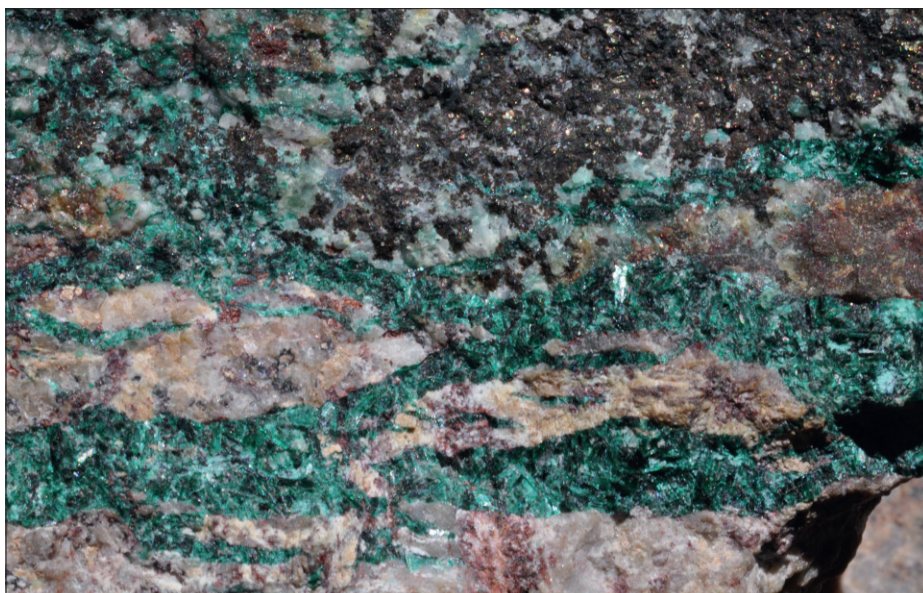
**Fig. 8.33** Exotic copper oxide.

A small exposure of the 7 km long exotic deposit. This is composed of altered gravels cemented by variable amounts of chrysocholla, minor atacamite, copper wad and copper pitch.

**Chiquicamata, Chile.**

Width of frame 1 m.

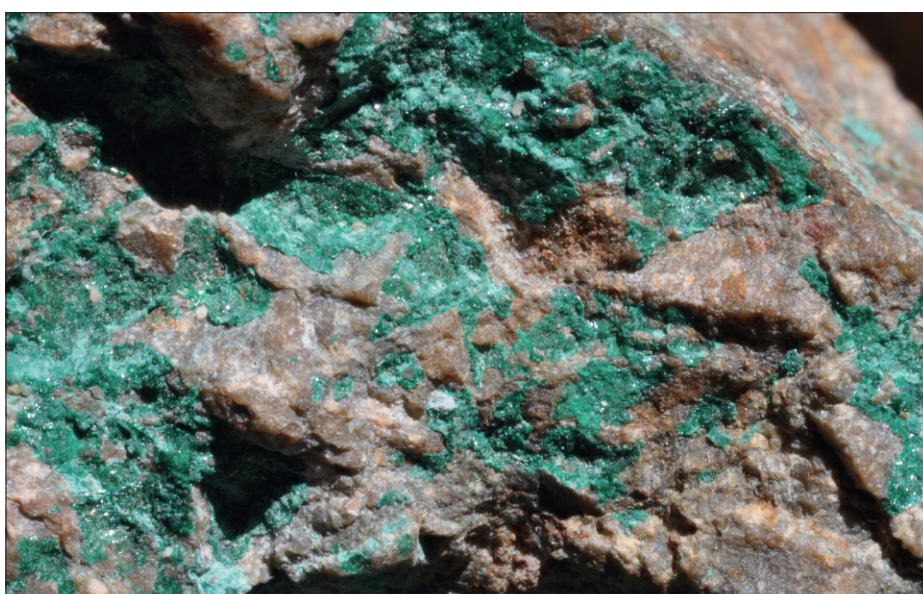




**Fig. 8.34** Brochantite (Copper hydroxysulphate). Chalcocite (dark) overprinted by veins of prismatic brochantite (green). Zaldívar mine, Chile. Width of frame 8 cm.



**Fig. 8.35** Chrysocholla (Hydrated copper silicate). Colloform chrysocholla (blue-green) precipitating in cavities. Miami mine, Arizona, USA. Width of frame 5 cm.



**Fig. 8.36** Atacamite (Copper hydroxychloride). Mantos Blancos, Chile. Width of frame 3.5 cm.

Fig. 8.37 Antlerite (Copper hydroxysulphate).  
Chiquicamata, Chile.  
Width of frame 3 cm

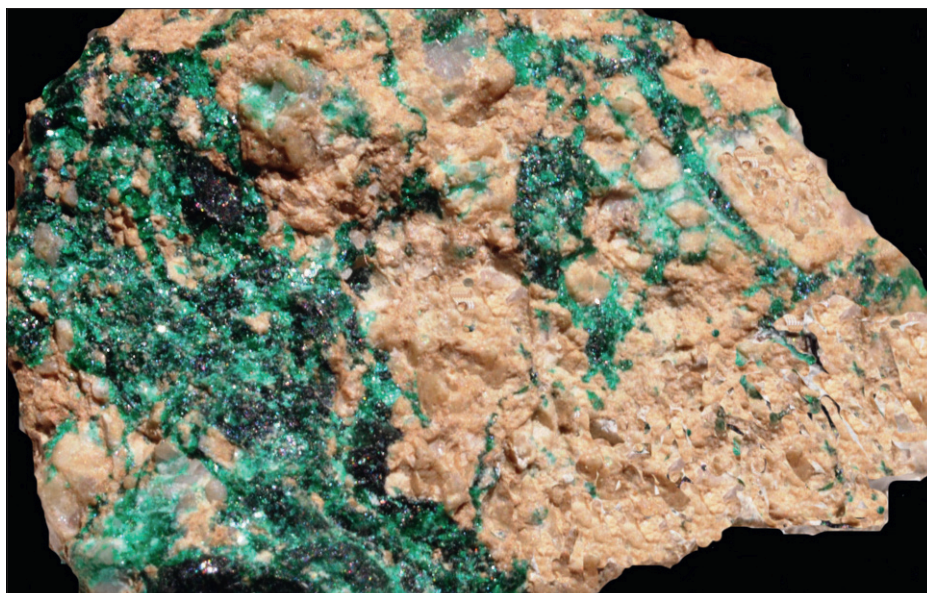


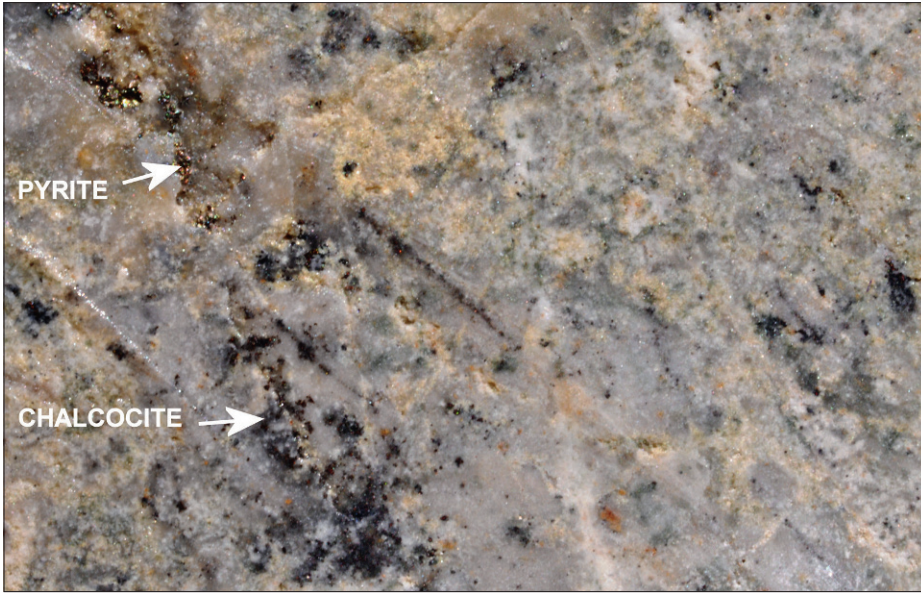
Fig. 8.38 Malachite (Copper carbonate).  
Botryoidal-colloform.  
Locality unknown.  
Width of frame 8 cm.



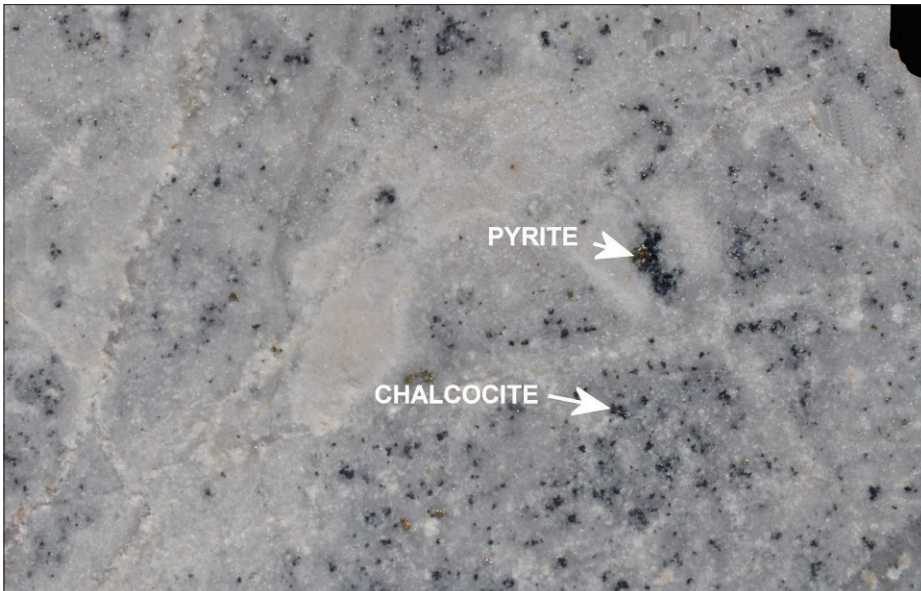
The various green minerals are often difficult to identify. For instance brochantite and antlerite can exhibit identical habits. Other examples are shown in [Figures 6.16–6.23](#).

The development of both leached capping materials and subsequent copper oxides are illustrated via samples from Escondida Norte ([Figures 8.39–8.48](#)).

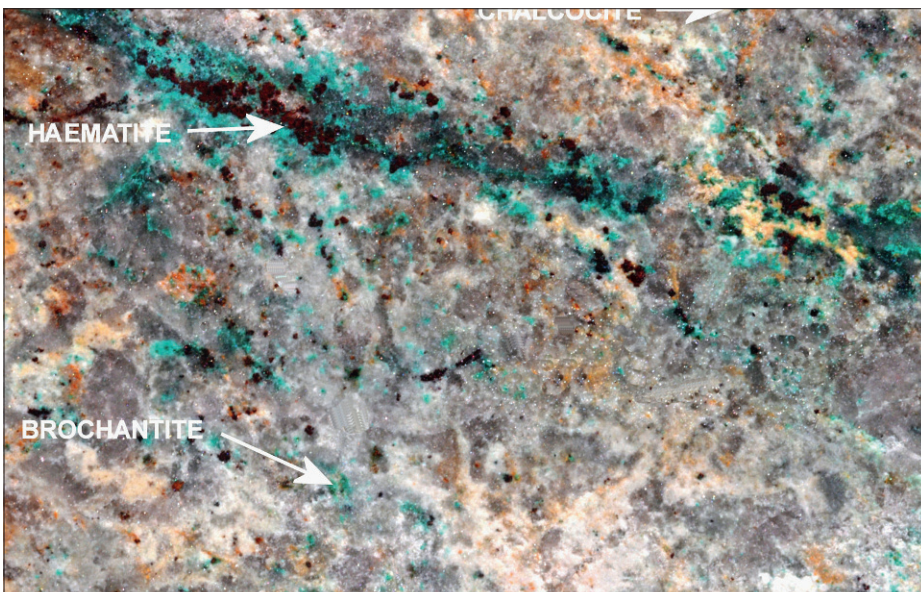
A different style of leached capping developing over a very immature high rainfall tropical terrain is given by the Grasberg example where supergene development is minimal ([Figures 8.49–8.54](#)).



**Fig. 8.39** Lower supergene region. DDH 118, 342 m. Chalcopyrite ± bornite converted to chalcocite (black) with pyrite unaffected (see Figure 8.12). Sericitic-sulphide alteration (see Figure 8.17) accompanying, quartz–sericite–sulphide infill (left). Late argillic overprint. Width of frame 3 cm.



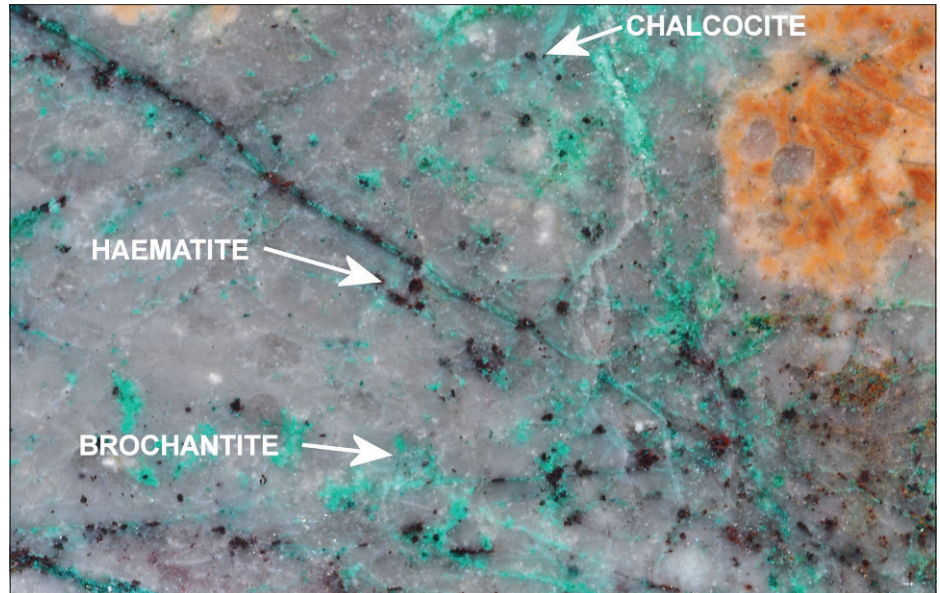
**Fig. 8.40** Mid to lower supergene region. DDH 118, 234.9 m. Original sulphides (see above and Figures 8.12 and 8.17) converted to supergene chalcocite (dark spots). Minor pyrite remains, although the process is essentially mature. The rock is broken with dominantly quartz (grey) veins, and associated sericitic-sulphide spot alteration. A crack style stockwork has channeled late supergene? clay alteration (creamy white). Width of frame 3 cm.



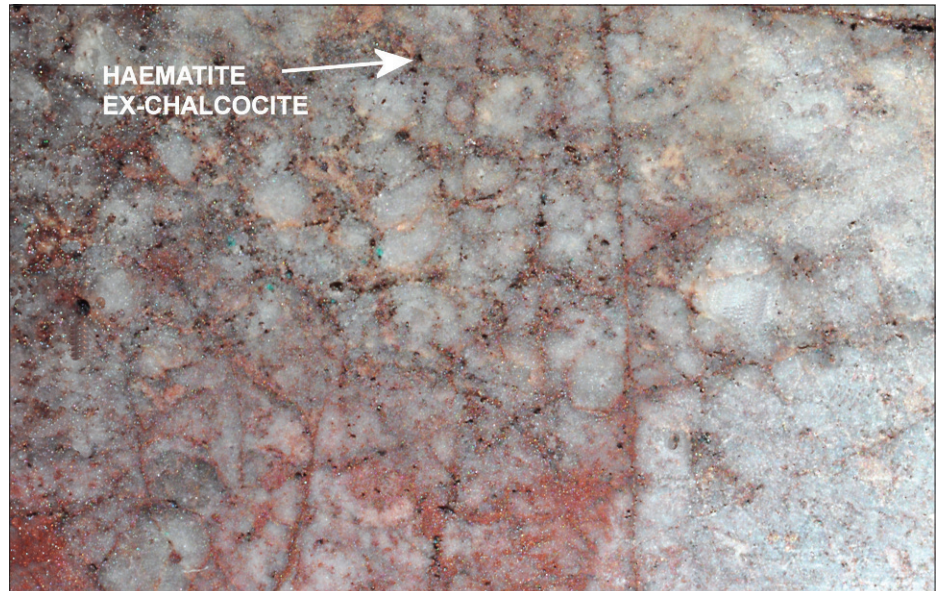
**Fig. 8.41** Upper supergene region. DDH 118 180 m. Supergene chalcocite with local conversion to haematite via late stage meteoric fluid entry (weakly acidic?). Leached copper has precipitated locally to produce brochantite – forming an overprinting immature copper oxide zone. Width of frame 3 cm.



**Fig. 8.42** Similar to Figure 8.41 – late stage percolation of fluids converting chalcocite to haematite, with the copper reappearing locally as mostly infill brochantite. It seems that primary chalcocite is required to allow the formation of an “oxide copper” zone? The grey zone is sericite-silica and the pink material is clay altered host rock, with minor late goethitic overprint. **Upper supergene region.** DDH 118, 156.75 m. Width of frame 3 cm.

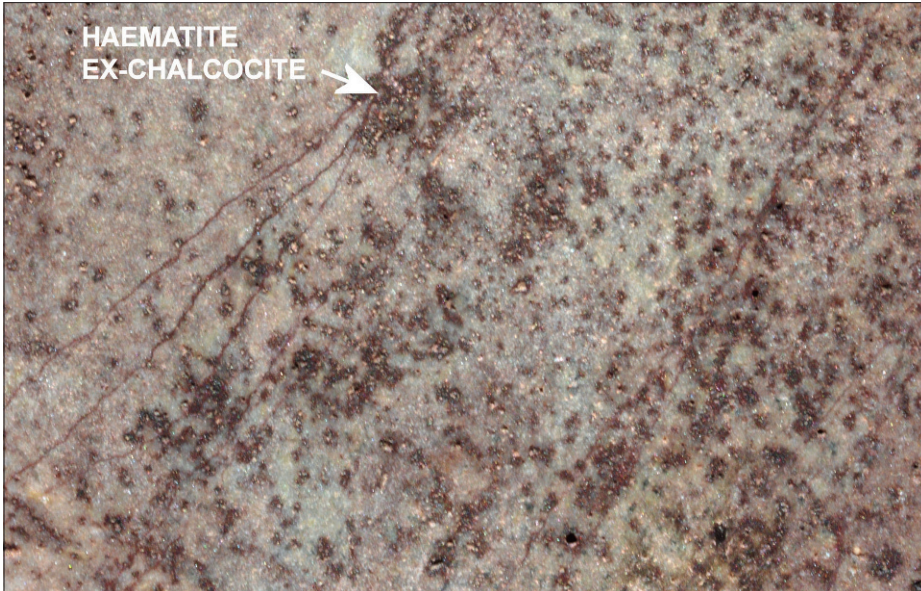


**Fig. 8.43** Chalcocite spots (arrow) converted to haematite (indigenous). Some transported haematite has also developed along the fracture system (see Figure 8.13). The host is sericite-silica altered porphyry ± later clay alteration. **Start of oxidised zone.** DDH 118, 153.1 m. Width of frame 3 cm.

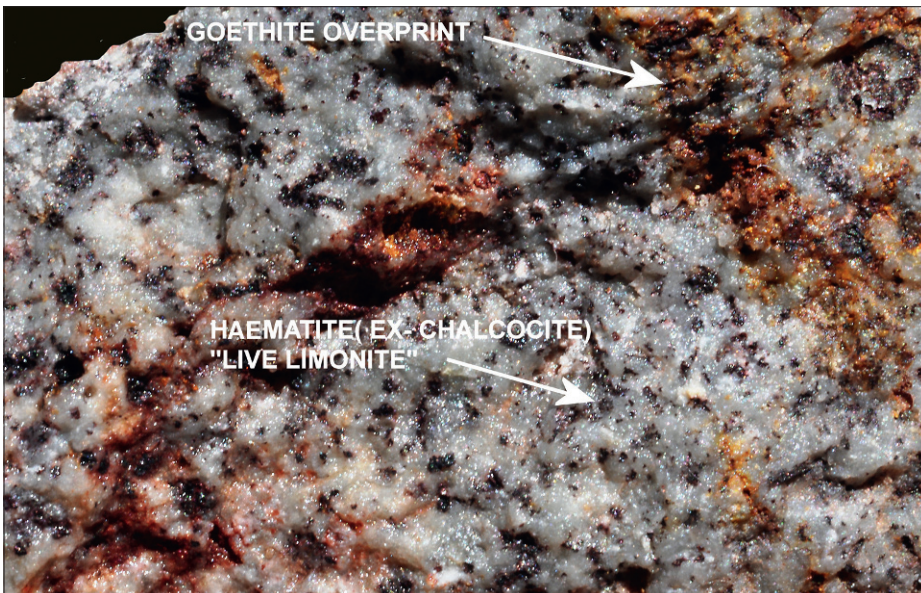


**Fig. 8.44** Chalcocite spots (arrow) converted to haematite (indigenous). Minor transported haematite (see Figure 8.13). Host rock is breccia with quartz and porphyry fragments ± sulphide infill – alteration, sericite alteration and late clay overprint. **Oxidised zone.** DDH 118, 132 m. Width of frame 3 cm

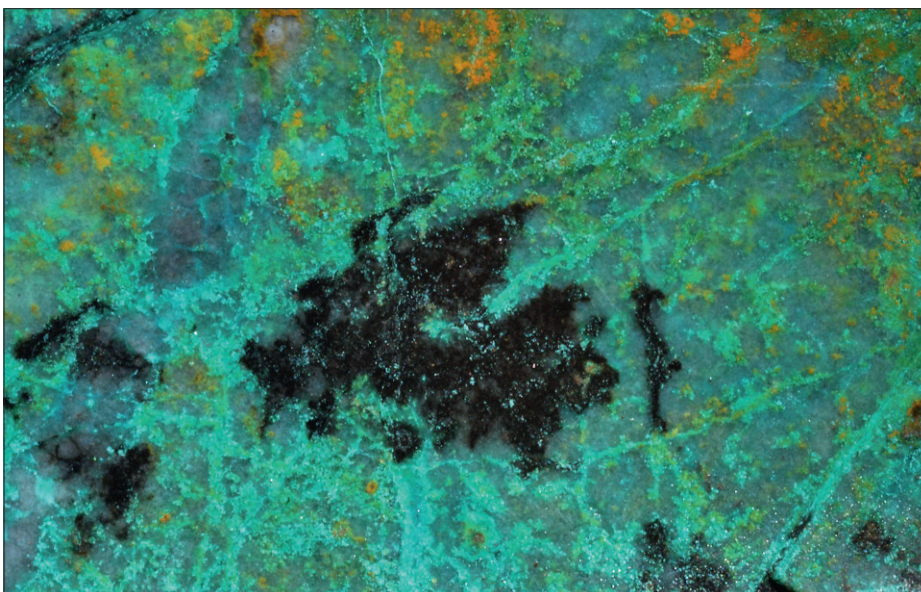




**Fig. 8.45** Surficial region. DDH 63, 103 m. Chalcocite spots converted to haematite. Haematite is only present as partial infill and some has been removed? resulting in slightly blurred edges. The host rock was originally porphyry, and then overprinted by sericite-sulphide alteration  $\pm$  sulphide infill. Width of frame 3 cm

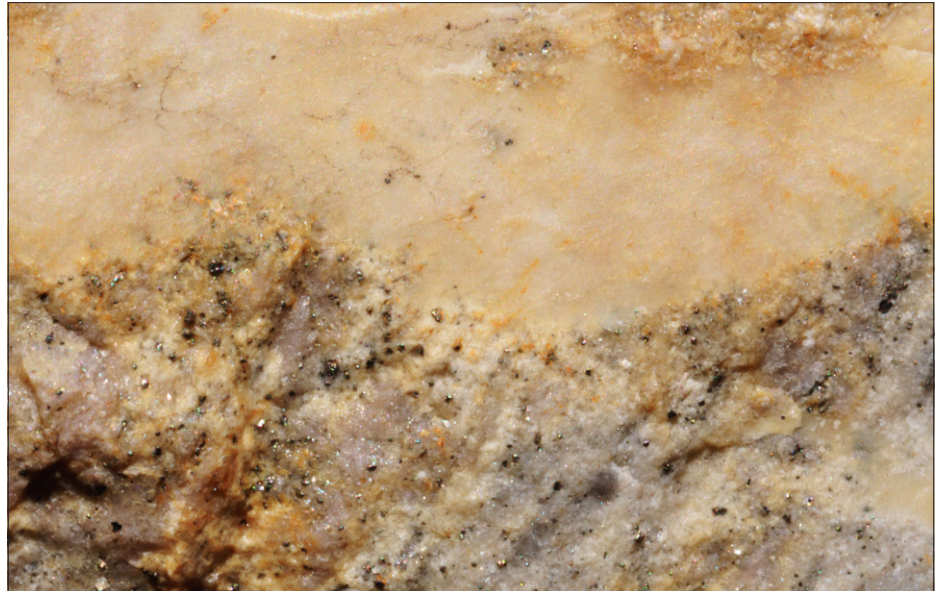


**Fig. 8.46** Surface. Surface rock collected above known chalcocite zone. Classic indigenous haematite spots (arrow-live limonite) denoting underlying chalcocite (see [Figures 4.2–4.4](#)). Later goethitic, orange-red limonite has formed along fractures. Width of frame 3 cm

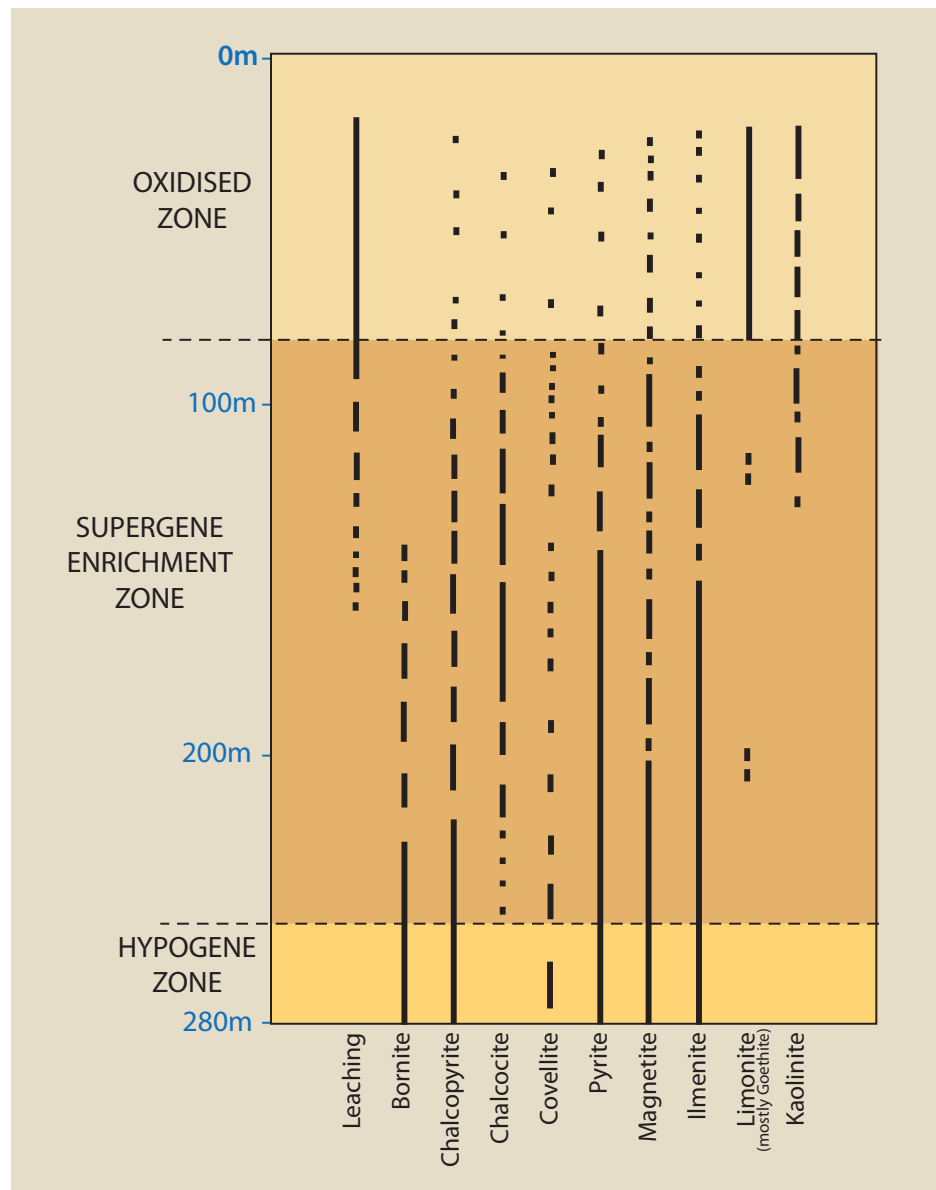


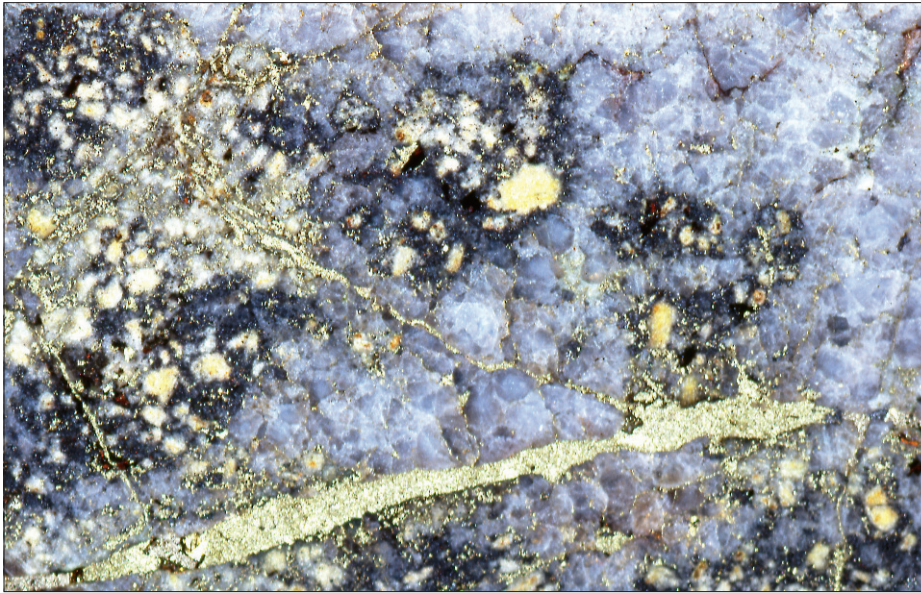
**Fig. 8.47** Other minerals in the local region. **1. Manganese oxide.** Specimen from the “copper oxide” zone (see [Figures 8.41–8.42](#)) to illustrate manganese oxide development (black). The green mineral is brochantite. **The exact location of this specimen is unknown, but it is from Escondida Norte at around 160 m depth.** Larger fluffy masses are referred to as manganese or copper wad. Width of frame 3 cm.

**Fig. 8.48** 2. Alunite? (Potassium aluminium hydroxysulphate). Secondary vein (top) of porcellanous materials-termed secondary alunite by local field geologists (possibly a mineraloid mixture rather than pure alunite? **Escondida, Chile.** Width of frame 4.5 cm.

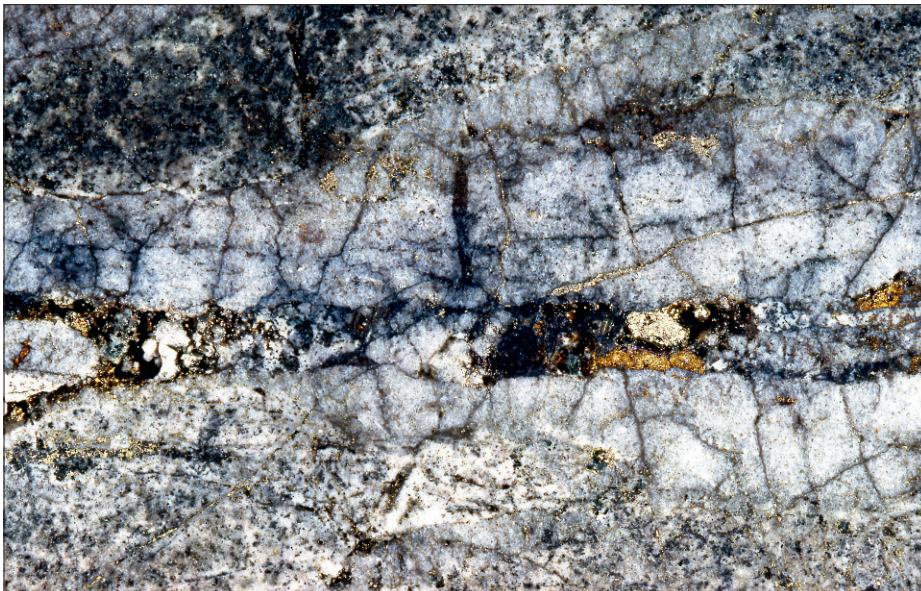


**Fig. 8.49** Oxidation profile at Grasberg Cu-Au mine, Irian Jaya, Indonesia. Generalised from the central pit region. Supergene enrichment is designated by partial replacement of chalcopyrite and bornite by chalcocite. Covellite at base may belong to a minor stage of late primary high sulphidation mineralisation.

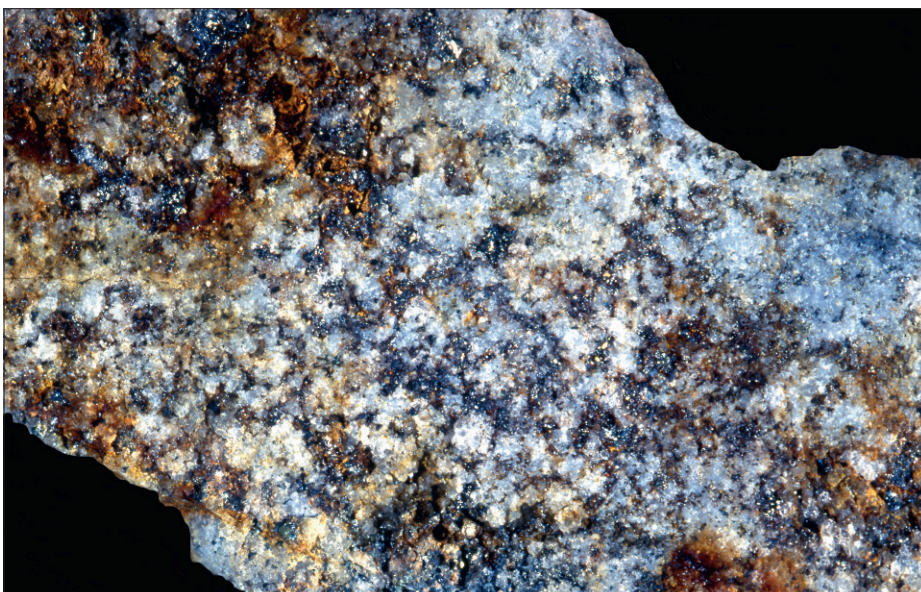




**Fig. 8.50 Primary ore.**  
DDH 58, 251 m.  
Chalcopyrite veins (yellow) cutting quartz veins containing fragments of early magnetite altered porphyry (black).  
Width of frame 6 cm.



**Fig. 8.51 DDH 58, 152 m.**  
Chalcocite (black) replacing chalcopyrite (yellow) with pyrite (pale yellow) unaffected. Sulphides overprint quartz vein (grey) and magnetite altered (dark spots) porphyry.  
Width of frame 6 cm  
(See also [Figure 8.50](#)).

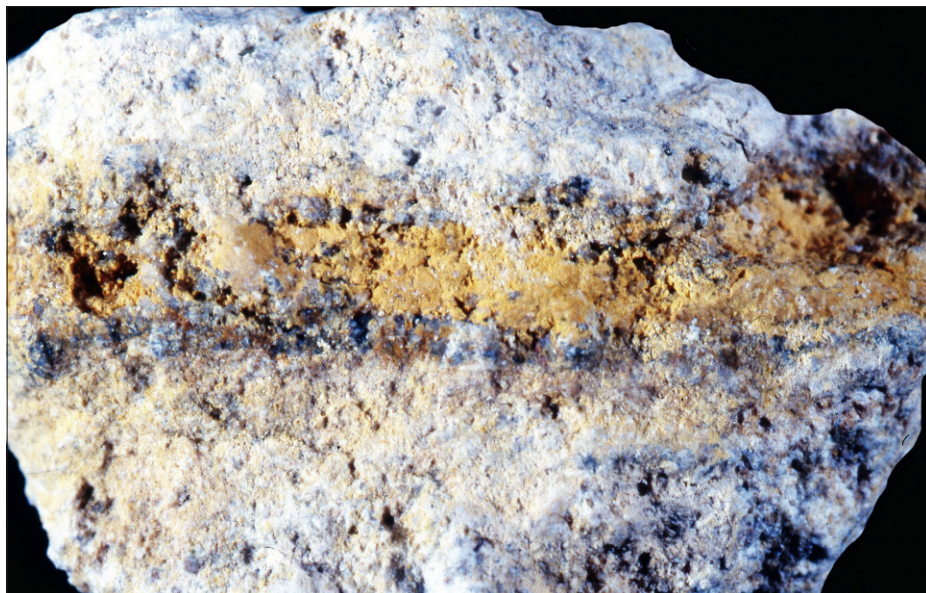


**Fig. 8.52 DDH 58, 8 m.**  
The rock has broken along the vein surface the sulphides (pyrite, chalcopyrite, bornite) are now altered to limonite (goethitic colours) creating some ovoid cellular structures. The dark spots are magnetite underlying the vein from a previous alteration. The magnetite is not converted to limonite.  
Width of frame 6 cm.

**Fig. 8.53** DDH 58, 50 m.  
The rock has broken along a vein surface which was originally sulphide rich (Figure 8.50). The sulphides are now represented as ovoid cellular limonite. Limonite has also precipitated along the fracture (transported limonite –mostly goethitic colours). Material of this nature persists to surface.  
Width of frame 6 cm.



**Fig. 8.54** DDH 58, 9 m.  
Clay altered porphyry (white), and quartz vein (grey) with late transported jarositic limonite (yellow). A highly acid fluid is implicated.  
Both goethitic and jarosite were well represented at the original surface.  
Width of frame 6 cm.



This text has focussed upon the geological aspects of leached cappings and gossans and obviously these activities should take place in tandem with sampling, geochemical analysis and any other instruments available (portable scintillometers, XRD analysers, etc). Ultimately geophysical techniques may be added to support field observations.

However, the author has experienced many situations which are quite normal in exploration activities where the only real aids available are geological aspects, perhaps supported by the usual field gear of a magnet, scriber and possibly an acid bottle.

Aside from the numerous field observations noted in the previous pages, there is also room for the common sense and/or experience factors.

In common sense terms there are not many common ore minerals and the regularly appearing candidates under suspicion are:

*Pyrite, pyrrhotite, galena, sphalerite, chalcopyrite, bornite and arsenopyrite along with carbonate quartz and chlorite gangue minerals.*

In this context general inference often be applied or considered in geological context.

Thus major clay/limonite zones are usually attributed to *pyrite* (acid leach effects, resulting from sulphuric acid production).

*Pyrrhotite* is a rarer option and iron rich *sphalerite* might also be considered.

Iron rich host rocks and/or gangue minerals such as mafic rocks or siderite, chlorite could be involved causing red gossanous style exposures, although these are generally easily eliminated or by superficial geological inspection.

Any hint of green copper minerals will have a major chance of ultimately coming from *chalcopyrite* and/or *bornite* combinations.

Similarly any hint of lead secondary products will almost certainly track back to *galena* and given the very strong association of *sphalerite* with galena, it too can be anticipated via the galena signal. Abundant smithsonite plus hemimorphite, hydrozincite and zinc clays in carbonate are probably signalling *sphalerite* dominant ores. Scorodite is usually associated with primary *arsenopyrite* or more rarely with the “enargite” group.

Experience factors obviously play a major role and if the observer has a strong working knowledge of different ore types and environments, this helps considerably with expectations and interpretations. A limonitic mass with jasperoidal overtones and nickel green colours (gaspeite) would arouse suspicions of pyrrhotite-pentlandite ores. Linear stratabound limonitic masses with volcanic associations would suggest volcanogenic styles where major *pyrite* would be expected with minor base metals and possible rare secondary minerals indicating *Cu, Pb and Zn base metal association*.

It is always recommended that the serious prospector or exploration geologist, takes the time to sit on (or collect from) old mine dumps. These frequently provide a set of samples ranging from fresh hypogene materials, through oxidising to leached surficial end products.

This is a very quick way to build up both local and general knowledge. Some follow up with a rock saw, and more detailed hand lens examination builds a valuable data base both for the individual concerned and ultimately for the general exploration team (especially field personal and newly arriving professionals).

The most valuable specimens are always the half/half transition samples where it is clearly seen that one mineral is changing to another, or becoming partially leached. This process cannot be recommended highly enough and is even worth some petrological follow up. As stated at the beginning of this text, the aim of the tome is to provide the basis for understanding the processes involved and improve field skills. A generalised geological check list of procedures is provided below.

- Obtain some obvious general impressions including size, shape and perceptions concerning amounts of clay, limonite and quartz. It is assumed that the general setting will also be noted (Section 4.o).
- Stand back a little (or a lot!) and look for general textural features. These are often well disguised via weathering and blurring via clay/limonite development. Breccias are extremely common and should be anticipated. Forms of layering are also widespread and easy to overlook. Take note of colour variations denoting different original assemblages (Sections 4.o–5.o). At the broader scale vegetation anomalies (especially poor growth due to toxic conditions) and topographic anomalies (hills, cliffs and depressions) are always of note.
- If quartz is a major contributor, record the nature and style of quartz (massive, crystalline, coarse-fine, vuggy, crustiform, colloform, etc.) (Section 4.o). Briefly check broad scale limonite colours and broad scale impression of transported versus indigenous (Section 4.o).
- Break open a considerable number of quartz boulders (or quartz + limonite) in an effort to locate unaltered ore minerals protected from oxidation within the quartz. These are usually minute and a good hand lens is essential.
- Spend considerable time, hunting for secondary minerals. These are most valuable indicators of primary ore composition and range from extremely obvious such as green copper minerals or yellow uranium secondary products, through to obscure small limonite/clay encrusted grains (Section 6.o).
- Search for boxwork textures. These are rarely visible to the eye, and it is a good idea to try and establish the grain size of sulphides involved, from one of the above steps. Most sulphides are at the millimetre scale. Clues from secondary minerals will assist considerably, and guide expectations (Section 7.o).
- Reflect geologically upon the possible style of mineralisation involved. Suspicions of a disseminated porphyry copper style would promote a different field approach, than discovery of a gossanous epithermal quartz vein (Section 8.o). Further investigation, style of sample collection and other regional activity may vary in line with deposit style expectation. Reflection should be done at the field level initially, as return visits are often not possible. The decision to walk around the corner or up the adjacent hill suspecting a breccia pipe may prove crucial (breccia pipes often cluster!).

- Alpers, C.N., and Brimhall, G.H., 1989, Paleohydrologic evolution and geochemical dynamics of cumulative supergene enrichment at La Escondida, Atacama desert, northern Chile: *Economic Geology*, v. 84, p. 229–255.
- Anderson, J.A., 1982, Characteristics of leached capping and techniques of appraisal, *in* Titley, S.R., ed., *Advances in geology of the porphyry copper deposits, southwestern North America*: Tucson, University of Arizona Press, p. 275–295.
- Balassone, G., Rossi, M., Boni, M., Stanley, G., and McDermott, P., 2008, Mineralogical and geochemical characterisation of non-sulphide Zn-Pb mineralisation at Silvermines and Galmoy (Irish Midlands): *Ore Geology Reviews*, v. 33, No.2, p. 168–186.
- Blain, C.F., and Andrew, R.L., 1977, Sulphide weathering and the evaluation of gossans in mineral exploration: *Minerals Science and Engineering*, v. 9, p. 119–149.
- Blanchard, R., 1968, Interpretation of leached outcrops: Nevada Bureau of Mines, Bulletin 66, 215 p.
- Blanchard, R., and Boswell, P.F., 1925, Notes on the oxidation products derived from chalcopyrite: *Economic Geology*, v. 20, p. 613–638.
- Boni, M., Balassone, M., Arseneau, V., Schmidt, P., 2009, The non sulphide zinc deposit at Accha (Southern Peru), geological and mineralogical characterisation: *Economic Geology*, v. 98, p. 749–771.
- Braxton, D.P., Cooke, D.P., Ignacio, A.M., Rye, R.O., and Waters, P.J., 2009, Ultra-deep oxidation and exotic copper formation at the late Pliocene Boyongan and Bayugo porphyry copper-gold deposits, Surigao, Philippines: Geology, mineralogy, paleoaltimetry and their implications for geologic, physiographic and tectonic controls, *in* Titley, S.R., ed., *Supergene environments, processes and products*: Society of Economic Geologists, Special publication No. 14, p. 103–120.
- Chavez, W.X., 2000, Supergene oxidation of copper deposits: zoning and distribution of copper oxide minerals: *Society of Economic Geologists newsletter*, No. 41, p. 10–21.
- Groves, I.M., Carman, C.E., and Dunlop, W.J., 2003, Geology of the Beltana willemite deposit, Flinders Ranges, South Australia: *Economic Geology*, v. 98, p. 797–818.
- Gustafson, L.B., and Hunt, J.P., 1975, The porphyry copper deposit at El Salvador, Chile: *Economic Geology*, v. 70, p. 875–912.
- Hitzman, M.W., Reynolds, N.A., Sangster, P.F., Allan, C.R., and Carman, C.E., 2003, Classification, genesis and exploration guides for nonsulphide zinc deposits: *Economic Geology*, v. 98, p. 685–714.
- Kelly, G.R., 1976, Oxidation and supergene enrichment of the Siberia lode vein system, Emuford, North Queensland: Unpublished M.Sc. Thesis, James Cook University, Queensland, Australia, p. 168
- Loghry, J.D., 1972, Characteristics of favourable cappings from several southwestern porphyry copper deposits: Unpublished M.S. thesis, Tucson, University of Arizona, p. 112.
- Munchmeyer, C., 1996, Exotic deposits products of lateral migration o supergene solutions from porphyry copper deposits: *Society of Economic Geologists special Publication No. 5*, p. 43–58.
- Nickel, E.H., Allchurch, P.D., Mason, M.G., and Wilmshurst, J.R., 1977, Supergene alteration at the Perseverance nickel deposit, Agnew, Western Australia: *Economic Geology*, v. 72, p. 184–203.
- Nickel, E.H., Ross, J.R., and Thornber, M.R., 1974. The supergene alteration of pyrrhotite-pentlandite ore at Kambalda, Australia: *Economic Geology*, v. 69, p. 93–107.

- Ortiz, F.J., 1995, Discovery of the Escondida porphyry copper deposit in the Antofagasta region, northern Chile, March 1982, *in* Pierce, R.W., and Bolm, J.G., eds., *Porphyry copper deposits of the American Cordillera: Arizona Geological Society digest* 20, p. 613–624.
- Reich, R., Palacios, C., Parada, A.M., Fehn, U., Cameron, E.M., Legbourne, M.I., and Zuniga, A., 2008, Atacamite formation by deep saline waters in copper deposits from the Atacama desert, Chile: evidence from fluid inclusions, groundwater geochemistry, TEM, and <sup>36</sup>Cl data: *Mineralium Deposita*, v. 43, p. 663–675.
- Reichert, J., 2009, A geochemical model of supergene carbonate hosted non sulphide zinc deposits, *in* Titley, S.R.; ed, *Supergene environments, processes and products: Society of Economic Geologists, Special publication No. 14*, p. 69–76.
- Reichert, J., and Borg, G., 2007, Numerical simulation and a geochemical model of supergene carbonate-hosted non-sulphide zinc deposits: *Ore Geology Reviews*, 33, p. 134–151.
- Rivera, S.L., Alcota, H., Fontecilla, C., and Kovacic, P., 2009, Supergene modification of porphyry columns and the application to exploration with special reference to the southern part and the Chuquicamata district, Chile, *in* Titley, S.R., ed., *Supergene environments, processes and products: Society of Economic Geologists, Special publication No. 14*, p. 1–14.
- Saegart, W.E., Madera, A., and Kilpatrick, B.E., 1974, *Geology and mineralogy of La Caridad porphyry copper deposit, Sonora, Mexico: Economic Geology*, v. 69, p. 1060–1077.
- Sillitoe, H.R., 2005, Supergene oxidised and enriched porphyry copper and related deposits: *Economic Geology 100<sup>th</sup> Anniversary Volume*, p. 723–768.
- Sillitoe, R.H., 2007, Hypogene reinterpretation of supergene silver enrichment at Chanarillo, northern Chile: *Economic Geology*, v. 102, p. 777–781.
- Sillitoe, R.H., 2009, Supergene silver enrichment reassessed: *in* Titley, S.R.; ed, *Supergene environments, processes and products: Society of Economic Geologists, Special publication No. 14*, p. 15–32.
- Szczerba, M., and Sawlowicz, Z., 2009, Remarks on the origin of cerussite in the upper Silesian Zn-Pb deposits, Poland: *Mineralogia*, v. 40, No. 1–4, p. 54–64.
- Taylor, R. G., 2009, *Ore textures: Berlin, Springer-Verlag*, 287 p.
- Thornber, M.R., and Taylor, G.F., 1992, The mechanisms of sulphide oxidation and gossan formation, *in* Butt, C.R.M., and Zeegers, H., eds, *Regolith exploration geochemistry in tropical and subtropical terrains (in Govett, G.J.S., ed., Handbook of exploration geochemistry) Amsterdam, Elsevier*, v. 4, p. 119–138.
- Titley, S.R., 1982, The style and progress of mineralisation and alteration in porphyry copper systems, American southwest, *in* Titley, S.R., ed., *Advances in geology of the porphyry copper deposits, southwestern North America: Tucson, University of Arizona Press*, p. 93–116.
- Titley, S.R., and Marozas, D.C., 1995, Processes and products of supergene copper enrichment, *in* Pierce, F.W., and Bolm, J.G., eds., *Porphyry copper deposits of the American Cordillera: Tucson, Arizona Geological Society Digest* 20, p. 156–168.
- Titley, S.R., Thompson, R.C., Haynes, F.M., Manske, S., Robinson, L.C., White, J.L., 1986, Evolution of fractures and alteration in Sierrita – Esperanza hydrothermal system, Pima County, Arizona: *Economic Geology*, v. 81, p. 343–370.

**A**

Acid forming sulphides 114  
 Adamite 62, 64, 66  
 Alunite 136  
 Anglesite 55, 56, 59  
 Annabergite 68, 69  
 Antlerite 40, 48, 51, 128, 132  
 Argillic alteration 16  
 Armouring 21  
 Arsenic secondary minerals 68  
 Arsenopyrite-Scorodite 98  
 Arsenopyrite-scorodite boxwork 98  
 Atacamite 40, 47, 51, 128, 131  
 Aurichalcite 62, 67  
 Autunite 75  
 Azurite 40, 46, 47, 128

**B**

Bismuth ochre 71, 72  
 Black oxide 130  
 Black oxide zones 126  
 Botryoidal limonite 27, 104  
 Boxwork 77  
 Boxworks and related features 77  
 Broad scale – first impressions 21  
 Brochantite 40, 48, 51, 128, 131, 133, 134, 135  
 Bromargyrite 71

**C**

Carbonate boxwork 99  
 Carnotite 73, 75  
 Cellular pyrite pseudomorphs 82  
 Cellular structures 77  
 Cerargyrite 71  
 Cerargyrite (Horn silver) 73  
 Cerussite 13, 30, 55, 56, 58  
 Cervantite 70  
 Chalcantite 40, 47, 50, 128  
 Chalcocite 40, 42, 45, 49, 54, 103, 121, 133, 134, 135, 137  
 Chalcocite supergene enrichment zone 121  
 Chalcopyrite boxworks 85  
 Chalcosiderite 40, 48, 53  
 Chalcotrichite 46

Chalcotrichite (Hair copper) 40  
 Chenevixite 126, 128  
 Chert-jasper 95  
 Chrysocolla 40, 47, 50, 128, 131  
 Classic epithermal layering 18  
 Clay 12, 16  
 Clay alteration 16  
 Columnar limonite 27  
 Composition of ribbing 79  
 Conichalcite 126, 128  
 Copper clays 128  
 Copper (native copper) 40  
 Copper “oxide” zone 129  
 Copper pitch 42, 128  
 Copper secondary minerals 41  
 Copper wad 128  
 Covellite 40, 49, 54  
 Crackle/stockwork recognition 108  
 Crednerite 128  
 Crocoite 55, 57, 61  
 Cuprite 40, 43, 44, 45, 128, 129

**D**

Dioptase 40, 48, 52

**E**

Eh/pH environment 8  
 Electrochemical reaction 4  
 Embolite 71  
 Erythrite 70, 102  
 Exotic copper oxide 130  
 Exotic copper oxide deposits 126  
 Exotic goethitic limonite 36  
 Exotic limonite 23  
 Exotic or transported limonite 26

**F**

False gossan – Century mine area 106  
 False gossan – Olivine gabbro 106  
 False gossans 104  
 False gossan –Serpentinite 105

Ferrimolybdate 71  
 Flooded boxwork 79  
 Fluorite 102  
 Fringing limonite 23

## G

Galena boxwork 94  
 Galena-cerussite-massicot-minium 93  
 Galena "gossan" 93  
 Galena residual kernels 93  
 Garnet boxwork 101  
 Garnet boxworks 100  
 Garnierite 68, 69  
 Gaspeite 68, 69, 95  
 General profile of oxidising ore 7  
 Goethite 13, 14, 22, 34, 123  
 Goethite dominant leached capping 123  
 Gossan 9  
 Granular cerussite 92

## H

Haematite 14, 22, 34, 36, 133, 134, 135  
 Haematite dominant capping 122  
 Haematite, goethite, jarosite proportions 114  
 Haematitic 36  
 Haematitic leached capping 109  
 Hemimorphite 13, 14, 15, 33, 62, 63, 66  
 Horn silver 71  
 Hydrolytic reaction 3  
 Hydrozincite 14, 62, 63, 66

## I

Indigenous and fringing limonite 25  
 Indigenous haematite 135  
 Indigenous limonite 23, 26, 81, 97, 115  
 Indigenous – Live limonite 25, 36  
 Initial Recognition 9  
 Iodargyrite 71  
 Iridescent limonite 27  
 Iron secondary minerals 34

## J

Jarosite 22, 34, 36  
 Jarosite dominant leached capping 124  
 Jarositic limonite 138

## K

Knobbly texture of breccia 29  
 Kröhnkite 128

## L

Layering 29  
 Leached capping – goethite/jarosite 112  
 Leached capping – jarositic ± minor goethite 112  
 Leached capping – oxidised copper style 111  
 Leached capping profile 109, 110  
 Leached cappings 9, 11  
 Leached cappings in porphyry copper systems 107  
 Lead secondary minerals 55  
 Lepidocrocite 22  
 Liebethenite 128  
 Limonite 9, 22, 23  
 Limonite colour charts 118  
 Limonite colours in relation to haematite – goethite  
 – jarosite proportions 119  
 Limonite mapping 118  
 Limonite nomenclature  
   Arborescent 23  
   Botryoidal 24  
   Caked 24  
   Cellular 24  
   Coagulated, Fused 24  
   Columnar 24  
   Concretionary 24  
   Craggy 24  
   Earthy 24  
   Flaky 24  
   Flat 24  
   Granular 24  
   Iridescent 24  
   Live 24  
   Mammilated 24  
   Massive 24  
   Nodular 24  
   Pitch 24  
   Pulverulent 24  
   Relief 24  
   Reniform 24  
   Stalactitic 24  
   Varnished 24  
   Vitreous 24  
 Limonitic gossan 12  
 Linarite 40, 48, 52  
 Litharge 55, 57  
 Live limonite 122  
 Loghry model 115  
 Ludjibaite 53

**M**

Malachite 19, 20, 40, 46, 47, 128, 132  
 Manganese oxides 14, 22, 38, 39, 104, 135  
 Manganese wad 38  
 Manganite 38  
 Maroon coloured indigenous limonite 110  
 Massicot 55, 59, 60  
 Melanterite 34, 35, 37  
 Metaautunite 75  
 Metaschoepite 75  
 Metatorbernite 75  
 Metatyuyamite 75  
 Metauranospinite 75  
 Mimetite 55, 57, 60  
 Minium 55, 57, 59, 60  
 Molybdic ochre 71, 72  
 Molybdite 71

**N**

Native copper 42, 44  
 Native silver 73  
 Negative pseudomorphs of molybdenite 103  
 Negative vegetation anomaly 12  
 Neotocite 38, 39, 128  
 Neutralising power of the host rocks 23  
 Nickel secondary minerals 68  
 Nickel sulphide “gossan-ironstone” 96

**O**

Ochres 71  
 Olivenite 40, 48, 53  
 Ovoid-cubic pseudomorphs of cobaltite 103  
 Oxidation collapse 29  
 Oxidation profile 8  
 Oxidation profile at Grasberg Cu-Au mine 136  
 Oxide copper ore 109  
 Oxide zone 126

**P**

Paramelaconite 128  
 Paratacamite 48  
 Pathways producing boxworks, in situ granular clusters and positive and negative pseudomorphs 78  
 Pitch limonite 44, 128  
 Plumbojarosite 55, 57, 60  
 Porphyry copper systems 107  
 Pseudomalachite 128

Pseudomalachite 40, 48, 53  
 Psilomilane 38  
 Pyrite cellular 82  
 Pyrite cellular sponge 83  
 Pyrite – cellular sponge boxwork 84  
 Pyrite – dominant leached capping and gossan 81  
 Pyrite – cellular boxwork 83  
 Pyrite – negative pseudomorphs 81  
 Pyrite – pseudomorphs 81  
 Pyrite – rectangular boxwork 84  
 Pyrite – remnant boxwork? 84  
 Pyrolusite 38  
 Pyromorphite 55, 57, 61  
 Pyrrhotite boxworks 85  
 Pyrrhotite cellular sponge 86

**Q**

Quartz textures 21  
 Quartz veining 9

**R**

Recent discoveries 11  
 Reichenbachite 53  
 Relief limonite 24, 25  
 Rib development 79  
 Ribs 78  
 Rodembolite 71  
 Rosasite 62, 67

**S**

Sampleite 128  
 Sauconite 13, 14, 62, 63  
 Schoepite 75  
 Schoepite-meteshoepite 76  
 Scorodite 19, 68, 70, 97  
 Secondary minerals 5, 9, 33  
 Secondary silver minerals 71  
 Siderite 22  
 Siderite (carbonate) boxwork 99  
 Siliceous jasperoidal alteration 96  
 Silver 73  
 Smithsonite 13, 14, 62, 63, 65  
 Sphalerite boxworks 87, 90, 91  
 Sphalerite crack/fracture 88  
 Sphalerite dissolution 89  
 Sphalerite replacement 89  
 Stability relations of some copper minerals 41  
 Stibiconite 70, 71  
 Structural preservation – breccia, shear fabric 31

- Structural preservation – layering 30
- Styles of ribbing 78
- Supergene copper sulphides 49
- Supergene enrichment 112, 113
- Supergene modification 5
- T**
- Tenorite 40, 43, 45, 128
- Theoretical Perspectives 3
- Torbernite 74, 75
- Torbernite-Metatorbernite 76
- Transported limonite 138
- Tungstic ochre 71, 72
- Tungstite 71
- Turquoise 40, 48, 52, 128
- Types of leached cappings and gossanous exposures
  - Clay dominant ± minor limonite ± secondary minerals – limited exposure inconspicuous 20
  - Clay dominated ± limonite – conspicuous 16
  - Inconspicuous with no obvious limonite, clay, or secondary minerals 20
  - Limonite dominant ± clay, secondary minerals – conspicuous 12
  - Limonite dominant ± secondary minerals – conspicuous 13
  - Limonite dominated – conspicuous 15
  - Limonite dominated – inconspicuous 16
  - Limonite dominated ± secondary minerals – conspicuous 15
  - Limonite dominated ± secondary minerals – conspicuous 14
  - Limonite dominated with significant clay – conspicuous 16
  - Quartz dominant – conspicuous 18
  - Quartz dominant – hidden 17, 18
  - Quartz dominant ± limonite ± secondary minerals – limited exposure – inconspicuous 19
  - Quartz dominant, minor limonite – concealed inconspicuous 19
  - Quartz – newly exposed 17
- Typical stockwork texture – porphyry copper system 121
- Tyuyamite 75
- Tyuyamunite-Carnotite 76
- U**
- Uranium secondary minerals 74
- Uranospinite 75
- Uranospinite-Metauranospinite 76
- V**
- Vanadinite 57
- Vivianite 34, 37
- Vuggy silica 9
- Vuggy-silica at surface 18
- Vuggy-silica capping 18
- W**
- Willemite 62, 64, 67
- Wulfenite 55, 57, 61
- Z**
- Zincian clay 63
- Zinc oxide or non sulphide zinc deposits 13
- Zinc secondary minerals 62